MULTISCALE METHODS AND ANALYSIS FOR HIGHLY OSCILLATORY DIFFERENTIAL EQUATIONS

ZHAO XIAOFEI

NATIONAL UNIVERSITY OF SINGAPORE

2014

MULTISCALE METHODS AND ANALYSIS FOR HIGHLY OSCILLATORY DIFFERENTIAL EQUATIONS

ZHAO XIAOFEI

(B.Sc., Beijing Normal University, China)

A THESIS SUBMITTED

FOR THE DEGREE OF DOCTOR OF PHILOSOPHY

DEPARTMENT OF MATHEMATICS

NATIONAL UNIVERSITY OF SINGAPORE

2014

DECLARATION

I hereby declare that this thesis is my original work and it has been written by me in its entirety.
I have duly acknowledged all the sources of information which have been used in the thesis.

This thesis has also not been submitted for any degree in any university previously.

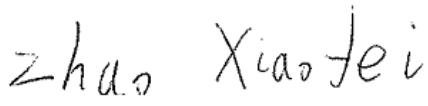

Zhao Xiaofei
28 July 2014

Acknowledgements

It is my great honor to take this opportunity to thank those who made this thesis possible.

First and foremost, I owe my deepest gratitude to my supervisor Prof. Bao Weizhu, whose generous support, patient guidance, constructive suggestion, invaluable help and encouragement enabled me to conduct such an interesting research project.

I would like to express my appreciation to my collaborators Dr. Xuanchun Dong for his contribution to the work. Specially, I thank Dr. Yongyong Cai for fruitful discussions and suggestions on my research. My sincere thanks go to all the former colleagues and fellow graduates in our group. My heartfelt thanks go to my friends for all the encouragement, emotional support, comradeship and entertainment they offered. I would also like to thank NUS for awarding me the Research Scholarship which financially supported me during my Ph.D candidature.

Last but not least, I am forever indebted to my beloved girl friend and family, for their encouragement, steadfast support and endless love when it was most needed.

Zhao Xiaofei

July 2014

Contents

Acknowledgements i

Summary v

List of Tables viii

List of Figures x

List of Symbols and Abbreviations xii

1 Introduction 1

1.1 The highly oscillatory problems 1

1.2 Existing methods 2

1.3 The subjects 4

1.3.1 Highly oscillatory second order differential equations 5

1.3.2 Nonlinear Klein-Gordon equation in the nonrelativistic limit regime 7

1.3.3 Klein-Gordon-Zakharov system in the high-plasma-frequency and subsonic limit regime 9

1.4 Purpose and outline of the thesis 11

2 For highly oscillatory second order differential equations 13

2.1 Introduction . . . 13
2.2 Finite difference methods . . . 17
2.3 Exponential wave integrators . . . 19
2.4 Multiscale decompositions . . . 21
2.4.1 Multiscale decomposition by frequency (MDF) . . . 22
2.4.2 Multiscale decomposition by frequency and amplitude (MDFA) 24
2.5 Multiscale time integrators for pure power nonlinearity . . . 25
2.5.1 A multiscale time integrator based on MDFA . . . 26
2.5.2 Another multiscale time integrator based on MDF . . . 30
2.5.3 Uniform convergence . . . 32
2.5.4 Proof of Theorem 2.5.1 . . . 34
2.5.5 Proof of Theorem 2.5.2 . . . 40
2.6 Multiscale time integrators for general nonlinearity . . . 42
2.6.1 A MTI based on MDFA . . . 42
2.6.2 Another MTI based on MDF . . . 45
2.7 Numerical results and comparisons . . . 45
2.7.1 For power nonlinearity . . . 46
2.7.2 For general gauge invariant nonlinearity . . . 49

3 Classical numerical methods for the Klein-Gordon equation 64

3.1 Introduction . . . 64
3.2 Existing numerical methods . . . 66
3.2.1 Finite difference time domain methods . . . 67
3.2.2 Exponential wave integrator with Gautschi's quadrature pseudospectral method . . . 68
3.3 Time splitting pseudospectral method . . . 70
3.4 EWI with Deuflhard's quadrature pseudospectral method . . . 74
3.4.1 Numerical scheme . . . 75
3.4.2 Error estimates . . . 76

3.5 Numerical results and comparisons 85
3.5.1 Accuracy tests for $\varepsilon = O(1)$ 86
3.5.2 Convergence and resolution studies for $0 < \varepsilon \ll 1$ 88

4 Multiscale methods for the Klein-Gordon equation 94
4.1 Existing results in the limit regime 94
4.2 Multiscale decomposition 97
4.3 Multiscale method 99
4.4 Error estimates 105
4.5 Numerical results 119

5 Applications to the Klein-Gordon-Zakharov system 126
5.1 Introduction 126
5.2 Exponential wave integrators 128
5.2.1 EWI-GSP 131
5.2.2 EWI-DSP 133
5.2.3 Convergence analysis 135
5.3 Multiscale method 147
5.3.1 Multiscale decomposition 148
5.3.2 MTI 150
5.4 Numerical results 156

6 Conclusion remarks and future work 166

Bibliography 170

List of Publications 181

Summary

The oscillatory phenomena happen almost everywhere in our life, ranging from macroscopic to microscopic level. They are usually described and governed by some highly oscillatory nonlinear differential equations from either classical mechanics or quantum mechanics. Effective and accurate approximations to the highly oscillatory equations become the key way of further studies of the nonlinear phenomena with oscillations in different scientific research fields.

The aim of this thesis is to propose and analyze some efficient numerical methods for approximating a class of highly oscillatory differential equations arising from quantum or plasma physics. The methods here include classical numerical discretizations and the multiscale methods with numerical implementations. Special attentions are paid to study the error bound of each numerical method in the highly oscillatory regime, which are geared to understand how the step size should be chosen in order to resolve the oscillations, and eventually to find out the uniformly accurate methods that could totally ignore the oscillations when approximating the equations.

This thesis is mainly separated into three parts. In the first part, two multiscale time integrators (MTIs), motivated from two types of multiscale decomposition by either frequency or frequency and amplitude, are proposed and analyzed for solving

highly oscillatory second order ordinary differential equations with a dimensionless parameter $0 < \varepsilon \leq 1$. This problem is considered as the fundamental model problem of all the studies in this thesis. In fact, the solution to this equation propagates waves with wavelength at $O(\varepsilon^2)$ when $0 < \varepsilon \ll 1$, which brings significantly numerical burdens in practical computation. We rigorously establish two independent error bounds for the two MTIs at $O(\tau^2/\varepsilon^2)$ and $O(\varepsilon^2)$ for $\varepsilon \in (0, 1]$ with $\tau > 0$ as step size, which imply that the two MTIs converge uniformly with linear convergence rate at $O(\tau)$ for $\varepsilon \in (0, 1]$ and optimally with quadratic convergence rate at $O(\tau^2)$ in the regimes when either $\varepsilon = O(1)$ or $0 < \varepsilon \leq \tau$. Thus the meshing strategy requirement (or ε-scalability) of the two MTIs is $\tau = O(1)$ for $0 < \varepsilon \ll 1$, which is significantly improved from $\tau = O(\varepsilon^3)$ and $\tau = O(\varepsilon^2)$ requested by finite difference methods and exponential wave integrators to the equation, respectively. Extensive numerical tests support the two error bounds very well, and comparisons with those classical numerical integrators offer better understanding on the convergence and resolution properties of the two MTIs.

The second part of the thesis studies the Klein-Gordon equation (KGE), involving a dimensionless parameter $\varepsilon \in (0, 1]$ which is inversely proportional to the speed of light. With a Gautschi-type exponential wave integrator (EWI) spectral method and some popular finite difference time domain methods reviewed at the beginning, a time-splitting Fourier pseudospectral (TSFP) discretization is considered for the KGE in the nonrelativistic limit regime, where the $0 < \varepsilon \ll 1$ leads to waves propagating in the exact solution of the KGE with wavelength of $O(\varepsilon^2)$ in time and $O(1)$ in space. Optimal error bound of TSFP is established for fixed $\varepsilon = O(1)$, thanks to a vital observation that the scheme coincides with a Deulfhard-type exponential wave integrator. Numerical studies of TSFP are carried out, with special efforts made in the nonrelativistic limit regime, which gear to suggest that TSFP has uniform spectral accuracy in space, and has an asymptotic temporal error bound $O(\tau^2/\varepsilon^2)$ whereas that of the Gautschi-type method is $O(\tau^2/\varepsilon^4)$. Comparisons show that TSFP offers the best approximation among all classical numerical

methods for solving the KGE in the highly oscillatory regime. Then a multiscale time integrator Fourier pseudospectral (MTI-FP) method is proposed for the KGE. The MTI-FP method is designed by adapting a multiscale decomposition by frequency (MDF) to the solution at each time step and applying an exponential wave integrator to the nonlinear Schrödinger equation with wave operator under well-prepared initial data for ε^2-frequency and $O(1)$-amplitude waves and a KG-type equation with small initial data for the reminder waves in the MDF. Two rigorous independent error bounds are established in H^2-norm to MTI-FP at $O(h^{m_0}+\tau^2+\varepsilon^2)$ and $O(h^{m_0}+\tau^2/\varepsilon^2)$ with h mesh size, τ time step and $m_0 \geq 2$ an integer depending on the regularity of the solution, which immediately imply that MTI-FP converges uniformly and optimally in space with exponential convergence rate if the solution is smooth, and uniformly in time with linear convergence rate at $O(\tau)$ for all $\varepsilon \in (0, 1]$ and optimally with quadratic convergence rate at $O(\tau^2)$ in the regimes when either $\varepsilon = O(1)$ or $0 < \varepsilon \leq \tau$. Numerical results are reported to confirm the error bounds and demonstrate the best efficiency and accuracy of the MTI-FP among all methods for solving the KGE, especially in the nonrelativistic limit regime.

The last part of the thesis is to apply and extend the proposed methods in previous parts to solve the Klein-Gordon-Zakharov system in the high-plasma-frequency and subsonic limit regimes. Numerical results show the success of the applications and shed some lights in future applications to other more oscillatory systems.

List of Tables

2.1 Error analysis of MTI-FA: $\mathrm{e}^{\varepsilon,\tau}(T)$ and $\mathrm{e}^{\tau}_{\infty}(T)$ with $T = 4$ and convergence rate. Here and after, the convergence rate is obtained by $\frac{1}{2}\log_2\left(\frac{\mathrm{e}^{\varepsilon,4\tau}(T)}{\mathrm{e}^{\varepsilon,\tau}(T)}\right)$. 47

2.2 Error analysis of MTI-F: $\mathrm{e}^{\varepsilon,\tau}(T)$ and $\mathrm{e}^{\tau}_{\infty}(T)$ with $T = 4$ and convergence rate. 54

2.3 Error analysis of EWI-G: $\mathrm{e}^{\varepsilon,\tau}(T)$ with $T = 4$ and convergence rate. . . 55

2.4 Error analysis of EWI-D: $\mathrm{e}^{\varepsilon,\tau}(T)$ with $T = 4$ and convergence rate. . . 56

2.5 Error analysis of EWI-F1: $\mathrm{e}^{\varepsilon,\tau}(T)$ with $T = 4$ and convergence rate. . 57

2.6 Error analysis of EWI-F2: $\mathrm{e}^{\varepsilon,\tau}(T)$ with $T = 4$ and convergence rate. . 58

2.7 Error analysis of CNFD : $\mathrm{e}^{\varepsilon,\tau}(T)$ with $T = 4$ and convergence rate. . 59

2.8 Error analysis of SIFD: $\mathrm{e}^{\varepsilon,\tau}(T)$ with $T = 4$ and convergence rate. . . . 60

2.9 Error analysis of EXFD: $\mathrm{e}^{\varepsilon,\tau}(T)$ with $T = 4$ and convergence rate. . . 61

2.10 Error of MTI-FA and MTI-F for HODE system: $\mathrm{e}^{\varepsilon,\tau}(T)$ with $T = 1$. . 61

2.11 Error analysis of MTI-FA for general nonlinearity: $\mathrm{e}^{\varepsilon,\tau}(T)$ with $T = 1$. 62

2.12 Error analysis of MTI-F for general nonlinearity: $\mathrm{e}^{\varepsilon,\tau}(T)$ with $T = 1$. 63

3.1 Spatial discretization errors of TSFP at time $t = 1$ for different mesh sizes h under $\tau = 10^{-5}$. 86

3.2 Temporal discretization errors of TSFP at time $t = 1$ for different time steps τ under $h = 1/16$ with convergence rate. 86
3.3 Conserved energy analysis of TSFP: $\tau = 10^{-3}$ and $h = 1/8$. 87
3.4 Spatial error analysis of TSFP for different ε and h at time $t = 1$ under $\tau = 10^{-5}$. 89
3.5 Temporal error analysis of TSFP for different ε and τ at time $t = 1$ under $h = 1/16$ with convergence rate. 90
3.6 Temporal error analysis of EWI-GFP for different ε and τ at time $t = 1$ under $h = 1/16$ with convergence rate. 91
3.7 ε-scalability analysis: temporal error at time $t = 1$ with $h = 1/16$ for different τ and ε under meshing requirement $\tau = c \cdot \varepsilon^2$. 92

4.1 Spatial error analysis: $\mathrm{e}_{\varepsilon}^{\tau,h}(T = 1)$ with $\tau = 5 \times 10^{-6}$ for different ε and h. 120
4.2 Temporal error analysis: $\mathrm{e}_{\varepsilon}^{\tau,h}(T = 1)$ a nd $\mathrm{e}_{\infty}^{\tau,h}(T = 1)$ with $h = 1/8$ for different ε and τ. 121

5.1 Spatial error analysis: $e_{\phi}^{\varepsilon}(T)$ at $T = 1$ with $\tau = 5 \times 10^{-6}$ for different ε and h. 158
5.2 Spatial error analysis: $e_{\psi}^{\varepsilon}(T)$ at $T = 1$ with $\tau = 5 \times 10^{-6}$ for different ε and h. 159
5.3 Temporal error analysis: $e_{\phi}^{\varepsilon}(T)$ and $e_{\phi}^{\infty}(T)$ at $T = 1$ with $h = 1/8$ for different ε and τ. 160
5.4 Temporal error analysis: $e_{\psi}^{\varepsilon}(T)$ and $e_{\psi}^{\infty}(T)$ at $T = 1$ with $h = 1/8$ for different ε and τ. 161

List of Figures

2.1 Time evolution of the solutions of (2.1.1) with $d = 2$ for different ε. . 15

2.2 Energy error $|E^n - E(0)|$ of SIFD and EWI-G for different τ during the computing under $\varepsilon = 0.2$. 50

2.3 Energy error $|E^n - E(0)|$ of MTI-F and MTI-FA for different τ during the computing under $\varepsilon = 0.2$. 51

2.4 Maximum energy error $e_E(t) := \max\limits_{0\le t_n\le t}\{|E^n - E(0)|\}$ of SIFD, EWI-G, MTI-F and MTI-FA under $\tau = 1E-3$ and $\varepsilon = 0.2$. 51

2.5 Solution of the HODE system (2.7.3) with $\varepsilon = 0.05$. 52

3.1 Energy error of TSFP in defocusing case ($\lambda = 1$) and focusing case ($\lambda = -1$): $|E(t) - E(0)|$ for different τ during the computing under $h = 1/8$ and $\varepsilon = 1$. 87

3.2 Dependence of the temporal discretization error on ε (in log-scale) for different τ at $t = 1$ under $h = 1/8$: (a) for TSFP and (b) for EWI-GFP. 89

4.1 The solution of (4.1.1) with $d = 1$, $f(u) = |u|^2u$, $\phi_1(x) = e^{-x^2/2}$ and $\phi_2(x) = \frac{3}{2}\phi_1(x)$ for different ε. 96

4.2 Profiles of the solutions of 1D KGE (4.5.1) under different ε. 122

4.3 Contour plots of the solutions of 2D KGE with (4.5.2) at different time t under $\varepsilon = 5E-3$. 123
4.4 Contour plots of the solutions of 2D KGE with (4.5.2) at different time t under $\varepsilon = 2.5E-3$. 124
4.5 Isosurface plots of the solutions of 3D KGE with (4.5.3) at different time t under ε. 125

5.1 Profile of the solutions of KGZ with $d = 1$ for different ε. 148
5.2 Solutions of the KGZ (5.3.1) with (5.4.1) in the high-plasma-frequency limit regime under different ε. 162
5.3 Solutions of the KGZ (5.2.1) with (5.4.1) in the simultaneously high-plasma-frequency and subsonic limit regime under different ε with $\gamma = 2\varepsilon$. 163
5.4 Solutions of the 2D KGZ (5.3.1) with (5.4.2) at different t under $\varepsilon = 5E-3$. 164
5.5 Solutions of the 2D KGZ (5.3.1) with (5.4.2) at different t under $\varepsilon = 2.5E-3$. 165

List of Symbols and Abbreviations

t	time
$\mathbf{x}$	space variable
$\mathbf{R}^d$	d dimensional Euclidean space
$\mathbf{C}^d$	d dimensional complex space
τ	time step size
h	space mesh size
i	imaginary unit
ε	a dimensionless parameter with its value $0 < \varepsilon \leq 1$
$\hbar$	Planck constant
∇	gradient
$\Delta = \nabla \cdot \nabla$	Laplacian
$\bar{f}$	conjugate of of a complex function f
$\mathrm{Re}(f)$	real part of a complex function f
$\mathrm{Im}(f)$	imaginary part of a complex function f
$A \lesssim B$	$A \leq C \cdot B$ for some generic constant $C > 0$ independent of τ, h and ε
1D	one dimension
2D	two dimension

3D	three dimension
KGE	Klein-Gordon equation
KGZ	Klein-Gordon-Zakharov
NLSE	Nonlinear Schrödinger equation
BC	boundary condition
EWI	exponential wave integrator
MTI	multiscale time integrator
MDF	multiscale decomposition by frequency
MDFA	multiscale decomposition by frequency and amplitude
EWI-GFP	exponential wave integrator with Gautschi's quadrature Fourier pseudospectral
EWI-DFP	exponential wave integrator with Deuflhard's quadrature Fourier pseudospectral
CNFD	Crank-Nicolson finite difference
SIFD	semi-implicit finite difference
EXFD	explicit finite difference
TSFP	time-splitting Fourier pseudospectral
Fig.	figure
Tab.	table

Chapter 1

Introduction

1.1 The highly oscillatory problems

Oscillate: 'to swing backward and forward like a pendulum; to move or travel back and forth between two points; to vary above and below a mean value.' (Webster's Ninth New Collegiate Dictionary (1985)). In our life, there are many oscillation phenomena from the macroscopic level for example, a vibrating spring, a pendulum et al, to the microscopic level like the motion of molecular [73, 92]. Due to the extensive background of oscillations from the studies of scientists, engineers and numerical analysts, it is almost not possible to give a precise mathematical definition of the word 'highly oscillatory' [88].

Our story begins with the simple harmonic oscillator, which is governed by the Newton's second law and Hooke's law as a second order differential equation:

$$m\ddot{x}(t) = -kx(t), \qquad t > 0,$$

where x denotes the displacement of the oscillator, m is the mass of it and k is the Young's modulus. When k is large, for example the stiff spring, the solution of the equation becomes highly oscillatory as time evolves. Although this is just a simple example, many physical phenomena in the Hamiltonian mechanics are in very similar situations. For example, the dynamics of the outer solar system, the

Hénon-Heiles model for stellar motion, the molecular dynamics [57] and even some stochastic differential equations [39] et al. They are all described by certain second order ordinary differential equations and the high oscillations occur when some large frequencies are involved into the forces in these systems. These oscillations, due to the nonlinear forces and nonlinear interactions, are not just simple periodic motions described as trigonometric functions in most cases. In general, the dynamics in the highly oscillatory system are quite complicated. The high oscillations do not only happen in the classical mechanics, but also happen frequently in the quantum mechanics and plasma physics especially under some limit physical regimes. In the quantum and plasma physics, things are usually described by nonlinear partial differential equations, and the oscillations could occur either in space or in time or in both. For example, the nonlinear Klein-Gordon equation in the nonrelativistic limit regime [10] is highly oscillatory in time, and so is the Klein-Gordon-Zakharov system in the high-plasma-frequency and subsonic limit regime. The nonlinear Schrödinger equation in the semiclassical limit regime [14] has oscillations in both time and space. Some other equations like the complex Ginzburg-Landau equation, Allen-Cahn equation et al, could possess more complicated oscillations usually known as layers [39].

These highly oscillatory problems find great interests in current research fronts and applications in industries. To solve the problems, exactly it is not possible since they are usually nonlinear coupled differential equations. Thus, finding effective approximations to the governing equations becomes the effective way to study these nonlinear phenomena with high oscillations.

1.2 Existing methods

The oscillatory differential equations have been studied for almost a century. The methods can be classified into two branches. One is developed from the applied mathematics and the methods are known as the analytical approaches in the

literature. The other is from the computational mathematical studies where people developed different numerical methods. Both branches share the same spirit: looking for good approximations to the oscillatory system.

On the analytical approaches, the first classical method is the standard averaging method, also known as Krylov-Bogolyubov method of averaging. This method is developed by N. Krylov and N. Bogoliubov in their very first French paper on oscillatory equations in 1935. One can refer to an English version in their book [72]. This method applies to find an effective model to replace the oscillatory equations which consists of slow variables and fast variables by averaging the original equations over the statistics of the fast variables properly. Extensions of the averaging method to study the elliptic type problems with multiple scales are known as the homogenization method [39, 86]. A special averaging known as the stroboscopic averaging was found as a very useful technique in analyzing the oscillatory equations in [90]. The key interest of stroboscopic averaging is that it allows to preserve the structure of the original problem along the averaging process, as pointed out in [23, 90]. Around 2000, E. Hair, Ch. Lubich and D. Cohen et al studied and developed the modulation Fourier expansion method in a series of their work [27–30, 55–57] to approximate and analyze the highly oscillatory differential equations arising from molecular dynamics (MD), where they found the method a powerful tool for analyzing the oscillating structures of the equations and the long time preserving properties of different numerical methods.

On the numerical approaches, various numerical methods have been proposed in the literature over the past decades. The early traditional methods like finite difference methods and Runge-Kutta methods, even though with the implicit stable versions, will lead to totally wrong approximations if the time step of the numerical methods is not small enough to fully resolve the highly oscillatory structure in the problem. The exponential wave integrators (EWIs) were then proposed to release the meshing requirements of early methods, where the very first two kinds were designed by W. Gautschi [45] and P. Deuflhard [36] in 1961 and 1979, respectively, based

on different quadratures. Later, the EWI methods were developed as the impulse methods and mollified impulse methods in [44,91] to overcome the convergence order reduction problems pointed out in [44]. The two EWI methods were also generalised to combine with different filter functions in order to get good long time energy preserving property in [55, 57]. Other numerical methods include some efficient quadratures for general highly oscillatory integrals studied by A. Iserles et al in [64–66] and the references therein.

Recently, combining the analytical methods and the numerical methods becomes a popular way to study the highly oscillatory problems. The numerical stroboscopic averaging method was proposed in [23,25]. The modulation Fourier expansion method has been used to design numerical methods for the equations from MD and linear second-order ODEs with stiff source terms in [27, 29, 54–57, 91]. The general framework for designing efficient numerical methods for problems with mulitscale and multiphysics is systematically developed as the heterogeneous multiscale method in [3, 39–41]. However, all these methods are strongly problem-dependent. That means for a different oscillatory equation arising from a certain background, different analytical tools and numerical methods should be chosen or designed properly. Thus, the studies of solving oscillatory problems never end. The combination of analytical methods and numerical methods is the one we are referring to in this thesis: the multiscale methods.

1.3 The subjects

Although many oscillatory problems such as the MD equations have been well studied in the literature, there are still lots of unclear but interesting highly oscillatory phenomena unsettled. This thesis considers the following problems with high oscillations in time which are mainly arising from quantum or plasma physics.

1.3.1 Highly oscillatory second order differential equations

The highly oscillatory second order differential equations (HODEs) read

$$\begin{cases} \varepsilon^2 \ddot{\mathbf{y}}(t) + A\mathbf{y}(t) + \dfrac{1}{\varepsilon^2}\mathbf{y}(t) + \mathbf{f}\left(\mathbf{y}(t)\right) = 0, \quad t > 0, \\ \mathbf{y}(0) = \Phi_1, \quad \dot{\mathbf{y}}(0) = \dfrac{\Phi_2}{\varepsilon^2}. \end{cases} \tag{1.3.1}$$

Here t is time, $\mathbf{y} := \mathbf{y}(t) = (y_1(t), \ldots, y_d(t))^T \in \mathbb{C}^d$ is a complex-valued vector function with d a positive integer, $\dot{\mathbf{y}}$ and $\ddot{\mathbf{y}}$ refer to the first and second order derivatives of $\mathbf{y}$, respectively, $0 < \varepsilon \leq 1$ is a dimensionless parameter which can be very small in some limit regimes, $A \in \mathbb{R}^{d\times d}$ is a symmetric positive semi-definite matrix, $\Phi_1,\ \Phi_2 \in \mathbb{C}^d$ are two given initial data at $O(1)$ in term of $0 < \varepsilon \ll 1$, and $\mathbf{f}(\mathbf{y}) = (f_1(\mathbf{y}), \ldots, f_d(\mathbf{y}))^T : \ \mathbb{C}^d \to \mathbb{C}^d$ describes the nonlinear interaction which is independent of ε. The *gauge invariance* implies that $\mathbf{f}(\mathbf{y})$ satisfies the following relation [77]

$$\mathbf{f}(\mathrm{e}^{is}\mathbf{y}) = \mathrm{e}^{is}\mathbf{f}(\mathbf{y}), \qquad \forall s \in \mathbb{R}. \tag{1.3.2}$$

We remark that if the initial data $\Phi_1, \Phi_2 \in \mathbb{R}^d$ and $\mathbf{f}(\mathbf{y}) : \ \mathbb{R}^d \to \mathbb{R}^d$, then the solution $\mathbf{y} \in \mathbb{R}^d$ is real-valued. In this case, the gauge invariance condition (1.3.2) for the nonlinearity in (1.3.1) is no longer needed.

The above problem is motivated from our recent numerical study of the nonlinear Klein–Gordon equation (KGE) in the nonrelativistic limit regime [10, 76, 77], where $0 < \varepsilon \ll 1$ is scaled to be inversely proportional to the speed of light. In fact, it can be viewed as a model resulted from a semi-discretization in space, e.g., by finite difference or spectral discretization with a fixed mesh size (see detailed equations (3.3) and (3.19) in [10]), to the nonlinear KGE. In order to propose new multiscale time integrators (MTIs) and compare with those classical numerical integrators including finite difference methods [10, 38, 73, 92, 99] and exponential wave integrators [44, 54, 55, 57, 91] efficiently, we thus focus on the above HODEs instead of the original nonlinear KGE. The solution to (1.3.1) propagates highly oscillatory waves with wavelength at $O(\varepsilon^2)$ and amplitude at $O(1)$.

The model problem (1.3.1) is quite different from the following oscillatory second order differential equations arising from Newtonian mechanics such as molecular dynamics [27, 29, 54, 55, 57, 91],

$$\begin{cases} \ddot{\mathbf{y}}(t) + \dfrac{A}{\varepsilon^2}\mathbf{y}(t) + \mathbf{f}(\mathbf{y}(t)) = 0, \qquad t > 0, \\ \mathbf{y}(0) = \varepsilon\Phi_1, \quad \dot{\mathbf{y}}(0) = \Phi_2. \end{cases} \tag{1.3.3}$$

In fact, the above problem (1.3.3) propagates waves with wave length and amplitude both at $O(\varepsilon)$, where the problem (1.3.1) propagates waves with wave length at $O(\varepsilon^2)$ and amplitude at $O(1)$, and thus the oscillation in the problem (1.3.1) is much more oscillating and wild. In addition, dividing ε^2 on both sides of the model equation (1.3.1), we obtain

$$\ddot{\mathbf{y}} + \frac{A\varepsilon^2 + 1}{\varepsilon^4}\mathbf{y} + \frac{1}{\varepsilon^2}\mathbf{f}(\mathbf{y}) = 0. \tag{1.3.4}$$

Of course, when $\varepsilon = O(1)$, both (1.3.3) and (1.3.4) are perturbations to the harmonic oscillator. However, in the regime of $0 < \varepsilon \ll 1$, due to the factor $\frac{1}{\varepsilon^2}$ in front of the nonlinear function, the nonlinear term in (1.3.4) is no longer a small perturbation to the harmonic oscillator! Resonance may occur at time $t = O(1)$. Another major difference is that the reduced energy [54–56, 56, 57] of the problem (1.3.3) $H_r := \dot{\mathbf{y}}^T\dot{\mathbf{y}} + \frac{1}{\varepsilon^2}\mathbf{y}^T A\mathbf{y}$ is uniformly bounded for $\varepsilon \in (0, 1]$, while that of the problem (1.3.1) $H_r := \varepsilon^2\dot{\mathbf{y}}^T\dot{\mathbf{y}} + \mathbf{y}^T A\mathbf{y} + \frac{1}{\varepsilon^2}\mathbf{y}^T\mathbf{y}$ is unbounded when $\varepsilon \to 0$. The unbounded energy could make the analysis and computations more difficult. In fact, with a scaling $\mathbf{y} \to \frac{1}{\varepsilon}\mathbf{y}$, one can convert the small initial data or the energy bounded case in (1.3.3) to

$$\begin{cases} \ddot{\mathbf{y}}(t) + \dfrac{A}{\varepsilon^2}\mathbf{y}(t) + \dfrac{1}{\varepsilon}\mathbf{f}(\varepsilon\mathbf{y}(t)) = 0, \qquad t > 0, \\ \mathbf{y}(0) = \Phi_1, \quad \dot{\mathbf{y}}(0) = \dfrac{1}{\varepsilon}\Phi_2. \end{cases} \tag{1.3.5}$$

In most practical cases, such as the Fermi-Pasta-Ulam problem, the Hénon-Heiles model from Newtonian dynamics [57] and the scalar field self-interaction in quantum dynamics, $\mathbf{f}(\mathbf{y})$ is a polynomial function and the nonlinearity $\frac{1}{\varepsilon}\mathbf{f}(\varepsilon\mathbf{y}) = o(1)$ in (1.3.5) is actually a very small perturbation to the linear problem and is much weaker than

that in (1.3.4). Thus, compared to (1.3.3), the model (1.3.1) is a much more highly oscillatory problem with a very strong nonlinearity, and consequently is much more challenging numerically. It is also believed that the study of (1.3.1) could also shed some lights on that of (1.3.3).

Different efficient and accurate numerical methods, including finite difference methods [10,38], exponential wave integrators (EWIs) [27,54,55], mollified impulse methods [29,57,91], modulated Fourier expansion methods [29,54,57,91], heterogeneous multiscale methods [42], flow averaging [101], Stroboscopic averaging [25] and Yong measure approach [4] have been proposed and analyzed as well as compared for the problem (1.3.3) in the literatures, especially in the regime when $0 < \varepsilon \ll 1$. However, based on the results in [10], all the above numerical methods do *not* converge uniformly for $\varepsilon \in (0, 1]$ for the problem (1.3.1) which usually arise from quantum and plasma physics.

1.3.2 Nonlinear Klein-Gordon equation in the nonrelativistic limit regime

The nonlinear Klein-Gordon equation (KGE) in d dimensions ($d = 1, 2, 3$) reads

$$\frac{\hbar^2}{mc^2}\partial_{tt}u(\mathbf{x},t) - \frac{\hbar^2}{m}\Delta u + mc^2 u + f(u) = 0, \quad \mathbf{x} \in \mathbb{R}^d, \ t > 0, \tag{1.3.6}$$

where t is time, $\mathbf{x}$ is the spatial coordinate, and c and $\hbar$ denote the speed of light and Plank constant, respectively. With the dimensionless variables: $t \to \frac{\hbar}{m\varepsilon^2 c^2}t$ and $\mathbf{x} \to \frac{\hbar}{m\varepsilon c}\mathbf{x}$, the KGE (1.3.6) takes the following non-dimensional form [10,75–77,81,104]:

$$\varepsilon^2\partial_{tt}u(\mathbf{x},t) - \Delta u(\mathbf{x},t) + \frac{1}{\varepsilon^2}u(\mathbf{x},t) + f(u(\mathbf{x},t)) = 0, \quad \mathbf{x} \in \mathbb{R}^d, \ t > 0, \tag{1.3.7a}$$

with initial conditions:

$$u(\mathbf{x},0) = \phi_1(\mathbf{x}), \qquad \partial_t u(\mathbf{x},0) = \frac{1}{\varepsilon^2}\phi_2(\mathbf{x}), \qquad \mathbf{x} \in \mathbb{R}^d. \tag{1.3.7b}$$

Here the dimensionless parameter $0 < \varepsilon \leq 1$ is inversely proportional to the speed of light c. The given initial data ϕ_1, ϕ_2 and the unknown $u := u(\mathbf{x}, t)$ are complex valued scalar functions. $f(u) : \mathbb{C} \to \mathbb{C}$ describing the nonlinear interaction is a given *gauge invariant* nonlinearity which is independent of ε and satisfies [43, 75–77, 89]

$$f(\mathrm{e}^{is}u) = \mathrm{e}^{is}f(u), \qquad \forall s \in \mathbb{R}. \tag{1.3.8}$$

Similarly as before, when everything is real, the condition (1.3.8) is not necessary. Thus (1.3.7) includes the classical KGE with the solution u real-valued as a special case [24, 38, 80, 93, 96, 99, 102]. In most applications and theoretical investigations in literatures [10, 21, 43, 47–50, 73, 75–77, 80, 87, 93, 96, 98], $f(u)$ is taken as the *pure power* nonlinearity, i.e.

$$f(u) = g(|u|^2)u, \text{ with } g(\rho) = \lambda\rho^p \text{ for some } \lambda \in \mathbb{R}, \ p \in \mathbb{N}_0 := \mathbb{N} \cup \{0\}. \tag{1.3.9}$$

The KGE is also known as the relativistic version of the Schrödinger equation and used to describe the motion of a spinless particle; see, e.g. [32, 89] for its derivation. The KGE (1.3.7) is time symmetry or time reversible, i.e. with $t \to -t$, $u(x, -t)$ is still the solution of the KGE (1.3.7).

When $\varepsilon > 0$ in (1.3.7) is fixed, for example $\varepsilon = 1$, which is corresponding to the $O(1)$-speed of light, i.e. the relativistic regime, the KGE (1.3.7) has been studied extensively in both analytical and numerical aspects. For analytical part, the global existence of solutions to the Cauchy problem was considered and well-established in [19, 21, 63, 71, 96]. Along the numerical aspect, many numerical schemes such as finite difference time domain methods, and the finite difference integrators with finite element or spectral discretization in space have been proposed in literatures [1, 24, 33, 38, 74, 99, 103]. Comparisons between these numerical methods in this regime have been given in [10, 67].

When $0 < \varepsilon \ll 1$ in (1.3.7), which is corresponding to the speed of light going to infinity and is known as the nonrelativistic limit regime, recent studies [10, 75–77, 81, 104] show that the solution of the KGE (1.3.7) propagates waves

with wavelength of $O(\varepsilon^2)$ and $O(1)$ in time and in space, respectively. Thus, the solution has high oscillations in time when $0 < \varepsilon \ll 1$. The highly oscillatory nature in time causes severe numerical burdens, making the computation in the nonrelativistic limit regime extremely challenging. Even for the stable numerical discretizations (or under stability restrictions on meshing strategies), the approximations may come out completely wrong unless the temporal oscillation is fully resolved numerically. Thus, developing and analyzing numerical methods for solving the KGE (1.3.7) with the allowance of step size as large as possible become a main and hot topic in the numerical study of KGE in the nonrelativistic limit regime.

1.3.3 Klein-Gordon-Zakharov system in the high-plasma-frequency and subsonic limit regime

The d-dimensional ($d = 1, 2, 3$) Klein-Gordon-Zakharov (KGZ) system for describing interaction between Langmuir waves and ion sound waves in plasma [20, 35, 78, 100] reads

$$\partial_{tt}\psi(\mathbf{x}, t) + \omega^2\psi - \gamma_{ee}\nu^2\nabla(\nabla \cdot \psi) + c_l^2\nabla \times \nabla \times \psi = -\frac{\omega^2}{c_0}\phi\psi, \tag{1.3.10a}$$

$$\partial_{tt}\phi(\mathbf{x}, t) - c_s^2\Delta\phi = \frac{\varepsilon_0}{2M}\Delta|\psi|^2, \quad \mathbf{x} \in \mathbb{R}^d, \ t > 0, \tag{1.3.10b}$$

where $\psi(\cdot, t) : \mathbb{R}^d \to \mathbb{R}^d$ is the electric field, $\phi(\cdot, t) : \mathbb{R}^d \to \mathbb{R}$ is the ion density fluctuation from the constant equilibrium $c_0 > 0$, ω denotes the plasma frequency, γ_{ee} is the electron heat ratio, ν denotes the thermal velocity, c_l is the speed of light, c_s is the ion sound speed, ε_0 is the vacuum dielectric constant and M is the ion mass. The physical parameters in details satisfy

$$\omega^2 = \frac{c_0 e^2}{m\varepsilon_0}, \quad \nu = \frac{\kappa T_e}{m}, \quad c_s^2 = \frac{\kappa(\gamma_{ie}T_e + \gamma_{ii}T_i)}{M}, \quad \gamma_{ie} = 1, \quad \gamma_{ee} = \gamma_{ii} = 3,$$

with e and m denote the eletron charge and mass, respectively, κ is the Boltzmann constant, T_e and T_i are the electron and ion temperatures, M is the ion mass, γ_{ie} and γ_{ii} are the heat ratios of the electrons and the ions. The KGZ system is derived from the Euler equations for the electrons and ions, coupled with the Maxwell equation for

the electric field [100, 108]. With a dimensionless parameter $\varepsilon > 0$, let the rescaling in (1.3.10) be

$$\psi(\mathbf{x},t) \to \sqrt{\frac{kT_e c_0}{\varepsilon_0 c^2}}\psi\left(\frac{\omega\mathbf{x}}{\varepsilon\nu}, \frac{\omega t}{\varepsilon^2}\right), \qquad \phi(\mathbf{x},t) \to \frac{c_0}{\varepsilon^2}\phi\left(\frac{\omega\mathbf{x}}{\varepsilon\nu}, \frac{\omega t}{\varepsilon^2}\right),$$

and denote $\gamma = \sqrt{\frac{m(\gamma_{ie}T_e+\gamma_{ii}T_i)}{MT_e}}$, then we get the dimensionless form

$$\begin{aligned}
&\varepsilon^2\partial_{tt}\psi(\mathbf{x},t) - 3\nabla(\nabla\cdot\psi) + \left(\frac{c_l}{v}\right)^2 \nabla\times\nabla\times\psi + \frac{1}{\varepsilon^2}\psi = -\phi\psi,\\
&\gamma^2\partial_{tt}\phi(\mathbf{x},t) - \Delta\phi = \frac{T_e}{2(\gamma_{ie}T_e+\gamma_{ii}T_i)}\Delta|\psi|^2, \quad \mathbf{x}\in\mathbb{R}^d,\ t>0.
\end{aligned}$$

Furthermore, let

$$\psi \to \sqrt{\frac{T_e}{2(\gamma_{ie}T_e+\gamma_{ii}T_i)}}\,\psi, \quad \text{and notice} \quad \nabla\times(\nabla\times\psi) = \nabla(\nabla\cdot\psi) - \Delta\psi,$$

with $\frac{c_l}{\nu} = O(1)$ [78], one considers the following simplified scalar dimensionless KGE system [78, 79, 84, 105]:

$$\varepsilon^2\partial_{tt}\psi(\mathbf{x},t) - \Delta\psi(\mathbf{x},t) + \frac{1}{\varepsilon^2}\psi(\mathbf{x},t) + \psi(\mathbf{x},t)\phi(\mathbf{x},t) = 0, \tag{1.3.11}$$

$$\gamma^2\partial_{tt}\phi(\mathbf{x},t) - \Delta\phi(\mathbf{x},t) - \Delta\left(\psi^2(\mathbf{x},t)\right) = 0, \qquad \mathbf{x}\in\mathbb{R}^d, \quad t>0, \tag{1.3.12}$$

with initial conditions

$$\psi(\mathbf{x},0) = \psi^{(0)}(\mathbf{x}),\ \partial_t\psi(\mathbf{x},0) = \psi^{(1)}(\mathbf{x}),\ \phi(\mathbf{x},0) = \phi^{(0)}(\mathbf{x}),\ \partial_t\phi(\mathbf{x},0) = \phi^{(1)}(\mathbf{x}). \tag{1.3.13}$$

Here, the real-valued scalar functions $\psi = \psi(\mathbf{x},t)$ and $\phi = \phi(\mathbf{x},t)$ are the fast time scale component of electric field raised by electrons and the derivation of ion density from its equilibrium, respectively; $0 < \varepsilon \le 1$ and $0 < \gamma \le 1$ are two dimensionless parameters which are inversely proportional to the plasma frequency and speed of sound, respectively.

For fixed $\varepsilon = \varepsilon_0 > 0$ and $\gamma = \gamma_0 > 0$, i.e. $O(1)$-plasma frequency and speed of sound regime, the above KGZ system (1.3.11)-(1.3.12) has been well-studied both analytically and numerically [84, 105]. For either $\varepsilon \to 0$ which is corresponding

to the high-plasma-frequency limit regime, or $(\varepsilon, \gamma) \to 0$ under $\varepsilon \lesssim \gamma$, which is corresponding to the simultaneous high-plasma-frequency and subsonic limit regime, the solution of the KGZ system becomes highly oscillatory in time, which makes the analysis and computation complicated and challenging.

1.4 Purpose and outline of the thesis

The purpose of this study is to propose and analyze efficient and accurate numerical methods for solving the mentioned highly oscillatory problems.

The following chapters are organized as follows. Chapter 2 is devoted to study the HODEs (1.3.1). Existing numerical integrators, namely finite difference integrators and exponential wave integrators (EWIs), are firstly reviewed to understand the sever restrictions on the time steps of the numerical methods for resolving the high oscillations and the numerical burden caused by it. To overcome the difficulty, two multiscale decompositions based on the frequency or frequency and amplitude are derived for the HODEs. Based on the decomposed systems, two multiscale time integrators (MTIs) are then proposed and analyzed to solve the HODEs, where the rigorous error estimates and extensive numerical results show that the MTIs are uniformly accurate and the time steps can be chosen despite of the oscillations. The result in Chapter 2 is also the fundament of studies in subsequent chapters.

Chapters 3 and 4 consider the KGE (1.3.7) in the nonrelativistic limit regime with the parameter $0 < \varepsilon \leq 1$. In Chapter 3, reviews on existing numerical methods including finite difference time domain (FDTD) methods and an EWI with Gautschi's quadratue Fourier pseudospectral (EWI-GFP) method are firstly listed to show the temporal error bounds of the two methods are $O(\tau^2/\varepsilon^6)$ and $O(\tau^2/\varepsilon^4)$, respectively, where τ denotes the time step. Then another classical numerical method namely the time-splitting Fourier pseudospectral (TSFP) method is proposed for solving the KGE by first rewriting the KGE into a first order system and then applying the operator splitting technique. Based on a vital observation that the TSFP is

equivalent to a Deulfhard-type EWI pseudospectral, rigorous and optimal error estimate of the TSFP method is obtained in regime $\varepsilon = O(1)$. Extensive numerical studies in the nonrelativistic limit regime show that the temporal error bound of the TSFP is $O(\tau^2/\varepsilon^2)$ as $0 < \varepsilon \ll 1$, which indicates TSFP is the optimum among all classical methods towards discretizating KGE directly. To further release the ε dependence in temporal error, in Chapter 4, a multiscale time integrator Fourier pseudospectral (MTI-FP) is proposed based on a multiscale decomposition by frequency to the KGE. The method is to first adapt the Fourier spectral method for spatial discretization and then apply the EWI for integrating second-order highly oscillating ODEs decomposed from the original problem. Rigorous error estimate of the MTI-FP for the KGE is established in energy space which show that MTI-FP is uniformly accurate for all $\varepsilon \in (0, 1]$, and optimally in space with spectral convergence rate, and uniformly in time with linear convergence rate for $\varepsilon \in (0, 1]$ and optimally with quadratic convergence rate in the regimes when either $\varepsilon = O(1)$ or $0 < \varepsilon \leq \tau$.

In Chapter 5, we apply the proposed EWIs and MTI method to solve the KGZ system in highly oscillatory regimes. To the end of this chapter, a Gautschi-type EWI sine pseudospectral method and a Deulhard-type sine pseudospectral method are proposed to solve the KGZ under the simultaneous high-plasma-frequency and subsonic limit regime. A MTI sine pseudospectral method is proposed to solve the KGZ system under high-plasma-frequency limit regime. Numerical results show that the performance of these methods are very much similar to those for KGE.

In Chapter 6, conclusions are drawn and some possible future studies are discussed.

Throughout this thesis, we adopt the notation $A \lesssim B$ to represent that there exists a generic constant $C > 0$, which is independent of τ (or n), h and ε, such that $|A| \leq CB$.

Chapter 2

For highly oscillatory second order differential equations

2.1 Introduction

This chapter considers the highly oscillatory second order differential equations as stated in Section 1.3.1,

$$\begin{cases} \varepsilon^2 \ddot{\mathbf{y}}(t) + A\mathbf{y}(t) + \frac{1}{\varepsilon^2}\mathbf{y}(t) + \mathbf{f}\left(\mathbf{y}(t)\right) = 0, \quad t > 0, \\ \mathbf{y}(0) = \Phi_1, \quad \dot{\mathbf{y}}(0) = \frac{\Phi_2}{\varepsilon^2}, \end{cases} \tag{2.1.1}$$

where t is time, $\mathbf{y} := \mathbf{y}(t) = (y_1(t), \ldots, y_d(t))^T \in \mathbb{C}^d$ is a complex-valued vector function in d-dimension, $\dot{\mathbf{y}}$ and $\ddot{\mathbf{y}}$ denote the first and second order derivatives of $\mathbf{y}$, respectively, $0 < \varepsilon \leq 1$ is a dimensionless parameter which can be very small in some limit regimes, $A \in \mathbb{R}^{d\times d}$ is a symmetric nonnegative definite matrix, $\Phi_1,\ \Phi_2 \in \mathbb{C}^d$ are two given initial data at $O(1)$ in terms of $0 < \varepsilon \ll 1$, and $\mathbf{f}(\mathbf{y}) = (f_1(\mathbf{y}), \ldots, f_d(\mathbf{y}))^T : \mathbb{C}^d \to \mathbb{C}^d$ is independent of ε and satisfies the *gauge invariance*

$$\mathbf{f}(\mathrm{e}^{is}\mathbf{y}) = \mathrm{e}^{is}\mathbf{f}(\mathbf{y}), \qquad \forall s \in \mathbb{R}, \tag{2.1.2}$$

in case $\mathbf{y}$ is complex valued.

The solution to (2.1.1) propagates high oscillatory waves with wavelength at $O(\varepsilon^2)$ and amplitude at $O(1)$. To illustrate this, Fig. 2.1 shows the solutions of

(2.1.1) with $d = 2$, $f_1(y_1, y_2) = y_1^2 y_2$, $f_2(y_1, y_2) = y_2^2 y_1$, $A = \mathrm{diag}(2, 2)$, $\Phi_1 = (1, 0.5)^T$ and $\Phi_2 = (1, 2)^T$ for different ε. The highly oscillatory nature of solutions to (2.1.1) causes severe burdens in practical computation, making the numerical approximation extremely challenging and costly in the regime of $0 < \varepsilon \ll 1$.

For the global well-posedness of the model problem (2.1.1), we refer to [58, 59]. For simplicity of notation, we will present our methods and comparison for (2.1.1) in its simplest case, i.e. $d = 1$, as

$$\begin{cases} \varepsilon^2 \ddot{y}(t) + \left(\alpha + \dfrac{1}{\varepsilon^2}\right) y(t) + f\left(y(t)\right) = 0, \quad t > 0, \\ y(0) = \phi_1, \quad \dot{y}(0) = \dfrac{\phi_2}{\varepsilon^2}, \end{cases} \tag{2.1.3}$$

where $y = y(t) \in \mathbb{C}$ is a complex-valued scalar function, $\alpha \geq 0$ is a real constant, $\phi_1,\ \phi_2 \in \mathbb{C}$, and $f(y) :\ \mathbb{C} \to \mathbb{C}$. In particular, in many applications [47–50, 76, 77, 87, 93, 96], $f(y)$ is taken as the *pure power* nonlinearity as

$$f(y) = g(|y|^2)y, \text{ with } g(\rho) = \lambda \rho^p \text{ for some } \lambda \in \mathbb{R},\ p \in \mathbb{N}_0 := \mathbb{N} \cup \{0\}. \tag{2.1.4}$$

In addition, if f is taken as the pure power nonlinearity (2.1.4), it is easy to see that (2.1.3) conserves the Hamiltonian or total energy, which is given by

$$\begin{aligned} E(t) &:= \varepsilon^2 \left|\dot{y}(t)\right|^2 + \left(\alpha + \frac{1}{\varepsilon^2}\right) |y(t)|^2 + F\left(|y(t)|^2\right) \\ &\equiv \frac{1}{\varepsilon^2} |\phi_2|^2 + \left(\alpha + \frac{1}{\varepsilon^2}\right) |\phi_1|^2 + F\left(|\phi_1|^2\right) := E(0), \quad t \geq 0, \end{aligned} \tag{2.1.5}$$

with $F(\rho) = \int_0^\rho g(\rho')d\rho'$. Although the numerical methods and their error estimates in this paper are for the model problem (2.1.3), they can be easily extended to solve the problem (2.1.1).

In fact, for existing numerical methods to solve the problem (2.1.3), in order to capture 'correctly' the oscillatory solutions, one has to restrict the time step τ in a numerical integrator to be quite small when $0 < \varepsilon \ll 1$. For instance, as suggested by the rigorous results in [10], for the frequently used finite difference (FD) time integrators in the literature [10, 38, 99], such as energy conservative, semi-implicit and explicit ones, which will be presented and reviewed in Section 2.2, the

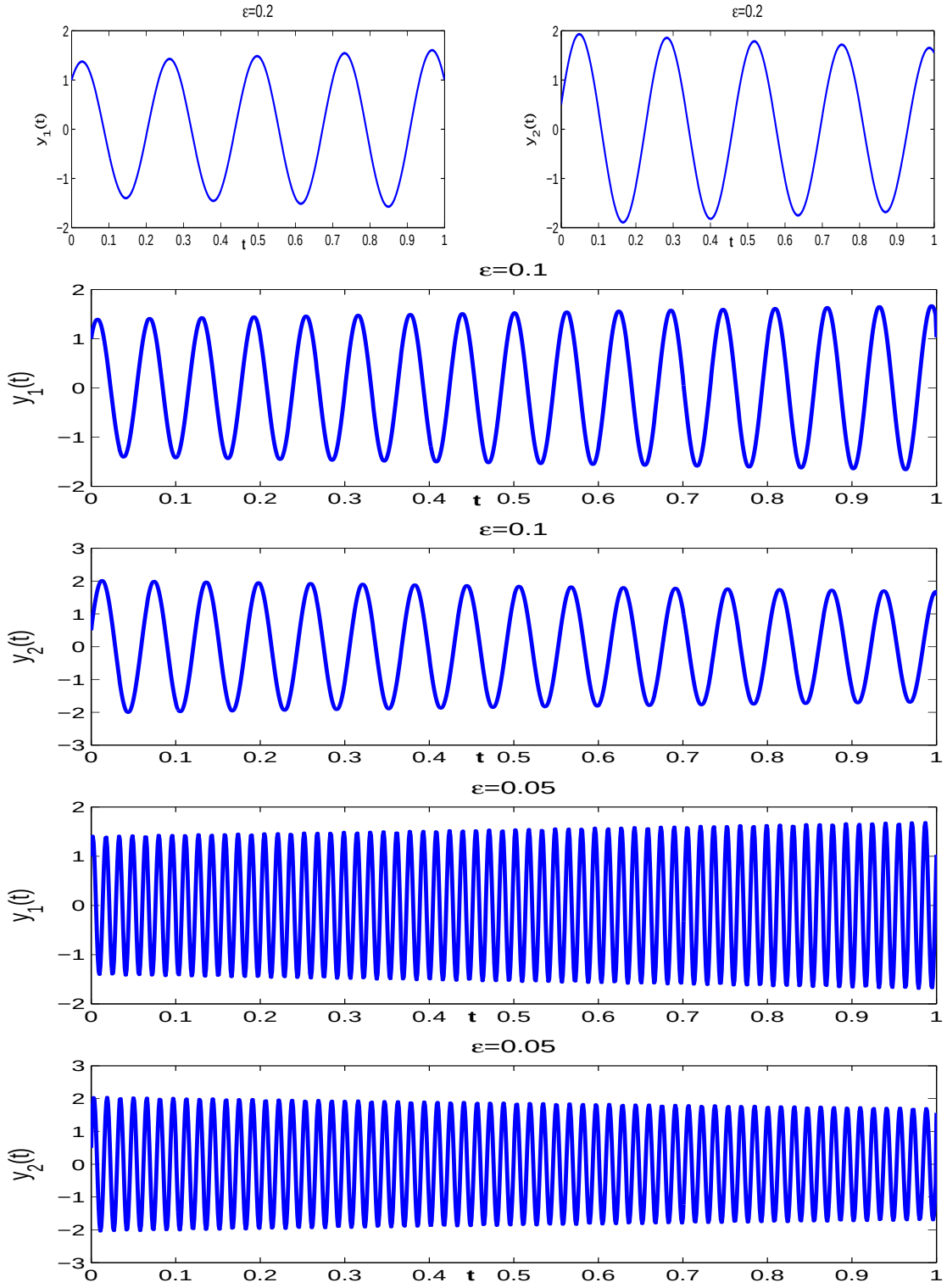

Figure 2.1: Time evolution of the solutions of (2.1.1) with $d = 2$ for different ε.

meshing strategy requirement (or ε-scalability) is $\tau = O(\varepsilon^3)$ [10]. Also, a class of trigonometric integrators which solves the linear part of (2.1.3) exactly [10, 44, 54, 55, 57, 91], namely the exponential wave integrators (EWIs), require $\tau = O(\varepsilon^2)$ for nonlinear problems [10]. In view of that the solutions to (2.1.3) are highly oscillatory with wavelength at $O(\varepsilon^2)$, the EWIs could be viewed as the optimal one among all the methods which integrate the oscillatory problem (2.1.3) directly. Section 2.3 will give a detailed review on the work of EWIs.

The rest and the main part of this chapter is going to propose and analyze multiscale time integrators (MTIs) to the problem (2.1.3), which will converge uniformly for $\varepsilon \in (0, 1]$ and thus possess much better improved ε-scalability than those classical FD and EWI methods in the regime $0 < \varepsilon \ll 1$, by taking into account the sophisticated multiscale structures (see details in (2.5)) in frequency and/or amplitude of the solutions to (2.1.3). The new proposed methods, at each time interval, adopt an ansatz same as the one used in [76, 77], then carry out multiscale decompositions of the solution to (2.1.3) by either frequency or frequency and amplitude, and obtain a coupled equations for two $O(1)$-in-amplitude non-oscillatory components and an $O(\varepsilon^2)$-in-amplitude oscillatory component. The coupled equations are then discretized by an explicit EWI method [54, 55, 57] with proper chosen transmission conditions between different time intervals. Our methods are different from the classical way of applying the modulated Fourier expansion methods for oscillatory ODEs [27, 29, 31] in terms of not only considering the leading order terms but also solving the equation of the remainder which is $O(\varepsilon^2)$ in the pure power nonlinear case so as to design a uniformly convergent integrator for any $0 < \varepsilon \leq 1$. For the MTIs, two independent error bounds at $O(\tau^2/\varepsilon^2)$ and $O(\varepsilon^2)$ for $\varepsilon \in (0, 1]$ are rigorously established by using the energy method and multiscale analysis [5, 8, 10]. These two error bounds immediately suggest that the MTIs converge uniformly with linear convergence rate at $O(\tau)$ for $\varepsilon \in (0, 1]$ and optimally with quadratic convergence rate at $O(\tau^2)$ in the regimes when either $\varepsilon = O(1)$ or $0 < \varepsilon \leq \tau$. Thus, the MTIs offer compelling advantages over those FD and EWI methods for the problem

(2.1.3), especially when $0 < \varepsilon \ll 1$. Extensions of the proposed MTIs from solving the power nonlinearity case to the general nonlinearity (2.1.2) are made in Sections 2.6. Numerical results are reported in Section 2.7.

2.2 Finite difference methods

Let $\tau = \Delta t > 0$ be the step size, and denote time steps by $t_n = n\tau$ for $n = 0, 1, \ldots$. For a sequence $\{y^n\}$, define the standard finite difference operators as

$$\delta_t^+ y^n := \frac{y^{n+1} - y^n}{\tau}, \quad \delta_t^- y^n := \frac{y^n - y^{n-1}}{\tau}, \quad \delta_t^2 y^n := \frac{y^{n+1} - 2y^n + y^{n-1}}{\tau^2}.$$

Then a conservative Crank-Nicolson finite difference (CNFD) integrator for solving (2.1.3) reads

$$\varepsilon^2 \delta_t^2 y^n + \left(\alpha + \frac{1}{\varepsilon^2}\right) \frac{y^{n+1} + y^{n-1}}{2} + G\left(y^{n+1}, y^{n-1}\right) = 0, \quad n = 1, 2, \ldots, \tag{2.2.1}$$

where

$$G\left(y^{n+1}, y^{n-1}\right) := \frac{F\left(|y^{n+1}|^2\right) - F\left(|y^{n-1}|^2\right)}{|y^{n+1}|^2 - |y^{n-1}|^2} \cdot \frac{y^{n+1} + y^{n-1}}{2}.$$

A semi-implicit finite difference (SIFD) integrator reads

$$\varepsilon^2 \delta_t^2 y^n + \left(\alpha + \frac{1}{\varepsilon^2}\right) \frac{y^{n+1} + y^{n-1}}{2} + g\left(|y^n|^2\right) y^n = 0, \quad n = 1, 2, \ldots. \tag{2.2.2}$$

An explicit finite difference (EXFD) integrator, which is known as the famous Störmer-Verlet or leap-frog method [55, 57, 73], reads

$$\varepsilon^2 \delta_t^2 y^n + \left(\alpha + \frac{1}{\varepsilon^2}\right) y^n + g\left(|y^n|^2\right) y^n = 0, \quad n = 1, 2, \ldots. \tag{2.2.3}$$

Here the initial conditions are discretized as

$$y^0 = \phi_1, \quad y^1 = \cos(\omega\tau)\, \phi_1 + \frac{\sin(\omega\tau)}{\varepsilon^2 \omega} \phi_2 - \frac{\tau \sin(\omega\tau)}{2\varepsilon^2 \omega} g\left(|\phi_1|^2\right) \phi_1. \tag{2.2.4}$$

In order that the methods CNFD and SIFD are stable uniformly in the regime $0 < \varepsilon \ll 1$, here y^1 is computed according to the exponential wave integrator (2.3.5)

introduced later with $n = 0$ instead of the classical way below. In fact, if one adapts the usual way to obtain y^1 as

$$y^1 = \phi_1 + \frac{\tau\phi_2}{\varepsilon^2} - \frac{\tau^2}{2\varepsilon^2}\left[\left(\alpha + \frac{1}{\varepsilon^2}\right)\phi_1 + g\left(|\phi_1|^2\right)\phi_1\right], \tag{2.2.5}$$

our numerical results suggest that it would cause severe instability issue when $\tau = O(1)$ and $0 < \varepsilon \ll 1$. Thus we adopt (2.2.4) instead of (2.2.5) to discretize the initial data since we want to consider $0 < \varepsilon \leq 1$, especially $0 < \varepsilon \ll 1$.

For the above FD integrators, all are time symmetric. CNFD is implicit, SIFD is implicit but can be solved very efficiently, and EXFD is explicit. For CNFD, it conserves the following energy in the discretized level, i.e.

$$\begin{aligned} E^n &:= \varepsilon^2\left|\delta_t^+ y^n\right|^2 + \left(\alpha + \frac{1}{\varepsilon^2}\right)\frac{|y^{n+1}|^2 + |y^n|^2}{2} + \frac{F\left(|y^{n+1}|^2\right) + F\left(|y^n|^2\right)}{2} \\ &\equiv E^0, \qquad n = 0, 1, \ldots \end{aligned}$$

However, at each step, a fully nonlinear equation needs to be solved, which might be quite time-consuming. In fact, if the nonlinear equation is not solved very accurately, then the above quantity will not be conserved in practical computation [7]. Thus CNFD is usually not adopted in practical computation, especially for partial differential equations in high dimensions. EXFD is very popular and powerful when $\varepsilon = O(1)$, however, it suffers from a server stability constraint $\tau \lesssim \varepsilon^2$ when $0 < \varepsilon \ll 1$ [10].

For the above finite difference integrators, defining the error functions as

$$e^n := y(t_n) - y^n, \quad \dot{e}^n := \dot{y}(t_n) - \dot{y}^n, \tag{2.2.6}$$

we have the following convergence result, providing the exact solution $y(t)$ to (2.1.3) satisfying

$$f \in C^3(\mathbb{R}), \quad y \in C^4(0,T), \quad \left\|\frac{d^m}{dt^m}y\right\|_{L^\infty(0,T)} \lesssim \frac{1}{\varepsilon^{2m}}, \quad m = 0, 1, 2, 3, 4, \tag{2.2.7}$$

where $0 < T < T^*$ with T^* denotes the maximum existence time of the solution. The proof proceed in analogous lines as the technique used in [10, Theorem 2 and 5], and we omit the details here for brevity.

Theorem 2.2.1 (Error bounds of FD). *For the CNFD (2.2.1), SIFD (2.2.2) and EXFD (2.2.3), under the assumption (2.2.7), there exists a constant $\tau_0 > 0$ independent of ε and n, such that for any $0 < \varepsilon \leq 1$ when $\tau \leq \tau_0 \varepsilon^3$, we have*

$$|e^n| + \varepsilon^2 |\dot{e}^n| \lesssim \frac{\tau^2}{\varepsilon^6}, \qquad 0 \leq n \leq \frac{T}{\tau}, \qquad 0 < \tau \leq \tau_0. \tag{2.2.8}$$

2.3 Exponential wave integrators

We rewrite the solution of (2.1.3) near $t = t_n$ by using the variation-of-constant formula, i.e.

$$y(t_n + s) = \cos(\omega s) y(t_n) + \frac{\sin(\omega s)}{\omega} \dot{y}(t_n) - \int_0^s \frac{\sin(\omega(s-\theta))}{\varepsilon^2 \omega} f^n(\theta) d\theta, \tag{2.3.1}$$

where $f^n(\theta) := f(y(t_n + \theta))$. Taking $s = \pm\tau$ in (2.3.1) and then summing them up, we have

$$y(t_{n+1}) + y(t_{n-1}) = 2\cos(\omega\tau) y(t_n) - \int_0^\tau \frac{\sin(\omega(\tau-\theta))}{\varepsilon^2 \omega} \left[f^n(\theta) + f^n(-\theta) \right] d\theta. \tag{2.3.2}$$

Then exponential wave integrators (EWIs) approximate the integral term by proper quadratures. For example, if a Gautschi's type quadrature [10, 45, 54, 57] is applied, one can end up with the following EWI in Gautschi's type (EWI-G). The stabilized EWI-G [10] reads

$$y^{n+1} = \begin{cases} -y^{n-1} + 2\cos\left(\omega^n \tau\right) y^n - 2G^n, & n \geq 1, \\ \cos\left(\omega^0 \tau\right) \phi_1 + \dfrac{\sin\left(\omega^0 \tau\right)}{\varepsilon^2 \omega^0} \phi_2 - G^0, & n = 0, \end{cases} \tag{2.3.3}$$

where

$$G^n = \frac{1 - \cos\left(\omega^n \tau\right)}{\varepsilon^2 (\omega^n)^2} \left[g\left(|y^n|^2\right) y^n - \alpha^n y^n \right], \qquad n \geq 0,$$
$$\omega^n = \frac{\sqrt{1 + \varepsilon^2(\alpha + \alpha^n)}}{\varepsilon^2}, \quad \alpha^n = \max\left\{ \alpha^{n-1}, g\left(|y^n|^2\right) \right\}, \text{ with } \alpha^{-1} = 0.$$

Here a linear stabilizing term with stabilizing constant α^n is introduced so that the method is unconditionally stable [10, Theorem 6]. Of course, one can use other

ways to filter oscillation in the resonance regime [55, 57–59, 91] instead of the above linear stabilizing term. In addition, if the approximation to $\dot{y}(t_n)$ is of interest, for example, evaluating the discrete energy, one can use

$$\dot{y}^{n+1} = \begin{cases} \dot{y}^{n-1} - 2\omega \sin(\omega\tau) y^n - 2\dfrac{\sin(\omega\tau)}{\varepsilon^2\omega} g(|y^n|^2) y^n, & n \geq 1, \\ -\omega \sin(\omega\tau) y^0 + \cos(\omega\tau)\dot{y}^0 - \dfrac{\sin(\omega\tau)}{\varepsilon^2\omega} g(|y^0|^2) y^0, & n = 0, \end{cases} \tag{2.3.4}$$

which is derived similarly from the differentiation of (2.3.1) with respect to s and then taking $s = \pm\tau$.

On the other hand, if the standard trapezoidal rule is applied to approximate the integral in (2.3.2), then one can end up with the following EWI in Deuflhard's type (EWI-D) [36, 55],

$$y^{n+1} = \begin{cases} -y^{n-1} + 2\cos(\omega\tau)\, y^n - 2D^n, & n \geq 1, \\ \cos(\omega\tau)\, \phi_1 + \dfrac{\sin(\omega\tau)}{\varepsilon^2\omega}\phi_2 - D^0, & n = 0, \end{cases} \tag{2.3.5}$$

where,

$$\omega = \frac{\sqrt{1+\alpha\varepsilon^2}}{\varepsilon^2}, \quad D^n = \frac{\tau \sin(\omega\tau)}{2\varepsilon^2\omega} g\left(|y^n|^2\right) y^n, \quad n \geq 0.$$

Similarly, to approximate $\dot{y}(t_n)$, we can use the scheme (2.3.4).

Generalizations of the above two EWIs based on (2.3.1) are the mollified impulse methods or EWIs with filters [44, 54, 55, 57], which have been well-developed for solving problem (1.3.3) with a uniform convergence and good energy preserving properties. Now with a stronger nonlinearity in the problem (2.1.3), the scheme reads

$$\begin{cases} y^{n+1} = \cos(\omega\tau) y^n + \dfrac{\sin(\omega\tau)}{\omega}\dot{y}^n + \dfrac{\tau^2}{2\varepsilon^2}\psi(\omega\tau) f\left(\phi(\omega\tau) y^n\right), \\ \dot{y}^{n+1} = -\omega \sin(\omega\tau) y^n + \cos(\omega\tau)\dot{y}^n + \dfrac{\tau}{2\varepsilon^2}\Big[\psi_0(\omega\tau) f\left(\phi(\omega\tau) y^n\right) \\ \qquad\qquad + \psi_1(\omega\tau) f\left(\phi(\omega\tau) y^{n+1}\right)\Big], \end{cases} \tag{2.3.6}$$

where ψ, ϕ, ψ_0 and ψ_1 are known as the filters under some consistent conditions [55, 57]. For example, two popular sets of filters mentioned in [55, 57] are chosen as

$$\psi_0(\rho) = \cos(\rho)\psi_1(\rho), \qquad \psi_1(\rho) = \frac{\psi(\rho)}{\operatorname{sinc}(\rho)}, \tag{2.3.7}$$

with

$$\psi(\rho) = \phi(\rho)\mathrm{sinc}(\rho), \qquad \phi(\rho) = \mathrm{sinc}(\rho), \tag{2.3.8}$$

or

$$\psi(\rho) = \mathrm{sinc}^2(\rho), \qquad \phi(\rho) = 1, \tag{2.3.9}$$

where $\mathrm{sinc}(\rho) = \sin(\rho)/\rho$ for $\rho \in \mathbb{R}$. Hereafter, we refer to the EWIs (2.3.6)-(2.3.7) with filters (2.3.8) as EWI-F1, and (2.3.6)-(2.3.7) with filters (2.3.9) as EWI-F2.

For convergence results of the EWIs, assuming that the solution of (2.1.3) satisfies

$$f \in C^3(\mathbb{R}), \quad y \in C^2(0,T), \quad \left\| \frac{d^m}{dt^m} y \right\|_{L^\infty(0,T)} \lesssim \frac{1}{\varepsilon^{2m}}, \quad m = 0, 1, 2, \tag{2.3.10}$$

for $0 < T < T^*$ with T^* the maximum existence time, we have the following theorem. The proof proceed in analogous lines as the technique used in [10, Theorem 9] towards the estimates in time or [54] and we omit the details here for brevity.

Theorem 2.3.1 (Error bounds of EWIs)**.** *For the EWI-G (2.3.3), EWI-D (2.3.5), EWI-F1 (2.3.8) and EWI-F2 (2.3.9), under the assumption (2.3.10), there exists a constant $\tau_0 > 0$ independent of ε and n, such that for any $0 < \varepsilon \leq 1$ when $0 < \tau \leq \tau_0 \varepsilon^2$,*

$$|e^n| + \varepsilon^2 |\dot{e}^n| \lesssim \frac{\tau^2}{\varepsilon^4}, \qquad 0 \leq n \leq \frac{T}{\tau}. \tag{2.3.11}$$

2.4 Multiscale decompositions

In this section, we present multiscale decompositions for the solution of (2.1.3) on the time interval $[t_n, t_{n+1}]$ with given initial data at $t = t_n$ as

$$y(t_n) = \phi_1^n = O(1), \qquad \dot{y}(t_n) = \frac{\phi_2^n}{\varepsilon^2} = O\left(\frac{1}{\varepsilon^2}\right), \tag{2.4.1}$$

by either frequency or frequency and amplitude.

2.4.1 Multiscale decomposition by frequency (MDF)

Similar to the analytical study of the nonrelativistic limit of the nonlinear Klein-Gordon equation [76,77], we take an ansatz to the solution $y(t) := y(t_n+s)$ of (2.1.3) on the time interval $[t_n, t_{n+1}]$ with (2.4.1) as

$$y(t_n+s) = \mathrm{e}^{is/\varepsilon^2} z_+^n(s) + \mathrm{e}^{-is/\varepsilon^2}\overline{z_-^n}(s) + r^n(s), \qquad 0 \le s \le \tau. \tag{2.4.2}$$

Hereafter, $\bar{z}$ denotes the complex conjugate of a complex-valued function z. Differentiating (2.4.2) with respect to s, we have

$$\dot{y}(t_n+s) = \mathrm{e}^{is/\varepsilon^2}\left[\dot{z}_+^n(s) + \frac{i}{\varepsilon^2} z_+^n(s)\right] + \mathrm{e}^{-is/\varepsilon^2}\left[\overline{\dot{z}_-^n}(s) - \frac{i}{\varepsilon^2}\overline{z_-^n}(s)\right] + \dot{r}^n(s). \tag{2.4.3}$$

Plugging (2.4.2) into (2.1.3), we get

$$\begin{aligned}&\left[2i\dot{z}_+^n(s) + \varepsilon^2\ddot{z}_+^n(s) + \alpha z_+^n(s)\right]\mathrm{e}^{is/\varepsilon^2} + \left[-2i\overline{\dot{z}_-^n}(s) + \varepsilon^2\overline{\ddot{z}_-^n}(s) + \alpha\overline{z_-^n}(s)\right]\mathrm{e}^{-is/\varepsilon^2}\\ &+ \varepsilon^2\ddot{r}^n(s) + \left(\alpha + \frac{1}{\varepsilon^2}\right) r^n(s) + f\left(y(t_n+s)\right) = 0, \quad 0 \le s \le \tau.\end{aligned} \tag{2.4.4}$$

Multiplying the above equation by $\mathrm{e}^{-is/\varepsilon^2}$ and $\mathrm{e}^{is/\varepsilon^2}$, respectively, we can decompose the above equation into a coupled system for two ε^2-frequency waves with the unknowns $z_\pm^n(s)$ and the rest frequency waves with the unknown $r^n(s)$ as

$$\begin{cases} 2i\dot{z}_\pm^n(s) + \varepsilon^2\ddot{z}_\pm^n(s) + \alpha z_\pm^n(s) + f_\pm\left(z_+^n(s), z_-^n(s)\right) = 0, \quad 0 < s \le \tau, \\ \varepsilon^2\ddot{r}^n(s) + \left(\alpha + \dfrac{1}{\varepsilon^2}\right) r^n(s) + f_r\left(z_+^n(s), z_-^n(s), r^n(s); s\right) = 0, \end{cases} \tag{2.4.5}$$

where

$$f_\pm\left(z_+, z_-\right) = \frac{1}{2\pi}\int_0^{2\pi} f\left(z_\pm + \mathrm{e}^{i\theta}\overline{z_\mp}\right) d\theta, \tag{2.4.6}$$

$$f_r\left(z_+, z_-, r; s\right) = f\left(\mathrm{e}^{\frac{is}{\varepsilon^2}} z_+ + \mathrm{e}^{-\frac{is}{\varepsilon^2}}\overline{z_-} + r\right) - f_+\left(z_+, z_-\right)\mathrm{e}^{\frac{is}{\varepsilon^2}} - \overline{f_-}\left(z_+, z_-\right)\mathrm{e}^{-\frac{is}{\varepsilon^2}}. \tag{2.4.7}$$

In order to find proper initial conditions for the above system (2.4.5), setting $s = 0$ in (2.4.2) and (2.4.3), noticing (2.4.1), we obtain

$$\begin{cases} z_+^n(0) + \overline{z_-^n}(0) + r^n(0) = y(t_n) = \phi_1^n, \\ \dfrac{i}{\varepsilon^2}\left[z_+^n(0) - \overline{z_-^n}(0)\right] + \dot{z}_+^n(0) + \overline{\dot{z}_-^n}(0) + \dot{r}^n(0) = \dot{y}(t_n) = \dfrac{\phi_2^n}{\varepsilon^2}. \end{cases} \tag{2.4.8}$$

Now we decompose the above initial data so as to: (i) equate $O\left(\frac{1}{\varepsilon^2}\right)$ and $O(1)$ terms in the second equation of (2.4.8), respectively, and (ii) be well-prepared for the first two equations in (2.4.5) when $0<\varepsilon\ll 1$, i.e. $\dot{z}_+^n(0)$ and $\dot{z}_-^n(0)$ are determined from the first two equations in (2.4.5), respectively, by setting $\varepsilon=0$ and $s=0$ [5,8]:

$$\begin{cases} z_+^n(0)+\overline{z_-^n}(0)=\phi_1^n, \qquad i\left[z_+^n(0)-\overline{z_-^n}(0)\right]=\phi_2^n, \\ 2i\dot{z}_\pm^n(0)+\alpha z_\pm^n(0)+f_\pm\left(z_+^n(0),z_-^n(0)\right)=0, \\ r^n(0)=0, \qquad \dot{r}^n(0)+\dot{z}_+^n(0)+\overline{\dot{z}_-^n}(0)=0. \end{cases} \tag{2.4.9}$$

Solving (2.4.9), we get the initial data for (2.4.5) as

$$\begin{cases} z_+^n(0)=\dfrac{1}{2}\left(\phi_1^n-i\phi_2^n\right), \qquad z_-^n(0)=\dfrac{1}{2}\left(\overline{\phi_1^n}-i\,\overline{\phi_2^n}\right), \\ \dot{z}_\pm^n(0)=\dfrac{i}{2}\left[\alpha z_\pm^n(0)+f_\pm\left(z_+^n(0),z_-^n(0)\right)\right], \\ r^n(0)=0, \qquad \dot{r}^n(0)=-\dot{z}_+^n(0)-\overline{\dot{z}_-^n}(0). \end{cases} \tag{2.4.10}$$

The above decomposition can be called as multiscale decomposition by frequency (MDF). In fact, it can also be regarded as to decompose slow waves at ε^2-wavelength and fast waves at other wavelengths, thus it can also be called as fast-slow frequency decomposition.

Specifically, for pure power nonlinearity, i.e. f satisfies (2.1.4), then the above MDF (2.4.5) collapses to

$$\begin{cases} 2i\dot{z}_\pm^n(s)+\varepsilon^2\ddot{z}_\pm^n(s)+\alpha z_\pm^n(s)+g_\pm\left(|z_+^n(s)|^2,|z_-^n(s)|^2\right)z_\pm^n(s)=0, \\ \varepsilon^2\ddot{r}^n(s)+\left(\alpha+\dfrac{1}{\varepsilon^2}\right)r^n(s)+g_r\left(z_+^n(s),z_-^n(s),r^n(s);s\right)=0, \quad 0<s\le\tau, \end{cases} \tag{2.4.11}$$

where

$$g_\pm\left(\rho_+,\rho_-\right)=\sum_{\langle p_1,p_2,p_3\rangle_0}\lambda\left(\rho_++\rho_-\right)^{p_1}\left(\rho_+\rho_-\right)^{p_2}(\rho_\mp)^{p_3}, \tag{2.4.12}$$

$$\begin{aligned} g_r\left(z_+,z_-,r;s\right)=&\sum_{k=1}^{p}\left(g_k\left(z_+,z_-\right)\mathrm{e}^{i(2k+1)s/\varepsilon^2}+\overline{g_k}\left(z_-,z_+\right)\mathrm{e}^{-i(2k+1)s/\varepsilon^2}\right) \\ &+h\left(z_+,z_-,r;s\right), \end{aligned} \tag{2.4.13}$$

with

$$g_k\left(z_+, z_-\right) = \lambda(z_+)^{k+1}(z_-)^k \sum_{\langle p_1,p_2,p_3\rangle_k} \left(|z_+|^2 + |z_-|^2\right)^{p_1} |z_+|^{2p_2}|z_-|^{2p_2+2p_3}, \quad (2.4.14)$$

$$\begin{aligned} h\left(z_+, z_-, r; s\right) = {} & g\left(|\mathrm{e}^{is/\varepsilon^2} z_+ + \mathrm{e}^{-is/\varepsilon^2}\overline{z_-} + r|^2\right)\left(\mathrm{e}^{is/\varepsilon^2} z_+ + \mathrm{e}^{-is/\varepsilon^2}\overline{z_-} + r\right) \\ & - g\left(|\mathrm{e}^{is/\varepsilon^2} z_+ + \mathrm{e}^{-is/\varepsilon^2}\overline{z_-}|^2\right)\left(\mathrm{e}^{is/\varepsilon^2} z_+ + \mathrm{e}^{-is/\varepsilon^2}\overline{z_-}\right), \end{aligned} \quad (2.4.15)$$

and $\langle p_1, p_2, p_3\rangle_k = \{p_1, p_2, p_3 \in \mathbb{N}_0 \mid p_1 + 2p_2 + p_3 = p - k,\ p_3 = 0, 1\}$ for $k = 0,\ldots,p$.

2.4.2 Multiscale decomposition by frequency and amplitude (MDFA)

Another way to decompose (2.4.4) is to decompose it into a coupled system for two ε^2-frequency waves at $O(1)$-amplitude with the unknowns $z_\pm^n(s)$ and the rest frequency and amplitude waves with the unknown $r^n(s)$ as

$$\begin{cases} 2i\dot{z}_\pm^n(s) + \alpha z_\pm^n(s) + f_\pm\left(z_+^n(s), z_-^n(s)\right) = 0, \qquad 0 < s \le \tau, \\ \varepsilon^2\ddot{r}^n(s) + \left(\alpha + \dfrac{1}{\varepsilon^2}\right) r^n(s) + f_r\left(z_+^n(s), z_-^n(s), r^n(s); s\right) + \varepsilon^2 u^n(s) = 0, \end{cases} \quad (2.4.16)$$

where

$$u^n(s) := \mathrm{e}^{is/\varepsilon^2}\ddot{z}_+^n(s) + \mathrm{e}^{-is/\varepsilon^2}\overline{\ddot{z}_-^n}(s). \quad (2.4.17)$$

Similarly, the initial data (2.4.1) can be decomposed as the following for the coupled ODEs (2.4.16)

$$\begin{cases} z_+^n(0) = \dfrac{1}{2}\left(\phi_1^n - i\phi_2^n\right), \qquad z_-^n(0) = \dfrac{1}{2}\left(\overline{\phi_1^n} - i\,\overline{\phi_2^n}\right), \\ r^n(0) = 0, \qquad \dot{r}^n(0) = -\dot{z}_+^n(0) - \overline{\dot{z}_-^n}(0), \end{cases} \quad (2.4.18)$$

with

$$\dot{z}_\pm^n(0) = \frac{i}{2}\left[\alpha z_\pm^n(0) + f_\pm\left(z_+^n(0), z_-^n(0)\right)\right].$$

In the following, for simplicity of notation, we denote

$$f_\pm^n(s) := f_\pm(z_+^n(s), z_-^n(s)), \quad f_r^n(s) := f_r\left(z_+^n(s), z_-^n(s), r^n(s); s\right). \quad (2.4.19)$$

The above decomposition can be called as multiscale decomposition by frequency and amplitude (MDFA). In fact, it can also be regarded as to decompose large amplitude waves at $O(1)$ and small amplitude waves at $O(\varepsilon^2)$, thus it can also be called as large-small amplitude decomposition.

Similarly, for pure power nonlinearity, i.e. f satisfies (2.1.4), then the above MDFA (2.4.16) collapses to

$$\begin{cases} 2i\dot{z}_{\pm}^n(s) + \alpha z_{\pm}^n(s) + g_{\pm}\left(|z_+^n(s)|^2, |z_-^n(s)|^2\right) z_{\pm}^n(s) = 0, \quad 0 < s \le \tau, \\ \varepsilon^2 \ddot{r}^n(s) + \left(\alpha + \dfrac{1}{\varepsilon^2}\right) r^n(s) + g_r\left(z_+^n(s), z_-^n(s), r^n(s); s\right) + \varepsilon^2 u^n(s) = 0. \end{cases} \tag{2.4.20}$$

After solving the MDF (2.4.5) or (2.4.11) with the initial data (2.4.10), or the MDFA (2.4.16) or (2.4.20) with the initial data (2.4.18), we get $z_{\pm}^n(\tau)$, $\dot{z}_{\pm}^n(\tau)$, $r^n(\tau)$ and $\dot{r}^n(\tau)$. Then we can reconstruct the solution to (2.1.3) at $t = t_{n+1}$ by setting $s = \tau$ in (2.4.2) and (2.4.3), i.e.,

$$\begin{cases} y(t_{n+1}) = \mathrm{e}^{i\tau/\varepsilon^2} z_+^n(\tau) + \mathrm{e}^{-i\tau/\varepsilon^2} \overline{z_-^n}(\tau) + r^n(\tau) := \phi_1^{n+1}, \\ \dot{y}(t_{n+1}) = \dfrac{1}{\varepsilon^2} \phi_2^{n+1}, \end{cases} \tag{2.4.21}$$

with

$$\phi_2^{n+1} := \mathrm{e}^{i\tau/\varepsilon^2}\left[\varepsilon^2 \dot{z}_+^n(\tau) + i z_+^n(\tau)\right] + \mathrm{e}^{-i\tau/\varepsilon^2}\left[\varepsilon^2 \overline{\dot{z}_-^n}(\tau) - i\overline{z_-^n}(\tau)\right] + \varepsilon^2 \dot{r}^n(\tau).$$

2.5 Multiscale time integrators for pure power nonlinearity

Based on the decomposed system in the pure power nonlinearity case, i.e. the MDFA (2.4.20) or MDF (2.4.11), we propose two multiscale time integrators (MTI) for solving (2.1.3), respectively. At each time grid $t = t_n$, we solve the decomposed system (2.4.20) or (2.4.11) by proper integrators within the time interval $[0, \tau]$, and then use (2.4.21) to reconstruct the solution to (2.1.3) at $t = t_{n+1}$.

2.5.1 A multiscale time integrator based on MDFA

Based on the MDFA (2.4.20), a MTI is designed as follows.

An exact integrator for $z_{\pm}^{n}(s)$ in (2.4.20):

Noting from (2.4.12) that $g_{\pm}\left(\rho_{+},\rho_{-}\right)$ is real-valued, similar to [13,14], multiplying the first two equations in (2.4.20) by $\overline{z_{\pm}^{n}}(s)$, respectively, then subtracting from their complex conjugates, we have

$$\left|z_{\pm}^{n}(s)\right| \equiv \left|z_{\pm}^{n}(0)\right|, \qquad 0 \leq s \leq \tau. \tag{2.5.1}$$

Therefore, the equations for $z_{\pm}^{n}(s)$ in (2.4.20) are exactly integrable, i.e.,

$$z_{\pm}^{n}(s) = \mathrm{e}^{is\left[g_{\pm}\left(|z_{+}^{n}(0)|^{2},|z_{-}^{n}(0)|^{2}\right)+\alpha\right]/2} z_{\pm}^{n}(0), \qquad 0 \leq s \leq \tau. \tag{2.5.2}$$

Taking $s=\tau$ in (2.5.2), we get

$$z_{\pm}^{n}(\tau) = \mathrm{e}^{i\tau\left[g_{\pm}\left(|z_{+}^{n}(0)|^{2},|z_{-}^{n}(0)|^{2}\right)+\alpha\right]/2} z_{\pm}^{n}(0). \tag{2.5.3}$$

Differentiating (2.5.2) with respect to s and then taking $s=0$ or τ, we get

$$\begin{cases} \dot{z}_{\pm}^{n}(\tau) = \dfrac{i}{2}\left[g_{\pm}\left(|z_{+}^{n}(0)|^{2},|z_{-}^{n}(0)|^{2}\right)+\alpha\right] z_{\pm}^{n}(\tau), \\ \ddot{z}_{\pm}^{n}(0) = -\dfrac{1}{4}\left[g_{\pm}\left(|z_{+}^{n}(0)|^{2},|z_{-}^{n}(0)|^{2}\right)+\alpha\right]^{2} z_{\pm}^{n}(0), \\ \ddot{z}_{\pm}^{n}(\tau) = -\dfrac{1}{4}\left[g_{\pm}\left(|z_{+}^{n}(0)|^{2},|z_{-}^{n}(0)|^{2}\right)+\alpha\right]^{2} z_{\pm}^{n}(\tau). \end{cases} \tag{2.5.4}$$

An EWI for $r^{n}(s)$ in (2.4.20):

For the third equation in (2.4.20), we apply the exponential wave integrator (EWI) [8,10,36,44,45,54,55,57,91] to solve it, which has favorable properties for solving the second-order oscillatory problems. By applying the variation-of-constant formula to $r^{n}(s)$, we get

$$r^{n}(s) = \frac{\sin(\omega s)}{\omega}\dot{r}^{n}(0) - \int_{0}^{s} \frac{\sin\left(\omega(s-\theta)\right)}{\varepsilon^{2}\omega}\left[g_{r}^{n}(\theta)+\varepsilon^{2}u^{n}(\theta)\right] d\theta, \tag{2.5.5}$$

where

$$\omega = \frac{\sqrt{1+\varepsilon^{2}\alpha}}{\varepsilon^{2}} = O\left(\frac{1}{\varepsilon^{2}}\right), \quad g_{r}^{n}(\theta) := g_{r}(z_{+}^{n}(\theta), z_{-}^{n}(\theta), r^{n}(\theta); \theta). \tag{2.5.6}$$

Taking $s = \tau$ in (2.5.5), we get

$$r^n(\tau) = \frac{\sin(\omega\tau)}{\omega}\dot{r}^n(0) - \int_0^\tau \frac{\sin\left(\omega(\tau-\theta)\right)}{\varepsilon^2\omega}\left[g_r^n(\theta) + \varepsilon^2 u^n(\theta)\right] d\theta. \tag{2.5.7}$$

Differentiating (2.5.5) with respect to s and then taking $s = \tau$, we get

$$\dot{r}^n(\tau) = \cos(\omega\tau)\dot{r}^n(0) - \int_0^\tau \frac{\cos\left(\omega(\tau-\theta)\right)}{\varepsilon^2}\left[g_r^n(\theta) + \varepsilon^2 u^n(\theta)\right] d\theta. \tag{2.5.8}$$

Plugging (2.4.13) into (2.5.7) and (2.5.8), we find

$$\begin{cases} r^n(\tau) = \dfrac{\sin(\omega\tau)}{\omega}\dot{r}^n(0) - \displaystyle\sum_{k=1}^{p}\left[I_{k,+}^n + \overline{I_{k,-}^n}\right] - J^n, \\ \dot{r}^n(\tau) = \cos(\omega\tau)\dot{r}^n(0) - \displaystyle\sum_{k=1}^{p}\left[\dot{I}_{k,+}^n + \overline{\dot{I}_{k,-}^n}\right] - \dot{J}^n, \end{cases} \tag{2.5.9}$$

where

$$\begin{cases} I_{k,\pm}^n = \displaystyle\int_0^\tau \frac{\sin(\omega(\tau-\theta))}{\varepsilon^2\omega} \mathrm{e}^{i(2k+1)\theta/\varepsilon^2} g_{k,\pm}^n(\theta) d\theta, \\ J^n = \displaystyle\int_0^\tau \frac{\sin(\omega(\tau-\theta))}{\varepsilon^2\omega}\left[h^n(\theta) + \varepsilon^2 u^n(\theta)\right] d\theta, \\ \dot{I}_{k,\pm}^n = \displaystyle\int_0^\tau \frac{\cos(\omega(\tau-\theta))}{\varepsilon^2} \mathrm{e}^{i(2k+1)\theta/\varepsilon^2} g_{k,\pm}^n(\theta) d\theta, \\ \dot{J}^n = \displaystyle\int_0^\tau \frac{\cos(\omega(\tau-\theta))}{\varepsilon^2}\left[h^n(\theta) + \varepsilon^2 u^n(\theta)\right] d\theta, \end{cases} \tag{2.5.10}$$

with

$$g_{k,\pm}^n(\theta) := g_k(z_\pm^n(\theta), z_\mp^n(\theta)), \qquad h^n(\theta) := h\left(z_+^n(\theta), z_-^n(\theta), r^n(\theta); \theta\right). \tag{2.5.11}$$

In order to have an explicit integrator and achieve uniform error bounds, we approximate the integral terms $I_{k,\pm}^n$ and $\dot{I}_{k,\pm}^n$ in (2.5.10) by a quadrature in the Gautschi's type [45] as the following which was discussed and used in [8, 10]

$$\begin{cases} I_{k,\pm}^n \approx \displaystyle\int_0^\tau \frac{\sin(\omega(\tau-\theta))}{\varepsilon^2\omega} \mathrm{e}^{i(2k+1)\theta/\varepsilon^2}\left[g_{k,\pm}^n(0) + \theta\dot{g}_{k,\pm}^n(0)\right] d\theta \\ \qquad = p_k g_{k,\pm}^n(0) + q_k \dot{g}_{k,\pm}^n(0), \\ \dot{I}_{k,\pm}^n \approx \displaystyle\int_0^\tau \frac{\cos(\omega(\tau-\theta))}{\varepsilon^2} \mathrm{e}^{i(2k+1)\theta/\varepsilon^2}\left[g_{k,\pm}^n(0) + \theta\dot{g}_{k,\pm}^n(0)\right] d\theta \\ \qquad = \dot{p}_k g_{k,\pm}^n(0) + \dot{q}_k \dot{g}_{k,\pm}^n(0), \end{cases} \tag{2.5.12}$$

where

$$p_k = \int_0^\tau \frac{\sin(\omega(\tau-\theta))}{\varepsilon^2\omega} \mathrm{e}^{i(2k+1)\theta/\varepsilon^2} d\theta, \quad q_k = \int_0^\tau \frac{\sin(\omega(\tau-\theta))}{\varepsilon^2\omega} \mathrm{e}^{i(2k+1)\theta/\varepsilon^2} \theta d\theta,$$
$$\dot{p}_k = \int_0^\tau \frac{\cos(\omega(\tau-\theta))}{\varepsilon^2} \mathrm{e}^{i(2k+1)\theta/\varepsilon^2} d\theta, \quad \dot{q}_k = \int_0^\tau \frac{\cos(\omega(\tau-\theta))}{\varepsilon^2} \mathrm{e}^{i(2k+1)\theta/\varepsilon^2} \theta d\theta.$$

After a detailed computation, we have

$$\begin{aligned}
p_k =& \frac{\varepsilon^2\omega\cos(\omega\tau) + i(2k+1)\sin(\omega\tau) - \varepsilon^2\omega \mathrm{e}^{i(2k+1)\tau/\varepsilon^2}}{(2k+1)^2\omega - \varepsilon^4\omega^3}, \\
\dot{p}_k =& \frac{i(2k+1)\cos(\omega\tau) - \varepsilon^2\omega\sin(\omega\tau) - i(2k+1)\mathrm{e}^{i(2k+1)\tau/\varepsilon^2}}{(2k+1)^2 - \varepsilon^4\omega^2}, \qquad 1 \le k \le p, \\
q_k =& \frac{\varepsilon^2}{\omega\left[\varepsilon^4\omega^2 - (2k+1)^2\right]^2}\Big[i(4k+2)\varepsilon^2\omega\cos(\omega\tau) - \left(\varepsilon^4\omega^2 + (2k+1)^2\right)\sin(\omega\tau) \\
& + \left(\varepsilon^4\omega^3\tau - (2k+1)^2\omega\tau - i(4k+2)\varepsilon^2\omega\right)\mathrm{e}^{i(2k+1)\tau/\varepsilon^2}\Big], \\
\dot{q}_k =& \frac{1}{\left[\varepsilon^4\omega^2 - (2k+1)^2\right]^2}\Big[-\left(\varepsilon^6\omega^2 + (2k+1)^2\varepsilon^2\right)\cos(\omega\tau) - i(4k+2)\varepsilon^4\omega\sin(\omega\tau) \\
& + \left(i(2k+1)\tau\varepsilon^4\omega^2 - i(2k+1)^3\tau + \varepsilon^6\omega^2 + (2k+1)^2\varepsilon^2\right)\mathrm{e}^{i(2k+1)\tau/\varepsilon^2}\Big].
\end{aligned}$$

In addition, approximating J^n and $\dot{J}^n$ in (2.5.10) by the standard single step trapezoidal rule and noticing $h^n(0) = 0$, we get

$$\begin{cases}
J^n \approx \dfrac{\tau}{2}\dfrac{\sin(\omega\tau)}{\varepsilon^2\omega}\left[h^n(0) + \varepsilon^2 u^n(0)\right] = \dfrac{\tau}{2}\dfrac{\sin(\omega\tau)}{\omega}u^n(0), \\
\dot{J}^n \approx \dfrac{\tau}{2}\left[\dfrac{\cos(\omega\tau)}{\varepsilon^2}\left(h^n(0) + \varepsilon^2 u^n(0)\right) + \dfrac{1}{\varepsilon^2}\left(h^n(\tau) + \varepsilon^2 u^n(\tau)\right)\right].
\end{cases} \tag{2.5.13}$$

Plugging (2.5.12), (2.5.13) and (2.5.10) into (2.5.9) and noticing $h^n(0) = 0$, we obtain

$$\begin{cases}
r^n(\tau) \approx -\displaystyle\sum_{k=1}^{p}\left[p_k g^n_{k,+}(0) + q_k \dot{g}^n_{k,+}(0) + \overline{p_k g^n_{k,-}(0)} + \overline{q_k \dot{g}^n_{k,-}(0)}\right] \\
\qquad\qquad + \dfrac{\sin(\omega\tau)}{\omega}\left[\dot{r}^n(0) - \dfrac{\tau}{2}u^n(0)\right], \\
\dot{r}^n(\tau) \approx -\displaystyle\sum_{k=1}^{p}\left[\dot{p}_k g^n_{k,+}(0) + \dot{q}_k \dot{g}^n_{k,+}(0) + \overline{\dot{p}_k g^n_{k,-}(0)} + \overline{\dot{q}_k \dot{g}^n_{k,-}(0)}\right] \\
\qquad\qquad + \cos(\omega\tau)\left[\dot{r}^n(0) - \dfrac{\tau}{2}u^n(0)\right] - \dfrac{\tau}{2}\left[\dfrac{h^n(\tau)}{\varepsilon^2} + u^n(\tau)\right].
\end{cases} \tag{2.5.14}$$

Detailed numerical scheme

For $n = 0, 1, \ldots$, let y^n and $\dot{y}^n$ be the approximations of $y(t_n)$ and $\dot{y}(t_n)$, $z_{\pm}^{n+1}$, $\dot{z}_{\pm}^{n+1}$, $\ddot{z}_{\pm}^{n+1}$, r^{n+1} and $\dot{r}^{n+1}$ be the approximations of $z_{\pm}^{n}(\tau)$, $\dot{z}_{\pm}^{n}(\tau)$, $\ddot{z}_{\pm}^{n}(\tau)$, $r^{n}(\tau)$ and $\dot{r}^{n}(\tau)$, respectively, where $z_{\pm}^{n}(s)$ and $r^{n}(s)$ are the solutions to the system (2.4.20) with initial data (2.4.18). Choosing $y^0 = y(0) = \phi_1$ and $\dot{y}^0 = \dot{y}(0) = \varepsilon^{-2}\phi_2$, for $n = 0, 1, \ldots$, y^{n+1} and $\dot{y}^{n+1}$ are updated as follows:

$$\begin{cases} y^{n+1} = \mathrm{e}^{i\tau/\varepsilon^2} z_+^{n+1} + \mathrm{e}^{-i\tau/\varepsilon^2}\overline{z_-^{n+1}} + r^{n+1}, \\ \dot{y}^{n+1} = \mathrm{e}^{i\tau/\varepsilon^2}\left(\dot{z}_+^{n+1} + \dfrac{i}{\varepsilon^2} z_+^{n+1}\right) + \mathrm{e}^{-i\tau/\varepsilon^2}\left(\overline{\dot{z}_-^{n+1}} - \dfrac{i}{\varepsilon^2}\overline{z_-^{n+1}}\right) + \dot{r}^{n+1}, \end{cases} \tag{2.5.15}$$

where

$$\begin{cases} z_{\pm}^{n+1} = \mathrm{e}^{i\mu_{\pm}\tau} z_{\pm}^{(0)}, \qquad \dot{z}_{\pm}^{n+1} = i\mu_{\pm} z_{\pm}^{n+1}, \qquad \ddot{z}_{\pm}^{n+1} = -(\mu_{\pm})^2 z_{\pm}^{n+1}, \\ r^{n+1} = \dfrac{\sin(\omega\tau)}{\omega}\left(\dot{r}^{(0)} - \dfrac{\tau}{2}u^{(0)}\right) - \displaystyle\sum_{k=1}^{p}\left[p_k g_{k,+}^{(0)} + q_k \dot{g}_{k,+}^{(0)} + \overline{p_k g_{k,-}^{(0)}} + \overline{q_k \dot{g}_{k,-}^{(0)}}\right], \\ \dot{r}^{n+1} = -\displaystyle\sum_{k=1}^{p}\left[\dot{p}_k g_{k,+}^{(0)} + \dot{q}_k \dot{g}_{k,+}^{(0)} + \overline{\dot{p}_k g_{k,-}^{(0)}} + \overline{\dot{q}_k \dot{g}_{k,-}^{(0)}}\right] \\ \qquad\qquad + \cos(\omega\tau)\left(\dot{r}^{(0)} - \dfrac{\tau}{2}u^{(0)}\right) - \dfrac{\tau}{2}\left(\dfrac{h^{n+1}}{\varepsilon^2} + u^{n+1}\right), \\ u^{n+1} = \mathrm{e}^{i\tau/\varepsilon^2}\ddot{z}_+^{n+1} + \mathrm{e}^{-i\tau/\varepsilon^2}\overline{\ddot{z}_-^{n+1}}, \\ h^{n+1} = g(|y^{n+1}|^2)y^{n+1} - g\left(\left|y^{n+1} - r^{n+1}\right|^2\right)\left(y^{n+1} - r^{n+1}\right), \end{cases} \tag{2.5.16}$$

with

$$\begin{cases} z_+^{(0)} = \dfrac{y^n - i\varepsilon^2\dot{y}^n}{2}, \quad z_-^{(0)} = \dfrac{\overline{y^n} - i\varepsilon^2\overline{\dot{y}^n}}{2}, \quad \dot{z}_{\pm}^{(0)} = i\mu_{\pm} z_{\pm}^{(0)}, \\ \dot{r}^{(0)} = -\dot{z}_+^{(0)} - \overline{\dot{z}_-^{(0)}}, \qquad u^{(0)} = -(\mu_+)^2 z_+^{(0)} - (\mu_-)^2\overline{z_-^{(0)}}, \\ \mu_{\pm} = \dfrac{1}{2}g_{\pm}\left(\left|z_+^{(0)}\right|^2, \left|z_-^{(0)}\right|^2\right) + \dfrac{\alpha}{2}, \qquad g_{k,\pm}^{(0)} = g_k\left(z_{\pm}^{(0)}, z_{\mp}^{(0)}\right), \\ \dot{g}_{k,\pm}^{(0)} = \dfrac{d}{ds}\left[g_k\left(z_+(s), z_-(s)\right)\right]\Big|_{\left\{z_{\pm}=z_{\pm}^{(0)},\ \dot{z}_{\pm}=\dot{z}_{\pm}^{(0)}\right\}}, \qquad k = 1, \ldots, p. \end{cases} \tag{2.5.17}$$

We call the proposed numerical integrator (2.5.15) with (2.5.16) as a multiscale time integrator based on MDFA which is abbreviated as MTI-FA in short. Clearly, MTI-FA is fully explicit, and easy to implement in practice. In fact, in this scheme,

at the beginning of each time interval $[t_n, t_{n+1}]$, we decompose the numerical solutions y^n and $\dot{y}^n$ to specify the initial conditions of the system (2.4.16); then we solve the decomposed system numerically; at the end of each time interval, we reconstruct the approximations y^{n+1} and $\dot{y}^{n+1}$ from the numerical solutions to (2.4.16). Therefore, at each time step, the algorithm proceeds as decomposition-solution-reconstruction.

2.5.2 Another multiscale time integrator based on MDF

Based on the MDF (2.4.11), we propose another MTI as follows. Since the system (2.4.11) consists of three second order oscillatory problems, so we use EWIs to solve it.

An EWI for (2.4.11):

By applying the variation-of-constant formula to the first two equations in (2.4.5), we have

$$z_{\pm}^n(s) = a(s) z_{\pm}^n(0) + \varepsilon^2 b(s) \dot{z}_{\pm}^n(0) - \int_0^s b(s-\theta) f_{\pm}^n(\theta) d\theta, \qquad 0 \le s \le \tau, \tag{2.5.18}$$

where

$$\begin{cases} a(s) := \dfrac{\lambda_+ \mathrm{e}^{is\lambda_-} - \lambda_- \mathrm{e}^{is\lambda_+}}{\lambda_+ - \lambda_-}, \quad b(s) := i\dfrac{\mathrm{e}^{is\lambda_+} - \mathrm{e}^{is\lambda_-}}{\varepsilon^2(\lambda_- - \lambda_+)}, \qquad 0 \le s \le \tau, \\ \lambda_+ = -\dfrac{1}{\varepsilon^2}\left(1 + \sqrt{1+\alpha\varepsilon^2}\right) = O\left(\dfrac{1}{\varepsilon^2}\right), \\ \lambda_- = -\dfrac{1}{\varepsilon^2}\left(1 - \sqrt{1+\alpha\varepsilon^2}\right) = O(1). \end{cases} \tag{2.5.19}$$

Taking $s = \tau$ in (2.5.18), we get

$$z_{\pm}^n(\tau) = a(\tau) z_{\pm}^n(0) + \varepsilon^2 b(\tau) \dot{z}_{\pm}^n(0) - \int_0^\tau b(\tau-\theta) f_{\pm}^n(\theta) d\theta. \tag{2.5.20}$$

Differentiating (2.5.18) with respect to s and then taking $s = \tau$, we get

$$\dot{z}_{\pm}^n(\tau) = \dot{a}(\tau) z_{\pm}^n(0) + \varepsilon^2 \dot{b}(\tau) \dot{z}_{\pm}^n(0) - \int_0^\tau \dot{b}(\tau-\theta) f_{\pm}^n(\theta) d\theta, \tag{2.5.21}$$

where

$$\dot{a}(s) = i\lambda_+\lambda_- \frac{\mathrm{e}^{is\lambda_-} - \mathrm{e}^{is\lambda_+}}{\lambda_+ - \lambda_-}, \qquad \dot{b}(s) = \frac{\lambda_+\mathrm{e}^{is\lambda_+} - \lambda_-\mathrm{e}^{is\lambda_-}}{\varepsilon^2(\lambda_+ - \lambda_-)}, \qquad 0 \le s \le \tau.$$

Then approximating the integral terms in (2.5.20) and (2.5.21) by the Gautschi's type quadrature similarly as (2.5.12), we have

$$\begin{cases} z_\pm^n(\tau) \approx a(\tau) z_\pm^n(0) + \varepsilon^2 b(\tau)\dot{z}_\pm^n(0) - c(\tau) f_\pm^n(0) - d(\tau)\dot{f}_\pm^n(0), \\ \dot{z}_\pm^n(\tau) \approx \dot{a}(\tau) z_\pm^n(0) + \varepsilon^2 \dot{b}(\tau)\dot{z}_\pm^n(0) - \dot{c}(\tau) f_\pm^n(0) - \dot{d}(\tau)\dot{f}_\pm^n(0), \end{cases} \tag{2.5.22}$$

where

$$\begin{aligned} c(\tau) &:= \int_0^\tau b(\tau-\theta)d\theta, \quad d(\tau) := \int_0^\tau b(\tau-\theta)\theta d\theta, \\ \dot{c}(\tau) &:= \int_0^\tau \dot{b}(\tau-\theta)d\theta, \quad \dot{d}(\tau) := \int_0^\tau \dot{b}(\tau-\theta)\theta d\theta. \end{aligned}$$

In details, we have

$$\begin{aligned} c(\tau) &= \frac{\lambda_-\mathrm{e}^{i\tau\lambda_+} - \lambda_+\mathrm{e}^{i\tau\lambda_-} + \lambda_+ - \lambda_-}{\varepsilon^2(\lambda_- - \lambda_+)\lambda_+\lambda_-}, \qquad \dot{c}(\tau) = i\frac{\mathrm{e}^{i\tau\lambda_+} - \mathrm{e}^{i\tau\lambda_-}}{\varepsilon^2(\lambda_- - \lambda_+)}, \\ d(\tau) &= i\frac{\lambda_-^2\mathrm{e}^{i\tau\lambda_+} - \lambda_+^2\mathrm{e}^{i\tau\lambda_-} + i\tau\lambda_+\lambda_-(\lambda_+ - \lambda_-) + \lambda_+^2 - \lambda_-^2}{\varepsilon^2(\lambda_+ - \lambda_-)\lambda_+^2\lambda_-^2}, \qquad \dot{d}(\tau) = c(\tau). \end{aligned}$$

Now, substituting

$$f_\pm^n(s) = g_\pm(|z_+^n(s)|^2, |z_-^n(s)|^2) z_\pm^n(s)$$

into (2.5.22), we obtain the approximations to $z_\pm^n(\tau)$ and $\dot{z}_\pm^n(\tau)$.

As for the last equation in (2.4.11), again by the variation-of-constant formula and noticing (2.4.13), we can derive the integral forms for $r^n(\tau)$ and $\dot{r}^n(\tau)$ same as (2.5.9) but without the u^n terms defined in J^n and $\dot{J}^n$. Then the rest approximations are similar to (2.5.14).

Detailed numerical scheme

Following the same notations introduced in subsection 2.5.1, choosing $y^0 = y(0) = \phi_1$ and $\dot{y}^0 = \dot{y}(0) = \varepsilon^{-2}\phi_2$, for $n = 0, 1, \ldots$, y^{n+1} and $\dot{y}^{n+1}$ are updated

in the same way as (2.5.15)-(2.5.17) except that

$$\begin{cases} z_{\pm}^{n+1} = a(\tau) z_{\pm}^{(0)} + \varepsilon^2 b(\tau) \dot{z}_{\pm}^{(0)} - c(\tau) f_{\pm}\left(z_{+}^{(0)}, z_{-}^{(0)}\right) - d(\tau) \dot{f}_{\pm}^{(0)}, \\ \dot{z}_{\pm}^{n+1} = \dot{a}(\tau) z_{\pm}^{(0)} + \varepsilon^2 \dot{b}(\tau) \dot{z}_{\pm}^{(0)} - \dot{c}(\tau) f_{\pm}\left(z_{+}^{(0)}, z_{-}^{(0)}\right) - \dot{d}(\tau) \dot{f}_{\pm}^{(0)}, \\ r^{n+1} = \dfrac{\sin(\omega\tau)}{\omega} \dot{r}^{(0)} - \displaystyle\sum_{k=1}^{p} \left[p_k g_{k,+}^{(0)} + q_k \dot{g}_{k,+}^{(0)} + \overline{p_k g_{k,-}^{(0)}} + \overline{q_k \dot{g}_{k,-}^{(0)}} \right], \\ \dot{r}^{n+1} = \cos(\omega\tau) \dot{r}^{(0)} - \dfrac{\tau}{2\varepsilon^2} h^{n+1} - \displaystyle\sum_{k=1}^{p} \left[\dot{p}_k g_{k,+}^{(0)} + \dot{q}_k \dot{g}_{k,+}^{(0)} + \overline{\dot{p}_k g_{k,-}^{(0)}} + \overline{\dot{q}_k \dot{g}_{k,-}^{(0)}} \right], \\ \dot{f}_{\pm}^{(0)} = \dfrac{d}{ds} \left[f_{\pm}(z_{+}(s), z_{-}(s)) \right] \Big|_{\left\{ z_{\pm} = z_{\pm}^{(0)},\ \dot{z}_{\pm} = \dot{z}_{\pm}^{(0)} \right\}}. \end{cases} \tag{2.5.23}$$

Again, we call the proposed numerical integrator (2.5.15) with (2.5.23) as a multiscale time integrator based on MDF which is abbreviated as MTI-F in short. Clearly, MTI-F is fully explicit, and easy to implement in practice.

2.5.3 Uniform convergence

Here, we shall give the convergence result of the proposed MTIs for the pure power nonlinearity case. In order to obtain rigorous error estimates, we assume that the exact solution $y(t)$ to (2.1.3) satisfies the same assumptions as (2.3.10). Denoting

$$C_0 := \max\left\{ \|y\|_{L^\infty(0,T)},\ \varepsilon^2 \|\dot{y}\|_{L^\infty(0,T)},\ \varepsilon^4 \|\ddot{y}\|_{L^\infty(0,T)} \right\}, \tag{2.5.24}$$

and the error functions same as (2.2.6), then we have the following error estimates for the MTIs [12].

Theorem 2.5.1 (Error bounds of MTI-FA)**.** *For numerical integrator MTI-FA, i.e. (2.5.15) with (2.5.16), under the assumption (2.3.10), there exits a constant $\tau_0 > 0$ independent of ε and n, such that for any $0 < \varepsilon \leq 1$ when $0 < \tau \leq \tau_0$,*

$$|e^n| + \varepsilon^2 |\dot{e}^n| \lesssim \frac{\tau^2}{\varepsilon^2}, \qquad |e^n| + \varepsilon^2 |\dot{e}^n| \lesssim \varepsilon^2, \tag{2.5.25}$$

$$|y^n| \leq C_0 + 1, \qquad |\dot{y}^n| \leq \frac{C_0 + 1}{\varepsilon^2}, \qquad 0 \leq n \leq \frac{T}{\tau}. \tag{2.5.26}$$

Thus by taking the minimum of two error bounds for $0 < \varepsilon \leq 1$*, we have a uniform error bound as*

$$|e^n| + \varepsilon^2|\dot{e}^n| \lesssim \min_{0<\varepsilon\leq 1}\left\{\frac{\tau^2}{\varepsilon^2}, \varepsilon^2\right\} \lesssim \tau, \quad 0 \leq n \leq \frac{T}{\tau}. \tag{2.5.27}$$

Theorem 2.5.2 (Error bounds of MTI-F)**.** *For the numerical integrator MTI-F, i.e. (2.5.15) with (2.5.23), under the assumption (2.3.10), there exists a constant* $\tau_0 > 0$ *independent of* ε *and* n*, such that for any* $0 < \varepsilon \leq 1$ *when* $0 < \tau \leq \tau_0$*,*

$$|e^n| + \varepsilon^2|\dot{e}^n| \lesssim \frac{\tau^2}{\varepsilon^2}, \qquad |e^n| + \varepsilon^2|\dot{e}^n| \lesssim \tau^2 + \varepsilon^2, \tag{2.5.28}$$

$$|y^n| \leq C_0 + 1, \qquad |\dot{y}^n| \leq \frac{C_0 + 1}{\varepsilon^2}, \qquad 0 \leq n \leq \frac{T}{\tau}. \tag{2.5.29}$$

Thus by taking the minimum of two error bounds for $0 < \varepsilon \leq 1$*, we have a uniform error bound as*

$$|e^n| + \varepsilon^2|\dot{e}^n| \lesssim \min_{0<\varepsilon\leq 1}\left\{\frac{\tau^2}{\varepsilon^2}, \ \tau^2 + \varepsilon^2\right\} \lesssim \tau, \quad 0 \leq n \leq \frac{T}{\tau}. \tag{2.5.30}$$

Remark 2.5.1. *If* ϕ_1*,* $\phi_2 \in \mathbb{R}$*,* $y := y(t)$ *is a real-valued function and* $f(y) : \mathbb{R} \to \mathbb{R}$ *in (2.1.3), then it is easy to see that* $z_-^n(s) = z_+^n(s)$ *for* $0 \leq s \leq \tau$ *in (2.4.2) from (2.4.5) and (2.4.10), and (2.4.16) and (2.4.18) for MDF and MDFA, respectively. Thus the multiscale decompositions MDF and MDFA and their numerical integrators MTI-F and MTI-FA as well as their error estimates are still valid and can be simplified. We omit the details here for brevity.*

Remark 2.5.2. *The two MTIs for the problem (2.1.3), i.e. MTI-FA and MTI-F, are completely different from the modulated Fourier expansion methods proposed in the literatures [27, 29, 54, 55, 57, 91] for the problem (1.3.3) in the following aspects. (i) As stated in Section 1.3.1, they are used to solve second order ODEs with different oscillatory behavior in the solutions. (ii) In our MTIs, we adapt the expansion (2.4.2) at each time interval* $[t_n, t_{n+1}]$ *and update its initial data via proper transmission conditions between different time intervals, and the decoupled system consists of only three equations including two equations for the two leading frequencies and one equation for reminder. However, in the modulated Fourier expansion methods,*

it expands the solution only once at $t = 0$ and up to finite terms with increasing frequencies by dropping the reminder, and thus the decoupled system consists of finite number of equations. (iii) Our MTIs are uniformly accurate for $\varepsilon \in (0, 1]$ for the problem (2.1.3) and the error only depends on the time step and is independent of ε and the terms in the expansion (2.4.2). However, if the modulated Fourier expansion methods are applied to the problem (2.1.3), they are usually asymptotic preserving methods instead of uniformly accurate methods. In addition, the errors depend on time step, ε and the number of terms used in the expansion. If high accuracy is needed, one needs to use many terms in the expansion and thus they might be expensive. (iv) Our MTIs work for the regimes when ε is small, large and intermediate; where the modulated Fourier expansion methods only work for the regime when ε is small.

2.5.4 Proof of Theorem 2.5.1

In order to proceed with the proof, we introduce the following auxiliary problem

$$\begin{cases} \varepsilon^2 \ddot{\tilde{y}}^n(s) + \left(\alpha + \dfrac{1}{\varepsilon^2}\right) \tilde{y}^n(s) + g\left(|\tilde{y}^n(s)|^2\right) \tilde{y}^n(s) = 0, \qquad s > 0, \\ \tilde{y}^n(0) = y^n, \qquad \dot{\tilde{y}}^n(0) = \dot{y}^n, \qquad n = 0, 1, \ldots, \end{cases} \tag{2.5.31}$$

and denote two local errors and an error energy as

$$\eta^n(s) := y(t_n + s) - \tilde{y}^n(s), \qquad \dot{\eta}^n(s) := \dot{y}(t_n + s) - \dot{\tilde{y}}^n(s), \qquad s \geq 0, \tag{2.5.32}$$

$$\xi^{n+1} := \tilde{y}^n(\tau) - y^{n+1}, \qquad \dot{\xi}^{n+1} := \dot{\tilde{y}}^n(\tau) - \dot{y}^{n+1}, \tag{2.5.33}$$

$$\mathcal{E}(e, \dot{e}) := \varepsilon^2 |\dot{e}|^2 + \left(\alpha + \frac{1}{\varepsilon^2}\right) |e|^2, \qquad \forall\, e,\, \dot{e} \in \mathbb{C}. \tag{2.5.34}$$

Noticing (2.2.6) and using the triangle inequality, we have

$$\eta^n(0) = e^n, \qquad \dot{\eta}^n(0) = \dot{e}^n, \tag{2.5.35}$$

$$\left|e^{n+1}\right| \leq |\eta^n(\tau)| + \left|\xi^{n+1}\right|, \qquad \left|\dot{e}^{n+1}\right| \leq |\dot{\eta}^n(\tau)| + \left|\dot{\xi}^{n+1}\right|. \tag{2.5.36}$$

Before we present the detailed proof, we first establish the following lemmas.

Lemma 2.5.1. *For any $n = 0, 1, \ldots,$ we have*

$$\mathcal{E}\left(e^{n+1}, \dot{e}^{n+1}\right) \leq (1+\tau)\mathcal{E}\left(\eta^n(\tau), \dot{\eta}^n(\tau)\right) + \left(1 + \frac{1}{\tau}\right)\mathcal{E}\left(\xi^{n+1}, \dot{\xi}^{n+1}\right). \quad (2.5.37)$$

Proof. Noticing (2.5.34), (2.5.36), the above inequality follows by using the Young inequality. □

Let C_0 be given in (2.5.24) and define

$$\tau_1 := (2C_0 + 4)^{-1} K_1^{-1}, \qquad \text{with} \qquad K_1 = \|g(\cdot)\|_{L^\infty\left(0,(2C_0+4)^2\right)}. \quad (2.5.38)$$

Lemma 2.5.2. *For the problem (2.5.31), if (2.5.26) holds for any fixed n ($n = 0, 1, \ldots, \frac{T}{\tau} - 1$), which will be proved by an induction argument later, then we have*

$$\|\tilde{y}^n\|_{L^\infty(0,\tau)} \leq 2C_0 + 3 \lesssim 1, \qquad 0 \leq \tau \leq \tau_1. \quad (2.5.39)$$

Proof. By using the variation-of-constant formula to (2.5.31), we get for $0 \leq s \leq \tau_1$

$$\tilde{y}^n(s) = \cos(\omega s) y^n + \frac{\sin(\omega s)}{\omega}\dot{y}^n - \int_0^s \frac{\sin(\omega(s-\theta))}{\varepsilon^2\omega} g(|\tilde{y}^n(\theta)|^2)\tilde{y}^n(\theta)d\theta. \quad (2.5.40)$$

Then the rest of the proof proceeds in the analogous lines as in [102] for nonlinear dispersive and wave equations by using the bootstrap principle and noticing (2.5.26). □

Lemma 2.5.3. *Under the same assumption as in Lemma 2.5.2, we have for $n = 0, 1, \ldots, \frac{T}{\tau} - 1$,*

$$\mathcal{E}\left(\eta^n(\tau), \dot{\eta}^n(\tau)\right) - \mathcal{E}\left(e^n, \dot{e}^n\right) \lesssim \tau\mathcal{E}\left(e^n, \dot{e}^n\right), \qquad 0 \leq \tau \leq \tau_1. \quad (2.5.41)$$

Proof. Subtracting (2.5.31) from (2.1.3) and noticing (2.5.32), we obtain

$$\begin{cases} \varepsilon^2\ddot{\eta}^n(s) + \left(\alpha + \dfrac{1}{\varepsilon^2}\right)\eta^n(s) + \tilde{g}^n(s) = 0, \qquad s > 0, \\ \eta^n(0) = e^n, \qquad \dot{\eta}^n(0) = \dot{e}^n, \qquad n = 0, 1, \ldots; \end{cases} \quad (2.5.42)$$

where

$$\tilde{g}^n(s) = g\left(|y(t_n+s)|^2\right) y(t_n+s) - g\left(|\tilde{y}^n(s)|^2\right)\tilde{y}^n(s). \tag{2.5.43}$$

By using the variation-of-constant formula and the triangle inequality, we get

$$\begin{cases} |\eta^n(\tau)| \le \left|\cos(\omega\tau)e^n + \dfrac{\sin(\omega\tau)}{\omega}\dot{e}^n\right| + \displaystyle\int_0^\tau \left|\frac{\sin(\omega(\tau-s))}{\varepsilon^2\omega}\tilde{g}^n(s)\right| ds, \\ |\dot{\eta}^n(\tau)| \le |-\omega\sin(\omega\tau)e^n + \cos(\omega\tau)\dot{e}^n| + \displaystyle\int_0^\tau \left|\frac{\cos(\omega(\tau-s))}{\varepsilon^2}\tilde{g}^n(s)\right| ds. \end{cases} \tag{2.5.44}$$

From (2.5.34) with $e = e^n$ and $\dot{e} = \dot{e}^n$, we have

$$\mathcal{E}\left(e^n, \dot{e}^n\right) = \varepsilon^2 |-\omega\sin(\omega\tau)e^n + \cos(\omega\tau)\dot{e}^n|^2 + \left(\alpha + \frac{1}{\varepsilon^2}\right)\left|\cos(\omega\tau)e^n + \frac{\sin(\omega\tau)}{\omega}\dot{e}^n\right|^2.$$

From (2.5.44) and (2.5.34), noticing the above equality and using the Young inequality, we get

$$\mathcal{E}\left(\eta^n(\tau), \dot{\eta}^n(\tau)\right) - (1+\tau)\mathcal{E}\left(e^n, \dot{e}^n\right) \le \left(1+\frac{1}{\tau}\right)\left(\alpha + \frac{2}{\varepsilon^2}\right)\left(\int_0^\tau |\tilde{g}^n(s)|\, ds\right)^2. \tag{2.5.45}$$

Noticing (2.5.24) and (2.5.39), we have

$$|\tilde{g}^n(s)| \lesssim |\eta^n(s)|, \qquad 0 \le s \le \tau \le \tau_1. \tag{2.5.46}$$

Plugging (2.5.46) into (2.5.45), noticing (2.5.34) and using the Hölder inequality, we get

$$\begin{aligned} \mathcal{E}\left(\eta^n(\tau), \dot{\eta}^n(\tau)\right) - (1+\tau)\mathcal{E}\left(e^n, \dot{e}^n\right) &\le \left(1+\frac{1}{\tau}\right)\left(\alpha+\frac{2}{\varepsilon^2}\right)\tau\int_0^\tau |\eta^n(s)|^2\, ds \\ &\lesssim \int_0^\tau \mathcal{E}\left(\eta^n(s), \dot{\eta}^n(s)\right) ds, \quad 0 \le \tau \le \tau_1. \end{aligned} \tag{2.5.47}$$

Then the estimate (2.5.41) can be obtained by applying the Gronwall inequality. □

Lemma 2.5.4. *(A prior estimate of MDFA) Let $z_\pm^n(s)$ and $r^n(s)$ be the solution of the MDFA (2.4.20) under the initial conditions (2.4.18) with $z_\pm^n(0) = z_\pm^{(0)}$ and $\dot{r}^n(0) = \dot{r}^{(0)}$ defined in (2.5.17). Under the same assumption as in Lemma 2.5.2, there exists a constant $\tau_2 > 0$, independent of ε and n, such that for $0 < \tau \le \tau_2$ and all $n = 0, 1, \ldots, \frac{T}{\tau} - 1$,*

$$\left\|\frac{d^m}{dt^m} z_\pm^n\right\|_{L^\infty(0,\tau)} \lesssim 1, \ m = 0,1,2,3; \qquad \varepsilon^{2l-2}\left\|\frac{d^l}{dt^l} r^n\right\|_{L^\infty(0,\tau)} \lesssim 1, \ l = 0,1,2. \tag{2.5.48}$$

Proof. From (2.4.18), noticing (2.5.26), (2.5.17) and (2.5.2), we obtain

$$\left|z_{\pm}^{(0)}\right| \lesssim 1, \quad \left|\dot{z}_{\pm}^{(0)}\right| \lesssim 1, \quad \left\|\frac{d^m}{dt^m} z_{\pm}^n\right\|_{L^\infty(0,\infty)} \lesssim 1, \quad m = 0, 1, 2, 3. \tag{2.5.49}$$

To estimate $r^n(s)$ in (2.4.20), using the variation-of-constant formula, noting (2.5.17), (2.4.13) and (2.5.11), we get

$$r^n(s) = \frac{\sin(\omega s)}{\omega}\dot{r}^{(0)} - \sum_{k=1}^{p}\left[I_{k,+}^n(s) + \overline{I_{k,-}^n(s)}\right] - J^n(s), \qquad s \geq 0, \tag{2.5.50}$$

where

$$\begin{cases} I_{k,\pm}^n(s) := \displaystyle\int_0^s \frac{\sin(\omega(s-\theta))}{\varepsilon^2\omega} \mathrm{e}^{i(2k+1)\theta/\varepsilon^2} g_{k,\pm}^n(\theta) d\theta, \\ J^n(s) := \displaystyle\int_0^s \frac{\sin(\omega(s-\theta))}{\varepsilon^2\omega}\left[h^n(\theta) + \varepsilon^2 u^n(\theta)\right] d\theta, \qquad s \geq 0. \end{cases} \tag{2.5.51}$$

Plugging (2.5.49) into (2.5.17) and using the triangle inequality, we have

$$\left|\dot{r}^{(0)}\right| \leq \left|\dot{z}_{+}^{(0)}\right| + \left|\dot{z}_{-}^{(0)}\right| \lesssim 1. \tag{2.5.52}$$

Let

$$T_k(\theta) = \frac{\varepsilon^2 \mathrm{e}^{i(2k+1)\theta/\varepsilon^2}}{\varepsilon^4\omega^2 - (2k+1)^2}\left[\cos\left(\omega(s-\theta)\right) + \frac{i(2k+1)}{\varepsilon^2\omega}\sin\left(\omega(s-\theta)\right)\right] = O(\varepsilon^2), \tag{2.5.53}$$

then we have

$$\frac{d}{d\theta}T_k(\theta) = \frac{\sin(\omega(s-\theta))}{\varepsilon^2\omega}\mathrm{e}^{i(2k+1)\theta/\varepsilon^2} = O(1), \qquad k = 1, 2, \ldots, p. \tag{2.5.54}$$

Plugging (2.5.54) into (2.5.51), noticing (2.5.53), (2.5.11), (2.4.14) and (2.5.49), we get

$$\begin{aligned} \left|I_{k,\pm}^n(s)\right| &= \left|\int_0^s g_{k,\pm}^n(\theta)\frac{d}{d\theta}T_k(\theta)d\theta\right| = \left|g_{k,\pm}^n(\theta)T_k(\theta)\big|_0^s - \int_0^s T_k(\theta)\frac{d}{d\theta}g_{k,\pm}^n(\theta)\, d\theta\right| \\ &\lesssim \varepsilon^2 + \int_0^s \varepsilon^2\, ds = \varepsilon^2(1+s), \qquad s \geq 0. \end{aligned} \tag{2.5.55}$$

From (2.5.51), noting (2.4.17), (2.5.11), (2.5.54) and (2.5.49), we obtain for $s \geq 0$

$$|J^n(s)| \lesssim \int_0^s \left[\varepsilon^2|u^n(\theta)| + |h^n(\theta)|\right] d\theta \lesssim \varepsilon^2 s + \int_0^s |h^n(\theta)|\, d\theta. \tag{2.5.56}$$

Plugging (2.5.55), (2.5.52) and (2.5.56) into (2.5.50), we have

$$|r^n(s)| \lesssim \varepsilon^2(1+s) + \int_0^s \left|h\left(z_+^n(\theta), z_-^n(\theta), r^n(\theta); \theta\right)\right| d\theta, \qquad s \geq 0. \tag{2.5.57}$$

By using the bootstrap argument to (2.5.57) [102], noting (2.5.49) and (2.4.15), there exists a constant $\tau_2 > 0$ independent of ε and n, such that for $0 < \tau \leq \tau_2$ and all $n = 0, 1, \ldots, \frac{T}{\tau} - 1$,

$$\|r^n\|_{L^\infty(0,\tau)} \lesssim \varepsilon^2, \qquad \|\dot{r}^n\|_{L^\infty(0,\tau)} \lesssim 1, \qquad \|\ddot{r}^n\|_{L^\infty(0,\tau)} \lesssim \varepsilon^{-2}. \tag{2.5.58}$$

The proof is completed by combining (2.5.49) and (2.5.58). □

Lemma 2.5.5. *(Estimate on local error ξ^{n+1}) Under the same assumption as in Lemma 2.5.2, for any $n = 0, 1, \ldots, \frac{T}{\tau} - 1$,, we have the following two independent bounds*

$$\mathcal{E}\left(\xi^{n+1}, \dot{\xi}^{n+1}\right) \lesssim \frac{\tau^6}{\varepsilon^6}, \qquad \mathcal{E}\left(\xi^{n+1}, \dot{\xi}^{n+1}\right) \lesssim \tau^2\varepsilon^2, \qquad 0 \leq \tau \leq \tau_2. \tag{2.5.59}$$

Proof. Similar to Sections 2&3, we can solve the problem (2.5.31) analytically via MDFA and obtain

$$\tilde{y}^n(\tau) = e^{i\tau/\varepsilon^2} z_+^n(\tau) + e^{-i\tau/\varepsilon^2}\overline{z_-^n}(\tau) + r^n(\tau), \tag{2.5.60}$$

where $z_\pm^n(\tau)$ and $r^n(\tau)$ are defined as (2.5.3) and (2.5.9), respectively with $\phi_1^n = y^n$ and $\phi_2^n = \varepsilon^2\dot{y}^n$ in (2.4.18). Plugging (2.5.60) and (2.5.15) into (2.5.33), noting (2.5.16), we have

$$\begin{aligned} \xi^{n+1} &= \mathrm{e}^{i\tau/\varepsilon^2}\left(z_+^n(\tau) - z_+^{n+1}\right) + \mathrm{e}^{-i\tau/\varepsilon^2}\left(\overline{z_-^n(\tau)} - \overline{z_-^{n+1}}\right) + r^n(\tau) - r^{n+1} \\ &= r^n(\tau) - r^{n+1} = \mathcal{J}^n + \sum_{k=1}^{p}\left[\mathcal{I}_{k,+}^n + \overline{\mathcal{I}_{k,-}^n}\right], \end{aligned} \tag{2.5.61}$$

where

$$\mathcal{J}^n := \frac{\tau\sin(\omega\tau)}{2\omega}u^{(0)} - J^n, \ \mathcal{I}_{k,\pm}^n := p_k g_{k,\pm}^{(0)} + q_k \dot{g}_{k,\pm}^{(0)} - I_{k,\pm}^n, \ k = 1, \ldots, p. \tag{2.5.62}$$

From (2.5.62), noting (2.5.10) and (2.5.14) where the Gautschi type or trapezoidal quadrature was used to approximate integrals and using the Taylor expansion, we

obtain for $0 < \tau \leq \tau_2$

$$\left|\mathcal{I}_{k,\pm}^n\right| = \left|\frac{1}{2}\int_0^\tau \theta^2 \frac{\sin(\omega(\tau-\theta))}{\varepsilon^2\omega} \mathrm{e}^{i(2k+1)\theta/\varepsilon^2} \ddot{g}_{k,\pm}^n(t(\theta))d\theta\right| \lesssim \int_0^\tau \theta^2 d\theta \lesssim \tau^3, \quad (2.5.63)$$

where $0 \leq t(\theta) \leq \tau$. In addition, similar to (2.5.55) by using integration by parts, we have

$$\left|\mathcal{I}_{k,\pm}^n\right| = \left|\frac{1}{2}\int_0^\tau \theta^2 \ddot{g}_{k,\pm}(t(\theta)) \frac{d}{d\theta} T_k(\theta) d\theta\right| \lesssim \tau^2\varepsilon^2, \qquad 0 < \tau \leq \tau_2. \quad (2.5.64)$$

Similarly, we can get two independent bounds for $\mathcal{J}^n$ as

$$|\mathcal{J}^n| \lesssim \frac{\tau^3}{\varepsilon^2}, \qquad |\mathcal{J}^n| \lesssim \tau\varepsilon^2, \qquad 0 < \tau \leq \tau_2. \quad (2.5.65)$$

From (2.5.61), noting (2.5.63), (2.5.64) and (2.5.65), we get two independent bounds for ξ^{n+1} as

$$\left|\xi^{n+1}\right| \lesssim \tau^3 + \frac{\tau^3}{\varepsilon^2} \lesssim \frac{\tau^3}{\varepsilon^2}, \qquad \left|\xi^{n+1}\right| \lesssim \varepsilon^2\tau + \tau^2\varepsilon^2 \lesssim \tau\varepsilon^2, \qquad 0 < \tau \leq \tau_2. \quad (2.5.66)$$

Similar to the above, we can obtain two independent bounds for $\dot{\xi}^{n+1}$ as

$$\left|\dot{\xi}^{n+1}\right| \lesssim \frac{\tau^3}{\varepsilon^4}, \qquad \left|\dot{\xi}^{n+1}\right| \lesssim \tau, \qquad 0 < \tau \leq \tau_2. \quad (2.5.67)$$

Then (2.5.59) is a combination of (2.5.66) and (2.5.67) by noting (2.5.34). □

Combining Lemmas 5.2.1, 2.5.2, 2.5.3 and 2.5.5, we can prove the Theorem 2.5.1.

Proof of Theorem 2.5.1 The proof proceeds by using the energy method with the help of the method of mathematical induction for establishing uniform boundedness of y^n and $\dot{y}^n$ [5, 7, 10]. Since $e^0 = 0$ and $\dot{e}^0 = 0$, $y^0 = y(0)$ and $\dot{y}^0 = \dot{y}(0)$, noting (2.5.24), we can get that (2.5.25)-(2.5.26) hold for $n = 0$.

Now assuming that (2.5.25)-(2.5.26) are valid for all $0 \leq n \leq m-1 \leq \frac{T}{\tau} - 1$, we need to show they are still valid for $n = m$. From Lemmas 5.2.1 and 2.5.3, we have

$$\mathcal{E}\left(e^{n+1}, \dot{e}^{n+1}\right) - \mathcal{E}\left(e^n, \dot{e}^n\right) \lesssim \tau\mathcal{E}\left(e^n, \dot{e}^n\right) + \frac{1}{\tau}\mathcal{E}\left(\xi^{n+1}, \dot{\xi}^{n+1}\right), \quad 0 < \tau \leq \tau_1. \quad (2.5.68)$$

Summing the above inequality for $n = 0, 1, \ldots, m-1$, noticing $\mathcal{E}\left(e^0, \dot{e}^0\right) = 0$, we obtain

$$\mathcal{E}\left(e^m, \dot{e}^m\right) \lesssim \tau \sum_{l=1}^{m-1} \mathcal{E}\left(e^l, \dot{e}^l\right) + \frac{1}{\tau}\sum_{l=1}^{m} \mathcal{E}\left(\xi^l, \dot{\xi}^l\right). \quad (2.5.69)$$

Applying the discrete Gronwall inequality to (2.5.69), we get

$$\mathcal{E}\left(e^m,\dot{e}^m\right)\lesssim\frac{1}{\tau}\sum_{l=1}^{m}\mathcal{E}\left(\xi^l,\dot{\xi}^l\right). \tag{2.5.70}$$

Plugging (2.5.59) into (2.5.70), we get two independent bounds as

$$\mathcal{E}\left(e^m,\dot{e}^m\right)\lesssim\frac{T}{\tau^2}\frac{\tau^6}{\varepsilon^6}\lesssim\frac{\tau^4}{\varepsilon^6},\quad \mathcal{E}\left(e^m,\dot{e}^m\right)\lesssim\frac{T}{\tau^2}\tau^2\varepsilon^2\lesssim\varepsilon^2,\quad 0<\tau\leq\min\{\tau_1,\tau_2\}. \tag{2.5.71}$$

Combing (2.5.71) and (2.5.34), we get

$$\begin{aligned}
&|e^m|\leq\varepsilon\sqrt{\mathcal{E}\left(e^m,\dot{e}^m\right)}\lesssim\frac{\tau^2}{\varepsilon^2},\qquad |e^m|\lesssim\varepsilon^2,\\
&\varepsilon^2|\dot{e}^m|\leq\varepsilon\sqrt{\mathcal{E}\left(e^m,\dot{e}^m\right)}\lesssim\frac{\tau^2}{\varepsilon^2},\qquad \varepsilon^2|\dot{e}^m|\lesssim\varepsilon^2,
\end{aligned}$$

which immediately imply that (2.5.25) is valid for $n=m$. In addition, we have [34, 68]

$$|y^m|-C_0\leq|e^m|\lesssim\min_{0<\varepsilon\leq1}\left\{\frac{\tau^2}{\varepsilon^2},\tau^2\right\}\lesssim\tau,\qquad \varepsilon^2\left|\dot{y}^m\right|-C_0\leq\varepsilon^2\left|\dot{e}^m\right|\lesssim\tau. \tag{2.5.72}$$

Thus there exists a $\tau_3>0$ independent of ε and m, such that

$$|y^m|\leq C_0+1,\qquad |\dot{y}^m|\leq\frac{C_0+1}{\varepsilon^2}.$$

Thus (2.5.26) is valid for $n=m$. By the method of mathematical induction, the proof is completed if we choose $\tau_0=\min\{\tau_1,\tau_2,\tau_3\}$. □

2.5.5 Proof of Theorem 2.5.2

The proof is quite similar to that of Theorem 2.5.1. Following the same notations introduced before, let y^n and $\dot{y}^n$ in (2.5.31) be obtained by the method MTI-F and assume (2.5.29) holds, then the regularity and stability results, i.e., Lemmas 5.2.1-2.5.3, for the auxiliary problem (2.5.31) still hold.

Lemma 2.5.6. *(A prior estimate of MDF) Let $z_{\pm}^n(s)$ and $r^n(s)$ be the solution of the MDF (2.4.11) under the initial conditions (2.4.10) with $z_{\pm}^n(0)=z_{\pm}^{(0)}$, $\dot{z}_{\pm}^n(0)=\dot{z}_{\pm}^{(0)}$*

and $\dot{r}^n(0) = \dot{r}^{(0)}$ *defined in (2.5.17). Under the assumption (2.5.29), there exists a constant* $\tau_4 > 0$ *independent of* ε *and* n*, such that for* $0 < \tau \le \tau_4$ *and all* $n = 0, 1, \ldots, \frac{T}{\tau} - 1$

$$\left\| \frac{d^m}{dt^m} z_\pm^n \right\|_{L^\infty(0,\tau)} + \varepsilon^2 \left\| \frac{d^3}{dt^3} z_\pm^n \right\|_{L^\infty(0,\tau)} + \varepsilon^{2m-2} \left\| \frac{d^m}{dt^m} r^n \right\|_{L^\infty(0,\tau)} \lesssim 1, \quad m = 0, 1, 2. \tag{2.5.73}$$

Proof. For the estimates on $z_\pm^n(s)$, we refer the readers to [5, Appendix] and omit the details here for brevity. For the estimates on $r^n(s)$, we can have a similar variation-of-constant formula as (2.5.50) but without the term u^n defined in $J^n(s)$. Then the rest part of the proof can be done in the same manner as Lemma 2.5.4. □

Lemma 2.5.7. *(Estimate on local error* ξ^{n+1}*) Under the same assumption as in Lemma 2.5.2 and assume (2.5.29) holds, for any* $n = 0, 1, \ldots, \frac{T}{\tau} - 1$*, we have two independent bounds*

$$\mathcal{E}\left(\xi^{n+1}, \dot{\xi}^{n+1}\right) \lesssim \frac{\tau^6}{\varepsilon^6}, \qquad \mathcal{E}\left(\xi^{n+1}, \dot{\xi}^{n+1}\right) \lesssim \frac{\tau^6}{\varepsilon^2} + \tau^2\varepsilon^2, \qquad 0 < \tau \le \tau_4. \tag{2.5.74}$$

Proof. Again, similar to Sections 2&3, we can solve the problem (2.5.31) analytically via MDF and obtain that $\tilde{y}^n(\tau)$ satisfies (2.5.60) with $z_\pm^n(\tau)$ and $r^n(\tau)$ defined as (2.5.18) and (2.5.5) with $u^n = 0$, respectively with $\phi_1^n = y^n$ and $\phi_2^n = \varepsilon^2 \dot{y}^n$ in (2.4.10). Plugging (2.5.60) and (2.5.15) into (2.5.33), using the triangle inequality, we get

$$\begin{aligned} |\xi^{n+1}| &= \left| \mathrm{e}^{i\tau/\varepsilon^2} \left(z_+^n(\tau) - z_+^{n+1} \right) + \mathrm{e}^{-i\tau/\varepsilon^2} \left(\overline{z_-^n(\tau)} - \overline{z_-^{n+1}} \right) + r^n(\tau) - r^{n+1} \right| \\ &\le \left| z_+^n(\tau) - z_+^{n+1} \right| + \left| z_-^n(\tau) - z_-^{n+1} \right| + \left| r^n(\tau) - r^{n+1} \right|. \end{aligned} \tag{2.5.75}$$

Similar to the proof in Lemma 2.5.5, we obtain the following two independent bounds

$$\left| r^n(\tau) - r^{n+1} \right| \lesssim \frac{\tau^3}{\varepsilon^2}, \qquad \left| r^n(\tau) - r^{n+1} \right| \lesssim \tau\varepsilon^2, \qquad 0 < \tau \le \tau_4. \tag{2.5.76}$$

Subtracting $z_\pm^{n+1}$ in (2.5.23) from (2.5.20), using the Taylor expansion, and noting (2.5.19), (2.4.19) and (2.5.73), we get

$$\left| z_\pm^n(\tau) - z_\pm^{n+1} \right| = \frac{1}{2} \left| \int_0^\tau \theta^2 b(\tau - \theta) \ddot{f}_\pm^n \left(t(\theta) \right) d\theta \right| \lesssim \int_0^\tau \theta^2 \, d\theta \lesssim \tau^3, \tag{2.5.77}$$

where $0 \leq t(\theta) \leq \tau$. Inserting (2.5.77) and (2.5.76) into (2.5.75), we obtain two independent bounds for ξ^{n+1} as

$$\left|\xi^{n+1}\right| \lesssim \frac{\tau^3}{\varepsilon^2}, \qquad \left|\xi^{n+1}\right| \lesssim \tau^3 + \tau\varepsilon^2, \qquad 0 < \tau \leq \tau_4. \tag{2.5.78}$$

Similarly, we can get two independent bounds for $\dot{\xi}^{n+1}$ as

$$\left|\dot{\xi}^{n+1}\right| \lesssim \frac{\tau^3}{\varepsilon^4}, \qquad \left|\dot{\xi}^{n+1}\right| \lesssim \frac{\tau^3 + \tau\varepsilon^2}{\varepsilon^2}, \qquad 0 < \tau \leq \tau_4. \tag{2.5.79}$$

Then (4.4.37) is a combination of (2.5.78) and (2.5.79) by noting (2.5.34). □

Combining Lemmas 5.2.1, 2.5.2, 2.5.3 and 2.5.7, we can prove the Theorem 2.5.2.

Proof of Theorem 2.5.2 The argument proceeds in analogous lines as for the Theorem 2.5.1 and we omit the details here for brevity. □

2.6 Multiscale time integrators for general nonlinearity

In this section, based on the MDFA (2.4.16) or MDF (2.4.5) for a general gauge invariant nonlinearity $f(y)$ in (2.1.3), we propose two multiscale time integrators (MTIs) for solving (2.1.3). We will adopt the notations introduced in Section 2.5.

2.6.1 A MTI based on MDFA

Based on the MDFA (2.4.16), we propose a MTI.

Integrating the first two equations for $z_{\pm}^n(s)$ in (2.4.16) over $[0, \tau]$, we get

$$z_{\pm}^n(\tau) = \mathrm{e}^{\frac{i\alpha}{2}\tau} z_{\pm}^n(0) + \frac{i}{2}\int_0^\tau \mathrm{e}^{\frac{i\alpha}{2}(\tau-s)} f_{\pm}^n(s) ds. \tag{2.6.1}$$

Similar to (2.5.12), we approximate the integral term by a quadrature in the Gautschi's type, i.e.,

$$\begin{aligned} z_{\pm}^n(\tau) &\approx \mathrm{e}^{\frac{i\alpha}{2}\tau} z_{\pm}^n(0) + \frac{i}{2}\int_0^\tau \mathrm{e}^{\frac{i\alpha}{2}(\tau-s)} \left[f_{\pm}^n(0) + s\dot{f}_{\pm}^n(0)\right] ds \\ &= \mathrm{e}^{\frac{i\alpha}{2}\tau} z_{\pm}^n(0) + \beta_1 f_{\pm}^n(0) + \beta_2 \dot{f}_{\pm}^n(0), \end{aligned} \tag{2.6.2}$$

where

$$\beta_1 = \frac{i}{2\alpha}\left(\mathrm{e}^{\frac{i\alpha}{2}\tau} - 1\right), \qquad \beta_2 = \frac{1}{2\alpha^2}\left(2\mathrm{e}^{\frac{i\alpha}{2}\tau} - i\alpha\tau - 2\right).$$

Taking $s = \tau$ in the first two equations in (2.4.16), we find

$$\dot{z}_{\pm}^n(\tau) = \frac{i\alpha}{2} z_{\pm}^n(\tau) + \frac{i}{2} f_{\pm}^n(\tau). \tag{2.6.3}$$

For the third equation in (2.4.16), we apply the EWI to solve it. Using the variation-of-constant formula, we obtain

$$\begin{cases} r^n(\tau) = \dfrac{\sin(\omega\tau)}{\omega}\dot{r}^n(0) - \displaystyle\int_0^\tau \frac{\sin\left(\omega(\tau-\theta)\right)}{\varepsilon^2\omega}\left[f_r^n(\theta) + \varepsilon^2 u^n(\theta)\right] d\theta, \\ \dot{r}^n(\tau) = \cos(\omega\tau)\dot{r}^n(0) - \displaystyle\int_0^\tau \frac{\cos\left(\omega(\tau-\theta)\right)}{\varepsilon^2}\left[f_r^n(\theta) + \varepsilon^2 u^n(\theta)\right] d\theta, \end{cases} \tag{2.6.4}$$

To have an explicit integrator and achieve uniform error bounds, we approximate the two integral terms in (2.6.4) by quadratures intended to preserve different scales produced by the two integrands. In order to do so, due to that $f_r^n(0) \neq 0$, we introduce two linear interpolations for $f_r^n(\theta)$ on the interval $[0, \tau]$ as

$$l_1^n(\theta) = \frac{\tau - \theta}{\tau} f_r^n(0), \qquad l_2^n(\theta) = \frac{\theta}{\tau} f_r^n(\tau) + \frac{\tau - \theta}{\tau} f_r^n(0), \qquad 0 \le \theta \le \tau. \tag{2.6.5}$$

In addition, differentiating the first two equations in (2.4.16) with respect to s and then taking $s = 0$ or τ, we get

$$\ddot{z}_{\pm}^n(0) = \frac{i\alpha}{2}\dot{z}_{\pm}^n(0) + \frac{i}{2}\dot{f}_{\pm}^n(0), \qquad \ddot{z}_{\pm}^n(\tau) = \frac{i\alpha}{2}\dot{z}_{\pm}^n(\tau) + \frac{i}{2}\dot{f}_{\pm}^n(\tau). \tag{2.6.6}$$

Combing the above and applying the trapezoidal rule, we have

$$\begin{aligned} &\int_0^\tau \frac{\sin(\omega(\tau-\theta))}{\varepsilon^2\omega}\left[f_r^n(\theta) + \varepsilon^2 u^n(\theta)\right] d\theta \\ &= \int_0^\tau \frac{\sin(\omega(\tau-\theta))}{\varepsilon^2\omega}\left[f_r^n(\theta) - l_1^n(\theta) + \varepsilon^2 u^n(\theta)\right] d\theta + \int_0^\tau \frac{\sin(\omega(\tau-\theta))}{\varepsilon^2\omega} l_1^n(\theta) d\theta \\ &\approx \frac{\tau\sin(\omega\tau)}{2\omega} u^n(0) + \gamma_1 f_r^n(0), \end{aligned} \tag{2.6.7}$$

$$\begin{aligned} &\int_0^\tau \frac{\cos(\omega(\tau-\theta))}{\varepsilon^2}\left[f_r^n(\theta) + \varepsilon^2 u^n(\theta)\right] d\theta \\ &= \int_0^\tau \frac{\cos(\omega(\tau-\theta))}{\varepsilon^2}\left[f_r^n(\theta) - l_2^n(\theta) + \varepsilon^2 u^n(\theta)\right] d\theta + \int_0^\tau \frac{\cos(\omega(\tau-\theta))}{\varepsilon^2} l_2^n(\theta) d\theta \\ &\approx \frac{\tau}{2}\left[\cos(\omega\tau)u^n(0) + u^n(\tau)\right] + \gamma_2 f_r^n(0) + \gamma_3 f_r^n(\tau), \end{aligned} \tag{2.6.8}$$

where

$$\gamma_1 = \frac{1-\cos(\omega\tau)}{\varepsilon^2\omega^2}, \quad \gamma_2 = \frac{\cos(\omega\tau)+\omega\tau\sin(\omega\tau)-1}{\varepsilon^2\omega^2\tau}, \quad \gamma_3 = \frac{1-\cos(\omega\tau)}{\varepsilon^2\omega^2\tau}.$$

Plugging (2.6.7) and (2.6.8) into (2.6.4), we obtain

$$\begin{cases} r^n(\tau) \approx \dfrac{\sin(\omega\tau)}{\omega}\left[\dot{r}^n(0) - \dfrac{\tau}{2}u^n(0)\right] - \gamma_1 f_r^n(0), \\ \dot{r}^n(\tau) \approx \cos(\omega\tau)\left[\dot{r}^n(0) - \dfrac{\tau}{2}u^n(0)\right] - \dfrac{\tau}{2}u^n(\tau) - \gamma_2 f_r^n(0) - \gamma_3 f_r^n(\tau), \end{cases} \tag{2.6.9}$$

where

$$u^n(0) = \ddot{z}_+^n(0) + \overline{\ddot{z}_-^n}(0), \qquad u^n(\tau) = \mathrm{e}^{i\tau/\varepsilon^2}\ddot{z}_+^n(\tau) + \mathrm{e}^{-i\tau/\varepsilon^2}\overline{\ddot{z}_-^n}(\tau).$$

Detailed numerical scheme

Following the same notations introduced in Subsection 2.5.1, choosing $y^0 = y(0) = \phi_1$ and $\dot{y}^0 = \dot{y}(0) = \varepsilon^{-2}\phi_2$, for $n = 0, 1, \ldots$, y^{n+1} and $\dot{y}^{n+1}$ are updated in the same way as (2.5.15)-(2.5.17) except that

$$\begin{cases} z_\pm^{n+1} = \mathrm{e}^{\frac{i\alpha}{2}\tau} z_\pm^{(0)} + \beta_1 f_\pm\left(z_+^{(0)}, z_-^{(0)}\right) + \beta_2 \dot{f}_\pm^{(0)}, \\ r^{n+1} = \dfrac{\sin(\omega\tau)}{\omega}\left(\dot{r}^{(0)} - \dfrac{\tau}{2}u^{(0)}\right) - \gamma_1 f_r\left(z_+^{(0)}, z_-^{(0)}, r^{(0)}; 0\right), \\ \dot{z}_\pm^{n+1} = \dfrac{i}{2}\left[\alpha z_\pm^{n+1} + f_\pm(z_+^{n+1}, z_-^{n+1})\right], \\ \dot{r}^{n+1} = \cos(\omega\tau)\left(\dot{r}^{(0)} - \dfrac{\tau}{2}u^{(0)}\right) - \dfrac{\tau}{2}u^{n+1} - \gamma_2 f_r(z_+^{(0)}, z_-^{(0)}, r^{(0)}; 0) \\ \qquad\qquad - \gamma_3 f_r(z_+^{n+1}, z_-^{n+1}, r^{n+1}; \tau), \\ \ddot{z}_\pm^{n+1} = \dfrac{i\alpha}{2}\dot{z}_\pm^{n+1} + \dfrac{i}{2}\dfrac{d}{ds}\left[f_\pm(z_+(s), z_-(s))\right]\Big|_{\left\{z_\pm = z_\pm^{n+1},\ \dot{z}_\pm = \dot{z}_\pm^{n+1}\right\}}, \end{cases} \tag{2.6.10}$$

with

$$\begin{cases} \dot{z}_\pm^{(0)} = \dfrac{i}{2}\left[\alpha z_\pm^{(0)} + f_\pm\left(z_+^{(0)}, z_-^{(0)}\right)\right], \\ u^{(0)} = \dfrac{i}{2}\left[\alpha\left(\dot{z}_+^{(0)} - \overline{\dot{z}_-^{(0)}}\right) + \dot{f}_+^{(0)} - \overline{\dot{f}_-^{(0)}}\right], \\ \dot{f}_\pm^{(0)} = \dfrac{d}{ds}\left[f_\pm(z_+(s), z_-(s))\right]\Big|_{\left\{z_\pm = z_\pm^{(0)},\ \dot{z}_\pm = \dot{z}_\pm^{(0)}\right\}}. \end{cases} \tag{2.6.11}$$

Remark 2.6.1. *As it can be seen from the above integrators, one needs to evaluate functions $f_{\pm}^n$ and $\dot{f}_{\pm}^n$ in the scheme. In fact, these functions are given in the integral forms as (2.4.6). In practice, if explicit formulas are not available, they can be computed numerically via the following composite trapezoidal rule*

$$f_{\pm}(z_+, z_-) \approx \frac{1}{N} \sum_{j=0}^{N-1} f\left(z_{\pm} + \mathrm{e}^{i\theta_j} \overline{z_{\mp}}\right), \qquad z_+, z_- \in \mathbb{C},$$

where $N \in \mathbb{N}$ is chosen to be large enough and $\theta_j = \frac{2\pi}{N} j$ for $j = 0, 1, \ldots, N$. Since the integrand $f\left(z_{\pm} + \mathrm{e}^{i\theta} \overline{z_{\mp}}\right)$ in (2.4.6) is a periodic function with period $T = 2\pi$, thus it is spectrally accurate to approximate the integrals in (2.4.6) via the composite trapezoidal rule!

2.6.2 Another MTI based on MDF

Based on the MDF (2.4.5), we propose another MTI as follows.

For the first two equations in (2.4.11), the integrator follows (2.5.18)-(2.5.22) totally. As for the approximations to $r^n(\tau)$ and $\dot{r}^n(\tau)$, we follow the EWIs (2.6.4)-(2.6.8) by setting $u^n = 0$.

Detailed numerical scheme

Following the same notations introduced in subsection 2.5.1, choosing $y^0 = y(0) = \phi_1$ and $\dot{y}^0 = \dot{y}(0) = \varepsilon^{-2}\phi_2$, for $n = 0, 1, \ldots$, y^{n+1} and $\dot{y}^{n+1}$ are updated in the same way as (2.5.15), (2.5.23) and (2.6.11) except that

$$\begin{cases} r^{n+1} = \dfrac{\sin(\omega\tau)}{\omega} \dot{r}^{(0)} - \gamma_1 f_r\left(z_+^{(0)}, z_-^{(0)}, r^{(0)}; 0\right), \\ \dot{r}^{n+1} = \cos(\omega\tau)\dot{r}^{(0)} - \gamma_2 f_r\left(z_+^{(0)}, z_-^{(0)}, r^{(0)}; 0\right) - \gamma_3 f_r\left(z_+^{n+1}, z_-^{n+1}, r^{n+1}; \tau\right). \end{cases} \tag{2.6.12}$$

2.7 Numerical results and comparisons

In this section, we present numerical comparison results between the proposed MTIs including MTI-FA and MTI-F, EWIs including EWI-G, EWI-D, EWI-F1 and EWI-F2, and classical finite difference integrators including CNFD, SIFD and

EXFD. We will compare their accuracy for fixed $\varepsilon = O(1)$ and their meshing strategy (or ε-resolution) in the parameter regime when $0 < \varepsilon \ll 1$. To quantify the convergence, we introduce two error functions:

$$\mathrm{e}^{\varepsilon,\tau}(T) := \left|y(T) - y^M\right|, \quad \mathrm{e}^{\tau}_{\infty}(T) := \max_{\varepsilon}\left\{e^{\varepsilon,\tau}(T)\right\}, \tag{2.7.1}$$

where $T = t_M$ with $t_M = M\tau$.

2.7.1 For power nonlinearity

Accuracy and meshing strategy

The nonlinearity in the problem (2.1.3) is taken as the pure power nonlinearity (2.1.4) with coefficients and initial conditions chosen as

$$\alpha = 2, \quad g\left(|y|^2\right) = |y|^2, \quad \phi_1 = 1, \quad \phi_2 = 1. \tag{2.7.2}$$

Since the analytical solution to this problem is not available, the 'exact' solution is obtained numerically by the MTI-FA (2.5.15) with (2.5.16) under a very small time step $\tau = 10^{-6}$.

Tab. 2.1 lists the errors of the method MTI-FA (2.5.15) with (2.5.16) under different ε and τ, and Tab. 2.2 shows similar results for the method MTI-F (2.5.15) with (2.5.23). For comparisons, Tab. 2.3 shows the errors of EWI-G (2.3.3) and EWI-D (2.3.5), Tab. 2.5 shows the errors of EWI-F1 (2.3.8) and EWI-F2 (2.3.9), and Tab. 2.7 shows the errors of CNFD (2.2.1), SIFD (2.2.2) and EXFD (2.2.3).

Based on Tabs. 2.1-2.9 and additional results not shown here for brevity, the following observations can be drawn:

1) For any fixed ε under $0 < \varepsilon \leq 1$, when τ is sufficiently small, e.g. $\tau \lesssim \varepsilon^2$, all the numerical methods are second-order accurate (cf. each row in the upper triangle of the tables). When $\varepsilon = O(1)$, e.g. $\varepsilon = 0.5$, the errors are in the same magnitude for all the numerical methods under fixed τ (cf. first row in the tables); on the contrary, when ε is small, under fixed τ small enough, the errors in MTI-FA

Table 2.1: Error analysis of MTI-FA: $\mathrm{e}^{\varepsilon,\tau}(T)$ and $\mathrm{e}^{\tau}_{\infty}(T)$ with $T = 4$ and convergence rate. Here and after, the convergence rate is obtained by $\frac{1}{2}\log_2\left(\frac{\mathrm{e}^{\varepsilon,4\tau}(T)}{\mathrm{e}^{\varepsilon,\tau}(T)}\right)$.

$\mathrm{e}^{\varepsilon,\tau}(T)$	$\tau_0 = 0.2$	$\tau_0/2^2$	$\tau_0/2^4$	$\tau_0/2^6$	$\tau_0/2^8$	$\tau_0/2^{10}$	$\tau_0/2^{12}$
$\varepsilon_0 = 0.5$	5.71E–1	5.28E–2	3.40E–3	2.14E–4	1.34E–5	8.36E–7	5.21E–8
rate	—	1.72	1.98	2.00	2.00	2.00	2.00
$\varepsilon_0/2^1$	3.14E–1	5.56E–2	5.70E–3	3.51E–4	2.17E–5	1.35E–6	8.43E–8
rate	—	1.25	1.64	2.01	2.01	2.00	2.00
$\varepsilon_0/2^2$	1.59E–1	1.53E–1	4.58E–2	2.80E–3	1.56E–4	9.36E–6	5.79E–7
rate	—	0.03	0.87	2.02	2.08	2.03	2.01
$\varepsilon_0/2^3$	5.90E–3	1.59E–2	1.25E–2	5.90E–3	2.51E–4	1.16E–5	6.58E–7
rate	—	-0.72	0.17	0.54	2.28	2.22	2.07
$\varepsilon_0/2^4$	6.70E–3	5.40E–3	8.60E–3	7.30E–3	2.60E–3	1.33E–4	6.82E–6
rate	—	0.16	0.34	0.12	0.74	2.14	2.14
$\varepsilon_0/2^5$	1.10E–3	1.00E–3	6.36E–4	1.30E–3	1.30E–3	2.77E–4	2.06E–5
rate	—	0.07	0.33	-0.52	0.00	1.12	1.87
$\varepsilon_0/2^6$	5.96E–4	2.18E–5	5.96E–4	4.10E–4	5.97E–4	5.18E–4	1.78E–4
rate	—	2.39	-2.39	0.27	-0.27	0.10	0.77
$\varepsilon_0/2^8$	6.51E–6	7.14E–6	1.04E–5	7.48E–6	7.00E–6	3.48E–6	1.03E–5
rate	—	-0.07	-0.27	0.24	0.05	0.50	0.78
$\varepsilon_0/2^{10}$	2.32E–7	4.85E–7	2.66E–7	2.79E–6	2.52E–6	5.01E–8	2.66E–6
rate	—	-0.53	0.43	-1.70	0.07	2.83	-2.87
$\varepsilon_0/2^{12}$	9.87E–8	4.34E–8	6.68E–8	2.33E–8	7.56E–8	1.19E–7	1.12E–7
rate	—	0.59	-0.31	0.76	-0.85	-0.33	0.04
$\varepsilon_0/2^{14}$	3.38E–8	3.77E–8	3.84E–8	3.55E–8	3.49E–8	3.45E–8	3.43E–8
rate	—	-0.08	-0.01	0.06	0.01	0.01	0.01
$\mathrm{e}^{\tau}_{\infty}(T)$	5.71E–1	1.53E–1	4.58E–2	7.30E–3	2.60E–3	5.18E–4	1.78E–4
rate	—	0.95	0.87	1.32	0.74	1.16	0.77

and MTI-F are several order smaller in magnitude than those in EWI-G, EWI-D, EWI-F1 and EWI-F2, and the errors in EWI-G, EWI-D, EWI-F1 and EWI-F2 are a few order smaller in magnitude than those in CNFD, SIFD and EXFD (cf. right bottom parts in the upper triangle of the tables).

2) Both MTI-FA and MTI-F are uniformly accurate for $0 < \varepsilon \leq 1$ and converge linearly in τ (cf. last row in Tabs. 2.1&2.2). In addition, for fixed τ, when $0 < \varepsilon \ll 1$, MTI-FA converges quadratically in term of ε (cf. each column in the lower triangle of Tab. 2.1); MTI-F is uniformly bounded (cf. each column in the lower triangle of Tab. 2.2). These results confirm our analytical results in (2.5.26), (2.5.27), (2.5.29) and (2.5.30). EWI-G, EWI-D, EWI-F1, EWI-F2, CNFD, SIFD and EXFD are not uniformly accurate for $0 < \varepsilon \leq 1$ (cf. each column in Tabs. 2.3&2.5). In fact, for fixed τ small enough, when ε decreases, the errors for EWI-G, EWI-D, EWI-F1 and EWI-F2 increase in term of ε^{-4} (cf. last row in Tab. 2.3), and resp., for CNFD, SIFD and EXFD in term of ε^{-6} (cf. last row in Tab. 2.5). These results confirm our analytical results in (2.2.8) and (2.3.11).

3) In summary, when $\varepsilon = O(1)$, all the methods perform the same in term of accuracy, however, EXFD is the simplest and cheapest one in term of computational cost. On the contrary, when $0 < \varepsilon < 1$, especially $0 < \varepsilon \ll 1$, both MTI-FA and MTI-F perform much better than the other classical methods. In fact, in order to compute 'correct' numerical solution, in the regime of $0 < \varepsilon \ll 1$, the ε-scalability (or meshing stragety) for MTI-FA and MTI-F is: $\tau = O(1)$ which is independent of ε, while EWI-G, EWI-D, EWI-F1 and EWI-F2 need to choose $\tau = O(\varepsilon^2)$ and CNFD, SIFD and EXFD need to choose $\tau = O(\varepsilon^3)$.

Energy comparisons

With the setup (2.7.2) and $\varepsilon = 0.2$ in (2.1.3), we test the energy behavior of the nonconservative numerical integrators. We compute the error between the numerical energy E^n:

$$E^n := \varepsilon^2 \left|\dot{y}^n\right|^2 + \left(\alpha + \frac{1}{\varepsilon^2}\right) \left|y^n\right|^2 + F\left(\left|y^n\right|^2\right),$$

and the exact energy $E(0) = E(t)$ (2.1.5) over a time interval $t \in [0, 80]$. The energy errors $|E^n - E(0)|$ of methods: SIFD and EWI-G under different step size are shown in Fig. 2.2, and that of MTI-F and MTI-FA is shown in Fig. 2.3. The corresponding results of other EWIs are similar to EWI-G. Comparisons between each method on the maximum energy error $e_E(t) := \max\limits_{0\le t_n\le t}\{|E^n - E(0)|\}$ are shown in Fig. 2.4. From the numerical results, we can see that: 1) the numerical energy of SIFD and EWIs is rapid bounded fluctuation from the exact energy, while that of MTI-F and MTI-FA is approximately linearly growing. 2) at early time of the computing, MTIs has much smaller maximum energy error than others. 3) until $t = 80$, the maximum energy error of the MTIs is still below that of the EWIs, and both of them are much smaller than SIFD.

An ODE system numerical example

Here we provide a numerical example, which is very similar to the famous Fermi-Pasta-Ulam problem in literatures [55–57, 91], for the proposed MTIs to solve the high oscillatory ODE system (2.1.1) with

$$d = 3,\ A = \begin{pmatrix} 2 & & \\ & 1 & \\ & & 0 \end{pmatrix},\ f(\mathbf{y}) = \begin{pmatrix} |y_2|^2 y_1 \\ |y_3|^2 y_2 \\ |y_1|^2 y_3 \end{pmatrix},\ \Phi_1 = \Phi_2 = \begin{pmatrix} 1 \\ 1 \\ 1 \end{pmatrix}. \tag{2.7.3}$$

The errors $\mathrm{e}^{\varepsilon,\tau}(T) := \max\{|y_1^n - y_1(T)|, |y_2^n - y_2(T)|, |y_2^n - y_2(T)|\}$ of MTI-FA and MTI-F at $T = 1$ are shown in Tab. 2.10.

2.7.2 For general gauge invariant nonlinearity

The nonlinearity and initial conditions in the problem (2.1.3) are chosen as

$$\alpha = 3, \qquad f(y) = \sin^2(|y|^2)y, \qquad \phi_1 = 1, \qquad \phi_2 = 1.$$

Again, the 'exact' solution is obtained numerically by the MTI-FA (2.5.15) with (2.6.10) and (2.6.11) under a very small time step.

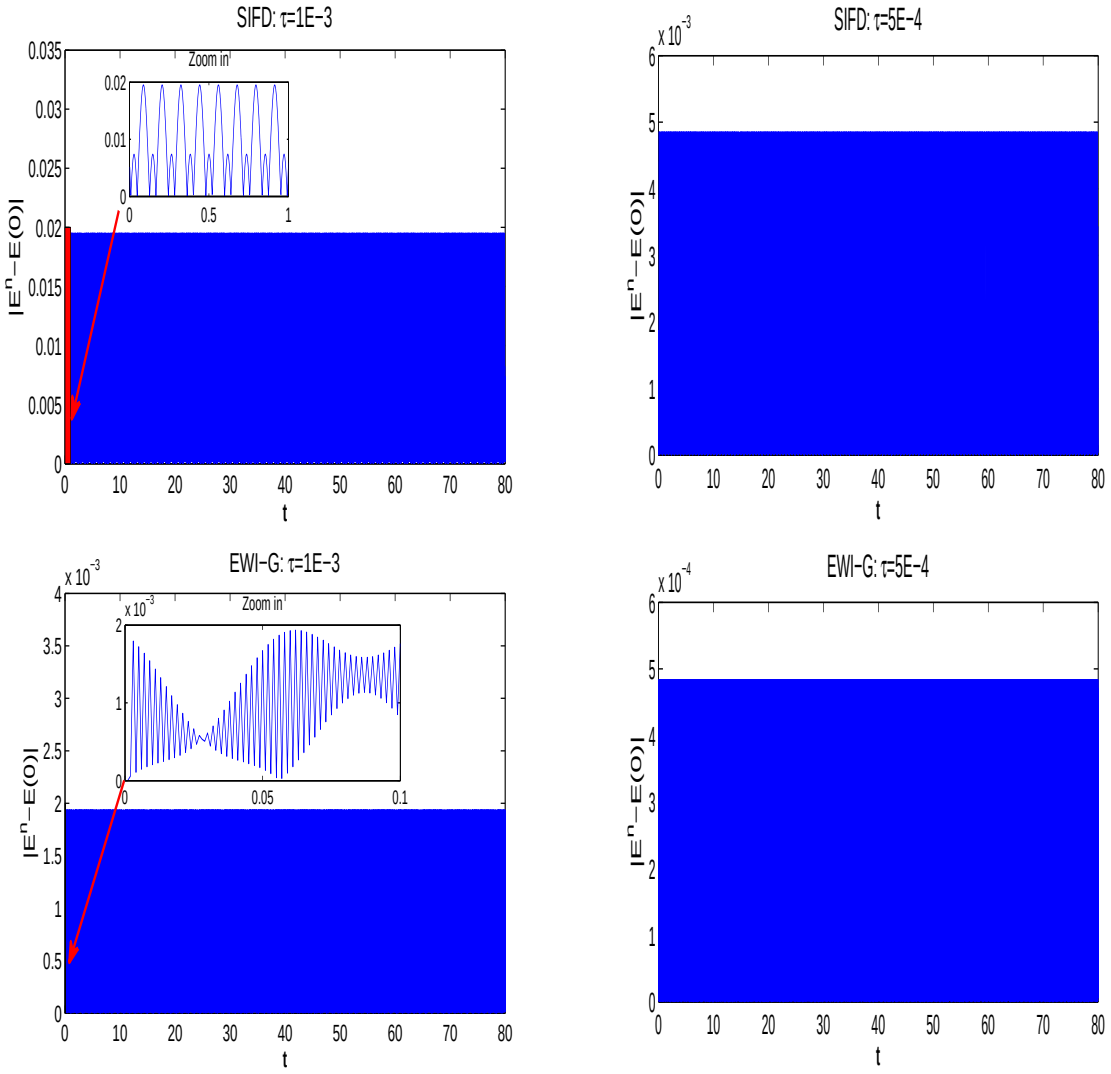

Figure 2.2: Energy error $|E^n - E(0)|$ of SIFD and EWI-G for different τ during the computing under $\varepsilon = 0.2$.

Tab. 2.11 shows the errors of the method MTI-FA (2.5.15) with (2.6.10) and (2.6.11) under different ε and τ, and Tab. 2.12 lists similar results for the method MTI-F (2.5.15) with (2.6.12). The results for EWI-G, EWI-D, EWI-F1, EWI-F2, CNFD, SIFD and EXFD are similar to the previous subsection and they are omitted here for brevity.

From Tabs. 2.11&2.12 and additional results not shown here for brevity, again

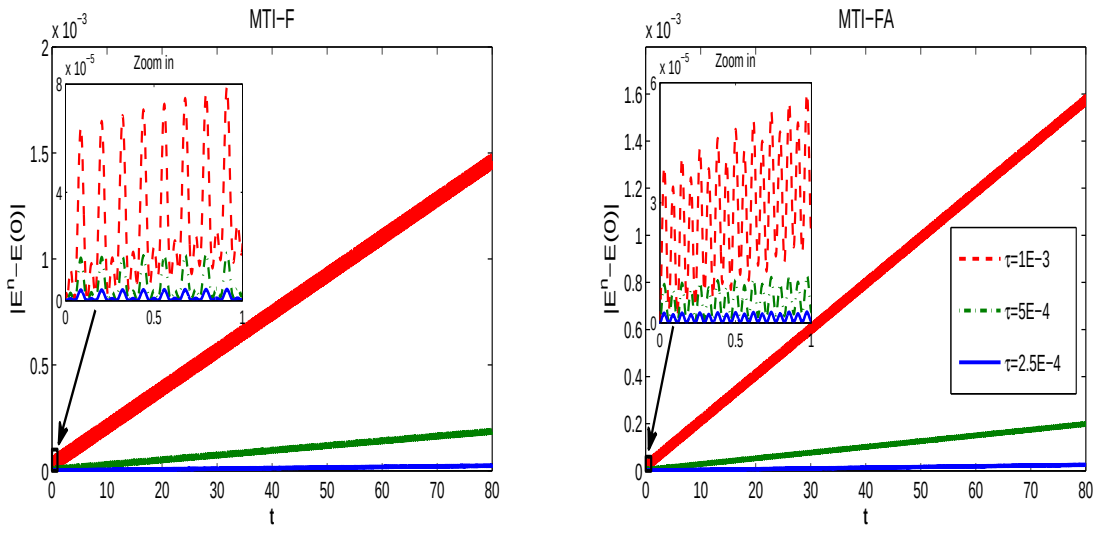

Figure 2.3: Energy error $|E^n - E(0)|$ of MTI-F and MTI-FA for different τ during the computing under $\varepsilon = 0.2$.

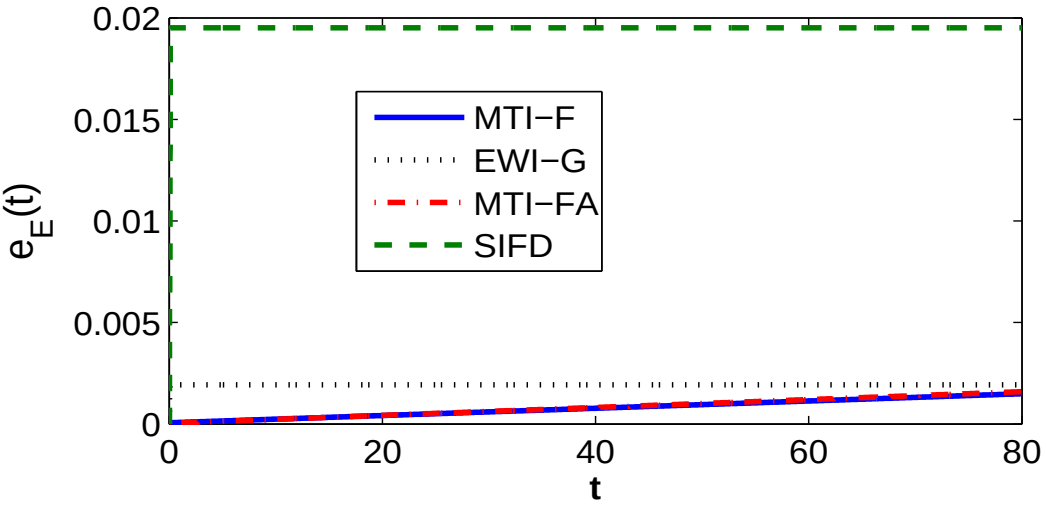

Figure 2.4: Maximum energy error $e_E(t) := \max\limits_{0\le t_n\le t}\{|E^n - E(0)|\}$ of SIFD, EWI-G, MTI-F and MTI-FA under $\tau = 1E-3$ and $\varepsilon = 0.2$.

we can see that both MTI-FA and MTI-F are uniformly accurate for $0 < \varepsilon \le 1$, especially when $0 < \varepsilon \ll 1$. In addition, the results suggest the following two independent error bounds for both MTI-FA and MTI-F under a general nonlinearity

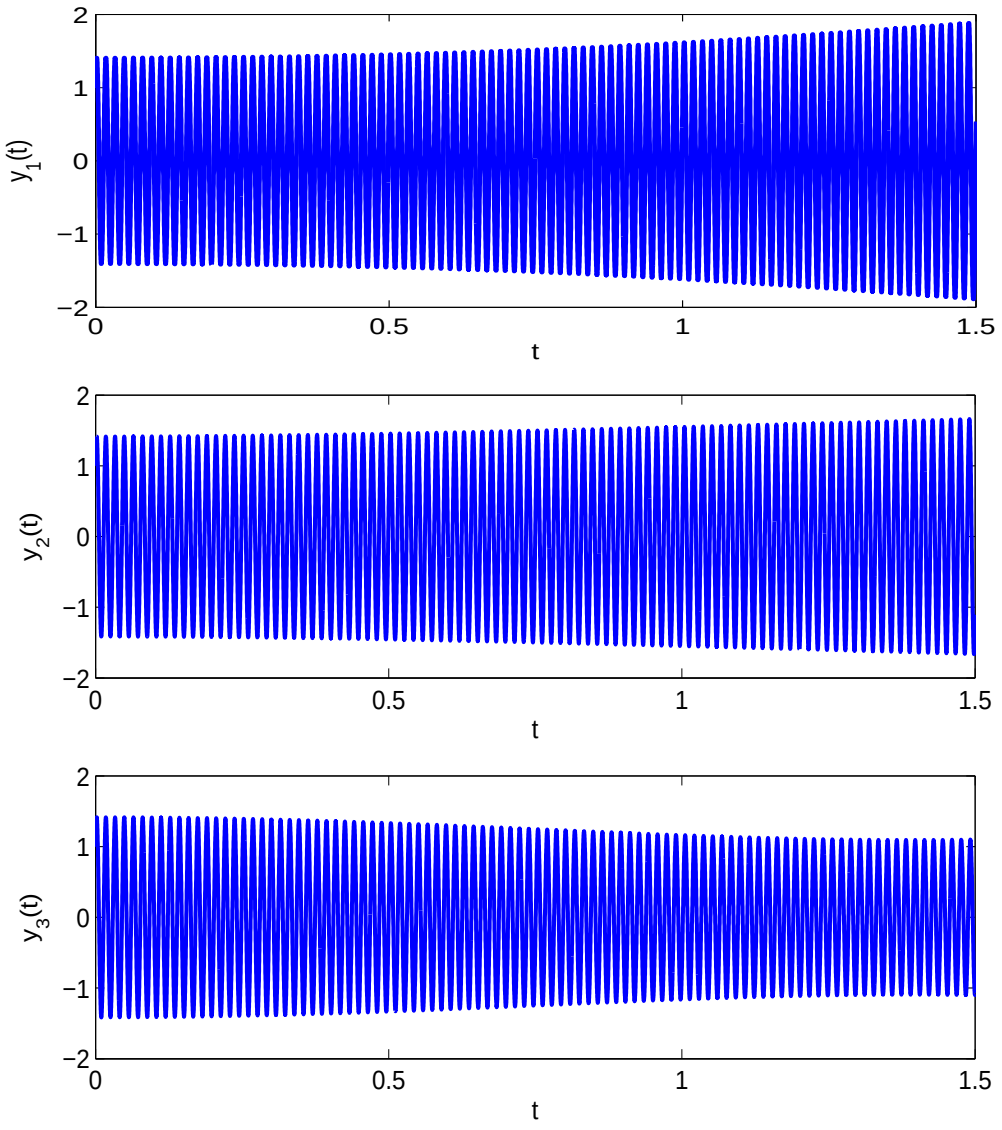

Figure 2.5: Solution of the HODE system (2.7.3) with $\varepsilon = 0.05$.

in (2.1.3)

$$|e^n| + \varepsilon^2|\dot{e}^n| \lesssim \frac{\tau^2}{\varepsilon^2}, \qquad |e^n| + \varepsilon^2|\dot{e}^n| \lesssim \tau^2 + \varepsilon^2, \qquad 0 < \tau \leq \tau_0.$$

Rigorous justification for the above observation is going to be the future study.

Table 2.2: Error analysis of MTI-F: $\mathrm{e}^{\varepsilon,\tau}(T)$ and $\mathrm{e}^{\tau}_{\infty}(T)$ with $T = 4$ and convergence rate.

$\mathrm{e}^{\varepsilon,\tau}(T)$	$\tau_0 = 0.2$	$\tau_0/2^2$	$\tau_0/2^4$	$\tau_0/2^6$	$\tau_0/2^8$	$\tau_0/2^{10}$	$\tau_0/2^{12}$
$\varepsilon_0 = 0.5$	5.33E−1	4.05E−2	2.80E−3	1.84E−4	1.16E−5	7.27E−7	4.53E−8
rate	—	1.86	1.93	1.96	1.99	2.00	2.00
$\varepsilon_0/2$	3.71E−1	5.54E−2	5.60E−3	3.48E−4	2.16E−5	1.34E−6	8.38E−8
rate	—	1.37	1.65	2.00	2.01	2.00	2.00
$\varepsilon_0/2^2$	2.78E−1	1.60E−1	4.51E−2	2.80E−3	1.55E−4	9.35E−6	5.79E−7
rate	—	0.40	0.91	2.00	2.09	2.03	2.01
$\varepsilon_0/2^3$	4.95E−2	1.68E−2	1.20E−2	5.80E−3	2.50E−4	1.16E−5	6.57E−7
rate	—	0.78	0.24	0.52	2.27	2.22	2.07
$\varepsilon_0/2^4$	1.07E−1	9.20E−3	8.70E−3	7.30E−3	2.60E−3	1.33E−4	6.82E−6
rate	—	1.77	0.04	0.13	0.87	2.14	2.14
$\varepsilon_0/2^5$	6.15E−2	3.90E−3	8.00E−4	1.40E−3	1.30E−3	2.76E−4	2.06E−5
rate	—	1.99	1.14	-0.40	0.05	1.12	1.87
$\varepsilon_0/2^6$	1.14E−1	4.80E−3	8.54E−4	4.24E−4	5.97E−4	5.18E−4	1.78E−4
rate	—	2.28	1.25	0.50	-0.25	0.10	0.77
$\varepsilon_0/2^8$	2.60E−2	1.40E−3	9.98E−5	1.31E−5	7.36E−6	3.50E−6	1.03E−5
rate	—	2.11	1.91	1.47	0.41	0.54	-0.78
$\varepsilon_0/2^{10}$	1.23E−1	5.30E−3	2.91E−4	2.04E−5	3.61E−6	1.20E−7	2.67E−6
rate	—	2.27	2.09	1.92	1.25	2.45	-2.24
$\varepsilon_0/2^{12}$	1.35E−1	6.00E−3	3.41E−4	2.08E−5	1.25E−6	2.36E−7	1.53E−7
rate	—	2.24	2.07	2.02	2.03	1.20	0.31
$\varepsilon_0/2^{14}$	4.57E−2	2.30E−3	1.36E−4	8.28E−6	3.27E−7	1.67E−7	1.97E−7
rate	—	2.15	2.04	2.02	2.32	0.49	-0.12
$\mathrm{e}^{\tau}_{\infty}(T)$	5.33E−1	1.60E−1	4.51E−2	7.30E−3	2.60E−3	5.18E−4	1.78E−4
rate	—	0.87	0.91	1.31	0.74	1.16	0.77

Table 2.3: Error analysis of EWI-G: $\mathrm{e}^{\varepsilon,\tau}(T)$ with $T = 4$ and convergence rate.

EWI-G	$\tau_0 = 0.2$	$\tau_0/2^2$	$\tau_0/2^4$	$\tau_0/2^6$	$\tau_0/2^8$	$\tau_0/2^{10}$
$\varepsilon_0 = 0.5$	1.09E–2	1.59E–3	1.01E–4	6.36E–6	3.97E–7	2.44E–8
rate	—	1.39	1.98	2.00	2.00	2.01
$\varepsilon_0/2$	2.34E+0	2.74E–2	1.75E–3	1.10E–4	6.86E–6	4.29E–7
rate	—	3.21	1.98	2.00	2.00	2.00
$\varepsilon_0/2^2$	9.65E–1	9.87E–1	6.50E–2	3.90E–3	2.43E–4	1.52E–5
rate	—	-0.02	1.96	2.03	2.00	2.00
$\varepsilon_0/2^3$	3.06E–1	1.90E–1	2.68E+0	2.20E–2	1.18E–3	7.33E–5
rate	—	0.34	1.91	3.46	2.11	2.01
$\varepsilon_0/2^4$	2.73E–1	3.01E–1	3.05E–1	2.41E+0	5.40E–2	3.08E–3
rate	—	-0.07	0.01	-1.49	2.74	2.07
$\varepsilon_0/2^6$	2.03E+0	2.06E+0	1.95E+0	2.09E+0	2.09E+0	3.56E–1
rate	—	-0.01	0.04	-0.05	0.00	1.28
$\varepsilon_0/2^8$	2.66E+0	2.66E+0	2.68E+0	2.65E+0	2.71E+0	2.63E+0
rate	—	0.00	-0.01	0.01	-0.02	0.02

Table 2.4: Error analysis of EWI-D: $e^{\varepsilon,\tau}(T)$ with $T = 4$ and convergence rate.

EWI-D	$\tau_0 = 0.2$	$\tau_0/2^2$	$\tau_0/2^4$	$\tau_0/2^6$	$\tau_0/2^8$	$\tau_0/2^{10}$
$\varepsilon_0 = 0.5$	1.02E−1	5.97E−3	3.66E−4	2.29E−5	1.43E−6	9.05E−8
rate	—	2.05	2.01	2.00	2.00	1.99
$\varepsilon_0/2$	7.61E−2	3.25E−2	1.52E−3	9.37E−5	5.85E−6	3.66E−7
rate	—	0.61	2.21	2.01	2.00	2.00
$\varepsilon_0/2^2$	5.66E−1	6.04E−1	2.19E−2	1.19E−3	7.36E−5	4.60E−6
rate	—	-0.05	2.39	2.10	2.01	2.00
$\varepsilon_0/2^3$	1.10E−1	2.83E−1	2.96E−1	2.56E−3	1.41E−4	8.76E−6
rate	—	0.68	-0.03	3.43	2.09	2.00
$\varepsilon_0/2^4$	3.78E−1	5.85E−2	1.52E−1	1.57E−1	1.16E−3	6.47E−5
rate	—	1.35	0.69	-0.02	3.54	2.08
$\varepsilon_0/2^6$	1.03E+0	2.09E−1	5.92E−2	5.74E−3	1.17E−2	1.20E−2
rate	—	1.15	0.91	1.68	-1.17	-0.02
$\varepsilon_0/2^8$	1.39E−1	1.32E−2	7.17E−3	1.92E−3	6.57E−4	6.80E−5
rate	—	1.70	0.44	0.95	0.77	1.64

Table 2.5: Error analysis of EWI-F1: $\mathrm{e}^{\varepsilon,\tau}(T)$ with $T = 4$ and convergence rate.

MI-F1	$\tau_0 = 0.2$	$\tau_0/2^2$	$\tau_0/2^4$	$\tau_0/2^6$	$\tau_0/2^8$	$\tau_0/2^{10}$
$\varepsilon_0 = 0.5$	9.73E−1	6.98E−2	4.40E−3	2.72E−4	1.70E−5	1.01E−6
rate	—	1.90	2.00	2.00	2.00	2.04
$\varepsilon_0/2$	1.70E+0	1.30E−1	4.87E−2	3.20E−3	2.03E−4	1.26E−5
rate	—	1.85	0.71	1.96	1.99	2.00
$\varepsilon_0/2^2$	3.49E−1	3.49E−1	9.81E−1	1.01E−1	6.40E−3	4.02E−4
rate	—	0.00	-0.74	1.64	1.99	2.00
$\varepsilon_0/2^3$	2.76E+0	2.76E+0	2.76E+0	1.01E+0	3.33E−2	1.90E−3
rate	—	0.00	0.00	0.73	2.46	2.08
$\varepsilon_0/2^4$	2.26E+0	2.26E+0	2.26E+0	2.26E+0	1.35E+0	7.63E−2
rate	—	0.00	0.00	0.00	0.37	2.07
$\varepsilon_0/2^6$	2.04E+0	2.04E+0	2.04E+0	2.04E+0	2.04E+0	2.04E+0
rate	—	0.00	0.00	0.00	0.00	0.00
$\varepsilon_0/2^8$	2.66E+0	2.66E+0	2.66E+0	2.66E+0	2.66E+0	2.66E+0
rate	—	0.00	0.00	0.00	0.00	0.00

Table 2.6: Error analysis of EWI-F2: $\mathrm{e}^{\varepsilon,\tau}(T)$ with $T = 4$ and convergence rate.

MI-F2	$\tau_0 = 0.2$	$\tau_0/2^2$	$\tau_0/2^4$	$\tau_0/2^6$	$\tau_0/2^8$	$\tau_0/2^{10}$
$\varepsilon_0 = 0.5$	2.18E–1	1.30E–2	8.15E–4	5.09E–5	3.13E–6	1.44E–7
rate	—	2.03	2.00	2.00	2.01	2.21
$\varepsilon_0/2$	2.00E+0	1.54E–1	1.17E–2	7.41E–4	4.63E–5	2.81E–6
rate	—	1.85	1.86	1.99	2.00	2.02
$\varepsilon_0/2^2$	2.12E–1	4.99E–1	3.68E–1	2.48E–2	1.60E–3	9.66E–5
rate	—	-0.62	0.22	1.95	2.00	2.02
$\varepsilon_0/2^3$	2.77E+0	2.77E+0	2.75E+0	1.74E–1	7.50E–3	4.55E–4
rate	—	0.00	0.00	1.99	2.26	2.02
$\varepsilon_0/2^4$	2.25E+0	2.30E+0	2.30E+0	2.21E+0	3.32E–1	1.86E–2
rate	—	-0.01	0.00	0.03	1.37	2.08
$\varepsilon_0/2^6$	2.04E+0	2.04E+0	2.03E+0	2.08E+0	2.09E+0	1.99E+0
rate	—	0.00	0.00	-0.01	0.00	0.03
$\varepsilon_0/2^8$	2.66E+0	2.66E+0	2.66E+0	2.66E+0	2.67E+0	2.63E+0
rate	—	0.00	0.00	0.00	0.00	0.01

Table 2.7: Error analysis of CNFD : $e^{\varepsilon,\tau}(T)$ with $T = 4$ and convergence rate.

CNFD	$\tau_0 = 0.2$	$\tau_0/2^2$	$\tau_0/2^4$	$\tau_0/2^6$	$\tau_0/2^8$	$\tau_0/2^{10}$
$\varepsilon_0 = 0.5$	3.24E−1	4.49E−1	2.75E−2	1.71E−3	1.07E−4	6.69E−6
rate	—	-0.24	2.01	2.00	2.00	2.00
$\varepsilon_0/2$	1.75E+0	2.42E+0	1.90E−1	3.41E−2	2.21E−3	1.38E−4
rate	—	-0.23	1.84	1.24	1.97	2.00
$\varepsilon_0/2^2$	1.05E+0	1.50E+0	5.02E−1	3.54E−1	1.94E−1	1.24E−2
rate	—	-0.26	0.79	0.25	0.43	1.98
$\varepsilon_0/2^3$	3.78E−1	1.78E+0	3.71E−1	2.69E+0	2.60E+0	3.93E−1
rate	—	1.11	1.13	1.43	0.02	1.36
$\varepsilon_0/2^4$	6.49E−2	1.51E−1	1.05E+0	7.87E−1	5.36E−2	2.48E+0
rate	—	0.61	-1.40	0.21	1.94	-2.76
$\varepsilon_0/2^6$	1.95E+0	1.95E+0	1.97E+0	3.55E−1	2.46E+0	1.25E+0
rate	—	0.00	-0.01	1.24	-1.40	0.49
$\varepsilon_0/2^8$	3.63E−1	3.64E−1	3.64E−1	3.63E−1	5.75E−2	2.49E+0
rate	—	0.00	0.00	0.00	1.33	-2.72

Table 2.8: Error analysis of SIFD: $e^{\varepsilon,\tau}(T)$ with $T = 4$ and convergence rate.

SIFD	$\tau_0 = 0.2$	$\tau_0/2^2$	$\tau_0/2^4$	$\tau_0/2^6$	$\tau_0/2^8$	$\tau_0/2^{10}$
$\varepsilon_0 = 0.5$	7.61E−1	2.88E−1	1.76E−2	1.09E−3	6.83E−5	4.27E−6
rate	—	0.70	2.02	2.00	2.00	2.00
$\varepsilon_0/2$	2.32E−1	1.25E+0	2.13E−1	2.82E−2	1.82E−3	1.14E−4
rate	—	-1.21	1.28	1.46	1.98	2.00
$\varepsilon_0/2^2$	1.61E+0	1.15E+0	1.73E+0	5.08E−1	1.83E−1	1.17E−2
rate	—	0.24	-0.29	0.88	0.74	1.98
$\varepsilon_0/2^3$	2.42E−1	6.85E−1	5.05E−1	2.21E+0	2.50E+0	3.85E−1
rate	—	-0.75	0.22	-1.06	-0.09	1.35
$\varepsilon_0/2^4$	1.13E−1	4.44E−2	1.91E+0	3.28E−1	1.58E+0	2.48E+0
rate	—	0.67	-2.71	1.27	-1.13	-0.33
$\varepsilon_0/2^6$	1.95E+0	1.95E+0	1.92E+0	6.89E−1	2.05E+0	6.26E−1
rate	—	0.00	0.01	0.74	-0.78	0.86
$\varepsilon_0/2^8$	3.63E−1	3.63E−1	3.65E−1	3.63E−1	9.42E−2	2.70E+0
rate	—	0.00	-0.01	0.01	0.97	-2.42

Table 2.9: Error analysis of EXFD: $e^{\varepsilon,\tau}(T)$ with $T = 4$ and convergence rate.

EXFD	$\tau_0 = 0.2$	$\tau_0/2^2$	$\tau_0/2^4$	$\tau_0/2^6$	$\tau_0/2^8$	$\tau_0/2^{10}$
$\varepsilon_0 = 0.5$	8.84E–1	7.52E–2	4.66E–3	2.90E–4	1.81E–5	1.13E–6
rate	—	1.78	2.01	2.00	2.00	2.00
$\varepsilon_0/2$	unstable	2.51E+0	1.15E–1	6.49E–3	4.03E–4	2.51E–5
rate	—	—	2.22	2.07	2.01	2.00
$\varepsilon_0/2^2$	unstable	unstable	1.76E+0	6.36E–1	3.87E–2	2.41E–3
rate	—	—	—	0.73	2.02	2.00
$\varepsilon_0/2^3$	unstable	unstable	unstable	1.34E+0	1.23E+0	3.25E–2
rate	—	—	—	—	0.06	2.62
$\varepsilon_0/2^4$	unstable	unstable	unstable	unstable	9.96E–1	3.37E–1
rate	—	—	—	—	—	0.78
$\varepsilon_0/2^6$	unstable	unstable	unstable	unstable	unstable	unstable
rate	—	—	—	—	—	—
$\varepsilon_0/2^8$	unstable	unstable	unstable	unstable	unstable	unstable
rate	—	—	—	—	—	—

Table 2.10: Error of MTI-FA and MTI-F for HODE system: $e^{\varepsilon,\tau}(T)$ with $T = 1$.

MTI-FA	$\tau_0 = 0.1$	$\tau_0/2$	$\tau_0/4$	$\tau_0/8$	$\tau_0/16$
$\varepsilon_0 = 5 * 10^{-1}$	4.21E-02	1.22E-02	3.20E-03	8.13E-04	2.05E-04
$\varepsilon_0 = 5 * 10^{-2}$	2.50E-03	1.10E-03	4.70E-03	4.31E-04	3.70E-03
$\varepsilon_0 = 5 * 10^{-3}$	8.35E-06	2.27E-05	1.43E-06	2.79E-05	2.47E-05
$\varepsilon_0 = 5 * 10^{-4}$	8.63E-07	8.98E-07	9.13E-07	1.15E-07	1.60E-07
MTI-FA	$\tau_0 = 0.1$	$\tau_0/2$	$\tau_0/4$	$\tau_0/8$	$\tau_0/16$
$\varepsilon_0 = 5 * 10^{-1}$	4.01E-02	1.12E-02	2.90E-03	7.51E-04	1.90E-04
$\varepsilon_0 = 5 * 10^{-2}$	8.00E-03	2.20E-03	5.00E-03	4.69E-04	3.70E-03
$\varepsilon_0 = 5 * 10^{-3}$	5.00E-03	1.10E-03	2.83E-04	9.71E-05	7.59E-06
$\varepsilon_0 = 5 * 10^{-4}$	3.10E-03	6.94E-04	1.63E-04	3.94E-05	9.51E-06

Table 2.11: Error analysis of MTI-FA for general nonlinearity: $\mathrm{e}^{\varepsilon,\tau}(T)$ with $T = 1$.

$\mathrm{e}^{\varepsilon,\tau}(T)$	$\tau_0 = 0.2$	$\tau_0/2^2$	$\tau_0/2^4$	$\tau_0/2^6$	$\tau_0/2^8$	$\tau_0/2^{10}$	$\tau_0/2^{12}$
$\varepsilon_0 = 1$	1.97E–2	1.22E–3	7.35E–5	4.54E–6	2.83E–7	1.78E–8	1.25E–9
$\varepsilon_0/2$	6.92E–3	1.34E–3	7.42E–5	4.43E–6	2.73E–7	1.71E–8	1.19E–9
$\varepsilon_0/2^2$	1.61E–4	4.01E–4	4.04E–4	2.63E–5	1.66E–6	1.04E–7	6.53E–9
$\varepsilon_0/2^3$	1.21E–2	2.25E–3	5.63E–4	8.47E–5	4.91E–6	3.00E–7	1.84E–8
$\varepsilon_0/2^4$	9.04E–3	9.78E–4	1.68E–3	1.50E–3	1.58E–6	5.97E–9	2.37E–9
$\varepsilon_0/2^5$	9.27E–3	2.50E–4	6.14E–6	1.62E–3	5.86E–5	7.52E–6	4.87E–7
$\varepsilon_0/2^6$	3.96E–3	3.29E–4	8.48E–6	6.34E–7	9.40E–4	1.19E–4	1.91E–6
$\varepsilon_0/2^8$	1.89E–3	2.35E–4	2.90E–5	1.41E–7	8.47E–7	3.70E–7	5.17E–5
$\varepsilon_0/2^{10}$	1.27E–2	8.46E–4	5.46E–5	6.29E–6	1.26E–6	1.27E–6	1.08E–6
$\varepsilon_0/2^{12}$	1.59E–4	1.47E–4	1.13E–5	7.51E–7	3.46E–8	9.93E–8	3.49E–8
$\varepsilon_0/2^{14}$	9.89E–3	5.33E–4	3.18E–5	1.96E–6	1.17E–7	1.72E–9	4.97E–9

Table 2.12: Error analysis of MTI-F for general nonlinearity: $\mathrm{e}^{\varepsilon,\tau}(T)$ with $T = 1$.

$\mathrm{e}^{\varepsilon,\tau}(T)$	$\tau_0 = 0.2$	$\tau_0/2^2$	$\tau_0/2^4$	$\tau_0/2^6$	$\tau_0/2^8$	$\tau_0/2^{10}$	$\tau_0/2^{12}$
$\varepsilon_0 = 1$	5.79E−3	8.19E−4	5.28E−5	3.31E−6	2.07E−7	1.31E−8	9.53E-10
$\varepsilon_0/2$	7.54E−3	1.28E−3	6.87E−5	3.93E−6	2.39E−7	1.50E−8	1.05E−9
$\varepsilon_0/2^2$	3.05E−2	3.58E−4	3.99E−4	2.61E−5	1.65E−6	1.03E−7	6.48E−9
$\varepsilon_0/2^3$	1.19E−2	2.81E−3	4.99E−4	8.07E−5	4.67E−6	2.85E−7	1.75E−8
$\varepsilon_0/2^4$	8.83E−3	6.63E−4	1.43E−3	1.49E−3	1.28E−6	2.40E−8	3.48E−9
$\varepsilon_0/2^5$	9.52E−3	3.02E−4	8.66E−5	1.54E−3	5.89E−5	7.52E−6	4.87E−7
$\varepsilon_0/2^6$	3.76E−3	3.55E−4	4.82E−6	4.65E−6	9.35E−4	1.19E−4	1.91E−6
$\varepsilon_0/2^8$	1.89E−3	2.41E−4	2.87E−5	2.55E−7	8.33E−7	3.91E−7	5.17E−5
$\varepsilon_0/2^{10}$	1.27E−2	8.46E−4	5.47E−5	6.33E−6	1.25E−6	1.27E−6	1.08E−6
$\varepsilon_0/2^{12}$	1.59E−4	1.47E−4	1.13E−5	7.51E−7	3.51E−8	9.88E−8	3.53E−8
$\varepsilon_0/2^{14}$	9.89E−3	5.33E−4	3.17E−5	1.95E−6	1.06E−7	9.43E−9	1.62E−8

Chapter 3

Classical numerical methods for the Klein-Gordon equation

3.1 Introduction

This chapter deals with the relativistic Klein-Gordon equation (KGE) in d-dimensions ($d = 1, 2, 3$) under a proper non-dimensionlization as stated in Section 1.3.2 as

$$\varepsilon^2 \partial_{tt} u(\mathbf{x}, t) - \Delta u(\mathbf{x}, t) + \frac{1}{\varepsilon^2} u(\mathbf{x}, t) + f(u(\mathbf{x}, t)) = 0, \quad \mathbf{x} \in \mathbb{R}^d, t > 0, \tag{3.1.1a}$$

with initial conditions:

$$u(\mathbf{x}, 0) = \phi_1(\mathbf{x}), \qquad \partial_t u(\mathbf{x}, 0) = \frac{1}{\varepsilon^2} \phi_2(\mathbf{x}), \qquad \mathbf{x} \in \mathbb{R}^d. \tag{3.1.1b}$$

In this chapter, for simplicity, $u = u(\mathbf{x}, t)$ is considered to be a real-valued scalar field, the dimensionless parameter $0 < \varepsilon \leq 1$ is inversely proportional to the speed of light, ϕ_1 and ϕ_2 are two given real-valued functions independent of ε. $f(\cdot)$ is a real-valued function independent of ε. Provided that $u(\cdot, t) \in H^1(\mathbb{R}^d)$ and $\partial_t u(\cdot, t) \in L^2(\mathbb{R}^d)$, the KGE (3.1.1) conserves the *energy*,

$$\begin{aligned} E(t) &:= \int_{\mathbb{R}^d} \left[\varepsilon^2 \left(\partial_t u(\mathbf{x}, t) \right)^2 + |\nabla u(\mathbf{x}, t)|^2 + \frac{1}{\varepsilon^2} \left(u(\mathbf{x}, t) \right)^2 + F\left(u(\mathbf{x}, t) \right) \right] \mathrm{d}\mathbf{x} \qquad (3.1.2) \\ &\equiv \int_{\mathbb{R}^d} \left[\frac{1}{\varepsilon^2} \left(\phi_2(\mathbf{x}) \right)^2 + |\nabla \phi_1(\mathbf{x})|^2 + \frac{1}{\varepsilon^2} \left(\phi_1(\mathbf{x}) \right)^2 + F\left(\phi_1(\mathbf{x}) \right) \right] \mathrm{d}\mathbf{x} := E(0), \quad t \geq 0, \end{aligned}$$

with $F(u) := 2\int_0^u f(\rho)\,\mathrm{d}\rho,\ u \in \mathbb{R}$.

For a fixed $\varepsilon > 0$ in (3.1.1), a surge of analysis and numerics results have been reported in literatures. For instance, the Cauchy problem was considered in [19, 21, 63, 71, 96]. In particular, global existence of solutions was established in [21] for $F(u) \geq 0$ (defocusing case); and possible blow-up was shown in [19] for $F(u) < 0$ (focusing case). For other interesting results in this regime, we refer the readers to [2, 80, 87, 94, 98] and references given therein. For the regime $0 < \varepsilon \ll 1$ in (3.1.1), which corresponds to the nonrelativistic limit or the speed of light goes to infinity, analytical results in [10, 75–77, 81, 104] reveal that the solution propagates waves with wavelength of $O(\varepsilon^2)$ and $O(1)$ in time and, respectively, in space when $0 < \varepsilon \ll 1$. Detailed discussions will be given in the next chapter. The high oscillations in time make the numerical approximations of the KGE (3.1.1) in the nonrelativistic limit regime very challenging.

In this chapter, we are going to review and study some popular classical numerical methods which are proposed based on directly discretizing the KGE (3.1.1) or its equivalent integral form. Special efforts are made to study how the error bound of the numerical method depends on ε, as $0 < \varepsilon \ll 1$. By the recent work in [10], frequently used finite difference time discretization including energy conservative type and semi-implicit type finite difference discretizations [1, 38, 74, 99], and a Gautschi-type exponential wave integrator (EWI) [52, 53, 57, 62] were shown to have the temporal error bounds as $O(\varepsilon^{-6}\tau^2)$ and $O(\varepsilon^{-4}\tau^2)$, respectively. So in order to guarantee 'correct' approximations for ε small, one needs the constraint on time step $\tau = O(\varepsilon^3)$ for the finite difference methods and $\tau = O(\varepsilon^2)$ for the EWIs, respectively. A detailed review on these existing results is provided in Section 3.2. In the rest sections of this chapter, we shall propose and study a time-splitting integrator (or so-called split-step method), coupled with Fourier pseudospectral (TSFP) discretization in space, for the nonlinear KGE (3.1.1). The time-splitting schemes for evolution equations can be even dated back to 1970s [60]; however, few results are available so far when they are applied to the KGE (3.1.1), even with $\varepsilon = O(1)$.

In the literature, although time-splitting schemes are widely used to compute the solutions to nonlinear Schrödinger equation (NLSE) (see, e.g. [6,106]) and especially successful for the semiclassical NLSE whose solutions exhibit spatial-temporal oscillations (see [14, 15]), it dose not give any clue to their performance for KGE in highly oscillatory regime. The detailed numerical scheme of TSFP is given in Section 3.3. A key observation that TSFP is totally equivalent to an exponential wave integrator with the Deuflhard-type quadrature [36] Fourier pseudospectral method is pointed in Section 3.4. Thanks to this observation, the rigorous error estimate of TSFP is established in the relativistic regime, i.e. $\varepsilon = O(1)$. Numerical studies of the TSFP method in various regimes, ranging from the smooth regime for $\varepsilon = O(1)$ to the highly oscillatory regime for $0 < \varepsilon \ll 1$ are done in Section 3.5, which gear to suggest that the temporal discretization error bound for TSFP is $O(\varepsilon^{-2}\tau^2)$ as $0 < \varepsilon \ll 1$. Therefore, the time-splitting pseudospectral discretization offers compelling better approximations over other classical schemes, especially in the nonrelativistic limit regime.

3.2 Existing numerical methods

In this section, we shall briefly review the existing numerical methods for solving the KGE which temporally are parallel to those integrators introduced in Sections 2.2 and 2.3 for the highly oscillatory ODEs. For simplicity of notation, the methods are presented in 1D, and generalization to higher dimensions are straightforward due to the tensor product grids. In practice, we truncate the whole space problem onto an interval $\Omega = (a, b)$ with periodic boundary conditions. In 1D, the KGE (3.1.1) with periodic boundary conditions collapses to

$$\varepsilon^2 \partial_{tt} u(x,t) - \partial_{xx} u(x,t) + \frac{1}{\varepsilon^2} u(x,t) + f(u(x,t)) = 0, \quad a < x < b, \ t > 0, \tag{3.2.1a}$$

$$u(a,t) = u(b,t), \qquad \partial_x u(a,t) = \partial_x u(b,t), \qquad t \geq 0, \tag{3.2.1b}$$

$$u(x,0) = \phi_1(x), \qquad \partial_t u(x,0) = \frac{1}{\varepsilon^2}\phi_2(x), \qquad a \leq x \leq b. \tag{3.2.1c}$$

Such truncations are due to the fast decay of the solution of the KGE at the far field, and the boundary conditions are inspired by the physical backgrounds as well as most studies in literatures [10, 24, 30, 38, 43, 67, 99]. The finite interval $\Omega = (a, b)$ are usually chosen sufficiently large such that the truncation error is negligible.

3.2.1 Finite difference time domain methods

Denote mesh size $h = \Delta x = (b-a)/M$ with an even positive integer M, time step $\tau = \Delta t$, and denote grid points as $x_j = a + jh, t_n = n\tau (n = 0, 1, \ldots, j = 0, \ldots, M)$. Introduce the finite difference operators as

$$\delta_t^2 u_j^n = \frac{u_j^{n+1} - 2u_j^n + u_j^{n-1}}{\tau^2}, \quad \delta_x^+ u_j^n = \frac{u_{j+1}^n - u_j^n}{h} \quad \delta_x^2 u_j^n = \frac{u_{j+1}^n - 2u_j^n + u_{j-1}^n}{h^2}.$$

Then for $j = 0, 1, \ldots, M-1, n = 1, 2, \ldots,$ the energy conservative finite difference (ECFD) method [10, 99] reads

$$\varepsilon^2 \delta_t^2 u_j^n - \delta_x^2 \frac{u_j^{n+1} + u_j^{n-1}}{2} + \frac{1}{\varepsilon^2} \frac{u_j^{n+1} + u_j^{n-1}}{2} + G(u_j^{n+1}, u_j^{n-1}) = 0, \tag{3.2.2}$$

where $G(v, w) = \frac{F(v)-F(w)}{2(v-w)}$, and a semi-implicit finite difference (SIFD) method [10, 74] reads

$$\varepsilon^2 \delta_t^2 u_j^n - \delta_x^2 \frac{u_j^{n+1} + u_j^{n-1}}{2} + \frac{1}{\varepsilon^2} \frac{u_j^{n+1} + u_j^{n-1}}{2} + F(u_j^n) = 0. \tag{3.2.3}$$

ECFD conserves the energy (3.1.2) in the discrete level [10], but the full implicit scheme makes it very time consuming due to a necessary nonlinear solver at each time level and that motives the SIFD method. For the two finite difference methods, under assumptions:

$$f(\cdot) \in C^3(\mathbf{R}), \quad u \in C^4([0, T], W_p^{5,\infty}), \quad \left\| \frac{\partial^{r+s}}{\partial x^s \partial t^r} \right\| \lesssim \frac{1}{\varepsilon^{2r}}, \tag{3.2.4}$$

where $W_p^{5,\infty} := \left\{ u \in W^{5,\infty}(\Omega) : \partial_x^l u(a) = \partial_x^l u(b),\ l = 0, 1 \ldots, 4 \right\}$ and $T > 0$ within the maximum existence time of solutions, the following error estimates results for $e_j^n = u(x_j, t^n) - u_j^n$ can be obtained as in [10]:

Theorem 3.2.1. *Under assumption (3.2.4), assume $\tau \lesssim h$, there exist constants $\tau_0 > 0$ and $h_0 > 0$ sufficiently small and independent of ε such that for $0 < \varepsilon \leq 1$, when $0 < \tau \leq \tau_0 \varepsilon^3$ and $0 < h \leq h_0$, the ECFD (3.2.2) and SIFD (3.2.3) satisfy*

$$\|e^n\|_{l^2} + \|\delta_x^+ e^n\|_{l^2} \lesssim h^2 + \frac{\tau^2}{\varepsilon^6}, \quad 0 \leq n \leq \frac{T}{\tau}.$$

From the above error bounds, indeed one can see that in order to make a correct approximation to the KGE (3.2.1), even for the full implicit method, one need to choose time step $\tau = O(\varepsilon^3)$ and mesh size $h = O(1)$. As $0 < \varepsilon \ll 1$, these FD methods will cause too much numerical burden.

3.2.2 Exponential wave integrator with Gautschi's quadrature pseudospectral method

To improve the resolution capacity of the FD methods, an exponential wave integrator (EWI) with the Gautschi's quadrature Fourier pseudospectral method is proposed in [10]. Here we shall briefly review the scheme.

To do the pseudospectral discretization in space, besides those introduced in the previous subsection, we furthermore introduce the following notations. Let

$$X_M := \text{span}\{\mathrm{e}^{i\mu_l(x-a)},\ \mu_l = \frac{2\pi l}{b-a},\ x \in \Omega,\ -M/2 \leq l \leq M/2-1\},$$
$$Y_M := \left\{w = (w_0, w_1, \ldots, w_M) \in \mathbb{R}^{M+1}\ :\ w_0 = w_M\right\}.$$

For a general periodic function $w(x)$ on $\overline{\Omega} = [a, b]$ and a vector $w \in Y_M$, let $P_M : L^2(\Omega) \to X_M$ be the standard L^2- projection operator onto X_M, $I_M : C(\Omega) \to X_M$ and $I_M : Y_M \to X_M$ be the trigonometric interpolation operator [51, 61, 95], i.e.

$$(P_M w)(x) = \sum_{l=-M/2}^{M/2-1} \widehat{w}_l \mathrm{e}^{i\mu_l(x-a)}, \quad (I_M w)(x) = \sum_{l=-M/2}^{M/2-1} \widetilde{w}_l \mathrm{e}^{i\mu_l(x-a)}, \quad x \in \Omega, \tag{3.2.5}$$

where

$$\widehat{w}_l = \frac{1}{b-a}\int_a^b w(x)\mathrm{e}^{-i\mu_l(x-a)}\mathrm{d}x, \qquad \widetilde{w}_l = \frac{1}{M}\sum_{j=0}^{M-1} w_j \mathrm{e}^{-i\mu_l(x_j-a)}, \tag{3.2.6}$$

with w_j interpreted as $w(x_j)$ for a function w. It is easy to check that P_M and I_M are identical operators on X_M. The spectral discretization begins with finding $u_M(x,t) \in X_M$ to solve

$$\varepsilon^2 \partial_{tt} u_M(x,t) - \partial_{xx} u_M(x,t) + \frac{1}{\varepsilon^2} u_M(x,t) + P_M f(u_M(x,t)) = 0.$$

By the orthogonality of the bases in X_M, one ends up for $l = -M/2,\ldots,M/2-1$,

$$\varepsilon^2 \widehat{(u_M)}_l''(t) + (\mu_l^2 + \frac{1}{\varepsilon^2})\widehat{(u_M)}_l(t) + (\widehat{f(u_M)})_l(t) = 0.$$

Then with the variation-of-constant formula and similar derivations introduced in Chapter 2 Section 2.3, one can get an EWI with Gautschi's quadrature Fourier spectral method. Finally replacing the projections by interpolations in (5.2.2), one can get the EWI with Gautschi's quadrature Fourier pseudospectral (EWI-GFP) discretization proposed in [10] for solving (3.3.5). The detailed method is as follows:

$$u_j^{n+1} = \sum_{l=-M/2}^{M/2-1} \widetilde{u}_l^{n+1} \mathrm{e}^{i\mu_l(x_j-a)}, \qquad v_j^{n+1} = \sum_{l=-M/2}^{M/2-1} \widetilde{v}_l^{n+1} \mathrm{e}^{i\mu_l(x_j-a)}, \tag{3.2.7}$$

for $j = 0,1,\ldots,M,\ n = 0,1,\ldots,$ with,

$$\widetilde{u}_l^1 = \left[\cos(\beta_l^0\tau) + \frac{\alpha^0\,(1-\cos(\beta_l^0\tau))}{(\varepsilon\beta_l^0)^2}\right]\widetilde{u}_l^0 + \frac{\sin(\beta_l^0\tau)}{\beta_l^0}\widetilde{v}_l^0 + \frac{\cos(\beta_l^0\tau)-1}{(\varepsilon\beta_l^0)^2}\widetilde{f}_l^0, \tag{3.2.8}$$

$$\widetilde{v}_l^1 = -\beta_l \sin(\beta_l\tau)\widetilde{v}_l^0 + \cos(\beta_l\tau)\widetilde{v}_l^0 - \frac{\sin(\beta_l\tau)}{\varepsilon^2\beta_l}\widetilde{f}_l^0 \tag{3.2.9}$$

$$\widetilde{u}_l^{n+1} = -\widetilde{u}_l^{n-1} + 2\left[\cos(\beta_l^n\tau) + \frac{\alpha^n\,(1-\cos(\beta_l^n\tau))}{(\varepsilon\beta_l^n)^2}\right]\widetilde{u}_l^n + \frac{2\,(\cos(\beta_l^n\tau)-1)}{(\varepsilon\beta_l^n)^2}\widetilde{f}_l^n, \tag{3.2.10}$$

$$\widetilde{v}_l^{n+1} = \widetilde{v}_l^{n-1} - 2\beta_l \sin(\beta_l\tau)\widetilde{u}_l^n - 2\frac{\sin(\beta_l\tau)}{\varepsilon^2\beta_l}\widetilde{f}_l^n, \qquad n \geq 1. \tag{3.2.11}$$

Here for $n = 0,1,\ldots,$

$$\beta_l^n = \frac{1}{\varepsilon^2}\sqrt{1+\varepsilon^2(\mu_l^2+\alpha^n)}, \quad \alpha^n = \max\left\{\alpha^{n-1},\ \max_{u_j^n\neq 0} f(u_j^n)/u_j^n\right\}, \quad \alpha^{-1} = 0,$$

where α^n is introduced to ensure the unconditional stability [10].

For some positive integer $m_0 > 0$ depends on the regularity of the solution, an error bound is established in [10] as

Theorem 3.2.2. *Assume $\tau \lesssim \varepsilon^2 h$, there exist constants $\tau_0 > 0$ and $h_0 > 0$ sufficiently small and independent of ε such that for $0 < \varepsilon \leq 1$, when $0 < \tau \leq \tau_0$ and $0 < h \leq h_0$, the EWI-GFP (3.2.7)-(3.2.11) satisfies*

$$\|u(\cdot, t_n) - I_M(u^n)\|_{H^1} \lesssim h^{m_0} + \frac{\tau^2}{\varepsilon^4}, \quad 0 \leq n \leq \frac{T}{\tau}.$$

From the error bound, clearly one can see that in order to capture the $O(\varepsilon^2)$-oscillation in time when $0 < \varepsilon \ll 1$, the meshing strategy constraint for EWI-GFP method is $\tau = O(\varepsilon^2)$ and $h = O(1)$ for nonlinear KGE problem. Compared to FD methods, the resolution capacity in time of EWI-GFP is remarkably improved. Extensive numerical comparisons are already given in [10].

3.3 Time splitting pseudospectral method

Now, we are going to the study another popular classical numerical integrator: the time splitting method for temporal discretizations, coupled with the Fourier pseudospectral method for spatial discretizations. The starting point of the time splitting Fourier pseudospectral (TSFP) method is to rewrite the second order equation as an equivalent but simple form of first order system in time. The key ideas of the method are: (i) split the evolution system in a proper way such that the nonlinear subproblem can be integrated exactly in time space; (ii) solve the linear subproblem in phase space by applying the Fourier pseudospectral approximation to the spatial derivative and integrating the equations (which is a first order linear ODE system) about the Fourier coefficients exactly.

As a preparatory step, we begin by recalling the construction of a time-splitting (or split-step) integrator for a general evolution system in the form:

$$\partial_t \mathbf{y} = \Phi(\mathbf{y}) = \mathcal{A}\mathbf{y} + \mathcal{B}\mathbf{y}, \tag{3.3.1}$$

where the mapping $\Phi(\mathbf{y})$ is usually a nonlinear operator and the decoupling $\Phi(\mathbf{y}) = \mathcal{A}\mathbf{y} + \mathcal{B}\mathbf{y}$ (or called operator-splitting) can be arbitrary; in particular, $\mathcal{A}$ and $\mathcal{B}$ can be two non-commutative operators. With a given time step $\tau > 0$, let $t_n = n\tau$, $n =$

$0, 1, 2, \ldots$, and $\mathbf{y}^n$ be the approximation of $\mathbf{y}(t_n)$. A commonly used second-order time-splitting integrator for (3.3.1), $\mathbf{y}^{n+1} = [\Phi_2(\tau)]\,(\mathbf{y}^n)$, can be constructed due to the Strang formula [97],

$$\mathbf{y}^{(1)} = \exp\left(\frac{1}{2}\tau\mathcal{A}\right)\mathbf{y}^n, \quad \mathbf{y}^{(2)} = \exp\left(\tau\mathcal{B}\right)\mathbf{y}^{(1)}, \quad \mathbf{y}^{n+1} = \exp\left(\frac{1}{2}\tau\mathcal{A}\right)\mathbf{y}^{(2)}, \tag{3.3.2}$$

which is explicit and symmetric, i.e., $\Phi_2(\tau)\Phi_2(-\tau) = 1$. A fourth-order symplectic time integrator for (3.3.1), $\mathbf{y}^{n+1} = [\Phi_4(\tau)]\,(\mathbf{y}^n)$, is constructed as follows (cf. [16, 107]):

$$\Phi_4(\tau) = \Phi_2(\omega\tau)\Phi_2((1-2\omega)\tau)\Phi_2(\omega\tau), \tag{3.3.3}$$

where,

$$\omega = \frac{1}{3}\left(2 + 2^{1/3} + 2^{-1/3}\right). \tag{3.3.4}$$

Clearly, the above fourth-order integrator is still explicit and time reversible. It is also possible to construct higher-order symplectic integrators (cf. [107]). In general, the operators $\mathcal{A}$ and $\mathcal{B}$ may be interchanged without affecting the accuracy order of the method.

Introducing $v(x,t) = \partial_t u(x,t)$, then (3.2.1) is equivalent to the following first-order-in-time system,

$$\partial_t u(x,t) - v(x,t) = 0, \qquad a < x < b, \quad t > 0, \tag{3.3.5a}$$

$$\varepsilon^2\partial_t v(x,t) - \partial_{xx}u(x,t) + \frac{1}{\varepsilon^2}u(x,t) + f(u(x,t)) = 0, \ a < x < b, \ t > 0, \tag{3.3.5b}$$

$$u(a,t) = u(b,t), \qquad \partial_x u(a,t) = \partial_x u(b,t), \quad v(a,t) = v(b,t), \quad t \geq 0, \tag{3.3.5c}$$

$$u(x,0) = \phi_1(x), \qquad v(x,0) = \frac{1}{\varepsilon^2}\phi_2(x), \qquad a \leq x \leq b. \tag{3.3.5d}$$

We now rewrite the system (3.3.5a)-(3.3.5b) in the form of (3.3.1) with

$$\mathbf{y} = \begin{pmatrix} u \\ v \end{pmatrix}, \quad \mathcal{A}\begin{pmatrix} u \\ v \end{pmatrix} = \begin{pmatrix} 0 \\ -\varepsilon^{-2}f(u) \end{pmatrix}, \quad \mathcal{B}\begin{pmatrix} u \\ v \end{pmatrix} = \begin{pmatrix} v \\ \varepsilon^{-2}\partial_{xx}u - \varepsilon^{-4}u \end{pmatrix}.$$

Thus, the key to an efficient implementation of the time-splitting integrator $\Phi_2(\tau)$ or $\Phi_4(\tau)$ is to solve efficiently the following two subproblems:

$$\partial_t u(x,t) = 0, \qquad a < x < b, \quad t > 0, \tag{3.3.6a}$$

$$\partial_t v(x,t) + \frac{1}{\varepsilon^2} f(u(x,t)) = 0, \qquad a < x < b, \quad t > 0, \tag{3.3.6b}$$

and

$$\partial_t u(x,t) - v(x,t) = 0, \qquad a < x < b, \quad t > 0, \tag{3.3.7a}$$

$$\partial_t v(v,t) - \frac{1}{\varepsilon^2}\partial_{xx} u(x,t) + \frac{1}{\varepsilon^4} u(x,t) = 0, \qquad a < x < b, \quad t > 0, \tag{3.3.7b}$$

$$u(a,t) = u(b,t), \quad \partial_x u(a,t) = \partial_x u(b,t), \quad v(a,t) = v(b,t), \quad t \geq 0. \tag{3.3.7c}$$

The solutions to (3.3.6) are trivial by noting that (3.3.6a) leaves $u(x,t)$ invariant in t and therefore (3.3.6b) can be integrated exactly, i.e., for $t \geq t_s$ (t_s any given time),

$$u(x,t) = u(x,t_s), \quad v(x,t) = v(x,t_s) - \frac{1}{\varepsilon^2}(t-t_s) f(u(x,t_s)), \quad a < x < b, \ t \geq t_s.$$

Now, the issue remains to find an efficient and accurate method for (3.3.7). We shall solve (3.3.7) below in phase space by applying the Fourier spectral or pseudospectral approximation in space discretization; and in particular, the equations about the Fourier coefficients are linear ODEs which can be solved exactly.

Following the same notations introduced in Section 3.4, the Fourier spectral method for (3.3.7) is to find $u_M(x,t) \in X_M$ and $v_M(x,t) \in X_M$ (cf. [95]), i.e.,

$$u_M(x,t) = \sum_{l=-M/2}^{M/2-1} \widehat{u}_l(t) \mathrm{e}^{i\mu_l(x-a)}, \quad v_M(x,t) = \sum_{l=-M/2}^{M/2-1} \widehat{v}_l(t) \mathrm{e}^{i\mu_l(x-a)}, \quad x \in \Omega, \quad t \geq 0, \tag{3.3.8}$$

such that,

$$\partial_t u_M(x,t) - v_M(x,t) = 0, \qquad x \in \Omega, \quad t \geq 0, \tag{3.3.9a}$$

$$\partial_t v_M(v,t) - \frac{1}{\varepsilon^2}\partial_{xx} u_M(x,t) + \frac{1}{\varepsilon^4} u_M(x,t) = 0, \qquad x \in \Omega, \quad t \geq 0. \tag{3.3.9b}$$

Plugging (3.3.8) into (3.3.9), noticing the orthogonality of Fourier functions, we find,

$$\widehat{u}_l'(t) - \widehat{v}_l(t) = 0, \qquad \widehat{v}_l'(t) + \beta_l^2 \widehat{u}_l(t) = 0, \qquad l = -\frac{M}{2}, \ldots, \frac{M}{2} - 1, \quad t \geq 0.$$

where $\beta_l = \varepsilon^{-2}\sqrt{\varepsilon^2 \mu_l^2 + 1}$. The above system is a first order linear ODE system, whose analytical solutions can be obtained directly, i.e. for $t \geq t_s$ (t_s any given time) and $l = -M/2, \ldots, M/2 - 1$,

$$\widehat{u}_l(t) = \cos\left(\beta_l (t - t_s)\right) \widehat{u}_l(t_s) + \frac{\sin\left(\beta_l (t - t_s)\right)}{\beta_l} \widehat{v}_l(t_s), \tag{3.3.10a}$$

$$\widehat{v}_l(t) = -\beta_l \sin\left(\beta_l (t - t_s)\right) \widehat{u}_l(t_s) + \cos\left(\beta_l (t - t_s)\right) \widehat{v}_l(t_s). \tag{3.3.10b}$$

The above procedure for solving (3.3.7) is not suitable in practice due to the difficulty in evaluating the integrals in (3.2.6). Thus, we shall approximate the integrals in (3.2.6) by a quadrature rule on the grids $\{x_j\}_{j=0}^M$, i.e., replacing the projections by the interpolations, which refers to the Fourier pseudospectral approximation [95].

For $j = 0, 1, \ldots, M$ and $n = 0, 1, \ldots$, let u_j^n and v_j^n be the approximations of $u(x_j, t_n)$ and $v(x_j, t_n)$, denote by u^n and v^n the solution vectors with components u_j^n and v_j^n, and choose $u_j^0 = \phi_1(x_j)$ and $v_j^0 = \phi_2(x_j)/\varepsilon^2$. Then the second order time-splitting Fourier pseudospectral (TSFP) discretization for the 1D KGE (3.3.5) is given by

$$u_j^{n,+} = u_j^n, \qquad v_j^{n,+} = v_j^n - \frac{\tau}{2\varepsilon^2} f(u_j^n), \tag{3.3.11a}$$

$$u_j^{n+1,-} = \mathcal{L}_u(\tau, u^{n,+}, v^{n,+})_j, \qquad v_j^{n+1,-} = \mathcal{L}_v(\tau, u^{n,+}, v^{n,+})_j, \tag{3.3.11b}$$

$$u_j^{n+1} = u_j^{n+1,-}, \qquad v_j^{n+1} = v_j^{n+1,-} - \frac{\tau}{2\varepsilon^2} f(u_j^{n+1,-}). \tag{3.3.11c}$$

Here, $\mathcal{L}_u(\tau, U, V)_j$ and $\mathcal{L}_u(\tau, U, V)_j$ ($j = 0, 1, \ldots, M$) are computed from any $\tau \in \mathbb{R}$, $U = (U_0, U_1, \ldots, U_M)^T$ and $V = (V_0, V_1, \ldots, V_M)^T$:

$$\mathcal{L}_u(\tau, U, V)_j = \sum_{l=-M/2}^{M/2-1} \left[\cos(\beta_l \tau)\widetilde{U}_l + \frac{\sin(\beta_l \tau)}{\beta_l}\widetilde{V}_l\right] \mathrm{e}^{i\mu_l(x_j - a)},$$

$$\mathcal{L}_v(\tau, U, V)_j = \sum_{l=-M/2}^{M/2-1} \left[-\beta_l \sin(\beta_l \tau)\widetilde{U}_l + \cos(\beta_l \tau)\widetilde{V}_l\right] \mathrm{e}^{i\mu_l(x_j - a)},$$

$$\widetilde{U}_l = \frac{1}{M}\sum_{j=0}^{M-1} U_j \, \mathrm{e}^{-i\mu_l(x_j - a)}, \quad \widetilde{V}_l = \frac{1}{M}\sum_{j=0}^{M-1} V_j \, \mathrm{e}^{-i\mu_l(x_j - a)}, \quad l = -\frac{M}{2}, \ldots, \frac{M}{2} - 1.$$

A fourth order TSFP discretization for (3.3.5) can be constructed according to (3.3.3) in a similar way. We omit the details here for brevity.

The time discretization error of the TSFP discretization is only the splitting error, which is second/fourth order in τ. Moreover, TSFP is explicit, time symmetric and easy to be extended to 2D and 3D. The memory cost is $O(M)$ and computational load per time step is $O(M \ln M)$ thanks to FFT.

Remark 3.3.1. *Clearly, (3.3.11a) and (3.3.11c) imply that* $u^{n+1,+} = u^{n+1} = u^{u+1,-}$, *so the TSFP (3.3.11) can be implemented according to*

$$u_j^{n+1} = \mathcal{L}_u(\tau, u^n, v^{n,+})_j, \qquad v_j^{n+1,-} = \mathcal{L}_v(\tau, u^n, v^{n,+})_j,$$
$$v_j^{n+1,+} = v_j^{n+1,-} - \frac{\Delta t}{\varepsilon^2} f(u_j^{n+1}).$$

Thus, it is not necessary to output v^{n+1} *unless it is of interests.*

Remark 3.3.2. *Note that for the special case* $f(u) = 0$, *i.e., the linear problem, the TSFP collapses to the following one-step formula:*

$$u_j^{n+1} = \mathcal{L}_u((n+1)\tau, u^0, v^0)_j, \quad v_j^{n+1} = \mathcal{L}_v((n+1)\tau, u^0, v^0)_j, \quad n = 0, 1, \ldots,$$

thereby introducing no time discretization error.

3.4 EWI with Deuflhard's quadrature pseudospectral method

As a fact pointed out in [57, Section XIII.1.3], for the first-order-in-time evolution equations, the split-step method is reduced to a trigonometric integrator proposed by P. Deuflhard [36]. Here, we discuss an alternative approach to derive the proposed TSFP (3.3.11) via using the EWI with Deuflhard's quadrature in temporal discretization and Fourier pseudospectral discretization in space, which in consequence gives rise to a simple way to analyze the convergence of the splitting method.

3.4.1 Numerical scheme

Similar as the solver to (3.3.7), we seek for $u_M(x,t)$, $v_M(x,t) \in X_M$ defined in (3.3.8) as spatial approximations to solutions $u(x,t)$ and $v(x,t)$, respectively. Plugging $u_M(x,t)$ into (3.2.1) and applying the L^2-projection, we get

$$\varepsilon^2 \partial_{tt} u_M - \partial_{xx} u_M + \frac{1}{\varepsilon^2} u_M + P_M f(u_M) = 0.$$

Noticing the orthogonality of Fourier bases, we get

$$\varepsilon^2 \widehat{u}_l''(t) + \mu_l^2 \widehat{u}_l(t) + \frac{1}{\varepsilon^2} \widehat{u}_l(t) + \widehat{f(u_M)}_l(t) = 0, \quad l = -\frac{M}{2}, \ldots, \frac{M}{2} - 1, \quad t > 0. \tag{3.4.1}$$

By using the variation-of-constant formula and noting $v = \partial_t u$, we get

$$\begin{aligned} \widehat{u}_l(t) = & \cos\left(\beta_l (t - t_s)\right) \widehat{u}_l(t_s) + \frac{\sin\left(\beta_l (t - t_s)\right)}{\beta_l} \widehat{v}_l(t_s) \\ & - \int_{t_s}^{t} \frac{\sin\left(\beta_l (t - s)\right)}{\varepsilon^2 \beta_l} \widehat{f(u_M)}_l(s) \mathrm{d}s, \quad 0 \le t_s \le t. \end{aligned} \tag{3.4.2}$$

Taking derivative with respect to t on both sides of (3.4.2), we get

$$\begin{aligned} \widehat{v}_l(t) = & -\beta_l \sin\left(\beta_l (t - t_s)\right) \widehat{u}_l(t_s) + \cos\left(\beta_l (t - t_s)\right) \widehat{v}_l(t_s) \\ & - \int_{t_s}^{t} \frac{\cos\left(\beta_l (t - s)\right)}{\varepsilon^2} \widehat{f(u_M)}_l(s) \mathrm{d}s. \end{aligned} \tag{3.4.3}$$

Applying the standard trapezoidal rule to the two unknown integrations in (3.4.2) and (3.4.3), we get

$$\begin{aligned} \widehat{u}_l(t) \approx & \cos\left(\beta_l (t - t_s)\right) \widehat{u}_l(t_s) + \frac{\sin\left(\beta_l (t - t_s)\right)}{\beta_l} \widehat{v}_l(t_s) \\ & - \frac{t - t_s}{2\varepsilon^2 \beta_l} \sin\left(\beta_l (t - t_s)\right) \widehat{f(u_M)}(t_s), \\ \widehat{v}_l(t) \approx & -\beta_l \sin\left(\beta_l (t - t_s)\right) \widehat{u}_l(t_s) + \cos\left(\beta_l (t - t_s)\right) \widehat{v}_l(t_s) \\ & - \frac{t - t_s}{2\varepsilon^2} \left[\cos\left(\beta_l (t - t_s)\right) \widehat{f(u_M)}(t_s) + \widehat{f(u_M)}(t)\right]. \end{aligned}$$

Replacing the above Fourier spectral approximations by pseudospectral discretization, we obtain the following EWI with Deuflhard's quadrature Fourier pseudospectral (EWI-DFP) method. For $j = 0, 1, \ldots, M$ and $n = 0, 1, \ldots$, choosing $u_j^0 = \phi_1(x_j)$

and $v_j^0 = \phi_2(x_j)/\varepsilon^2$, then

$$u_j^{n+1} = \sum_{l=-M/2}^{M/2-1} \widetilde{u}_l^{n+1} \mathrm{e}^{i\mu_l(x_j-a)}, \quad v_j^{n+1} = \sum_{l=-M/2}^{M/2-1} \widetilde{v}_l^{n+1} \mathrm{e}^{i\mu_l(x_j-a)}, \quad n \geq 0, \tag{3.4.4a}$$

$$\widetilde{u}_l^{n+1} = \cos(\beta_l\tau)\, \widetilde{u}_l^n + \frac{\sin(\beta_l\tau)}{\beta_l} \widetilde{v}_l^n - \frac{\tau}{2\varepsilon^2\beta_l} \sin(\beta_l\tau)\, \widetilde{f}_l^n, \tag{3.4.4b}$$

$$\widetilde{v}_l^{n+1} = -\beta_l \sin(\beta_l\tau)\, \widetilde{u}_l^n + \cos(\beta_l\tau)\, \widetilde{v}_l^n - \frac{\tau}{2\varepsilon^2} \left[\cos(\beta_l\tau)\, \widetilde{f}_l^n + \widetilde{f}_l^{n+1}\right], \tag{3.4.4c}$$

where,

$$\widetilde{u}_l^n = \frac{1}{M} \sum_{j=0}^{M-1} u_j^n\, \mathrm{e}^{-i\mu_l(x_j-a)}, \quad \widetilde{v}_l^n = \frac{1}{M} \sum_{j=0}^{M-1} v_j^n\, \mathrm{e}^{-i\mu_l(x_j-a)},$$

$$\widetilde{f}_l^n = \frac{1}{M} \sum_{j=0}^{M-1} f(u_j^n)\, \mathrm{e}^{-i\mu_l(x_j-a)}.$$

A simple calculation shows that [37]

Theorem 3.4.1 (Equivalence of EWI-DFP and TSSP)**.** *The TSFP method (3.3.11) coincides with the EWI-DFP method (3.4.4). Thus, EWI-DFP is time symmetric.*

Proof. First, the initial choices of TSFP and EWI-DFP are the same, i.e. $u_j^0 = \phi_1(x_j)$, $v_j^0 = \phi_2(x_j)/\varepsilon^2$. From the TSFP method (3.3.11), plugging (3.3.11a) into (3.3.11b) and noticing from (3.3.11c) that $u^{n+1} = u^{n+1,-}$, we get

$$\widetilde{u}_l^{n+1} = \cos(\beta_l\tau)\widetilde{u}_l^n + \frac{\sin(\beta_l\tau)}{\beta_l} \left(\widetilde{v}_l^n - \frac{\tau}{2\varepsilon^2} \widetilde{f}_l^n\right), \tag{3.4.5}$$

which is indeed (3.4.4b) in the EWI-DFP method, and

$$\widetilde{v}_l^{n+1,-} = -\beta_l \sin(\beta_l\tau)\widetilde{u}_l^n + \cos(\beta_l\tau) \left(\widetilde{v}_l^n - \frac{\tau}{2\varepsilon^2} \widetilde{f}_l^n\right). \tag{3.4.6}$$

Plugging (3.4.6) into (3.3.11c), we are led to (3.4.4c) in the EWI-DFP method, which completes the proof. □

3.4.2 Error estimates

In this section, we will establish rigorously the error bounds of the TSFP method (3.3.11) in the energy space $H^1 \times L^2$ for fixed $\varepsilon = \varepsilon_0 = O(1)$ (the $O(1)$-speed of light

regime). Without loss of generality and for simplicity of notation, we set $\varepsilon = 1$ in this section. The rigorous arguments are achieved thanks to its equivalent formulation, i.e. the EWI-DFP method (3.4.4).

Let T_* be the maximum existence time for the solutions to the KGE (3.2.1). In order to establish the error estimates for the TSFP method, we make the following assumptions on the nonlinearity and the exact solutions: for $0 < T < T_*$,

$$f \in C^k(\mathbb{R}),\ u \in C\left([0,T]; W^{1,\infty} \cap H_p^{m_0+1}\right) \cap C^1\left([0,T]; W^{1,4} \cap H_p^{m_0}\right) \cap C^2\left([0,T]; H^1\right), \tag{3.4.7}$$

for some integer k, $m_0 \geq 2$. Under assumption (3.4.7), we let

$$m = \min\{k,\, m_0\}, \qquad K_1 = \|u\|_{L^\infty([0,T];L^\infty(\Omega)\cap H^1(\Omega))}, \qquad K_2 = \|\partial_t u\|_{L^\infty([0,T];L^2(\Omega))}.$$

Denote the trigonometric interpolations of numerical solutions as $u_I^n(x) := I_M(u^n)(x)$, $v_I^n(x) := I_M(v^n)(x)$, and define the error functions as

$$e^n(x) := u(x,t_n) - u_I^n(x), \quad \dot{e}^n(x) := \partial_t u(x,t_n) - v_I^n(x), \qquad x \in \Omega, \quad n \geq 0,$$

then we have the following main error estimate result [37]:

Theorem 3.4.2. *Let u^n and v^n be the numerical approximations obtained from the TSFP method (3.3.11). Under the assumption (3.4.7), there exit two constants τ_0, $h_0 > 0$, independent of τ (or n) and h, such that for any $0 < \tau < \tau_0$, $0 < h < h_0$,*

$$\|e^n\|_{H^1} + \|\dot{e}^n\|_{L^2} \lesssim \tau^2 + h^m, \qquad n = 0, \ldots, \frac{T}{\tau}, \tag{3.4.8a}$$

$$\|u_I^n\|_{H^1} \leq K_1 + 1, \qquad \|v_I^n\|_{L^2} \leq K_2 + 1, \qquad \|u^n\|_{l^\infty} \leq K_1 + 1. \tag{3.4.8b}$$

Thanks to the EWI-DFP formulism, the error estimates can be done in analogous lines as [10] by means of energy method. We first introduce the following notations.

Suppose u, v are exact solutions to KGE (3.3.5). Denote the L^2-projected solutions as [1]

$$\begin{aligned} u_M(x,t) &:= P_M(u(x,t)) = \sum_{l=-M/2}^{M/2-1} \widehat{u}_l(t) \mathrm{e}^{i\mu_l(x-a)}, \\ v_M(x,t) &:= P_M(v(x,t)) = \sum_{l=-M/2}^{M/2-1} \widehat{v}_l(t) \mathrm{e}^{i\mu_l(x-a)}, \end{aligned} \qquad x \in \Omega, \quad t \geq 0, \tag{3.4.9}$$

and the projected error functions as

$$\begin{aligned} e_M^n(x) &:= P_M(e^n(x)) = \sum_{l=-M/2}^{M/2-1} \widehat{e}_l^n \mathrm{e}^{i\mu_l(x-a)}, \\ \dot{e}_M^n(x) &:= P_M(\dot{e}^n(x)) = \sum_{l=-M/2}^{M/2-1} \widehat{\dot{e}}_l^n \mathrm{e}^{i\mu_l(x-a)}, \end{aligned} \qquad n = 0, \ldots, \frac{T}{\tau}. \tag{3.4.10}$$

Then we should have

$$\widehat{e}_l^n = \widehat{u}_l(t_n) - \widetilde{u}_l^n, \qquad \widehat{\dot{e}}_l^n = \widehat{v}_l(t_n) - \widetilde{v}_l^n, \qquad n = 0, \ldots, \frac{T}{\tau}. \tag{3.4.11}$$

Based on (3.4.4b) and (3.4.4c), define the local truncation errors as

$$\xi^n(x) := \sum_{l=-M/2}^{M/2-1} \widehat{\xi}_l \mathrm{e}^{i\mu_l(x-a)}, \quad \dot{\xi}^n(x) := \sum_{l=-M/2}^{M/2-1} \widehat{\dot{\xi}}_l \mathrm{e}^{i\mu_l(x-a)}, \ x \in \Omega, \ n = 0, \ldots, \frac{T}{\tau} - 1. \tag{3.4.12}$$

where

$$\begin{aligned} \widehat{\xi}_l^n &= \widehat{u}_l(t_{n+1}) - \cos(\beta_l \tau)\, \widehat{u}_l(t_n) - \frac{\sin(\beta_l \tau)}{\beta_l} \widehat{v}_l(t_n) \\ &\quad + \frac{\tau}{2\beta_l} \sin(\beta_l \tau)\, \widehat{(f_M)}_l(t_n), \end{aligned} \tag{3.4.13a}$$

$$\begin{aligned} \widehat{\dot{\xi}}_l^n &= \widehat{v}_l(t_{n+1}) + \beta_l \sin(\beta_l \tau)\, \widehat{u}_l(t_n) - \cos(\beta_l \tau)\, \widehat{v}_l(t_n) \\ &\quad + \frac{\tau}{2} \left(\cos(\beta_l \tau)\, \widehat{(f_M)}_l(t_n) + \widehat{(f_M)}_l(t_{n+1}) \right), \end{aligned} \tag{3.4.13b}$$

[1] We remark that the u_M defined in (3.4.9) is different with the one in spectral method formulation, since for the later case $u_M \approx P_M u$, and similar for v_M. Here we adopt the same notations for simplicity.

and $\beta_l = \sqrt{\mu_l^2 + 1}$, with $\widehat{(f_M)}_l(t)$ the Fourier coefficient of $f(u_M(x,t))$. Subtracting the local truncation errors (3.4.13) from the scheme (3.4.4b) and (3.4.4c), we are led to the error equations

$$\widehat{e}_l^{n+1} = \cos(\beta_l\tau)\,\widehat{e}_l^n + \frac{\sin(\beta_l\tau)}{\beta_l}\widehat{\dot{e}}_l^n + \widehat{\xi}_l^n - \widehat{\eta}_l^n, \tag{3.4.14a}$$

$$\widehat{\dot{e}}_l^{n+1} = -\beta_l \sin(\beta_l\tau)\,\widehat{e}_l^n + \cos(\beta_l\tau)\,\widehat{\dot{e}}_l^n + \widehat{\dot{\xi}}_l^n - \widehat{\dot{\eta}}_l^n, \tag{3.4.14b}$$

where

$$\widehat{\eta}_l^n = \frac{\tau}{2\beta_l}\sin(\beta_l\tau)\left(\widehat{(f_M)}_l(t_n) - \widetilde{f}_l^n\right), \tag{3.4.15a}$$

$$\widehat{\dot{\eta}}_l^n = \frac{\tau}{2}\left[\cos(\beta_l\tau)\left(\widehat{(f_M)}_l(t_n) - \widetilde{f}_l^n\right) + \left(\widehat{(f_M)}_l(t_{n+1}) - \widetilde{f}_l^{n+1}\right)\right], \tag{3.4.15b}$$

with the nonlinear error functions defined as

$$\eta^n(x) := \sum_{l=-M/2}^{M/2-1} \widehat{\eta}_l(t_n)\mathrm{e}^{i\mu_l(x-a)}, \quad \dot{\eta}^n(x) := \sum_{l=-M/2}^{M/2-1} \widehat{\dot{\eta}}_l(t_n)\mathrm{e}^{i\mu_l(x-a)}, \qquad x \in \Omega.$$

Define the error energy as

$$\mathcal{E}(P,Q) := \|P\|_{H^1}^2 + \|Q\|_{L^2}^2, \tag{3.4.16}$$

for two arbitrary functions $P(x)$ and $Q(x)$.

In order to proceed with the proof of Theorem 3.4.2, we give the following lemmas. Firstly, we have estimates for the local truncation errors, stated in the following lemma.

Lemma 3.4.1. *Based on assumption (3.4.7), we have estimates for the local truncation errors as*

$$\|\xi^n\|_{H^1} + \|\dot{\xi}^n\|_{L^2} \lesssim \tau^3 + \tau \cdot h^{m_0+1}, \qquad n = 0, \ldots, \frac{T}{\tau} - 1. \tag{3.4.17}$$

Proof. Applying L^2-projection on both sides of (3.2.1), due to the orthogonality and variation-of-constant formula, the Fourier coefficients $\widehat{u}_l(t_n), \widehat{u}_l(t_n)$ should satisfy

$$\widehat{u}_l(t_{n+1}) = \cos(\beta_l\tau)\,\widehat{u}_l(t_n) + \frac{\sin(\beta_l\tau)}{\beta_l}\widehat{v}_l(t_n) - \int_{t_n}^{t_{n+1}} \frac{\sin(\beta_l(t_{n+1}-s))}{\beta_l}\widehat{f}_l(s)\mathrm{d}s, \tag{3.4.18a}$$

$$\widehat{v}_l(t_{n+1}) = -\beta_l \sin(\beta_l\tau)\,\widehat{u}_l(t_n) + \cos(\beta_l\tau)\,\widehat{v}_l(t_n) - \int_{t_n}^{t_{n+1}} \cos(\beta_l(t_{n+1}-s))\,\widehat{f}_l(s)\mathrm{d}s, \tag{3.4.18b}$$

for $n = 0, \ldots, T/\tau$, where $\widehat{f_l}(t)$ denotes the Fourier coefficient of $f(u(x,t))$ for short, provided that no confusion occurs. Subtracting (3.4.18) from the local truncation errors (3.4.13), we get

$$\widehat{\xi}_l^n = \frac{\tau}{2\beta_l}\sin(\beta_l\tau)\,\widehat{(f_M)}_l(t_n) - \int_{t_n}^{t_{n+1}} \frac{\sin(\beta_l(t_{n+1}-s))}{\beta_l}\widehat{f_l}(s)\mathrm{d}s, \tag{3.4.19a}$$

$$\widehat{\dot{\xi}}_l^n = \frac{\tau}{2}\left[\cos(\beta_l\tau)\,\widehat{(f_M)}_l(t_n) + \widehat{(f_M)}_l(t_{n+1})\right] - \int_{t_n}^{t_{n+1}} \cos(\beta_l(t_{n+1}-s))\,\widehat{f_l}(s)\mathrm{d}s. \tag{3.4.19b}$$

For a general function $g(s) \in C^2$, we have the quadrature error for the standard trapezoidal rule written in the second order Peano form [46],

$$\frac{\tau}{2}(g(0)+g(\tau)) - \int_0^\tau g(s)\mathrm{d}s = \frac{\tau^3}{2}\int_0^1 \theta(1-\theta)g''(\theta\tau)\mathrm{d}\theta.$$

Rewriting $\widehat{\xi}_l^n$ in (3.4.19a) as

$$\begin{aligned}\widehat{\xi}_l^n =& \frac{\tau}{2\beta_l}\sin(\beta_l\tau)\,\widehat{f_l}(t_n) - \int_{t_n}^{t_{n+1}} \frac{\sin(\beta_l(t_{n+1}-s))}{\beta_l}\widehat{f_l}(s)\mathrm{d}s \\ &+ \frac{\tau}{2\beta_l}\sin(\beta_l\tau)\left[\widehat{(f_M)}_l(t_n) - \widehat{f_l}(t_n)\right],\end{aligned}$$

we then have,

$$\begin{aligned}\left|\widehat{\xi}_l^n\right| \lesssim& \tau^3\int_0^1 \theta(1-\theta)\left[\beta_l\left|\widehat{f_l}(t_n+\theta\tau)\right| + \left|\frac{\mathrm{d}}{\mathrm{d}s}\widehat{f_l}(t_n+\theta\tau)\right|\right]\mathrm{d}\theta \\ &+ \tau^3\int_0^1 \frac{\theta(1-\theta)}{\beta_l}\left|\frac{\mathrm{d}^2}{\mathrm{d}s^2}\widehat{f_l}(t_n+\theta\tau)\right|\mathrm{d}\theta + \frac{\tau}{\beta_l}\left|\widehat{(f_M)}_l(t_n) - \widehat{f_l}(t_n)\right|.\end{aligned} \tag{3.4.20}$$

Taking square on both sides of (3.4.20) and using the Cauchy's inequality, we get

$$\begin{aligned}\left|\widehat{\xi}_l^n\right|^2 \lesssim& \tau^6\int_0^1 \left[\beta_l^2\left|\widehat{f_l}(t_n+\theta\tau)\right|^2 + \left|\frac{\mathrm{d}}{\mathrm{d}s}\widehat{f_l}(t_n+\theta\tau)\right|^2\right]\mathrm{d}\theta \\ &+ \tau^6\int_0^1 \frac{1}{\beta_l^2}\left|\frac{\mathrm{d}^2}{\mathrm{d}s^2}\widehat{f_l}(t_n+\theta\tau)\right|^2\mathrm{d}\theta + \frac{\tau^2}{\beta_l^2}\left|\widehat{(f_M)}_l(t_n) - \widehat{f_l}(t_n)\right|^2.\end{aligned} \tag{3.4.21}$$

Multiplying both sides of (3.4.21) by $\beta_l^2 = (1+\mu_l^2)$ and then summing up for $l = -M/2, \ldots, M/2-1$, thanks to the Parseval's identity, we get

$$\begin{aligned}\|\xi^n\|_{H^1}^2 \lesssim& \tau^6 \cdot \sup_{0<t<T}\left[\|f(u)\|_{H^2}^2 + \|\partial_t f(u)\|_{H^1}^2 + \|\partial_{tt} f(u)\|_{L^2}^2\right] \\ &+ \tau^2\left\|f(u_M(\cdot,t_n)) - f(u(\cdot,t_n))\right\|_{L^2}^2.\end{aligned}$$

Then based on assumption (3.4.7) and the standard projection error bounds [95], we have

$$\|\xi^n\|_{H^1}^2 \lesssim \tau^6 + \tau^2 \cdot h^{2(m_0+1)}, \qquad n = 0, \ldots, \frac{T}{\tau} - 1. \tag{3.4.22}$$

Similarly, from (3.4.19b) we could get

$$\|\dot{\xi}^n\|_{L^2}^2 \lesssim \tau^6 + \tau^2 \cdot h^{2(m_0+1)}, \qquad n = 0, \ldots, \frac{T}{\tau} - 1. \tag{3.4.23}$$

Combining (3.4.22) and (3.4.23) gives the assertion (5.2.44). □

For the nonlinear error terms, we have estimates stated as the following lemma.

Lemma 3.4.2. *Based on assumption (3.4.7), and assume (3.4.8b) holds for some* $0 \le n \le T/\tau - 1$ *(which will be given by induction later), then we have*

$$\|\eta^n\|_{H^1} + \|\dot{\eta}^n\|_{L^2} \lesssim \tau \left(\|e_M^n\|_{L^2} + \|e_M^{n+1}\|_{L^2}\right) + \tau \cdot h^m. \tag{3.4.24}$$

Proof. From (5.2.42), we have

$$|\widehat{\eta}_l^n| \le \frac{\tau}{2\beta_l} \left| \widehat{(f_M)}_l(t_n) - \widetilde{f}_l^n \right|, \quad \left|\widehat{\dot{\eta}}_l^n\right| \le \frac{\tau}{2} \left[\left| \widehat{(f_M)}_l(t_n) - \widetilde{f}_l^n \right| + \left| \widehat{(f_M)}_l(t_{n+1}) - \widetilde{f}_l^{n+1} \right| \right].$$

For the first part, similarly as before, we can get

$$\|\eta^n\|_{H^1}^2 \le \frac{\tau^2}{4} \|P_M f(u_M(\cdot, t_n)) - I_M f(u^n)\|_{L^2}^2 .$$

Under assumption (3.4.7), we should have $f(u_M(x,t)) \in C([0,T]; H_p^m)$, then

$$\begin{aligned}
\|\eta^n\|_{H^1}^2 &\le \frac{\tau^2}{4} \|I_M f(u_M(\cdot, t_n)) - I_M f(u^n)\|_{L^2}^2 \\
&\quad + \frac{\tau^2}{4} \|P_M f(u_M(\cdot, t_n)) - I_M f(u_M(\cdot, t_n))\|_{L^2}^2 \\
&\lesssim \frac{\tau^2}{4} \|I_M f(u_M(\cdot, t_n)) - I_M f(u^n)\|_{L^2}^2 + \frac{\tau^2}{4} h^{2m}.
\end{aligned} \tag{3.4.25}$$

By Parseval's identity, together with the assumption (3.4.7) and (3.4.8b), we have

$$\begin{aligned}
&\|I_M f(u_M(\cdot, t_n)) - I_M f(u^n)\|_{L^2} = \|f(u_M(\cdot, t_n)) - f(u^n)\|_{l^2} \\
&= \left\| \int_0^1 f'\left(s u_M(\cdot, t_n) + (1-s) u^n\right) \mathrm{d}s \cdot \left(u_M(\cdot, t_n) - u^n\right) \right\|_{l^2} \\
&\lesssim \|u_M(\cdot, t_n) - u^n\|_{l^2} = \|u_M(\cdot, t_n) - I_M u^n\|_{L^2} = \|e_M^n\|_{L^2}.
\end{aligned} \tag{3.4.26}$$

Plugging the above estimate back to (3.4.25), we get

$$\|\eta^n\|_{H^1} \lesssim \tau\|e_M^n\|_{L^2} + \tau \cdot h^m. \tag{3.4.27}$$

For the second part, similarly, we can have

$$\begin{aligned}\|\dot{\eta}^n\|_{L^2}^2 \leq & \frac{\tau^2}{4}\left\|P_M f(u_M(\cdot,t_n)) - I_M f(u^n)\right\|_{L^2}^2 \\ & + \frac{\tau^2}{4}\left\|P_M f(u_M(\cdot,t_{n+1})) - I_M f(u^{n+1})\right\|_{L^2}^2 \\ \lesssim & \tau^2\|e_M^n\|_{L^2}^2 + \tau^2 \cdot h^{2m} + \tau^2\left\|I_M f(u_M(\cdot,t_{n+1})) - I_M f(u^{n+1})\right\|_{L^2}^2.\end{aligned} \tag{3.4.28}$$

To carry out a similar argument as (3.4.26), now we only need to show the maximum value of the numerical solution at t_{n+1} level, i.e. $\|u^{n+1}\|_{l^\infty}$, is bounded by some generic constant under assumption (3.4.8b). By the Sobolev's inequality,

$$\|u^{n+1}\|_{l^\infty} \leq \|u_I^{n+1}\|_{L^\infty} \lesssim \|u_I^{n+1}\|_{H^1} = \sqrt{(b-a)\sum_{l=-M/2}^{M/2-1}(1+\mu_l^2)|\widetilde{u}_l^{n+1}|^2}.$$

From (3.4.4b), we get

$$|\widetilde{u}_l^{n+1}| \leq |\widetilde{u}_l^n| + \frac{1}{\beta_l}|\widetilde{v}_l^n| + \frac{\tau}{2\beta_l}|\widetilde{f}_l^n|.$$

Then with $\tau \leq 1$ similarly as before, we can get

$$\begin{aligned}\|u_I^{n+1}\|_{H^1} &\leq 2\|u_I^n\|_{H^1} + 2\|v_I^n\|_{L^2} + \|f(u^n)\|_{l^2} \leq 2\|u_I^n\|_{H^1} + 2\|v_I^n\|_{L^2} + \|f(u^n)\|_{l^\infty} \\ &\leq 2(K_1+K_2+2) + \|f(\cdot)\|_{L^\infty(0,K_1+1)}.\end{aligned}$$

Thus, following the argument done as (3.4.26), we can get a further estimate for (3.4.28) as

$$\|\dot{\eta}^n\|_{L^2} \lesssim \tau\left(\|e_M^n\|_{L^2} + \|e_M^{n+1}\|_{L^2}\right) + \tau \cdot h^m. \tag{3.4.29}$$

Combing (3.4.27) and (3.4.29), we finish the proof. □

With the error energy functional notation (5.2.43), it is ready to show the following fact.

Lemma 3.4.3. *For $n = 0, \ldots, T/\tau - 1$, we have*

$$\mathcal{E}(e_M^{n+1}, \dot{e}_M^{n+1}) - \mathcal{E}(e_M^n, \dot{e}_M^n) \leq \tau \mathcal{E}(e_M^n, \dot{e}_M^n) + \frac{2}{\tau}\left[\mathcal{E}(\xi^n, \dot{\xi}^n) + \mathcal{E}(\eta^n, \dot{\eta}^n)\right]. \quad (3.4.30)$$

Proof. Multiplying (3.4.14a) with its complex conjugate, and by Cauchy's inequality, we have

$$\left|\widehat{e}_l^{n+1}\right|^2 \leq (1+\tau)\left|\cos(\beta_l\tau)\,\widehat{e}_l^n + \frac{\sin(\beta_l\tau)}{\beta_l}\widehat{\dot{e}}_l^n\right|^2 + \frac{1}{\tau}\left|\widehat{\xi}_l^n - \widehat{\eta}_l^n\right|^2. \quad (3.4.31)$$

Similarly for (3.4.14b), we have

$$\left|\widehat{\dot{e}}_l^{n+1}\right|^2 \leq (1+\tau)\left|-\beta_l \sin(\beta_l\tau)\,\widehat{e}_l^n + \cos(\beta_l\tau)\,\widehat{\dot{e}}_l^n\right|^2 + \frac{1}{\tau}\left|\widehat{\dot{\xi}}_l^n - \widehat{\dot{\eta}}_l^n\right|^2. \quad (3.4.32)$$

Multiplying (3.4.31) by $\beta_l^2 = 1 + \mu_l^2$ and then adding to (3.4.32), we get

$$\beta_l^2\left|\widehat{e}_l^{n+1}\right|^2 + \left|\widehat{\dot{e}}_l^{n+1}\right|^2 \leq (1+\tau)\left(\beta_l^2\left|\widehat{e}_l^n\right|^2 + \left|\widehat{\dot{e}}_l^n\right|^2\right) + \frac{1}{\tau}\left(\beta_l^2\left|\widehat{\xi}_l^n - \widehat{\eta}_l^n\right|^2 + \left|\widehat{\dot{\xi}}_l^n - \widehat{\dot{\eta}}_l^n\right|^2\right).$$

Summing the above inequalities up for $l = -M/2, \ldots, M/2-1$, and noticing (5.2.43) we get

$$\mathcal{E}(e_M^{n+1}, \dot{e}_M^{n+1}) \leq (1+\tau)\mathcal{E}(e_M^n, \dot{e}_M^n) + \frac{1}{\tau}\mathcal{E}(\xi^n - \eta^n, \dot{\xi}^n - \dot{\eta}^n),$$

and then by applying Cauchy's inequality again, we get assertion (5.2.61). □

Now, combining the Lemmas 5.2.1-5.2.3, we give the proof of Theorem 3.4.2 with the help of mathematical induction argument [10], or the so called cut-off technique [7] for the boundedness of numerical solutions.

Proof of Theorem 3.4.2. For $n = 0$, from the scheme and assumption (3.4.7),

$$\|e^0\|_{H^1} + \|\dot{e}^0\|_{L^2} = \|\phi_1 - I_M\phi_1\|_{H^1} + \|\phi_2 - I_M\phi_2\|_{L^2} \lesssim h^{m_0}.$$

Then by triangle inequality,

$$\|u_I^0\|_{H^1} \leq \|\phi_1\|_{H^1} + \|e^0\|_{H^1} \leq K_1 + 1,\ \|v_I^0\|_{L^2} \leq \|\phi_2\|_{L^2} + \|\dot{e}^0\|_{L^2} \leq K_2 + 1,\ 0 < h \leq h_1,$$

for some $h_1 > 0$ independent of τ and h, and obviously $\|u^0\|_{l^\infty} \leq K_1 + 1$. Thus, (3.4.8) is true for $n = 0$.

Assume (3.4.8) holds for $n \le N \le T/\tau - 1$. Now we need to show the results are still true for $n = N+1$. First, by triangle inequality,

$$\begin{aligned}\|e^n\|_{H^1} + \|\dot{e}^n\|_{L^2} &\le \|e_M^n\|_{H^1} + \|\dot{e}_M^n\|_{L^2} + \|u(\cdot,t_n) - u_M(\cdot,t_n)\|_{H^1} \\ &\quad + \|v(\cdot,t_n) - v_M(\cdot,t_n)\|_{L^2} \\ &\lesssim \|e_M^n\|_{H^1} + \|\dot{e}_M^n\|_{L^2} + h^{m_0}. \end{aligned} \tag{3.4.33}$$

Then from Lemma 5.2.3, we have for $n = 0, \dots, N$,

$$\mathcal{E}(e_M^{n+1}, \dot{e}_M^{n+1}) - \mathcal{E}(e_M^n, \dot{e}_M^n) \lesssim \tau \mathcal{E}(e_M^n, \dot{e}_M^n) + \frac{1}{\tau}\left[\mathcal{E}(\xi^n, \dot{\xi}^n) + \mathcal{E}(\eta^n, \dot{\eta}^n)\right].$$

Since (3.4.8b) is assumed to be true for all $n \le N$, we can plug the estimates in Lemmas 5.2.1 and 5.2.2 into the above estimate and get

$$\mathcal{E}(e_M^{n+1}, \dot{e}_M^{n+1}) - \mathcal{E}(e_M^n, \dot{e}_M^n) \lesssim \tau\left[\mathcal{E}(e_M^{n+1}, \dot{e}_M^{n+1}) + \mathcal{E}(e_M^n, \dot{e}_M^n)\right] + \tau^5 + \tau \cdot h^{2m}. \tag{3.4.34}$$

Summing (3.4.34) up for $n = 0, \dots, N$, and then by the discrete Gronwall's inequality, we get

$$\mathcal{E}(e_M^{N+1}, \dot{e}_M^{N+1}) \lesssim \tau^4 + h^{2m}.$$

Thus, we have $\|e_M^{N+1}\|_{H^1} + \|\dot{e}_M^{N+1}\|_{L^2} \le \tau^2 + h^m$, which together with (3.4.33) show (3.4.8b) is valid for $n = N+1$. Then by triangle inequality,

$$\begin{aligned} &\|u_I^{N+1}\|_{H^1} \le \|u(\cdot,t_{N+1})\|_{H^1} + \|e^{N+1}\|_{H^1} \le K_1 + 1, \\ &\|v_I^{N+1}\|_{L^2} \le \|v(\cdot,t_{N+1})\|_{L^2} + \|\dot{e}^{N+1}\|_{L^2} \le K_2 + 1, \end{aligned} \qquad 0 < \tau \le \tau_1, \;\; 0 < h \le h_2,$$

for some τ_1, $h_2 > 0$ independent of τ and h. Noting the Sobolev's inequality $\|e^N\|_{L^\infty} \lesssim \|e^N\|_{H^1}$, we also have

$$\|u^{N+1}\|_{l^\infty} \le \|u_I^{N+1}\|_{L^\infty} \le \|u(\cdot,t_{N+1})\|_{L^\infty} + \|e^{N+1}\|_{L^\infty} \le K_1 + 1,$$

for $0 < \tau \le \tau_2$, $0 < h \le h_3$ and τ_2, $h_3 > 0$ independent of τ and h. Therefore, the proof is completed by choosing $\tau_0 = \min\{\tau_1, \tau_2\}$ and $h_0 = \min\{h_1, h_2, h_3\}$. □

Remark 3.4.1. *In higher dimensional space, the Sobolev's inequality reads* $\|\rho\|_{L^\infty} \lesssim \|\rho\|_{H^2}$*, then one only need to rise the energy space for error functions to* $H^2 \times H^1$*, under a stronger regularity assumption than (3.4.7).*

Remark 3.4.2. *In the nonrelativistic limit regime, i.e. (3.2.1) with* $0 < \varepsilon \ll 1$*, following the analogous procedure made in this section, one can establish an error bound of the TSFP method (3.3.11) as*

$$\|e^n\|_{H^1} + \varepsilon\|\nabla e^n\|_{H^1} + \varepsilon^2\|\dot{e}^n\|_{H^1} \lesssim \frac{\tau^2}{\varepsilon^4} + h^m, \tag{3.4.35}$$

under a stronger regularity assumption than (3.4.7) and an oscillation assumption

$$\|u\| + \varepsilon^2\|\partial_t u\| + \varepsilon^4\|\partial_{tt} u\| \lesssim 1,$$

for certain norms. We omit the detailed arguments here for brevity.

The error bound (3.4.35) is quite similar to the one obtained in [10] for EWI-GFP, of which the ε*-dependence* $\tau \lesssim \varepsilon^2$ *has been numerically shown to be optimal for EWI-GFP. On the other hand, the error bound (3.4.35) also agrees with the expectation since the local truncation errors mainly come from trapezoidal quadrature, which is second-order accurate with a factor before* τ^2 *of the same order as* $\partial_{tt} u$*. However, our extensive numerical results, presented in the forthcoming section, will show that the* ε*-dependence in the estimate (3.4.35) is indeed not optimal for TSFP when* $0 < \varepsilon \ll 1$*. In fact, it suggests that the error of TSFP would asymptoticly behave like*

$$\|e^n\|_{H^1} \lesssim \frac{\tau^2}{\varepsilon^2} + h^m. \tag{3.4.36}$$

Thus, rigorous arguments towards an optimal error estimate of TSFP for $0 < \varepsilon \ll 1$ *are still absent, which will be the substantial work.*

3.5 Numerical results and comparisons

In this section, we report the numerical results of the classical method for solving the KGE (3.2.1) together with comparisons. Numerical comparisons between the FD methods and EWI-GFP are already systematically done in [10]. Here we focus on results for TSFP and comparisons with EWI-GFP. We will first test the TSFP method in the $O(1)$-speed of light regime. Then we will study the accuracy of

Table 3.1: Spatial discretization errors of TSFP at time $t = 1$ for different mesh sizes h under $\tau = 10^{-5}$.

$e^{\tau,h}$	$h = 1$	$h = 1/2$	$h = 1/4$	$h = 1/8$
$\lambda = 1$	$3.71E-2$	$1.70E-3$	$1.34E-6$	$2.22E-12$
$\lambda = -1$	$3.95E-2$	$1.70E-3$	$1.58E-6$	$2.53E-12$

Table 3.2: Temporal discretization errors of TSFP at time $t = 1$ for different time steps τ under $h = 1/16$ with convergence rate.

$e^{\tau,h}$	$\tau = 1/5$	$\tau = 1/10$	$\tau = 1/20$	$\tau = 1/40$	$\tau = 1/80$
$\lambda = 1$	$1.50E-3$	$3.65E-4$	$9.06E-5$	$2.26E-5$	$5.64E-6$
rate	–	2.03	2.01	2.00	2.00
$\lambda = -1$	$2.40E-3$	$6.14E-4$	$1.54E-4$	$3.84E-5$	$9.61E-6$
rate	–	1.97	2.00	2.00	2.00

TSFP for solving the KGE for $\varepsilon \in (0, 1)$, especially when $0 < \varepsilon \ll 1$. Since the oscillations of the problem happen in time and the temporal error is mainly concerned, so 1D problems are solved as examples. We choose the pure power nonlinearity $f(u) = \lambda u^{p+1}$ with $p = 2, \lambda = \pm 1$ in (3.2.1), and choose the initial conditions (3.2.1c) as

$$u(x,0) = \frac{3\sin(x)}{e^{0.5x^2} + e^{-0.5x^2}}, \qquad v(x,0) = \frac{2e^{-x^2}}{\sqrt{\pi}\varepsilon^2}, \qquad x \in \mathbb{R}.$$

We truncate the problem onto a finite domain $\Omega = [-16, 16]$, i.e. $b = -a = 16$, which is large enough to ignore the aliasing errors relative to the whole space problem.

3.5.1 Accuracy tests for $\varepsilon = O(1)$

We take fixed $\varepsilon = 1$ (i.e. the $O(1)$-speed of light regime). In this case, there is no analytical solution and we let $u(x,t)$ be the 'exact' solution which is obtained

Table 3.3: Conserved energy analysis of TSFP: $\tau = 10^{-3}$ and $h = 1/8$.

$E(t)$	$t = 0$	$t = 0.5$	$t = 1.0$	$t = 1.5$	$t = 2.0$
$\lambda = 1$	10.0957456	10.0957438	10.0957437	10.0957450	10.0957441
$\lambda = -1$	7.6534166	7.6534174	7.6534178	7.6534176	7.6534175

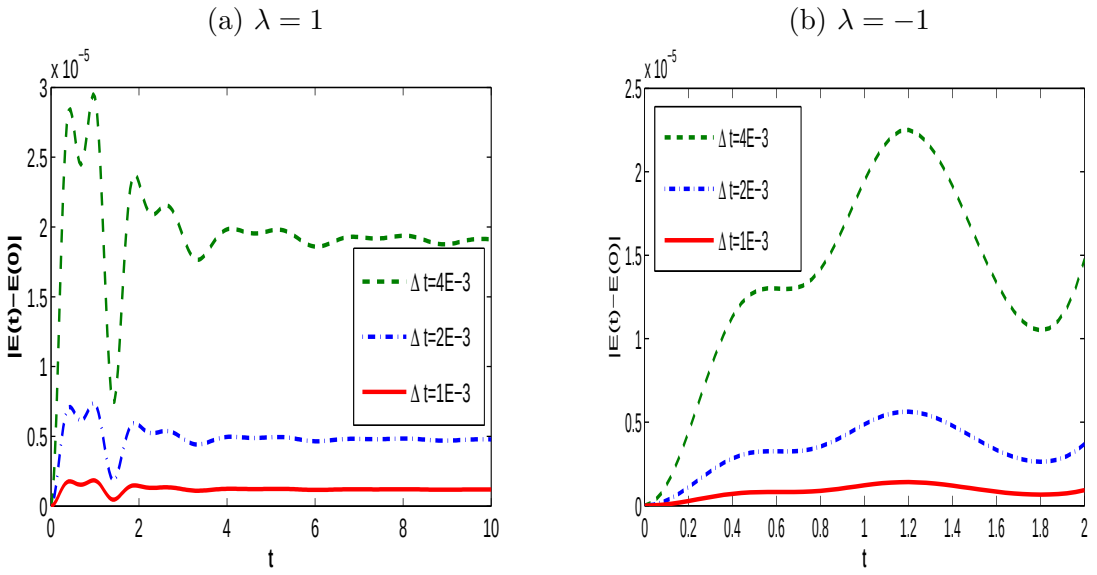

Figure 3.1: Energy error of TSFP in defocusing case ($\lambda = 1$) and focusing case ($\lambda = -1$): $|E(t) - E(0)|$ for different τ during the computing under $h = 1/8$ and $\varepsilon = 1$.

numerically by using TSFP method with very fine mesh size and small time step, e.g., $h = 1/32$ and $\tau = 10^{-5}$. We solve the problem on the interval $\Omega = [-16, 16]$ till time $t = 2$ in two cases: $\lambda = 1$ (defocusing case) and $\lambda = -1$ (focusing case). Here, we test the spatial and temporal discretization errors separately, and then test the conservation of the conserved energy of TSFP. To quantify the numerical results, we present the error:

$$\mathrm{e}^{\tau,h}(t = t_n) = \|e^n\|_{H^1} = \|u(\cdot, t_n) - I_M(u^n)\|_{H^1}\,. \tag{3.5.1}$$

Firstly, we test the discretization error in space, and in order to do this we take a very fine time step $\tau = 10^{-5}$ such that the error from time discretization is negligible compared to the spatial discretization error. Tab. 3.1 lists the errors (3.5.1) at time $t = 1$ with different mesh sizes h and parameters λ. Secondly, we test the discretization error in time, and mesh size is chosen as $h = 1/16$ such that the error from space discretization is negligible. Tab. 3.2 shows the errors (3.5.1) at time $t = 1$ with different time steps τ and parameters λ. Thirdly, we test the conservation of the energy $E(t)$ (3.1.2). Here we choose a small mesh size in space such that the energy $E(t = 0)$ which is approximated spectrally from the initial data is very close to the exact conserved energy. Tab. 3.3 lists the discrete energy at different time points with $\tau = 10^{-3}$ and $h = 1/8$. Fig. 3.1 shows the convergence of the energy error as τ decreases. Here for the focusing case, i.e. $\lambda = -1$, the results are only shown till $T = 2$ because of the finite time blow up of the solution.

From Tabs. 3.1-3.3 and Fig. 3.1, we can draw the following observations:

1. In the $O(1)$-speed of light regime, the TSFP (3.3.11) is of spectral-order accuracy in space, and is of second-order accuracy in time (cf. Tabs. 3.1&3.2), which verifies our error estimate (3.4.8a) and indicates the result is optimal.

2. TSFP conserves the energy very well. The energy obtained from the numerical solution is just a small fluctuation from the exact energy during the computation (cf. Tab. 3.3). As time step τ decreases to zero, the energy error during the computing converges to zero (cf. Fig. 3.1).

3.5.2 Convergence and resolution studies for $0 < \varepsilon \ll 1$

We now consider $\varepsilon \in (0, 1)$ in (3.2.1), in particular $0 < \varepsilon \ll 1$, i.e. the non-relativistic limit regime. Here we study the temporal and spatial errors of TSFP under different mesh sizes and time steps as $\varepsilon \to 0$. By doing so, we mainly want to investigate two questions. The first question is how the convergence/accuracy of the numerical method be affected as ε decays. The second question is within the

Table 3.4: Spatial error analysis of TSFP for different ε and h at time $t = 1$ under $\tau = 10^{-5}$.

TSFP	$h_0 = 1$	$h_0/2$	$h_0/4$	$h_0/8$
$\varepsilon_0 = 0.5$	7.99E-02	4.20E-03	3.01E-06	2.78E-12
$\varepsilon_0/2$	8.13E-02	5.40E-03	2.28E-06	2.84E-12
$\varepsilon_0/2^2$	2.77E-02	1.30E-03	1.07E-06	1.75E-12
$\varepsilon_0/2^3$	4.88E-02	4.60E-03	3.05E-06	1.67E-12
$\varepsilon_0/2^4$	8.24E-02	4.30E-03	2.74E-06	1.72E-12
$\varepsilon_0/2^6$	4.57E-02	5.00E-03	3.02E-06	1.89E-12

(a) TSFP (b) EWI-GFP

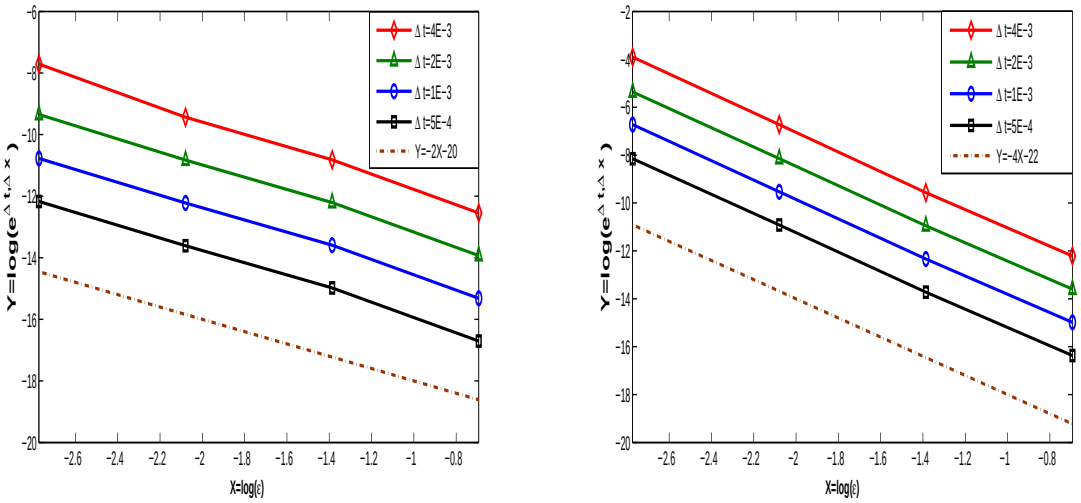

Figure 3.2: Dependence of the temporal discretization error on ε (in log-scale) for different τ at $t = 1$ under $h = 1/8$: (a) for TSFP and (b) for EWI-GFP.

convergence regime, how the error bound depends on ε. Again, the 'exact' solution $u(x, t)$ is obtained by a similar way as before. Since the numerical results of TSFP are similar in defocusing and focusing cases, so we here only consider a defocusing

Table 3.5: Temporal error analysis of TSFP for different ε and τ at time $t = 1$ under $h = 1/16$ with convergence rate.

TSFP	$\tau_0 = 0.2$	$\tau_0/2^2$	$\tau_0/2^4$	$\tau_0/2^6$	$\tau_0/2^8$	$\tau_0/2^{10}$
$\varepsilon_0 = 0.5$	1.52E-02	5.66E-04	3.49E-05	2.18E-06	1.36E-07	8.37E-09
rate	–	2.37	2.01	2.00	2.00	2.01
$\varepsilon_0/2^1$	1.27E-01	3.80E-03	1.97E-04	1.22E-05	7.62E-07	4.69E-08
rate	–	2.53	2.13	2.00	2.00	2.01
$\varepsilon_0/2^2$	1.13E-01	1.13E-01	8.93E-04	4.85E-05	3.01E-06	1.85E-07
rate	–	0.00	3.49	2.10	2.01	2.01
$\varepsilon_0/2^3$	1.21E-01	4.57E-02	4.52E-02	2.33E-04	1.27E-05	7.76E-07
rate	–	0.70	0.01	3.80	2.10	2.02
$\varepsilon_0/2^4$	1.35E-01	8.90E-03	1.02E-02	1.04E-02	6.75E-05	3.69E-06
rate	–	1.97	-0.98	-0.01	3.62	2.10
$\varepsilon_0/2^6$	1.38E-01	1.42E-02	3.70E-03	4.90E-04	6.70E-04	6.83E-04
rate	–	1.64	0.97	1.46	-0.22	-0.01
$\varepsilon_0/2^8$	8.80E-02	1.99E-02	2.10E-02	7.54E-04	2.32E-04	1.62E-05
rate	–	1.07	-0.04	2.40	0.85	1.92
$\varepsilon_0/2^{10}$	1.14E-01	5.43E-02	1.50E-03	1.00E-03	1.10E-03	3.78E-05
rate	–	0.53	2.58	0.26	-0.09	2.43

case with $\lambda = 1$ as a numerical example.

The spatial error and temporal error here are computed in a similar way as before. For the error in space, either from our numerical experience or from the theoretical result (3.4.35) and estimates in [10] , the spatial errors of TSFP and EWI-GFP are almost the same due to the same spectral discretization used in space. Thus here we omit the results of EWI-GFP for brevity and tabulate the spatial error of TSFP under different ε and mesh sizes h in Tab. 3.4. Tabs. 3.5&3.6 show the temporal error of TSFP and EWI-GFP, respectively, under different ε and time steps τ. To

Table 3.6: Temporal error analysis of EWI-GFP for different ε and τ at time $t = 1$ under $h = 1/16$ with convergence rate.

EWI-GFP	$\tau_0 = 0.2$	$\tau_0/2^2$	$\tau_0/2^4$	$\tau_0/2^6$	$\tau_0/2^8$	$\tau_0/2^{10}$
$\varepsilon_0 = 0.5$	1.96E-02	7.82E-04	4.87E-05	3.04E-06	1.90E-07	1.20E-08
rate	–	2.32	2.00	2.00	2.00	1.99
$\varepsilon_0/2$	4.37E-01	1.16E-02	6.86E-04	4.29E-05	2.68E-06	1.68E-07
rate	–	2.61	2.04	2.00	2.00	2.00
$\varepsilon_0/2^2$	1.19E-01	4.98E-01	1.17E-02	7.09E-04	4.43E-05	2.77E-06
rate	–	-1.03	2.71	2.02	2.00	2.00
$\varepsilon_0/2^3$	1.68E-01	1.64E-01	4.73E-01	1.19E-02	7.06E-04	4.41E-05
rate	–	0.02	-0.46	2.66	2.04	2.00
$\varepsilon_0/2^4$	1.76E-01	1.85E-01	1.96E-01	6.85E-01	1.12E-02	6.63E-04
rate	–	-0.04	-0.04	-0.90	2.96	2.04
$\varepsilon_0/2^6$	1.13E-01	2.04E-01	2.22E-01	2.17E-01	2.20E-01	8.77E-01
rate	–	-0.42	-0.06	0.02	-0.01	-0.99
$\varepsilon_0/2^8$	1.53E-01	1.94E-01	2.01E-01	4.00E-01	2.13E-01	5.72E-01
rate	–	-0.17	-0.03	-0.04	0.45	-0.71
$\varepsilon_0/2^{10}$	1.76E-01	1.99E-01	2.09E-01	2.12E-01	2.16E-01	2.14E-01
rate	–	-0.08	-0.04	-0.01	-0.01	0.01

study the error bounds of the numerical methods inside the convergence regime, we plot the temporal discretization errors of TSFP and EWI-GFP as functions of ε for some fixed τ in log-scale. The results are shown in Fig. 3.2. Moreover, we study the performance of TSFP in temporal approximations in Tab. 3.7 under the meshing strategy $\tau = O(\varepsilon^2)$, which is the exact ε-scalability of EWI-GFP [10].

From Tabs. 3.5-3.7 and Fig. 3.2, we can draw the following observations:

1. TSFP has uniform spectral accuracy in space for all $\varepsilon \in (0, 1]$ (cf. each column

Table 3.7: ε-scalability analysis: temporal error at time $t = 1$ with $h = 1/16$ for different τ and ε under meshing requirement $\tau = c \cdot \varepsilon^2$.

TSFP	$\varepsilon_0 = 0.5$	$\varepsilon_0/2$	$\varepsilon_0/4$	$\varepsilon_0/8$	$\varepsilon_0/16$
$c = 0.8$	1.52E-02	3.80E-03	8.93E-04	2.33E-04	6.75E-05
$c = 0.4$	2.40E-03	8.10E-04	1.99E-04	5.20E-05	1.52E-05
$c = 0.2$	5.66E-04	1.97E-04	4.85E-05	1.27E-05	3.69E-06
EWI-GFP	$\varepsilon_0 = 0.5$	$\varepsilon_0/2$	$\varepsilon_0/4$	$\varepsilon_0/8$	$\varepsilon_0/16$
$c = 0.8$	1.96E-02	1.16E-02	1.17E-02	1.19E-02	1.12E-02
$c = 0.4$	3.20E-03	2.70E-03	2.90E-03	2.90E-03	2.70E-03
$c = 0.2$	7.82E-04	6.86E-04	7.09E-04	7.06E-04	6.63E-04

in Tab. 3.4). The spatial discretization error is totally independent of ε. Thus the spatial resolution of TSFP is

$$h = O(1), \qquad 0 < \varepsilon \ll 1,$$

i.e. the mesh size can be chosen independent of ε, which is the same as EWI-GFP [10].

2. As ε vanishes, both TSFP and EWI-GFP are second-order accurate in time when τ is sufficiently small, i.e. within the convergence regime $\tau \lesssim \varepsilon^2$, (cf. the upper diagonal part of Tabs. 3.5&3.6). Both methods either have some convergence order reductions or lose the convergence outside the convergence regime (cf. the lower diagonal part of Tabs. 3.5&3.6). Between the two numerical methods, TSFP always offers better temporal approximations than EWI-GFP under the same time step, especially when ε becomes small (cf. Tabs. 3.5&3.6).

3. The temporal discretization error bound of EWI-GFP within the convergence regime behaves like $O(\varepsilon^{-4}\tau^2)$ (cf. Fig. 3.2(b)) and the ε-scalability is $\tau =$

$O(\varepsilon^2)$ which are consistent with the results in [10]. Fig. 3.2(a) indicates that the temporal error bound of TSFP would asymptotically behave like $O(\varepsilon^{-2}\tau^2)$ within the convergence regime, which on the other hand indicates that the estimate provided in (3.4.35) is not optimal in time. Tab. 3.7 illustrates a clearly second convergence in terms of ε for the temporal error of TSFP as $\varepsilon \to 0$ under the mesh strategy $\tau = O(\varepsilon^2)$, while EWI-GFP shows no convergence, which again indicate the temporal error bounds for the two methods and shows that TSFP will dominant in the highly oscillatory regime.

Chapter 4

Multiscale methods for the Klein-Gordon equation

4.1 Existing results in the limit regime

In this section, we continue with the KGE given in Section 1.3.2:

$$\varepsilon^2 \partial_{tt} u(\mathbf{x},t) - \Delta u(\mathbf{x},t) + \frac{1}{\varepsilon^2} u(\mathbf{x},t) + f(u(\mathbf{x},t)) = 0, \quad \mathbf{x} \in \mathbb{R}^d, \ t > 0, \tag{4.1.1a}$$

$$u(\mathbf{x},0) = \phi_1(\mathbf{x}), \qquad \partial_t u(\mathbf{x},0) = \frac{1}{\varepsilon^2}\phi_2(\mathbf{x}), \qquad \mathbf{x} \in \mathbb{R}^d, \tag{4.1.1b}$$

with the dimensionless parameter $0 < \varepsilon \leq 1$. Here we consider the initial data ϕ_1, ϕ_2 and the unknown u as complex-valued scalar functions, and the nonlinearity $f(\cdot) : \mathbb{C} \to \mathbb{C}$ is independent of ε satisfying the gauge invariance (1.3.8). Provided that $u(\cdot,t) \in H^1(\mathbb{R}^d)$ and $\partial_t u(\cdot,t) \in L^2(\mathbb{R}^d)$, for $f(u) = g(|u|^2)u$ with $g(\cdot)$ a real-valued function, the KGE (1.3.7) conserves the *energy*:

$$\begin{aligned} E(t) &:= \int_{\mathbb{R}^d} \left[\varepsilon^2 \left|\partial_t u(\mathbf{x},t)\right|^2 + \left|\nabla u(\mathbf{x},t)\right|^2 + \frac{1}{\varepsilon^2}\left|u(\mathbf{x},t)\right|^2 + F\left(|u(\mathbf{x},t)|^2\right) \right] \mathrm{d}\mathbf{x} \quad (4.1.2) \\ &\equiv \int_{\mathbb{R}^d} \left[\frac{1}{\varepsilon^2}\left|\phi_2(\mathbf{x})\right|^2 + \left|\nabla \phi_1(\mathbf{x})\right|^2 + \frac{1}{\varepsilon^2}\left|\phi_1(\mathbf{x})\right|^2 + F\left(|\phi_1(\mathbf{x})|^2\right) \right] \mathrm{d}\mathbf{x} := E(0), \ t \geq 0, \end{aligned}$$

with $F(\varrho) := \int_0^\varrho g(\rho)\mathrm{d}\rho$.

Over the past decade, more attentions on the study of KGE have been paid to the regime $0 < \varepsilon \ll 1$, which corresponds to the nonrelativistic limit or the

speed of light goes to infinity. In this regime, the analysis and efficient simulation are mathematically rather complicated issues; see, e.g. [10, 75–77, 81, 104]. In fact, due to that the energy $E(t) = O(\varepsilon^{-2})$ in (4.1.2) becomes unbounded when $\varepsilon \to 0$, significant difficulties are brought into the mathematical analysis of the problem (4.1.1) in the nonrelativistic limit regime. Recently, Machihara *et al.* [76] studied the nonrelativistic limit in the energy space, and Masmoudi *et al.* [77] analyzed the similar limit in a strong topology of the energy space. Their results show that the nonlinear KGE converges to two coupled nonlinear Schrödinger equations (NLSE) as the speed of light tends to infinity, that is for the solution $u(\mathbf{x}, t)$ of (4.1.1),

$$u(\mathbf{x},t) - \mathrm{e}^{it/\varepsilon^2} z_+(\mathbf{x},t) - \mathrm{e}^{-it/\varepsilon^2}\overline{z_-}(\mathbf{x},t) \to 0 \quad \text{in } C([0,T^*);H^1), \quad \text{as } \varepsilon \to 0, \tag{4.1.3}$$

where $z_\pm(\mathbf{x}, t)$ is the solution of the coupled NLSE

$$\begin{aligned} &2i\partial_t z_\pm(\mathbf{x},t) - \Delta z_\pm(\mathbf{x},t) + f_\pm(z_+(\mathbf{x},t), z_-(\mathbf{x},t)) = 0, \quad \mathbf{x} \in \mathbf{R}^d, \ t > 0, \\ &z_+(\mathbf{x},0) = \frac{1}{2}(\phi_1(\mathbf{x}) - i\phi_2(\mathbf{x})), \quad z_-(\mathbf{x},0) = \frac{1}{2}(\overline{\phi_1}(\mathbf{x}) - i\overline{\phi_2}(\mathbf{x})), \end{aligned} \tag{4.1.4}$$

with the maximal existence time of solutions $T^* > 0$ and $f_\pm(z_+, z_-) = \frac{1}{2\pi}\int_0^{2\pi} f(z_\pm + \mathrm{e}^{i\theta}\overline{z_\mp})d\theta$. For more recent progresses made to understand this limit, we refer to [81, 104]. Based on their results, the solution propagates waves with wavelength of $O(\varepsilon^2)$ and $O(1)$ in time and in space, respectively, when $0 < \varepsilon \ll 1$. To illustrate this, Fig. 4.1 shows the solution of the KGE (4.1.1) with $d = 1$, $f(u) = |u|^2 u$, $\phi_1(x) = e^{-x^2/2}$ and $\phi_2(x) = \frac{3}{2}\phi_1(x)$ for different ε. As discussed in previous chapters, the high oscillations in time bring challenges to the computations of the KGE in the nonrelativistic limit regime. The time step of classical numerical methods such as FD and EWIs, is severely restricted by the ε. Thus, recent studies turns to design numerical methods based on some proper transformed formulism of the KGE instead of approximating it directly. By (4.1.3), an asymptotic preserving method that requests $h = O(1)$ and $\tau = O(1)$ when $0 < \varepsilon \ll 1$, is proposed in [43] by solving the NLSE (4.1.4), but it clearly brings $O(1)$-error when $\varepsilon = \varepsilon_0 = O(1)$. Thus all the above numerical methods for the problem (4.1.1) do not converge uniformity

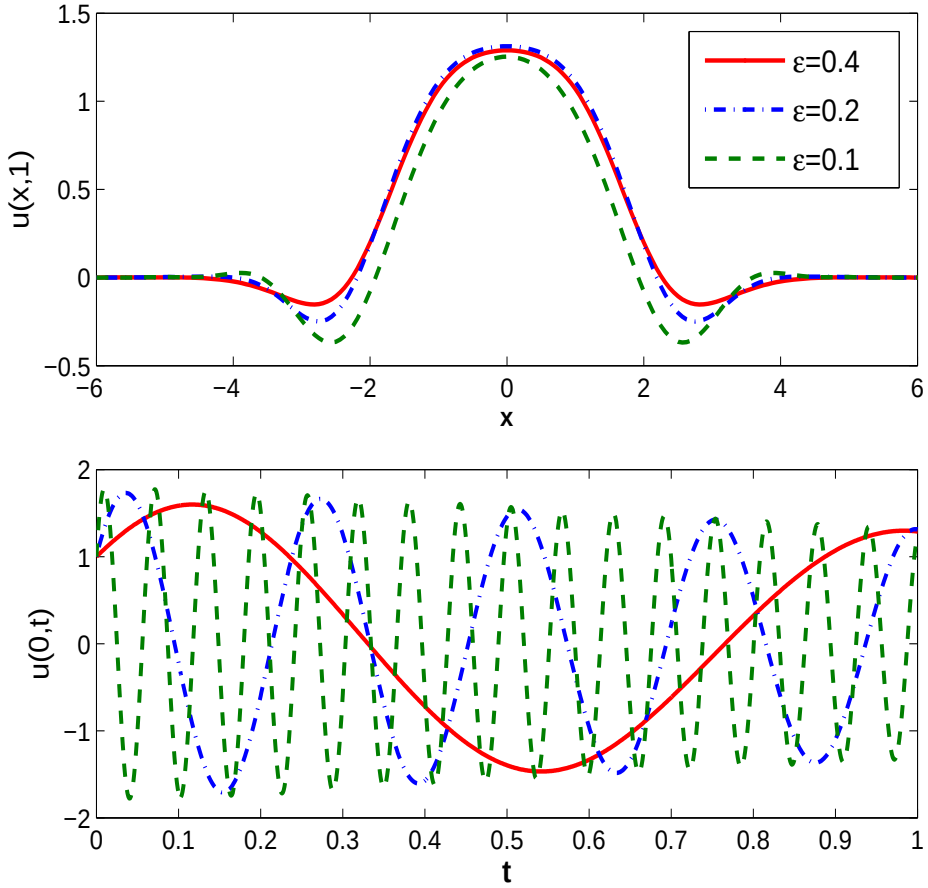

Figure 4.1: The solution of (4.1.1) with $d = 1$, $f(u) = |u|^2 u$, $\phi_1(x) = e^{-x^2/2}$ and $\phi_2(x) = \frac{3}{2}\phi_1(x)$ for different ε.

for $\varepsilon \in (0, 1]$ [10, 43]. Very recently, some uniformly accurate numerical schemes for high oscillatory Klein-Gordon and nonlinear Schrödinger equations have been proposed and analyzed [26] based on embedding the problem in a suitable "two-scale" reformulation with the induction of an additional variable and using the Chapman-Enskog expansion to separate the fast time scale and the slow one.

In Chapter 2, by using the highly oscillatory second-order ordinary differential equation (2.1.1) which has the same oscillatory nature as the problem (4.1.1) in time, we proposed and analyzed two multiscale time integrators (MTIs) based on multiscale decompositions of the solution. The two MTIs converge uniformly for $\varepsilon \in (0, 1]$ and have some advantages compared to the FDTD and EWIs as well as

asymptotic preserving methods in integrating highly oscillatory second order ODEs for $\varepsilon \in (0, 1]$, especially when ε is not too big and too small, i.e. in the intermediate regime. This chapter is to design and analyze a multiscale time integrator Fourier pseudospectral (MTI-FP) method for the problem (4.1.1) based on a multiscale decomposition of the KGE and the MTIs to the highly oscillatory second order ODEs studied in Chapter 2. The proposed MTI-FP method to (4.1.1) is explicit, efficient and accurate in practical computation, and converges in time uniformly at linear convergence rate for all $\varepsilon \in (0, 1]$ and optimally at quadratic convergence rate in the regimes $\varepsilon = O(1)$ or $0 < \varepsilon \leq \tau$. Thus our method is different with those numerical methods in [10, 26, 43].

4.2 Multiscale decomposition

Let $\tau = \Delta t > 0$ be the step size, and denote time steps by $t_n = n\tau$ for $n = 0, 1, \ldots$. In this section, we present a multiscale decomposition for the solution of (4.1.1) on the time interval $[t_n, t_{n+1}]$. The decomposition is similar to that studied in Section 2.4.1. With given initial data at $t = t_n$ as

$$u(\mathbf{x}, t_n) = \phi_1^n(\mathbf{x}) = O(1), \qquad \partial_t u(\mathbf{x}, t_n) = \frac{1}{\varepsilon^2}\phi_2^n(\mathbf{x}) = O\left(\frac{1}{\varepsilon^2}\right). \tag{4.2.1}$$

Similarly to the analytical study of the nonrelativistic limit of the nonlinear KGE in [75–77], we take an ansatz to the solution $u(\mathbf{x}, t) := u(\mathbf{x}, t_n + s)$ of (4.1.1) on the time interval $[t_n, t_{n+1}]$ with (4.2.1) as

$$u(\mathbf{x}, t_n+s) = \mathrm{e}^{is/\varepsilon^2} z_+^n(\mathbf{x}, s)+\mathrm{e}^{-is/\varepsilon^2}\overline{z_-^n}(\mathbf{x}, s)+r^n(\mathbf{x}, s), \quad \mathbf{x} \in \mathbb{R}^d, \ 0 \leq s \leq \tau. \tag{4.2.2}$$

Differentiating (4.2.2) with respect to s, we have

$$\begin{aligned}\partial_s u(\mathbf{x}, t_n + s) =& \mathrm{e}^{\frac{is}{\varepsilon^2}}\left[\partial_s z_+^n(\mathbf{x}, s) + \frac{i}{\varepsilon^2} z_+^n(\mathbf{x}, s)\right] + \mathrm{e}^{-\frac{is}{\varepsilon^2}}\left[\partial_s \overline{z_-^n}(\mathbf{x}, s) - \frac{i}{\varepsilon^2}\overline{z_-^n}(\mathbf{x}, s)\right] \\ &+ \partial_s r^n(\mathbf{x}, s), \quad \mathbf{x} \in \mathbb{R}^d, \quad 0 \leq s \leq \tau. \end{aligned} \tag{4.2.3}$$

Plugging (4.2.2) into (4.1.1), we get for $\mathbf{x}\in\mathbb{R}^d$ and $0\le s\le\tau$

$$\begin{aligned}&\mathrm{e}^{\frac{is}{\varepsilon^2}}\left[\varepsilon^2\partial_{ss}z_+^n(\mathbf{x},s)+2i\partial_s z_+^n(\mathbf{x},s)-\Delta z_+^n(\mathbf{x},s)\right]+\varepsilon^2\partial_{ss}r^n(\mathbf{x},s)+\Delta r^n(\mathbf{x},s)\\&+\mathrm{e}^{-\frac{is}{\varepsilon^2}}\left[\varepsilon^2\partial_{ss}\overline{z_-^n}(\mathbf{x},s)-2i\partial_s\overline{z_-^n}(\mathbf{x},s)-\Delta\overline{z_-^n}(\mathbf{x},s)\right]+\frac{r^n(\mathbf{x},s)}{\varepsilon^2}\\&+f(u(\mathbf{x},t_n+s))=0.\end{aligned}$$

Multiplying the above equation by $\mathrm{e}^{-is/\varepsilon^2}$ and $\mathrm{e}^{is/\varepsilon^2}$, respectively, we can decompose it into a coupled system for two ε^2-frequency waves with the unknowns $z_\pm^n(\mathbf{x},s):=z_\pm^n$ and the rest frequency waves with the unknown $r^n(\mathbf{x},s):=r^n$ as

$$\begin{cases}\varepsilon^2\partial_{ss}z_\pm^n+2i\partial_s z_\pm^n-\Delta z_\pm^n+f_\pm\left(z_+^n,z_-^n\right)=0,\\ \varepsilon^2\partial_{ss}r^n-\Delta r^n+\dfrac{1}{\varepsilon^2}r^n+f_r\left(z_+^n,z_-^n,r^n;s\right)=0,\end{cases}\qquad \mathbf{x}\in\mathbb{R}^d,\quad 0\le s\le\tau,\ (4.2.4)$$

where

$$\begin{aligned}&f_\pm\left(z_+,z_-\right)=\frac{1}{2\pi}\int_0^{2\pi}f\left(z_\pm+\mathrm{e}^{i\theta}\overline{z_\mp}\right)d\theta,\qquad z_\pm,r\in\mathbb{C},\qquad 0\le s\le\tau,\\&f_r\left(z_+,z_-,r;s\right)=f\left(\mathrm{e}^{is/\varepsilon^2}z_++\mathrm{e}^{-is/\varepsilon^2}\overline{z_-}+r\right)-f_+\left(z_+,z_-\right)\mathrm{e}^{is/\varepsilon^2}-\overline{f_-}\left(z_+,z_-\right)\mathrm{e}^{-is/\varepsilon^2}.\end{aligned}$$

To find initial conditions for the above system (4.2.4), setting $s=0$ in (4.2.2) and (4.2.3) and noticing (4.2.1), we get

$$\begin{cases}z_+^n(\mathbf{x},0)+\overline{z_-^n}(\mathbf{x},0)+r^n(\mathbf{x},0)=\phi_1^n(\mathbf{x}),\quad \mathbf{x}\in\mathbb{R}^d,\\ \dfrac{i}{\varepsilon^2}\left[z_+^n(\mathbf{x},0)-\overline{z_-^n}(\mathbf{x},0)\right]+\partial_s z_+^n(\mathbf{x},0)+\partial_s\overline{z_-^n}(\mathbf{x},0)+\partial_s r^n(\mathbf{x},0)=\dfrac{\phi_2^n(\mathbf{x})}{\varepsilon^2}.\end{cases}\ (4.2.5)$$

Then we choose initial data with the principles from Section 2.4.1: (i) equate $O\left(\frac{1}{\varepsilon^2}\right)$ and $O(1)$ terms in the second equation of (4.2.5), respectively, and (ii) be well-prepared for the first two equations in (4.2.4) when $0<\varepsilon\ll 1$, i.e. $\partial_s z_+^n(\mathbf{x},0)$ and $\partial_s z_-^n(\mathbf{x},0)$ are determined from the first two equations in (4.2.4), respectively, by setting $\varepsilon=0$ and $s=0$ [5, 8]:

$$\begin{cases}z_+^n(\mathbf{x},0)+\overline{z_-^n}(\mathbf{x},0)=\phi_1^n(\mathbf{x}),\qquad i\left[z_+^n(\mathbf{x},0)-\overline{z_-^n}(\mathbf{x},0)\right]=\phi_2^n(\mathbf{x}),\\ 2i\partial_s z_\pm^n(\mathbf{x},0)-\Delta z_\pm^n(\mathbf{x},0)+f_\pm\left(z_+^n(\mathbf{x},0),z_-^n(\mathbf{x},0)\right)=0,\qquad \mathbf{x}\in\mathbb{R}^d,\\ r^n(\mathbf{x},0)=0,\qquad \partial_s r^n(\mathbf{x},0)+\partial_s z_+^n(\mathbf{x},0)+\partial_s\overline{z_-^n}(\mathbf{x},0)=0.\end{cases}\ (4.2.6)$$

Solving (4.2.6), we get the initial data for (4.2.4) as

$$\begin{cases} z_+^n(\mathbf{x},0) = \dfrac{1}{2}\left[\phi_1^n(\mathbf{x}) - i\phi_2^n(\mathbf{x})\right], \qquad z_-^n(\mathbf{x},0) = \dfrac{1}{2}\left[\overline{\phi_1^n}(\mathbf{x}) - i\ \overline{\phi_2^n}(\mathbf{x})\right], \\ \partial_s z_\pm^n(\mathbf{x},0) = \dfrac{i}{2}\left[-\Delta z_\pm^n(\mathbf{x},0) + f_\pm\left(z_+^n(\mathbf{x},0), z_-^n(\mathbf{x},0)\right)\right], \qquad \mathbf{x}\in\mathbb{R}^d, \\ r^n(\mathbf{x},0) = 0, \qquad \partial_s r^n(\mathbf{x},0) = -\partial_s z_+^n(\mathbf{x},0) - \partial_s\overline{z_-^n}(\mathbf{x},0). \end{cases} \tag{4.2.7}$$

Again, we call the above decomposition (4.2.2) as multiscale decomposition by frequency (MDF). Specifically, for the pure power nonlinearity, i.e. f satisfies (2.1.4), explicit formulas for $f_\pm$ and f_r have been given in Chapter 2.

After solving the decomposed system (4.2.4) with the initial data (4.2.7), we get $z_\pm^n(\mathbf{x},\tau)$, $\partial_s z_\pm^n(\mathbf{x},\tau)$, $r^n(\mathbf{x},\tau)$ and $\partial_s r^n(\mathbf{x},\tau)$. Then we can reconstruct the solution to (4.1.1) at $t = t_{n+1}$ by setting $s = \tau$ in (4.2.2) and (4.2.3), i.e.,

$$\begin{cases} u(\mathbf{x},t_{n+1}) = \mathrm{e}^{i\tau/\varepsilon^2} z_+^n(\mathbf{x},\tau) + \mathrm{e}^{-i\tau/\varepsilon^2}\overline{z_-^n}(\mathbf{x},\tau) + r^n(\mathbf{x},\tau) := \phi_1^{n+1}(\mathbf{x}), \\ \partial_t u(\mathbf{x},t_{n+1}) = \dfrac{1}{\varepsilon^2}\phi_2^{n+1}(\mathbf{x}), \qquad \mathbf{x}\in\mathbb{R}^d, \end{cases} \tag{4.2.8}$$

with

$$\begin{aligned} \phi_2^{n+1}(\mathbf{x}) =& \mathrm{e}^{i\tau/\varepsilon^2}\left[\varepsilon^2\partial_s z_+^n(\mathbf{x},\tau) + i z_+^n(\mathbf{x},\tau)\right] + \mathrm{e}^{-i\tau/\varepsilon^2}\left[\varepsilon^2\partial_s\overline{z_-^n}(\mathbf{x},\tau) - i\overline{z_-^n}(\mathbf{x},\tau)\right] \\ &+ \varepsilon^2\partial_s r^n(\mathbf{x},\tau). \end{aligned}$$

4.3 Multiscale method

In this section, based on the MDF (4.2.4), we propose a new numerical method for solving the KGE (4.1.1) with the pure power nonlinearity (2.1.4), which is uniformly accurate for $\varepsilon \in (0,1]$. For the simplicity of notation, we present the numerical method in 1D with a cubic nonlinearity, i.e. $d = 1$ in (4.1.1) and $f(u) = \lambda|u|^2u$ with $\lambda\in\mathbb{R}$ a given constant in (2.1.4). In this case, we have

$$\begin{cases} f_\pm\left(z_+,z_-\right) = \lambda\left(|z_\pm|^2 + 2|z_\mp|^2\right)z_\pm, \qquad z_\pm, r\in\mathbb{C}, \qquad 0\le s\le\tau, \\ f_r\left(z_+,z_-,r;s\right) = \mathrm{e}^{3is/\varepsilon^2} g_+(z_+,z_-) + \mathrm{e}^{-3is/\varepsilon^2}\overline{g_-}(z_+,z_-) + w(z_+,z_-,r;s), \end{cases} \tag{4.3.1}$$

with

$$\begin{cases} g_\pm(z_+, z_-) = \lambda\, z_\pm^2\, z_\mp, \qquad z_\pm, r \in \mathbb{C}, \qquad 0 \le s \le \tau, \\ w(z_+, z_-, r; s) = f\left(\mathrm{e}^{is/\varepsilon^2} z_+ + \mathrm{e}^{-is/\varepsilon^2}\overline{z_-} + r\right) - f\left(\mathrm{e}^{is/\varepsilon^2} z_+ + \mathrm{e}^{-is/\varepsilon^2}\overline{z_-}\right). \end{cases} \tag{4.3.2}$$

Generalizations to higher dimensions and general power nonlinearity are straightforward and all the results presented in this paper are still valid with minor modifications. Due to fast decay of the solution to the KGE (4.1.1) at far field, similar as Chapter 3, the whole space problem (4.1.1) in 1D is truncated onto a finite interval $\Omega = (a, b)$ with periodic boundary conditions:

$$\begin{cases} \varepsilon^2 \partial_{tt} u(x,t) - \partial_{xx} u(x,t) + \dfrac{u(x,t)}{\varepsilon^2} + f\left(u(x,t)\right) = 0, \quad x \in \Omega = (a,b),\ t > 0, \\ u(a,t) = u(b,t), \quad \partial_x u(a,t) = \partial_x u(b,t), \qquad t \ge 0, \\ u(x,0) = \phi_1(x), \quad \partial_t u(x,0) = \dfrac{1}{\varepsilon^2}\phi_2(x), \qquad x \in \overline{\Omega} = [a,b]. \end{cases} \tag{4.3.3}$$

Consequently, for $n \ge 0$, the decomposed system MDF (4.2.4) in 1D collapses to

$$\begin{cases} \varepsilon^2 \partial_{ss} z_\pm^n + 2i\partial_s z_\pm^n - \partial_{xx} z_\pm^n + f_\pm\left(z_+^n, z_-^n\right) = 0, \\ \varepsilon^2 \partial_{ss} r^n - \partial_{xx} r^n + \dfrac{1}{\varepsilon^2} r^n + f_r\left(z_+^n, z_-^n, r^n; s\right) = 0, \quad a < x < b,\ 0 < s \le \tau. \end{cases} \tag{4.3.4}$$

The initial and boundary conditions for the above system are

$$\begin{cases} z_\pm^n(a,s) = z_\pm^n(b,s), \qquad \partial_x z_\pm^n(a,s) = \partial_x z_\pm^n(b,s), \\ r^n(a,s) = r^n(b,s), \qquad \partial_x r^n(a,s) = \partial_x r^n(b,s), \qquad 0 \le s \le \tau; \\ z_+^n(x,0) = \dfrac{1}{2}\left[\phi_1^n(x) - i\phi_2^n(x)\right], \quad z_-^n(x,0) = \dfrac{1}{2}\left[\overline{\phi_1^n}(x) - i\,\overline{\phi_2^n}(x)\right], \\ \partial_s z_\pm^n(x,0) = \dfrac{i}{2}\left[-\partial_{xx} z_\pm^n(x,0) + f_\pm\left(z_+^n(x,0), z_-^n(x,0)\right)\right], \qquad a \le x \le b, \\ r^n(x,0) = 0, \qquad \partial_s r^n(x,0) = -\partial_s z_+^n(x,0) - \partial_s\,\overline{z_-^n}(x,0). \end{cases} \tag{4.3.5}$$

In order to discretize (4.3.4) with (4.3.5), we first apply the Fourier spectral method in space and then use the exponential wave integrator (EWI) for time integration. Choose the mesh size $h := \Delta x = (b-a)/M$ with M a positive integer and denote grid points as $x_j := a + jh$ for $j = 0, 1, \ldots, M$. Again, denote

$$X_M := \operatorname{span}\left\{\phi_l(x) = \mathrm{e}^{i\mu_l(x-a)} \mid l = -\frac{M}{2}, \ldots, \frac{M}{2} - 1\right\} \quad \text{with } \mu_l = \frac{2\pi l}{b-a},$$

$$Y_M := \left\{\mathbf{v} = (v_0, v_1, \ldots, v_M) \in \mathbb{C}^{M+1} \mid v_0 = v_M\right\} \quad \text{with } \|\mathbf{v}\|_{l^2} = h\sum_{j=0}^{M-1} |v_j|^2.$$

For a periodic function $v(x)$ on $\overline{\Omega}$ and a vector $\mathbf{v} \in Y_M$, let $P_M : L^2(\Omega) \to X_M$ be the standard L^2-projection operator, and $I_M : C(\Omega) \to X_M$ or $Y_M \to X_M$ be the trigonometric interpolation operator [95], i.e.

$$(P_M v)(x) = \sum_{l=-M/2}^{M/2-1} \widehat{v}_l \, \mathrm{e}^{i\mu_l(x-a)}, \quad (I_M \mathbf{v})(x) = \sum_{l=-M/2}^{M/2-1} \widetilde{v}_l \, \mathrm{e}^{i\mu_l(x-a)}, \quad a \le x \le b, \tag{4.3.6}$$

where $\widehat{v}_l$ and $\widetilde{v}_l$ are the Fourier and discrete Fourier transform coefficients of the periodic function $v(x)$ and vector $\mathbf{v}$, respectively, defined as

$$\widehat{v}_l = \frac{1}{b-a}\int_a^b v(x)\, \mathrm{e}^{-i\mu_l(x-a)}dx, \qquad \widetilde{v}_l = \frac{1}{M}\sum_{j=0}^{M-1} v_j \, \mathrm{e}^{-i\mu_l(x_j-a)}. \tag{4.3.7}$$

Then a Fourier spectral method for discretizing (4.3.4) reads:
Find $z^n_{\pm,M} := z^n_{\pm,M}(x,s)$, $r^n_M := r^n_M(x,s) \in X_M$ for $0 \le s \le \tau$, i.e.

$$z^n_{\pm,M}(x,s) = \sum_{l=-M/2}^{M/2-1} \widehat{(z^n_\pm)}_l(s)\mathrm{e}^{i\mu_l(x-a)}, \quad r^n_M(x,s) = \sum_{l=-M/2}^{M/2-1} \widehat{(r^n)}_l(s)\mathrm{e}^{i\mu_l(x-a)}, \tag{4.3.8}$$

such that for $0 < s < \tau$

$$\begin{cases} \varepsilon^2 \partial_{ss} z^n_{\pm,M} + 2i\partial_s z^n_{\pm,M} - \partial_{xx} z^n_{\pm,M} + P_M f_\pm\left(z^n_{+,M}, z^n_{-,M}\right) = 0, \quad a < x < b, \\ \varepsilon^2 \partial_{ss} r^n_M - \partial_{xx} r^n_M + \dfrac{1}{\varepsilon^2} r^n_M + P_M f_r\left(z^n_{+,M}, z^n_{-,M}, r^n_M; s\right) = 0. \end{cases} \tag{4.3.9}$$

Substituting (4.3.8) into (4.3.9) and noticing the orthogonality of $\phi_l(x)$, we get

$$\begin{cases} \varepsilon^2 \widehat{(z^n_\pm)}''_l(s) + 2i\widehat{(z^n_\pm)}'_l(s) + \mu_l^2 \widehat{(z^n_\pm)}_l(s) + \widehat{(f^n_\pm)}_l(s) = 0, \quad 0 < s \le \tau, \\ \varepsilon^2 \widehat{(r^n)}''_l(s) + \left(\mu_l^2 + \dfrac{1}{\varepsilon^2}\right)\widehat{(r^n)}_l(s) + \widehat{(f^n_r)}_l(s) = 0, \quad -\dfrac{M}{2} \le l \le \dfrac{M}{2} - 1, \end{cases} \tag{4.3.10}$$

where $\widehat{(f^n_\pm)}_l(s)$ and $\widehat{(f^n_r)}_l(s)$ are the Fourier coefficients of $f^n_\pm(x,s) := f_\pm(z^n_{+,M}(x,s), z^n_{-,M}(x,s))$ and $f^n_r(x,s) := f_r\left(z^n_{+,M}(x,s), z^n_{-,M}(x,s), r^n_M(x,s); s\right)$, respectively. In order to apply the EWIs for integrating (4.3.10) in time, for each fixed $-M/2 \le l \le M/2-1$, we rewrite (4.3.10) by using the variation-of-constant formulas

$$\begin{cases} \widehat{(z^n_\pm)}_l(s) = a_l(s)\widehat{(z^n_\pm)}_l(0) + \varepsilon^2 b_l(s)\widehat{(z^n_\pm)}'_l(0) - \displaystyle\int_0^s b_l(s-\theta)\widehat{(f^n_\pm)}_l(\theta)\, d\theta, \\ \widehat{(r^n)}_l(s) = \dfrac{\sin(\omega_l s)}{\omega_l}\widehat{(r^n)}'_l(0) - \displaystyle\int_0^s \frac{\sin\left(\omega_l(s-\theta)\right)}{\varepsilon^2\omega_l}\widehat{(f^n_r)}_l(\theta)\, d\theta, \quad 0 \le s \le \tau, \end{cases} \tag{4.3.11}$$

where $\omega_l = \frac{1}{\varepsilon^2}\sqrt{1+\mu_l^2\varepsilon^2}$ and

$$\begin{cases} a_l(s) := \dfrac{\lambda_l^+ \mathrm{e}^{is\lambda_l^-} - \lambda_l^- \mathrm{e}^{is\lambda_l^+}}{\lambda_l^+ - \lambda_l^-}, \qquad b_l(s) := i\dfrac{\mathrm{e}^{is\lambda_l^+} - \mathrm{e}^{is\lambda_l^-}}{\varepsilon^2(\lambda_l^- - \lambda_l^+)}, \quad 0 \le s \le \tau, \\ \lambda_l^+ = -\dfrac{1+\sqrt{1+\mu_l^2\varepsilon^2}}{\varepsilon^2} = O\left(\dfrac{1}{\varepsilon^2}\right), \quad \lambda_l^- = -\dfrac{1-\sqrt{1+\mu_l^2\varepsilon^2}}{\varepsilon^2} = O(1). \end{cases} \tag{4.3.12}$$

Differentiating (4.3.11) with respect to s, we obtain

$$\begin{cases} \widehat{(z_\pm^n)}_l'(s) = a_l'(s)\widehat{(z_\pm^n)}_l(0) + \varepsilon^2 b_l'(s)\widehat{(z_\pm^n)}_l'(0) - \displaystyle\int_0^s b_l'(s-\theta)\widehat{(f_\pm^n)}_l(\theta)\,d\theta, \\ \widehat{(r^n)}_l'(s) = \cos(\omega_l s)\widehat{(r^n)}_l'(0) - \displaystyle\int_0^s \frac{\cos\left(\omega_l(s-\theta)\right)}{\varepsilon^2}\widehat{(f_r^n)}_l(\theta)\,d\theta, \quad 0 \le s \le \tau, \end{cases} \tag{4.3.13}$$

where

$$a_l'(s) = i\lambda_l^+\lambda_l^- \frac{\mathrm{e}^{is\lambda_l^-} - \mathrm{e}^{is\lambda_l^+}}{\lambda_l^+ - \lambda_l^-}, \qquad b_l'(s) = \frac{\lambda_l^+ \mathrm{e}^{is\lambda_l^+} - \lambda_l^- \mathrm{e}^{is\lambda_l^-}}{\varepsilon^2(\lambda_l^+ - \lambda_l^-)}, \qquad 0 \le s \le \tau. \tag{4.3.14}$$

Taking $s = \tau$ in (4.3.11) and (4.3.13), noticing (4.3.1) and (4.3.2), and approximating the integrals either by the Gautschi's type quadrature [45, 57] or by the Deuflhard's type quadrature (the standard trapezoidal rule) [36, 57], we get

$$\begin{cases} \widehat{(z_\pm^n)}_l(\tau) \approx a_l(\tau)\widehat{(z_\pm^n)}_l(0) + \varepsilon^2 b_l(\tau)\widehat{(z_\pm^n)}_l'(0) - c_l(\tau)\widehat{(f_\pm^n)}_l(0) - d_l(\tau)\widehat{(f_\pm^n)}_l'(0), \\ \widehat{(r^n)}_l(\tau) \approx \dfrac{\sin(\omega_l\tau)}{\omega_l}\widehat{(r^n)}_l'(0) - p_l(\tau)\widehat{(g_+^n)}_l(0) - q_l(\tau)\widehat{(g_+^n)}_l'(0) \\ \qquad\qquad -\overline{p_l}(\tau)\widehat{\left(\overline{g^n}\right)}_l(0) - \overline{q_l}(\tau)\widehat{\left(\overline{g^n}\right)}_l'(0), \\ \widehat{(z_\pm^n)}_l'(\tau) \approx a_l'(\tau)\widehat{(z_\pm^n)}_l(0) + \varepsilon^2 b_l'(\tau)\widehat{(z_\pm^n)}_l'(0) - c_l'(\tau)\widehat{(f_\pm^n)}_l(0) - d_l'(\tau)\widehat{(f_\pm^n)}_l'(0), \\ \widehat{(r^n)}_l'(\tau) \approx \cos(\omega_l\tau)\widehat{(r^n)}_l'(0) - p_l'(\tau)\widehat{(g_+^n)}_l(0) - q_l'(\tau)\widehat{(g_+^n)}_l'(0) - \overline{p_l'}(\tau)\widehat{\left(\overline{g^n}\right)}_l(0) \\ \qquad\qquad -\overline{q_l'}(\tau)\widehat{\left(\overline{g^n}\right)}_l'(0) - \dfrac{\tau}{2\varepsilon^2}\widehat{(w^n)}_l(\tau), \end{cases} \tag{4.3.15}$$

where $\widehat{(g_\pm^n)}_l(s)$, $\widehat{(w^n)}_l(s)$, $\widehat{(f_\pm^n)}_l'(s) = \widehat{(\partial_s f_\pm^n)}_l(s)$ and $\widehat{(g_\pm^n)}_l'(s) = \widehat{(\partial_s g_\pm^n)}_l(s)$ are the Fourier coefficients of $g_\pm^n = g_\pm\left(z_{+,M}^n, z_{-,M}^n\right)$, $w^n = w\left(z_{+,M}^n, z_{-,M}^n, r_M^n; s\right)$, $\partial_s f_\pm^n = 2\lambda z_\pm^n \operatorname{Re}\left[\overline{z_\pm^n}\partial_s z_\pm^n + 2\overline{z_\mp^n}\partial_s z_\mp^n\right] + \lambda\partial_s z_\pm^n\left[|z_\pm^n|^2 + 2|z_\mp^n|^2\right] =: \dot{f}_\pm\left(z_+^n, z_-^n; \partial_s z_+^n, \partial_s z_-^n\right)$ and $\partial_s g_\pm^n = 2\lambda z_\pm^n z_\mp^n \partial_s z_\pm^n + \lambda\left(z_\pm^n\right)^2 \partial_s z_\mp^n =: \dot{g}_\pm\left(z_+^n, z_-^n; \partial_s z_+^n, \partial_s z_-^n\right)$, respectively, and (their

detailed explicit formulas are shown in Chapter 2)

$$\begin{cases} c_l(\tau) = \displaystyle\int_0^\tau b_l(\tau-\theta)\,d\theta, & p_l(\tau) = \int_0^\tau \frac{\sin\left(\omega_l(\tau-\theta)\right)}{\varepsilon^2\omega_l}\mathrm{e}^{3i\theta/\varepsilon^2}\,d\theta, \\ d_l(\tau) = \displaystyle\int_0^\tau b_l(\tau-\theta)\theta\,d\theta, & q_l(\tau) = \int_0^\tau \frac{\sin\left(\omega_l(\tau-\theta)\right)}{\varepsilon^2\omega_l}\mathrm{e}^{3i\theta/\varepsilon^2}\theta\,d\theta, \\ c_l'(\tau) = \displaystyle\int_0^\tau b_l'(\tau-\theta)\,d\theta, & p_l'(\tau) = \int_0^\tau \frac{\cos\left(\omega_l(\tau-\theta)\right)}{\varepsilon^2}\mathrm{e}^{3i\theta/\varepsilon^2}\,d\theta, \\ d_l'(\tau) = \displaystyle\int_0^\tau b_l'(\tau-\theta)\theta\,d\theta, & q_l'(\tau) = \int_0^\tau \frac{\cos\left(\omega_l(\tau-\theta)\right)}{\varepsilon^2}\mathrm{e}^{3i\theta/\varepsilon^2}\theta\,d\theta. \end{cases} \tag{4.3.16}$$

Inserting (4.3.15) into (4.3.8) and its time derivative with setting $s=\tau$, and noticing (4.2.8), we immediately obtain a *MTI-FP* discretization for the problem (4.3.3).

In practice, the integrals for computing the Fourier transform coefficients in (4.3.7), (4.3.11) and (4.3.13) are usually approximated by numerical quadratures [8,10,95]. Let u_j^n and $\dot{u}_j^n$ be approximations of $u(x_j,t_n)$ and $\partial_t u(x_j,t_n)$, respectively; and $z_{\pm,j}^{n+1}$, $\dot{z}_{\pm,j}^{n+1}$, r_j^{n+1} and $\dot{r}_j^{n+1}$ be approximations of $z_\pm^n(x_j,\tau)$, $\partial_s z_\pm^n(x_j,\tau)$, $r^n(x_j,\tau)$ and $\partial_s r^n(x_j,\tau)$, respectively, for $j=0,\ldots,M$. Choosing $u_j^0=\phi_1(x_j)$ and $\dot{u}_j^0=\phi_2(x_j)/\varepsilon^2$ for $0\le j\le M$ and noticing (4.2.8), (4.3.8) with $s=\tau$, (4.3.15), (4.3.5) and (4.2.1), then a MTI-FP discretization for the problem (4.3.3) reads for $n\ge 0$

$$\begin{cases} u_j^{n+1} = \mathrm{e}^{i\tau/\varepsilon^2} z_{+,j}^{n+1} + \mathrm{e}^{-i\tau/\varepsilon^2}\overline{z_{-,j}^{n+1}} + r_j^{n+1}, \qquad j=0,1,\ldots,M, \\ \dot{u}_j^{n+1} = \mathrm{e}^{i\tau/\varepsilon^2}\left(\dot{z}_{+,j}^{n+1} + \dfrac{i}{\varepsilon^2} z_{+,j}^{n+1}\right) + \mathrm{e}^{-i\tau/\varepsilon^2}\left(\overline{\dot{z}_{-,j}^{n+1}} - \dfrac{i}{\varepsilon^2}\overline{z_{-,j}^{n+1}}\right) + \dot{r}_j^{n+1}, \end{cases} \tag{4.3.17}$$

where

$$\begin{cases} z_{\pm,j}^{n+1} = \displaystyle\sum_{l=-M/2}^{M/2-1} \widetilde{(z_\pm^{n+1})}_l \mathrm{e}^{i\mu_l(x_j-a)}, & r_j^{n+1} = \sum_{l=-M/2}^{M/2-1} \widetilde{(r^{n+1})}_l \mathrm{e}^{i\mu_l(x_j-a)}, \\ \dot{z}_{\pm,j}^{n+1} = \displaystyle\sum_{l=-M/2}^{M/2-1} \widetilde{(\dot{z}_\pm^{n+1})}_l \mathrm{e}^{i\mu_l(x_j-a)}, & \dot{r}_j^{n+1} = \sum_{l=-M/2}^{M/2-1} \widetilde{(\dot{r}^{n+1})}_l \mathrm{e}^{i\mu_l(x_j-a)}, \end{cases} \tag{4.3.18}$$

with

$$\begin{cases} \widetilde{(z_{\pm}^{n+1})}_l = a_l(\tau)\widetilde{(z_{\pm}^{0})}_l + \varepsilon^2 b_l(\tau)\widetilde{(\dot{z}_{\pm}^{0})}_l - c_l(\tau)\widetilde{(f_{\pm}^{0})}_l - d_l(\tau)\widetilde{(\dot{f}_{\pm}^{0})}_l, \\ \widetilde{(\dot{z}_{\pm}^{n+1})}_l = a_l'(\tau)\widetilde{(z_{\pm}^{0})}_l + \varepsilon^2 b_l'(\tau)\widetilde{(\dot{z}_{\pm}^{0})}_l - c_l'(\tau)\widetilde{(f_{\pm}^{0})}_l - d_l'(\tau)\widetilde{(\dot{f}_{\pm}^{0})}_l, \\ \widetilde{(r^{n+1})}_l = \frac{\sin(\omega_l\tau)}{\omega_l}\widetilde{(\dot{r}^{0})}_l - p_l(\tau)\widetilde{(g_{+}^{0})}_l - q_l(\tau)\widetilde{(\dot{g}_{+}^{0})}_l - \overline{p_l}(\tau)\widetilde{\left(\overline{g_{-}^{0}}\right)}_l - \overline{q_l}(\tau)\widetilde{\left(\overline{\dot{g}_{-}^{0}}\right)}_l, \\ \widetilde{(\dot{r}^{n+1})}_l = \cos(\omega_l\tau)\widetilde{(\dot{r}^{0})}_l - p_l'(\tau)\widetilde{(g_{+}^{0})} - q_l'(\tau)\widetilde{(\dot{g}_{+}^{0})}_l - \overline{p_l'}(\tau)\widetilde{\left(\overline{g_{-}^{0}}\right)}_l \\ \qquad -\overline{q_l'}(\tau)\widetilde{\left(\overline{\dot{g}_{-}^{0}}\right)}_l - \frac{\tau}{2\varepsilon^2}\widetilde{(w^{n+1})}_l, \quad -\frac{M}{2} \le l \le \frac{M}{2} - 1, \end{cases} \tag{4.3.19}$$

and

$$\begin{cases} \widetilde{(z_{+}^{0})}_l = \frac{1}{2}\left[\widetilde{(u^n)}_l - i\varepsilon^2\widetilde{(\dot{u}^n)}_l\right], \quad \widetilde{(z_{-}^{0})}_l = \frac{1}{2}\left[\widetilde{(\overline{u^n})}_l - i\varepsilon^2\widetilde{(\overline{\dot{u}^n})}_l\right], \\ \widetilde{(\dot{z}_{\pm}^{0})}_l = \frac{i}{2}\left[\frac{2}{\tau}\sin\left(\frac{1}{2}\mu_l^2\tau\right)\widetilde{(z_{\pm}^{0})}_l + \widetilde{(f_{\pm}^{0})}_l\right], \quad \widetilde{(\dot{r}^{0})}_l = -\widetilde{(\dot{z}_{+}^{0})}_l - \widetilde{\left(\overline{\dot{z}_{-}^{0}}\right)}_l; \\ f_{\pm,j}^0 = f_{\pm}\left(z_{+,j}^0, z_{-,j}^0\right), \quad \dot{f}_{\pm,j}^0 = \dot{f}_{\pm}\left(z_{+,j}^0, z_{-,j}^0; \dot{z}_{+,j}^0, \dot{z}_{-,j}^0\right), \\ g_{\pm,j}^0 = g_{\pm}\left(z_{+,j}^0, z_{-,j}^0\right), \quad \dot{g}_{\pm,j}^0 = \dot{g}_{\pm}\left(z_{+,j}^0, z_{-,j}^0; \dot{z}_{+,j}^0, \dot{z}_{-,j}^0\right), \\ w_j^{n+1} = f\left(u_j^{n+1}\right) - f\left(\mathrm{e}^{i\tau/\varepsilon^2} z_{+,j}^{n+1} + \mathrm{e}^{-i\tau/\varepsilon^2}\overline{z_{-,j}^{n+1}}\right), \qquad 0 \le j \le M. \end{cases} \tag{4.3.20}$$

This MTI-FP method for the KGE (4.3.3) (or (4.1.1)) is explicit, accurate, easy to implement and very efficient due to the fast Fourier transform (FFT), and its memory cost is $O(M)$ and the computational cost per time step is $O(M \log M)$.

Remark 4.3.1. *Instead of discretizing the initial velocity $\partial_s z_{\pm}^n(x,0)$ from (4.3.5) in Fourier space as $\widetilde{(z_{\pm}^n)}_l'(0) = \frac{i}{2}[\mu_l^2\widetilde{(z_{\pm}^n)}_l(0) + \widetilde{(f_{\pm}^n)}_l(0)]$ which will result a second order decreasing in the spatial accuracy, we change to the modified coefficients given in (4.3.20) as filters where the accuracy is now controlled by the time step τ (cf. (4.4.51)). There are other possible choices of the filters.*

Remark 4.3.2. *When the initial data $\phi_1(x)$ and $\phi_2(x)$ are real-valued functions and $f(u) : \mathbb{R} \to \mathbb{R}$ in (4.1.1), then the solution $u(x,t)$ is real-valued. In this case, for $n \ge 0$, it is easy to see that $z_+^n(x,s) = z_-^n(x,s)$ for $x \in \Omega$ and $0 \le s \le \tau$ in the MDF (4.2.4). In the corresponding numerical scheme, we have $z_{+,j}^n = z_{-,j}^n$ for $j = 0, \ldots, M$ in the MTI-FP (4.3.17). Thus the scheme can be simplified and the computational cost can be reduced.*

4.4 Error estimates

In this section, we establish an error bound for the MTI-FP (4.3.17) of the problem (4.3.3), which is uniform for $\varepsilon \in (0,1]$. Let $0 < T < T^*$ with T^* the maximum existence time of the solution u to the problem (4.3.3), motivated by the analytical results in [75–77], here we make the following assumption on the solution u to the problem (4.3.3) — there exists an integer $m_0 \geq 2$ such that

$$u \in C^1\left([0,T]; H_p^{m_0+4}(\Omega)\right), \quad \|u\|_{L^\infty([0,T];H^{m_0+4})} + \varepsilon^2 \|\partial_t u\|_{L^\infty([0,T];H^{m_0+4})} \lesssim 1, \tag{4.4.1}$$

where $H_p^m(\Omega) = \left\{\phi(x) \in H^m(\Omega) \mid \phi^{(k)}(a) = \phi^{(k)}(b),\ k = 0,1,\ldots,m-1\right\} \subset H^m(\Omega)$. Denote

$$C_0 = \max_{0<\varepsilon\leq 1} \left\{ \|u\|_{L^\infty([0,T];H^{m_0+4})},\ \varepsilon^2 \|\partial_t u\|_{L^\infty([0,T];H^{m_0+4})} \right\}. \tag{4.4.2}$$

Let $\mathbf{u}^n = (u_0^n, u_1^n, \ldots, u_M^n) \in \mathbb{C}^{M+1}$, $\dot{\mathbf{u}}^n = (\dot{u}_0^n, \dot{u}_1^n, \ldots, \dot{u}_M^n) \in \mathbb{C}^{M+1}$ $(n \geq 0)$ be the numerical solution obtained from the MTI-FP method (4.3.17), denote their interpolations as

$$u_I^n(x) := (I_M \mathbf{u}^n)(x), \qquad \dot{u}_I^n(x) := (I_M \dot{\mathbf{u}}^n)(x), \qquad x \in \overline{\Omega}, \tag{4.4.3}$$

and define the error functions as

$$e^n(x) := u(x,t_n) - u_I^n(x), \quad \dot{e}^n(x) := \partial_t u(x,t_n) - \dot{u}_I^n(x), \quad x \in \overline{\Omega},\ 0 \leq n \leq \frac{T}{\tau}, \tag{4.4.4}$$

then we have the following error estimates for the MTI-FP method (4.3.17) [9].

Theorem 4.4.1 (Error bounds of MTI-FP). *Under the assumption (4.4.1), there exist two constants $0 < h_0 \leq 1$ and $0 < \tau_0 \leq 1$ sufficiently small and independent of ε such that, for any $0 < \varepsilon \leq 1$, when $0 < h \leq h_0$ and $0 < \tau \leq \tau_0$, we have*

$$\|e^n\|_{H^2} + \varepsilon^2 \|\dot{e}^n\|_{H^2} \lesssim h^{m_0} + \frac{\tau^2}{\varepsilon^2}, \ \|e^n\|_{H^2} + \varepsilon^2 \|\dot{e}^n\|_{H^2} \lesssim h^{m_0} + \tau^2 + \varepsilon^2, \tag{4.4.5}$$

$$\|u_I^n\|_{H^2} \leq C_0 + 1, \quad \|\dot{u}_I^n\|_{H^2} \leq \frac{C_0+1}{\varepsilon^2}, \qquad 0 \leq n \leq \frac{T}{\tau}. \tag{4.4.6}$$

Thus, by taking the minimum of the two error bounds in (4.4.5) for $\varepsilon \in (0,1]$, we obtain an error bound which is uniformly convergent for $\varepsilon \in (0,1]$

$$\|e^n\|_{H^2} + \varepsilon^2 \|\dot{e}^n\|_{H^2} \lesssim h^{m_0} + \tau^2 + \min_{0<\varepsilon\leq 1} \left\{ \frac{\tau^2}{\varepsilon^2}, \varepsilon^2 \right\} \lesssim h^{m_0} + \tau, \quad 0 \leq n \leq \frac{T}{\tau}. \tag{4.4.7}$$

In order to prove the above theorem, for $0 \le n \le \frac{T}{\tau}$, we introduce

$$e_M^n(x) := (P_M u)(x,t_n) - u_I^n(x), \quad \dot{e}_M^n(x) := P_M(\partial_t u)(x,t_n) - \dot{u}_I^n(x), \quad x \in \overline{\Omega}. \tag{4.4.8}$$

Using the triangle inequality and noticing the assumption (4.4.1), we have

$$\|e^n\|_{H^2} \le \|u(\cdot,t_n) - P_M u(\cdot,t_n)\|_{H^2} + \|e_M^n\|_{H^2} \lesssim h^{m_0+2} + \|e_M^n\|_{H^2}, \tag{4.4.9a}$$

$$\|\dot{e}^n\|_{H^2} \le \|\partial_t u(\cdot,t_n) - P_M \partial_t u(\cdot,t_n)\|_{H^2} + \|\dot{e}_M^n\|_{H^2} \lesssim \frac{1}{\varepsilon^2} h^{m_0+2} + \|\dot{e}_M^n\|_{H^2}. \tag{4.4.9b}$$

Thus we only need to obtain estimates for $\|e_M^n\|_{H^2}$ and $\|\dot{e}_M^n\|_{H^2}$, which will be done by introducing the following error energy functional

$$\mathcal{E}\left(e_M^n, \dot{e}_M^n\right) := \varepsilon^2 \left\|\dot{e}_M^n\right\|_{H^2}^2 + \left\|\partial_x e_M^n\right\|_{H^2}^2 + \frac{1}{\varepsilon^2}\left\|e_M^n\right\|_{H^2}^2, \qquad 0 \le n \le \frac{T}{\tau}, \tag{4.4.10}$$

and establishing the following several lemmas.

Lemma 4.4.1 (Formulation of the exact solution)**.** *Denote the Fourier expansion of the exact solution $u(x,t)$ of the problem (4.3.3) as*

$$u(x,t) = \sum_{l=-\infty}^{\infty} \widehat{u}_l(t)\, e^{i\mu_l(x-a)}, \qquad x \in \bar{\Omega}, \quad t \ge 0, \tag{4.4.11}$$

then we have

$$\begin{aligned}\widehat{u}_l(t_{n+1}) = {} & \cos(\omega_l\tau)\widehat{u}_l(t_n) + \frac{\sin(\omega_l\tau)}{\omega_l}\widehat{u}_l'(t_n) - \int_0^\tau \frac{\sin(\omega_l(\tau-\theta))}{\varepsilon^2\omega_l}\Big[\mathrm{e}^{i\theta/\varepsilon^2}\widehat{(f_+^n)}_l(\theta) \\ & + \mathrm{e}^{-i\theta/\varepsilon^2}\widehat{\left(\overline{f_-^n}\right)}_l(\theta) + \mathrm{e}^{3i\theta/\varepsilon^2}\widehat{(g_+^n)}_l(\theta) + \mathrm{e}^{-3i\theta/\varepsilon^2}\widehat{\left(\overline{g_-^n}\right)}_l(\theta) + \widehat{(w^n)}_l(\theta)\Big]\, d\theta, \end{aligned} \tag{4.4.12a}$$

$$\begin{aligned}\widehat{u}_l'(t_{n+1}) = {} & \cos(\omega_l\tau)\widehat{u}_l'(t_n) - \omega_l\sin(\omega_l\tau)\widehat{u}_l(t_n) - \int_0^\tau \frac{\cos(\omega_l(\tau-\theta))}{\varepsilon^2}\Big[\mathrm{e}^{i\theta/\varepsilon^2}\widehat{(f_+^n)}_l(\theta) \\ & + \mathrm{e}^{-i\theta/\varepsilon^2}\widehat{\left(\overline{f_-^n}\right)}_l(\theta) + \mathrm{e}^{3i\theta/\varepsilon^2}\widehat{(g_+^n)}_l(\theta) + \mathrm{e}^{-3i\theta/\varepsilon^2}\widehat{\left(\overline{g_-^n}\right)}_l(\theta) + \widehat{(w^n)}_l(\theta)\Big]\, d\theta. \end{aligned} \tag{4.4.12b}$$

Proof. Substituting (4.4.11) with $t = t_n + s$ into (4.3.3), we have

$$\varepsilon^2\widehat{u}_l''(t_n+s) + \left(\mu_l^2 + \frac{1}{\varepsilon^2}\right)\widehat{u}_l(t_n+s) + \widehat{f(u)}_l(t_n+s) = 0, \quad s > 0. \tag{4.4.13}$$

Applying the variation-of-constant formula to (4.4.13) and noticing (4.3.12), we get

$$\begin{aligned}\widehat{u}_l(t_n+s) = {} & \cos(\omega_l s)\widehat{u}_l(t_n) + \frac{\sin(\omega_l s)}{\omega_l}\widehat{u}_l'(t_n) \\ & - \int_0^s \frac{\sin(\omega_l(s-\theta))}{\varepsilon^2\omega_l}\widehat{f(u)}_l(t_n+\theta)\, d\theta, \quad 0 \le s \le \tau. \end{aligned} \tag{4.4.14}$$

For the cubic nonlinearity $f(u) = \lambda|u|^2u$ and noticing (4.2.2), (4.3.1) and (4.3.2), we have

$$\begin{aligned} f(u(x,t_n+s)) &= \mathrm{e}^{is/\varepsilon^2} f_+^n(x,s) + \mathrm{e}^{-is/\varepsilon^2}\overline{f_-^n}(x,s) + \mathrm{e}^{3is/\varepsilon^2} g_+^n(x,s) \\ &\quad + \mathrm{e}^{-3is/\varepsilon^2}\overline{g_-^n}(x,s) + w^n(x,s), \quad x\in\bar{\Omega},\ 0\le s\le\tau, \end{aligned} \tag{4.4.15}$$

where

$$\begin{cases} f_\pm^n(x,s) = f_\pm(z_+^n(x,s), z_-^n(x,s)), \qquad g_\pm^n(x,s) = g_\pm(z_+^n(x,s), z_-^n(x,s)), \\ w^n(x,s) = w^n(z_+^n(x,s), z_-^n(x,s), r^n(x,s); s), \qquad x\in\overline{\Omega},\quad 0\le s\le\tau. \end{cases} \tag{4.4.16}$$

Plugging (4.4.15) and (4.4.16) into (4.4.14), we get

$$\begin{aligned} \widehat{u}_l(t_n+s) &= \cos(\omega_l s)\widehat{u}_l(t_n) + \frac{\sin(\omega_l s)}{\omega_l}\widehat{u}_l'(t_n) - \int_0^s \frac{\sin(\omega_l(s-\theta))}{\varepsilon^2\omega_l}\Big[\mathrm{e}^{i\theta/\varepsilon^2}\widehat{(f_+^n)}_l(\theta) \\ &\quad + \mathrm{e}^{-i\theta/\varepsilon^2}\widehat{(\overline{f_-^n})}_l(\theta) + \mathrm{e}^{3i\theta/\varepsilon^2}\widehat{(g_+^n)}_l(\theta) + \mathrm{e}^{-3i\theta/\varepsilon^2}\widehat{(\overline{g_-^n})}_l(\theta) + \widehat{(w^n)}_l(\theta)\Big]\,d\theta. \end{aligned} \tag{4.4.17}$$

Then we can obtain (4.4.12a) by setting $s=\tau$ in (4.4.17) and get (4.4.12b) by taking derivative with respect to s in (4.4.17) and then letting $s=\tau$. □

Lemma 4.4.2 (A new formulation of MTI-FP)**.** *For $n\ge 0$, expanding $u_I^n(x)$ and $\dot{u}_I^n(x)$ in (4.4.3) into Fourier series as*

$$u_I^n(x) = \sum_{l=-M/2}^{M/2-1} \widetilde{(u_I^n)}_l\, \mathrm{e}^{i\mu_l(x-a)}, \quad \dot{u}_I^n(x) = \sum_{l=-M/2}^{M/2-1} \widetilde{(\dot{u}_I^n)}_l\, \mathrm{e}^{i\mu_l(x-a)}, \qquad x\in\bar{\Omega}, \tag{4.4.18}$$

then we have

$$\begin{cases} \widetilde{(u_I^{n+1})}_l = \cos(\omega_l\tau)\widetilde{(u_I^n)}_l + \dfrac{\sin(\omega_l\tau)}{\omega_l}\widetilde{(\dot{u}_I^n)}_l - \widetilde{G_l^n}, \\ \widetilde{(\dot{u}_I^{n+1})}_l = -\omega_l\sin(\omega_l\tau)\widetilde{(u_I^n)}_l + \cos(\omega_l\tau)\widetilde{(\dot{u}_I^n)}_l - \widetilde{\dot{G}_l^n}, \quad l = -\dfrac{M}{2},\ldots,\dfrac{M}{2}-1, \end{cases} \tag{4.4.19}$$

where

$$\begin{aligned} \widetilde{G_l^n} &= \mathrm{e}^{i\tau/\varepsilon^2}\Big[c_l(\tau)\widetilde{(f_+^0)}_l + d_l(\tau)\widetilde{(\dot{f}_+^0)}_l\Big] + \mathrm{e}^{-i\tau/\varepsilon^2}\Big[\overline{c_l}(\tau)\widetilde{\Big(\overline{f_-^0}\Big)}_l + \overline{d_l}(\tau)\widetilde{\Big(\overline{\dot{f}_-^0}\Big)}_l\Big] \\ &\quad + p_l(\tau)\widetilde{(g_+^0)}_l + q_l(\tau)\widetilde{(\dot{g}_+^0)}_l + \overline{p_l}(\tau)\widetilde{\Big(\overline{g_-^0}\Big)}_l + \overline{q_l}(\tau)\widetilde{\Big(\overline{\dot{g}_-^0}\Big)}_l, \end{aligned} \tag{4.4.20}$$

$$\begin{aligned}\widetilde{\dot{G}_l^n} &= \mathrm{e}^{i\tau/\varepsilon^2}\left[c_l'(\tau)+\frac{i}{\varepsilon^2}c_l(\tau)\right]\widetilde{(f_+^0)}_l+\mathrm{e}^{i\tau/\varepsilon^2}\left[d_l'(\tau)+\frac{i}{\varepsilon^2}d_l(\tau)\right]\widetilde{(\dot{f}_+^0)}_l \\ &+\mathrm{e}^{-i\tau/\varepsilon^2}\left[\overline{c}_l'(\tau)-\frac{i}{\varepsilon^2}\overline{c}_l(\tau)\right]\widetilde{\left(\overline{f_-^0}\right)}_l+\mathrm{e}^{-i\tau/\varepsilon^2}\left[\overline{d}_l'(\tau)-\frac{i}{\varepsilon^2}\overline{d}_l(\tau)\right]\widetilde{\left(\overline{\dot{f}_-^0}\right)}_l \\ &+p_l'(\tau)\widetilde{(g_+^0)}_l+q_l'(\tau)\widetilde{(\dot{g}_+^0)}_l+\overline{p}_l'(\tau)\widetilde{\left(\overline{g_-^0}\right)}_l+\overline{q}_l'(\tau)\widetilde{\left(\overline{\dot{g}_-^0}\right)}_l+\frac{\tau}{2\varepsilon^2}\widetilde{(w^{n+1})}_l.\end{aligned} \tag{4.4.21}$$

Proof. Combining (4.3.20), (4.4.18) and (4.4.3), we have

$$\begin{cases}\widetilde{(z_+^0)}_l=\dfrac{1}{2}\left[\widetilde{(u_I^n)}_l-i\varepsilon^2\widetilde{(\dot{u}_I^n)}_l\right], \qquad \widetilde{(z_-^0)}_l=\dfrac{1}{2}\left[\widetilde{\left(\overline{u_I^n}\right)}_l-i\varepsilon^2\widetilde{\left(\overline{\dot{u}_I^n}\right)}_l\right], \\ \widetilde{(\dot{r}^0)}_l=-\widetilde{(\dot{z}_+^0)}_l-\widetilde{\left(\overline{\dot{z}_-^0}\right)}_l, \qquad l=-\dfrac{M}{2},\ldots,\dfrac{M}{2}-1.\end{cases} \tag{4.4.22}$$

Inserting (4.4.22) into (4.3.19) and noticing (4.3.17), (4.3.18), (4.4.18) and (4.4.3), we get

$$\begin{aligned}&\widetilde{(u_I^{n+1})}_l=\mathrm{e}^{i\tau/\varepsilon^2}\widetilde{(z_+^{n+1})}_l+\mathrm{e}^{-i\tau/\varepsilon^2}\widetilde{\left(\overline{z_-^{n+1}}\right)}_l+\widetilde{(r^{n+1})}_l \\ &=\mathrm{Re}\left\{\mathrm{e}^{i\tau/\varepsilon^2}a_l(\tau)\right\}\widetilde{(u_I^n)}_l+\varepsilon^2\,\mathrm{Im}\left\{\mathrm{e}^{i\tau/\varepsilon^2}a_l(\tau)\right\}\widetilde{(\dot{u}_I^n)}_l+\varepsilon^2\mathrm{e}^{i\tau/\varepsilon^2}b_l(\tau)\widetilde{(\dot{z}_+^0)}_l \\ &+\varepsilon^2\mathrm{e}^{-i\tau/\varepsilon^2}\overline{b}_l(\tau)\widetilde{\left(\overline{\dot{z}_-^0}\right)}_l+\frac{\sin(\omega_l\tau)}{\omega_l}\widetilde{(\dot{r}^0)}_l-\widetilde{G_l^n}, \quad l=-\frac{M}{2},\ldots,\frac{M}{2}-1,\end{aligned} \tag{4.4.23a}$$

$$\begin{aligned}&\widetilde{(\dot{u}_I^{n+1})}_l=\mathrm{e}^{i\tau/\varepsilon^2}\left[\widetilde{(\dot{z}_+^{n+1})}_l+\frac{i}{\varepsilon^2}\widetilde{(z_+^{n+1})}_l\right]+\mathrm{e}^{-i\tau/\varepsilon^2}\left[\widetilde{\left(\overline{\dot{z}_-^{n+1}}\right)}_l-\frac{i}{\varepsilon^2}\widetilde{\left(\overline{z_-^{n+1}}\right)}_l\right]+\widetilde{(\dot{r}^{n+1})}_l \\ &=\mathrm{Re}\left\{\mathrm{e}^{i\tau/\varepsilon^2}a_l'(\tau)+\frac{i}{\varepsilon^2}\mathrm{e}^{\frac{i\tau}{\varepsilon^2}}a_l(\tau)\right\}\widetilde{(u_I^n)}_l+\varepsilon^2\mathrm{e}^{-i\tau/\varepsilon^2}\left[\overline{b}_l'(\tau)-\frac{i}{\varepsilon^2}\overline{b}_l(\tau)\right]\widetilde{\left(\overline{\dot{z}_-^0}\right)}_l \\ &+\varepsilon^2\,\mathrm{Im}\left\{\mathrm{e}^{i\tau/\varepsilon^2}a_l'(\tau)+\frac{i}{\varepsilon^2}\mathrm{e}^{\frac{i\tau}{\varepsilon^2}}a_l(\tau)\right\}\widetilde{(\dot{u}_I^n)}_l+\varepsilon^2\mathrm{e}^{i\tau/\varepsilon^2}\left[b_l'(\tau)+\frac{i}{\varepsilon^2}b_l(\tau)\right]\widetilde{(\dot{z}_+^0)}_l \\ &+\cos(\omega_l\tau)\widetilde{(\dot{r}^0)}_l-\widetilde{\dot{G}_l^n}, \quad l=-\frac{M}{2},\ldots,\frac{M}{2}-1,\end{aligned} \tag{4.4.23b}$$

where $\mathrm{Re}(\alpha)$ and $\mathrm{Im}(\alpha)$ denote the real and imaginary parts of a complex number α, respectively. Thus we can obtain (4.4.19) from (4.4.23) by using the fact that $a_l(\tau)=a_{-l}(\tau)$ and $b_l(\tau)=b_{-l}(\tau)$ for $l=-M/2,\ldots,M/2-1$ in (4.3.12). □

For $0\le n\le\frac{T}{\tau}$, let $z_\pm^n(x,s)$ and $r^n(x,s)$ be the solution of the MDF (4.3.4)-(4.3.5) with $\phi_1^n(x)=u(x,t_n)$ and $\phi_2^n(x)=\varepsilon^2\partial_t u(x,t_n)$ for $x\in\bar{\Omega}$, then we have

Lemma 4.4.3 (A prior estimate of MDF). *Under the assumption (4.4.1), there exists a constant $\tau_1>0$ independent of $0<\varepsilon\le 1$ and $h>0$, such that for*

$0 < \tau \le \tau_1$

$$\left\|z_{\pm}^{n}\right\|_{L^{\infty}([0,\tau];H^{m_0+2})} + \left\|\partial_s z_{\pm}^{n}\right\|_{L^{\infty}([0,\tau];H^{m_0+1})} + \left\|\partial_{ss} z_{\pm}^{n}\right\|_{L^{\infty}([0,\tau];H^{m_0})} \lesssim 1, \quad (4.4.24)$$

$$\left\|r^{n}\right\|_{L^{\infty}([0,\tau];H^{4})} + \varepsilon^{2}\left\|\partial_s r^{n}\right\|_{L^{\infty}([0,\tau];H^{3})} + \varepsilon^{4}\left\|\partial_{ss} r^{n}\right\|_{L^{\infty}([0,\tau];H^{2})} \lesssim \varepsilon^{2}. \quad (4.4.25)$$

Proof. From (4.3.5) and noticing the assumption (4.4.1) and (4.3.1), we have

$$\|z_{\pm}^{n}(\cdot,0)\|_{H^{m_0+4}} \lesssim \|u(\cdot,t_n)\|_{H^{m_0+4}} + \varepsilon^{2}\|\partial_t u(\cdot,t_n)\|_{H^{m_0+4}} \lesssim 1,$$

$$\|\partial_s z_{\pm}^{n}(\cdot,0)\|_{H^{m_0+2}} \lesssim \|\partial_{xx} z_{\pm}^{n}(\cdot,0)\|_{H^{m_0+2}} + \|f_{\pm}(z_{+}^{n}(\cdot,0), z_{-}^{n}(\cdot,0))\|_{H^{m_0+2}} \lesssim 1,$$

which immediately imply

$$\|\partial_s r^{n}(\cdot,0)\|_{H^{m_0+2}} \le \|\partial_s z_{+}^{n}(\cdot,0)\|_{H^{m_0+2}} + \|\partial_s z_{-}^{n}(\cdot,0)\|_{H^{m_0+2}} \lesssim 1. \quad (4.4.26)$$

Similar to the proof for the nonlinear Schrödinger equation with wave operator [5,8], we can easily establish (4.4.24) and the details are omitted here for brevity. Taking the Fourier expansion of $r^n(x,s)$ and noticing (4.3.4), (4.3.5), (4.3.1) and (4.3.2), we obtain

$$r^{n}(x,s) = \sum_{l=-\infty}^{\infty} \widehat{(r^n)}_l(s)\, e^{i\mu_l(x-a)}, \qquad x \in \bar{\Omega}, \quad 0 \le s \le \tau, \quad (4.4.27)$$

where for $l \in \mathbb{Z}$

$$\widehat{(r^n)}_l(s) = \frac{\sin(\omega_l s)}{\omega_l}\widehat{(r^n)}_l'(0) - \int_0^s \frac{\sin\left(\omega_l(s-\theta)\right)}{\varepsilon^2\omega_l} \mathrm{e}^{3i\theta/\varepsilon^2}\widehat{(g_{+}^{n})}_l(\theta)\, d\theta \quad (4.4.28)$$

$$- \int_0^s \frac{\sin\left(\omega_l(s-\theta)\right)}{\varepsilon^2\omega_l} \mathrm{e}^{-3i\theta/\varepsilon^2}\widehat{(\overline{g_{-}^{n}})}_l(\theta)\, d\theta - \int_0^s \frac{\sin\left(\omega_l(s-\theta)\right)}{\varepsilon^2\omega_l}\widehat{(w^n)}_l(\theta)\, d\theta.$$

Let $M_\varepsilon := \left[\frac{b-a}{2\pi\varepsilon}\right] = O\left(\frac{1}{\varepsilon}\right)$ be the integer part of $\frac{b-a}{2\pi\varepsilon}$. From (4.4.28), integrating by parts and using the Cauchy's and Hölder's inequalities, we obtain for $|l| \le M_\varepsilon$

$$\begin{aligned}
|\widehat{(r^n)}_l(s)|^2 \lesssim\ & \Big|\varepsilon^2|\widehat{(r^n)}_l'(0)| + \varepsilon^2\left[|\widehat{(g_{+}^{n})}_l(s)| + |\widehat{(g_{+}^{n})}_l(0)| + |\widehat{(\overline{g_{-}^{n}})}_l(s)| + |\widehat{(\overline{g_{-}^{n}})}_l(0)|\right] \\
& + \int_0^s \left[\varepsilon^2\left(|\widehat{(g_{+}^{n})}_l'(\theta)| + |\widehat{(\overline{g_{-}^{n}})}_l'(\theta)|\right) + |\widehat{(w^n)}_l(\theta)|\right] d\theta\Big|^2 \\
\lesssim\ & \varepsilon^4\left[|\widehat{(r^n)}_l'(0)|^2 + |\widehat{(g_{+}^{n})}_l(s)|^2 + |\widehat{(g_{+}^{n})}_l(0)|^2 + |\widehat{(\overline{g_{-}^{n}})}_l(s)|^2 + |\widehat{(\overline{g_{-}^{n}})}_l(0)|^2\right] \\
& + \int_0^s \left[\varepsilon^4\left(|\widehat{(g_{+}^{n})}_l'(\theta)|^2 + |\widehat{(\overline{g_{-}^{n}})}_l'(\theta)|^2\right) + |\widehat{(w^n)}_l(\theta)|^2\right] d\theta. \quad (4.4.29)
\end{aligned}$$

Here we use the fact that for $|l| \le M_\varepsilon$

$$\begin{aligned} T_l(\theta) &= \frac{\varepsilon^2 \mathrm{e}^{3i\theta/\varepsilon^2}}{\varepsilon^4\omega_l^2 - 9}\left[\cos(\omega_l(s-\theta)) + \frac{3i}{\varepsilon^2\omega_l}\sin(\omega_l(s-\theta))\right] = O(\varepsilon^2), \\ T_l'(\theta) &= \frac{\sin(\omega_l(s-\theta))}{\varepsilon^2\omega_l}\mathrm{e}^{3i\theta/\varepsilon^2} = O(1), \quad 0 \le \theta \le s \le \tau, \qquad 0 < \varepsilon \le 1. \end{aligned}$$

Similarly, we can get for $|l| > M_\varepsilon$

$$|\widehat{(r^n)}_l(s)|^2 \lesssim \varepsilon^4|\widehat{(r^n)}_l'(0)|^2 + \int_0^s \left[|\widehat{(g_+^n)}_l(\theta)|^2 + |\widehat{(g_-^n)}_l(\theta)|^2 + |\widehat{(w^n)}_l(\theta)|^2\right] d\theta. \quad (4.4.30)$$

Multiplying (4.4.29) and (4.4.30) by $1 + \mu_l^2 + \ldots + \mu_l^8$, then summing them up for $l \in \mathbb{Z}$, we obtain

$$\begin{aligned} \|r^n(\cdot,s)\|_{H^4}^2 &\lesssim \sum_{l=-\infty}^{\infty}\left(1+\mu_l^2+\ldots+\mu_l^8\right)|\widehat{(r^n)}_l(s)|^2 \\ &\lesssim \sum_{l=-\infty}^{\infty}\left(\sum_{m=0}^{4}\mu_l^{2m}\right)\int_0^s |\widehat{(w^n)}_l(\theta)|^2 d\theta + \varepsilon^4\Big[\|\partial_s r^n(\cdot,0)\|_{H^4}^2 + \|g_+^n\|_{L^\infty([0,\tau];H^4)} \\ &\quad + \|g_-^n\|_{L^\infty([0,\tau];H^4)} + s\|\partial_s g_+^n\|_{L^\infty([0,\tau];H^4)} + s\|\partial_s g_-^n\|_{L^\infty([0,\tau];H^4)}\Big] \\ &\quad + s\Big[\|g_+^n - P_{M_\varepsilon}g_+^n\|_{L^\infty([0,\tau];H^4)}^2 + \|g_-^n - P_{M_\varepsilon}g_-^n\|_{L^\infty([0,\tau];H^4)}^2\Big] \\ &\lesssim \varepsilon^4 + \int_0^s \|w^n(\cdot,\theta)\|_{H^4}^2\, d\theta \lesssim \varepsilon^4 + \int_0^s \|r^n(\cdot,\theta)\|_{H^4}^2\, d\theta, \quad 0 \le s \le \tau. \quad (4.4.31) \end{aligned}$$

Combining (4.4.31), (4.4.26), noticing $r^n(x,0) \equiv 0$ for $x \in \bar{\Omega}$, and adapting the standard bootstrap argument for the nonlinear wave equation [102], we have that there exists a positive constant $\tau_1 > 0$ independent of ε and h such that

$$\|r^n\|_{L^\infty([0,\tau];H^4)} \lesssim \varepsilon^2. \quad (4.4.32)$$

Similarly we can obtain

$$\|\partial_s r^n\|_{L^\infty([0,\tau];H^3)} \lesssim 1, \qquad \|\partial_{ss} r^n\|_{L^\infty([0,\tau];H^2)} \lesssim \frac{1}{\varepsilon^2}, \quad (4.4.33)$$

which, together with (4.4.32), immediately imply the desired inequality (4.4.25). □

Combining the above lemmas and defining the local truncation error as

$$\xi^n(x) = \sum_{l=-M/2}^{M/2-1} \widehat{\xi_l^n}\, e^{i\mu_l(x-a)}, \qquad \dot{\xi}^n(x) = \sum_{l=-M/2}^{M/2-1} \widehat{\dot{\xi}_l^n}\, e^{i\mu_l(x-a)}, \qquad x \in \bar{\Omega}, \quad (4.4.34)$$

where

$$\begin{cases} \widehat{\xi_l^n} := \widehat{u}_l(t_{n+1}) - \left[\cos(\omega_l\tau)\widehat{u}_l(t_n) + \dfrac{\sin(\omega_l\tau)}{\omega_l}\widehat{u}_l'(t_n) - \widehat{\mathcal{G}_l^n}\right], \\ \widehat{\dot{\xi}_l^n} := \widehat{u}_l'(t_{n+1}) - \left[-\omega_l\sin(\omega_l\tau)\widehat{u}_l(t_n) + \cos(\omega_l\tau)\widehat{u}_l'(t_n) - \widehat{\mathcal{G}_l^n}\right], \end{cases} \tag{4.4.35}$$

with

$$\begin{aligned} \widehat{\mathcal{G}_l^n} &= \mathrm{e}^{i\tau/\varepsilon^2}\left[c_l(\tau)\widehat{(f_+^n)}_l(0) + d_l(\tau)\widehat{(f_+^n)}_l'(0)\right] + \mathrm{e}^{-i\tau/\varepsilon^2}\left[\overline{c_l}(\tau)\widehat{(\overline{f_-^n})}_l(0) + \overline{d_l}(\tau)\widehat{(\overline{f_-^n})}_l'(0)\right] \\ &\quad + p_l(\tau)\widehat{(g_+^n)}_l(0) + q_l(\tau)\widehat{(g_+^n)}_l'(0) + \overline{p_l}(\tau)\widehat{(\overline{g_-})}_l(0) + \overline{q_l}(\tau)\widehat{(\overline{g_-})}_l'(0), \qquad (4.4.36a) \\ \widehat{\dot{\mathcal{G}}_l^n} &= \mathrm{e}^{i\tau/\varepsilon^2}\left[c_l'(\tau) + \frac{i}{\varepsilon^2}c_l(\tau)\right]\widehat{(f_+^n)}_l(0) + \mathrm{e}^{i\tau/\varepsilon^2}\left[d_l'(\tau) + \frac{i}{\varepsilon^2}d_l(\tau)\right]\widehat{(f_+^n)}_l'(0) \qquad (4.4.36b) \\ &\quad + \mathrm{e}^{-i\tau/\varepsilon^2}\left[\overline{c_l'}(\tau) - \frac{i}{\varepsilon^2}\overline{c_l}(\tau)\right]\widehat{(\overline{f_-^n})}_l(0) + \mathrm{e}^{-i\tau/\varepsilon^2}\left[\overline{d_l'}(\tau) - \frac{i}{\varepsilon^2}\overline{d_l}(\tau)\right]\widehat{(\overline{f_-^n})}_l'(0) \\ &\quad + p_l'(\tau)\widehat{(g_+^n)}_l(0) + q_l'(\tau)\widehat{(g_+^n)}_l'(0) + \overline{p_l'}(\tau)\widehat{(\overline{g_-^n})}_l(0) + \overline{q_l'}(\tau)\widehat{(\overline{g_-^n})}_l'(0) + \frac{\tau}{2\varepsilon^2}\widehat{(w^n)}_l(\tau). \end{aligned}$$

Then we have the following estimates for them.

Lemma 4.4.4 (Estimates on ξ^n and $\dot{\xi}^n$)**.** *Under the assumption (4.4.1), when* $0 < \tau \le \tau_1$, *we have two independent estimates for* $0 < \varepsilon \le 1$

$$\mathcal{E}\left(\xi^n, \dot{\xi}^n\right) \lesssim \frac{\tau^6}{\varepsilon^2} + \tau^2\varepsilon^2 \quad \textit{and} \quad \mathcal{E}\left(\xi^n, \dot{\xi}^n\right) \lesssim \frac{\tau^6}{\varepsilon^6}, \qquad n = 0, 1, \ldots, \frac{T}{\tau} - 1. \tag{4.4.37}$$

Proof. Noticing the fact

$$b_l(\tau-\theta)\mathrm{e}^{i\tau/\varepsilon^2} = \frac{\sin(\omega_l(\tau-\theta))}{\varepsilon^2\omega_l}\mathrm{e}^{i\theta/\varepsilon^2}, \qquad 0 \le \theta \le \tau, \tag{4.4.38}$$

subtracting (4.4.35) from (4.4.12) and then using the Taylor's expansion, we get

$$\begin{aligned} \widehat{\xi_l^n} = -\int_0^\tau \frac{\sin(\omega_l(\tau-\theta))}{\varepsilon^2\omega_l}\Big[\theta^2\Big(\mathrm{e}^{i\theta/\varepsilon^2}\int_0^1 \widehat{(f_+^n)}_l''(\theta\rho)(1-\rho)d\rho \qquad (4.4.39) \\ + \mathrm{e}^{-i\theta/\varepsilon^2}\int_0^1 \widehat{(\overline{f_-^n})}_l''(\theta\rho)(1-\rho)d\rho + \mathrm{e}^{3i\theta/\varepsilon^2}\int_0^1 \widehat{(g_+^n)}_l''(\theta\rho)(1-\rho)d\rho \\ + \mathrm{e}^{-3i\theta/\varepsilon^2}\int_0^1 \widehat{(\overline{g_-^n})}_l''(\theta\rho)(1-\rho)d\rho\Big) + \widehat{(w^n)}_l(\theta)\Big]d\theta, \quad l = -\frac{M}{2}, \ldots, \frac{M}{2} - 1. \end{aligned}$$

Using the triangle inequality, we obtain for $l = -\frac{M}{2}, \ldots, \frac{M}{2} - 1$,

$$\begin{aligned} |\widehat{\xi_l^n}| \lesssim \frac{\tau^2}{\varepsilon^2\omega_l}\int_0^\tau \Bigg[\int_0^1 \left|\widehat{(f_+^n)}_l''(\theta\rho)\right|d\rho + \int_0^1 \left|\widehat{(\overline{f_-^n})}_l''(\theta\rho)\right|d\rho + \int_0^1 \left|\widehat{(g_+^n)}_l''(\theta\rho)\right|d\rho \\ + \int_0^1 \left|\widehat{(\overline{g_-^n})}_l''(\theta\rho)\right|d\rho\Bigg]d\theta + \frac{1}{\varepsilon^2\omega_l}\int_0^\tau \left|\widehat{(w^n)}_l(\theta)\right|d\theta. \end{aligned}$$

Noting $\frac{1}{\varepsilon^2\omega_l}=\frac{1}{\sqrt{1+\varepsilon^2\mu_l^2}}\leq 1$ for $l=-\frac{M}{2},\ldots,\frac{M}{2}-1$ and by Lemma 4.4.3, we get

$$\begin{aligned}\|\xi^n\|_{H^2}^2\lesssim\tau^6\Big[&\|\partial_{ss}f_+^n\|_{L^\infty([0,\tau];H^2)}^2+\|\partial_{ss}f_-^n\|_{L^\infty([0,T];H^2)}^2+\|\partial_{ss}g_+^n\|_{L^\infty([0,\tau];H^2)}^2\\&+\|\partial_{ss}g_-^n\|_{L^\infty([0,\tau];H^2)}^2\Big]+\tau^2\|w^n\|_{L^\infty([0,\tau];H^2)}^2\lesssim\tau^6+\tau^2\varepsilon^4,\quad 0<\tau\leq\tau_1.\end{aligned}\tag{4.4.40}$$

Similarly, noting $\frac{|\mu_l|}{\varepsilon^2\omega_l}=\frac{|\mu_l|}{\sqrt{1+\varepsilon^2\mu_l^2}}\leq\frac{1}{\varepsilon}$ for $l=-\frac{M}{2},\ldots,\frac{M}{2}-1$, we obtain

$$\|\partial_x\xi^n\|_{H^2}^2\lesssim\frac{\tau^6}{\varepsilon^2}+\tau^2\varepsilon^2\quad\text{and}\quad\|\dot\xi^n\|_{H^2}^2\lesssim\frac{\tau^6}{\varepsilon^4}+\tau^2,\quad 0<\tau\leq\tau_1.\tag{4.4.41}$$

Plugging (4.4.40) and (4.4.41) into (4.4.10) with $e_M^n=\xi^n$ and $\dot e_M^n=\dot\xi^n$, we immediately get the first inequality in (4.4.37). On the other hand, for $l=-M/2,\ldots,M/2-1$, noticing $\widehat{(w^n)}_l(0)=0$ and using the error formula of trapezoidal rule for an integral, we get

$$\left|\int_0^\tau\frac{\sin(\omega_l(\tau-\theta))}{\varepsilon^2\omega_l}\widehat{(w^n)}_l(\theta)d\theta\right|\lesssim\int_0^\tau\frac{\theta(\tau-\theta)}{\varepsilon^2\omega_l}\left|\frac{d^2}{d\theta^2}\left[\sin(\omega_l(\tau-\theta))\widehat{(w^n)}_l(\theta)\right]\right|d\theta.\tag{4.4.42}$$

Combining (4.4.42) and (4.4.39), we have

$$\begin{aligned}|\widehat{\xi_l^n}|\lesssim&\frac{\tau^2}{\varepsilon^2\omega_l}\int_0^\tau\Bigg[\int_0^1\left|\widehat{(f_+^n)}_l''(\theta\rho)\right|d\rho+\int_0^1\left|\widehat{(f_-^n)}_l''(\theta\rho)\right|d\rho+\int_0^1\left|\widehat{(g_+^n)}_l''(\theta\rho)\right|d\rho\\&+\int_0^1\left|\widehat{(g_-^n)}_l''(\theta\rho)\right|d\rho+\omega_l^2\left|\widehat{(w^n)}_l(\theta)\right|+\omega_l\left|\widehat{(w^n)}_l'(\theta)\right|+\left|\widehat{(w^n)}_l''(\theta)\right|\Bigg]d\theta.\end{aligned}$$

Noting $\omega_l\lesssim(1+|\mu_l|)/\varepsilon^2$ for $l=-\frac{M}{2},\ldots,\frac{M}{2}-1$, we obtain

$$\begin{aligned}\|\xi^n\|_{H^2}^2\lesssim\tau^6\Big[&\|\partial_{ss}f_+^n\|_{L^\infty([0,\tau];H^2)}^2+\|\partial_{ss}f_-^n\|_{L^\infty([0,\tau];H^2)}^2+\|\partial_{ss}g_+^n\|_{L^\infty([0,\tau];H^2)}^2\\&+\|\partial_{ss}g_-^n\|_{L^\infty([0,\tau];H^2)}^2+\frac{1}{\varepsilon^8}\|w^n\|_{L^\infty([0,\tau];H^4)}^2+\frac{1}{\varepsilon^4}\|\partial_s w^n\|_{L^\infty([0,\tau];H^3)}^2\\&+\|\partial_{ss}w^n\|_{L^\infty([0,\tau];H^2)}^2\Big]\lesssim\frac{\tau^6}{\varepsilon^4},\qquad 0<\tau\leq\tau_1.\end{aligned}\tag{4.4.43}$$

Similarly, we can get

$$\|\partial_x\xi^n\|_{H^2}^2\lesssim\frac{\tau^6}{\varepsilon^6},\qquad\|\dot\xi^n\|_{H^2}^2\lesssim\frac{\tau^6}{\varepsilon^8},\qquad 0<\tau\leq\tau_1.\tag{4.4.44}$$

Again, substituting (4.4.43) and (4.4.44) into (4.4.10) with $e_M^n=\xi^n$ and $\dot e_M^n=\dot\xi^n$, we immediately get the second inequality in (4.4.37). □

For any $\mathbf{v} \in Y_M$, we denote $v_{-1} = v_{M-1}$ and $v_{n+1} = v_1$ and then define the difference operators $\delta_x^+ \mathbf{v} \in Y_M$ and $\delta_x^2 \mathbf{v} \in Y_M$ as

$$\delta_x^+ \mathbf{v}_j = \frac{v_{j+1} - v_j}{h}, \qquad \delta_x^2 \mathbf{v}_j = \frac{v_{j+1} - 2v_j + v_{j-1}}{h^2}, \qquad j = 0, 1, \ldots, M.$$

In addition, we define the following norms as $\|\mathbf{v}\|_{Y,1}^2 = \|\mathbf{v}\|_{l^2}^2 + \|\delta_x^+ \mathbf{v}\|_{l^2}^2$ and $\|\mathbf{v}\|_{Y,2}^2 = \|\mathbf{v}\|_{l^2}^2 + \|\delta_x^+ \mathbf{v}\|_{l^2}^2 + \|\delta_x^2 \mathbf{v}\|_{l^2}^2$ and it is easy to see that

$$\|I_M \mathbf{v}\|_{H^1} \lesssim \|\mathbf{v}\|_{Y,1} \lesssim \|I_M \mathbf{v}\|_{H^1}, \quad \|I_M \mathbf{v}\|_{H^2} \lesssim \|\mathbf{v}\|_{Y,2} \lesssim \|I_M \mathbf{v}\|_{H^2}, \quad \forall \mathbf{v} \in Y_M. \tag{4.4.45}$$

Let $\mathbf{z}_\pm^0 \in Y_M$, $\dot{\mathbf{z}}_\pm^0 \in Y_M$, $\mathbf{f}_\pm^0 \in Y_M$, $\dot{\mathbf{f}}_\pm^0 \in Y_M$, $\mathbf{g}_\pm^0 \in Y_M$ and $\dot{\mathbf{g}}_\pm^0 \in Y_M$ with $z_{\pm,j}^0$, $\dot{z}_{\pm,j}^0$, $f_{\pm,j}^0$, $\dot{f}_{\pm,j}^0$, $g_{\pm,j}^0$ and $\dot{g}_{\pm,j}^0$, respectively, for $j = 0, 1, \ldots, M$ be defined in (4.3.20), and define the following error functions $\mathbf{e}_{z_\pm}^n \in Y_M$, $\dot{\mathbf{e}}_{z_\pm}^n \in Y_M$, $\mathbf{e}_{f_\pm}^n \in Y_M$, $\dot{\mathbf{e}}_{f_\pm}^n \in Y_M$, $\mathbf{e}_{g_\pm}^n \in Y_M$ and $\dot{\mathbf{e}}_{g_\pm}^n \in Y_M$ as

$$\begin{cases} e_{z_\pm,j}^n = z_\pm^n(x_j, 0) - z_{\pm,j}^0, \quad \dot{e}_{z_\pm,j}^n = \partial_s z_\pm^n(x_j, 0) - \dot{z}_{\pm,j}^0, \\ e_{f_\pm,j}^n = f_\pm^n(x_j, 0) - f_{\pm,j}^0, \quad \dot{e}_{f_\pm,j}^n = \partial_s f_\pm^n(x_j, 0) - \dot{f}_{\pm,j}^0, \qquad 0 \le j \le M, \\ e_{g_\pm,j}^n = g_\pm^n(x_j, 0) - g_{\pm,j}^0, \quad \dot{e}_{g_\pm,j}^n = \partial_s g_\pm^n(x_j, 0) - \dot{g}_{\pm,j}^0. \end{cases} \tag{4.4.46}$$

Lemma 4.4.5 (Interpolation error)**.** *Under the assumption (4.4.1) and assume (4.4.6) holds (which will be proved by induction later), then we have*

$$\begin{aligned} &\|I_M \mathbf{e}_{f_\pm}^n\|_{H^2} + \|I_M \mathbf{e}_{g_\pm}^n\|_{H^2} \lesssim \|e_M^n\|_{H^2} + \varepsilon^2 \|\dot{e}_M^n\|_{H^2} + h^{m_0}, \\ &\|I_M \dot{\mathbf{e}}_{f_\pm}^n\|_{H^2} + \|I_M \dot{\mathbf{e}}_{g_\pm}^n\|_{H^2} \lesssim \frac{1}{\tau} \left(\|e_M^n\|_{H^2} + \varepsilon^2 \|\dot{e}_M^n\|_{H^2} + h^{m_0} + \tau^2 \right). \end{aligned} \tag{4.4.47}$$

Proof. From (4.4.46), (4.4.45), (4.3.20) and (4.4.16), we have

$$\begin{aligned} \|I_M \mathbf{e}_{f_\pm}^n\|_{H^2} &\lesssim \|\mathbf{e}_{f_\pm}^n\|_{Y,2} \\ &\le \int_0^1 \left[\left\| \partial_{z_+} f_\pm \left(\mathbf{z}_+^\theta, \mathbf{z}_-^n \right) \cdot \mathbf{e}_{z_+}^n \right\|_{Y,2} + \left\| \partial_{z_-} f_\pm \left(\mathbf{z}_+^0, \mathbf{z}_-^\theta \right) \cdot \mathbf{e}_{z_-}^n \right\|_{Y,2} \right] d\theta, \end{aligned} \tag{4.4.48}$$

where $\mathbf{z}_\pm^\theta \in Y_M$ and $\mathbf{z}_\pm^n \in Y_M$ are defined as $\mathbf{z}_{\pm,j}^\theta = \theta z_\pm^n(x_j, 0) + (1 - \theta) z_{\pm,j}^0$ and $\mathbf{z}_\pm^n = z_{\pm,j}^n$, respectively, for $j = 0, 1, \ldots, M$ and $0 \le \theta \le 1$. Under the assumption

(4.4.6) and using the Sobolev's inequality, we get

$$\begin{aligned}
&\int_0^1 \left\|\partial_{z_+} f_\pm\left(\mathbf{z}_+^\theta, \mathbf{z}_-^n\right)\cdot \mathbf{e}_{z_+}^n\right\|_{Y,2} d\theta \lesssim \left\|\mathbf{e}_{z_+}^n\right\|_{l^\infty}\cdot \int_0^1 \left\|\delta_x^2\partial_{z_+} f_\pm\left(\mathbf{z}_+^\theta, \mathbf{z}_-^n\right)\right\|_{l^2} d\theta \\
&+\left\|\mathbf{e}_{z_+}^n\right\|_{Y,1}\cdot \int_0^1 \left\|\delta_x^+\partial_{z_+} f_\pm\left(\mathbf{z}_+^\theta, \mathbf{z}_-^n\right)\right\|_{l^\infty} d\theta + \left\|\mathbf{e}_{z_+}^n\right\|_{Y,2}\cdot \int_0^1 \left\|\partial_{z_+} f_\pm\left(\mathbf{z}_+^\theta, \mathbf{z}_-^n\right)\right\|_{l^\infty} d\theta \\
&\lesssim \left\|\mathbf{e}_{z_+}^n\right\|_{Y,2}.
\end{aligned}$$

Similarly, we have

$$\int_0^1 \left\|\partial_{z_-} f_\pm\left(z_+^0, \mathbf{z}_-^\theta\right)\cdot \mathbf{e}_{z_-}^n\right\|_{Y,2} d\theta \lesssim \left\|\mathbf{e}_{z_-}^n\right\|_{Y,2}.$$

Plugging the above two inequalities into (4.4.48), we get

$$\begin{aligned}
\|I_M \mathbf{e}_{f_\pm}^n\|_{H^2} &\lesssim \left\|\mathbf{e}_{z_+}^n\right\|_{Y,2} + \left\|\mathbf{e}_{z_-}^n\right\|_{Y,2} \lesssim \left\|I_M \mathbf{e}_{z_+}^n\right\|_{H^2} + \left\|I_M \mathbf{e}_{z_-}^n\right\|_{H^2} \\
&\lesssim \|I_M u(\cdot,t_n) - u_I^n\|_{H^2} + \varepsilon^2 \|I_M \partial_t u(\cdot,t_n) - \dot{u}_I^n\|_{H^2} \\
&\lesssim \|e_M^n\|_{H^2} + \varepsilon^2 \|\dot{e}_M^n\|_{H^2} + h^{m_0}. \qquad (4.4.49)
\end{aligned}$$

In addition, combining (4.2.7) and (4.3.20), we obtain

$$\begin{aligned}
\|I_M \dot{\mathbf{e}}_{f_\pm}^n\|_{H^2} \lesssim &\|\dot{\mathbf{e}}_{f_\pm}^n\|_{Y,2} \lesssim \left\|I_M \mathbf{e}_{z_+}^n\right\|_{H^2} + \left\|I_M \mathbf{e}_{z_-}^n\right\|_{H^2} + \left\|I_M \dot{\mathbf{e}}_{z_+}^n\right\|_{H^2} + \left\|I_M \dot{\mathbf{e}}_{z_-}^n\right\|_{H^2} \\
&\lesssim \|e_M^n\|_{H^2} + \varepsilon^2 \|\dot{e}_M^n\|_{H^2} + h^{m_0} + \left\|\partial_s z_+^n(\cdot,0) - I_M \dot{z}_+^0\right\|_{H^2} \\
&\quad + \left\|\partial_s z_-^n(\cdot,0) - I_M \dot{z}_-^0\right\|_{H^2}. \qquad (4.4.50)
\end{aligned}$$

Noticing $\partial_s z_\pm^n(x,0) = \frac{i}{2}[-\partial_{xx} z_\pm^n(x,0) + f_\pm^n(z_+(x,0), z_-(x,0))]$, we have in Fourier space

$$\begin{aligned}
\widehat{(\partial_s z_\pm^n)_l} =& \frac{i}{2}\left[\mu_l^2 \widehat{(z_\pm^n)_l} + \widehat{(f_\pm^n)_l}\right] \qquad (4.4.51)\\
=& \frac{i}{2}\left[2\frac{\sin(\frac{1}{2}\tau\mu_l^2)}{\tau}\widehat{(z_\pm^n)_l} + \widehat{(f_\pm^n)_l}\right] + \frac{i\mu_l^2}{2}\left(1 - \frac{\sin(\frac{1}{2}\tau\mu_l^2)}{\frac{1}{2}\tau\mu_l^2}\right)\widehat{(z_\pm^n)_l}.
\end{aligned}$$

Since the 'sinc' function $\mathrm{sinc}(s) = \frac{\sin s}{s}$ if $s \neq 0$ and $\mathrm{sinc}(0) = 1$ has the property that $\mathrm{sinc}'(0) = 0$ and all the derivatives of sinc are bounded, we find

$$\left|1 - \frac{\sin\left(\frac{1}{2}\tau\mu_l^2\right)}{\frac{1}{2}\tau\mu_l^2}\right| = \left|\mathrm{sinc}(0) - \mathrm{sinc}\left(\frac{1}{2}\tau\mu_l^2\right)\right| \leq \frac{1}{2}\tau\mu_l^2 \|\mathrm{sinc}'(\cdot)\|_{L^\infty}.$$

Then from (4.3.20) and Lemma 4.4.3 we have for small τ,

$$\left\|\partial_s z_\pm^n(\cdot,0) - I_M \dot{z}_\pm^0\right\|_{H^2} \lesssim \frac{1}{\tau}\left(\|e_M^n\|_{H^2} + \varepsilon^2\|\dot{e}_M^n\|_{H^2} + h^{m_0}\right) + \tau\|z_\pm^n(\cdot,0)\|_{H^6}. \quad (4.4.52)$$

Plugging (4.4.52) into (4.4.50), we get

$$\|I_M\dot{\mathbf{e}}_{f_\pm}^n\|_{H^2} \lesssim \frac{1}{\tau}\left(\|e_M^n\|_{H^2} + \varepsilon^2\|\dot{e}_M^n\|_{H^2} + h^{m_0} + \tau^2\right).$$

Similarly, we can get the estimate results for $\|I_M\mathbf{e}_{g_\pm}^n\|_{H^2}$ and $\|I_M\dot{\mathbf{e}}_{g_\pm}^n\|_{H^2}$. Combining all, we immediately get (4.4.47). □

Defining the errors from the nonlinear terms as

$$\eta^n(x) := \sum_{l=-M/2}^{M/2-1} \widetilde{\eta_l^n}\ \mathrm{e}^{i\mu_l(x-a)}, \quad \dot{\eta}^n(x) := \sum_{l=-M/2}^{M/2-1} \widetilde{\dot{\eta}_l^n}\ \mathrm{e}^{i\mu_l(x-a)}, \quad x\in\overline{\Omega}, \quad n\geq 0, \tag{4.4.53}$$

where

$$\widetilde{\eta_l^n} = \widehat{\mathcal{G}_l^n} - \widetilde{G_l^n}, \qquad \widetilde{\dot{\eta}_l^n} = \widehat{\dot{\mathcal{G}}_l^n} - \widetilde{\dot{G}_l^n}, \qquad l = -\frac{M}{2},\ldots\frac{M}{2}-1, \tag{4.4.54}$$

then we have

Lemma 4.4.6 (Estimates on η^n and $\dot{\eta}^n$)**.** *Under the same assumptions as in Lemma 4.4.5, we have for any* $0<\tau\leq\tau_1$,

$$\mathcal{E}\left(\eta^n,\dot{\eta}^n\right) \lesssim \tau^2\mathcal{E}\left(e_M^n,\dot{e}_M^n\right) + \frac{\tau^2h^{2m_0}}{\varepsilon^2} + \frac{\tau^6}{\varepsilon^2}, \quad n=0,1,\ldots,\frac{T}{\tau}-1. \tag{4.4.55}$$

Proof. Denote

$$\begin{cases} e_{f_\pm}^n(x) = f_\pm^n(x) - (I_M\mathbf{f}_\pm^0)(x), \quad \dot{e}_{f_\pm}^n(x) = \partial_s f_\pm^n(x) - (I_M\dot{\mathbf{f}}_\pm^0)(x), \\ e_{g_\pm}^n(x) = f_\pm^n(x) - (I_M\mathbf{f}_\pm^0)(x), \quad \dot{e}_{g_\pm}^n(x) = \partial_s g_\pm^n(x) - (I_M\dot{\mathbf{g}}_\pm^0)(x), \quad x\in\Omega. \end{cases} \tag{4.4.56}$$

For $l=-M/2,\ldots,M/2-1$, from (4.4.56), (4.4.54) and (4.4.36), using the triangle inequality, we have

$$\begin{aligned} |\eta_l^n| \ \leq\ & |c_l(\tau)|\left[\left|\widehat{(e_{f_+}^n)_l}\right| + \left|\widehat{(e_{f_-}^n)_l}\right|\right] + |d_l(\tau)|\left[\left|\widehat{(\dot{e}_{f_+}^n)_l}\right| + \left|\widehat{(\dot{e}_{f_-}^n)_l}\right|\right] \\ & + |p_l(\tau)|\left[\left|\widehat{(e_{g_+}^n)_l}\right| + \left|\widehat{(e_{g_-}^n)_l}\right|\right] + |q_l(\tau)|\left[\left|\widehat{(\dot{e}_{g_+}^n)_l}\right| + \left|\widehat{(\dot{e}_{g_-}^n)_l}\right|\right]. \end{aligned} \tag{4.4.57}$$

From (4.3.16) directly, we have

$$\begin{aligned} &|c_l(\tau)| + |p_l(\tau)| \lesssim \frac{\tau}{\sqrt{1+\mu_l^2\varepsilon^2}} \lesssim \tau, \qquad \mu_l(|c_l(\tau)| + |p_l(\tau)|) \lesssim \frac{\tau}{\varepsilon}, \\ &|d_l(\tau)| + |q_l(\tau)| \lesssim \frac{\tau^2}{\sqrt{1+\mu_l^2\varepsilon^2}} \lesssim \tau^2, \qquad \mu_l(|d_l(\tau)| + |q_l(\tau)|) \lesssim \frac{\tau^2}{\varepsilon}. \end{aligned} \tag{4.4.58}$$

Inserting (4.4.58) into (4.4.57) and using the Cauchy's inequality, we obtain

$$\begin{aligned}\|\eta^n\|_{H^2}^2 &\lesssim \tau^2\left[\left\|P_M e_{f_+}^n\right\|_{H^2}^2+\left\|P_M e_{f_-}^n\right\|_{H^2}^2+\left\|P_M e_{g_+}^n\right\|_{H^2}^2+\left\|P_M e_{g_-}^n\right\|_{H^2}^2\right]\\ &\quad+\tau^4\left[\left\|P_M \dot{e}_{f_+}^n\right\|_{H^2}^2+\left\|P_M \dot{e}_{f_-}^n\right\|_{H^2}^2+\left\|P_M \dot{e}_{g_+}^n\right\|_{H^2}^2+\left\|P_M \dot{e}_{g_-}^n\right\|_{H^2}^2\right]\\ &\lesssim \tau^2\left[\left\|I_M e_{f_+}^n\right\|_{H^2}^2+\left\|I_M e_{f_-}^n\right\|_{H^2}^2+\left\|I_M e_{g_+}^n\right\|_{H^2}^2+\left\|I_M e_{g_-}^n\right\|_{H^2}^2\right]\\ &\quad+\tau^4\left[\left\|I_M \dot{e}_{f_+}^n\right\|_{H^2}^2+\left\|I_M \dot{e}_{f_-}^n\right\|_{H^2}^2+\left\|I_M \dot{e}_{g_+}^n\right\|_{H^2}^2+\left\|I_M \dot{e}_{g_-}^n\right\|_{H^2}^2\right]+\tau^2 h^{2m_0}\\ &\lesssim \tau^2\|e_M^n\|_{H^2}^2+\tau^2\varepsilon^4\|\dot{e}_M^n\|_{H^2}^2+\tau^2 h^{2m_0}+\tau^6, \end{aligned}\tag{4.4.59}$$

and

$$\|\partial_x\eta^n\|_{H^2}^2\lesssim\frac{\tau^2}{\varepsilon^2}\|e_M^n\|_{H^2}^2+\tau^2\varepsilon^2\|\dot{e}_M^n\|_{H^2}^2+\frac{\tau^2 h^{2m_0}}{\varepsilon^2}+\frac{\tau^6}{\varepsilon^2}.\tag{4.4.60}$$

Similarly,

$$\varepsilon^2\|\dot{\eta}^n\|_{H^2}^2\lesssim\frac{\tau^2}{\varepsilon^2}\|e_M^n\|_{H^2}^2+\tau^2\varepsilon^2\|\dot{e}_M^n\|_{H^2}^2+\frac{\tau^2 h^{2m_0}}{\varepsilon^2}+\frac{\tau^6}{\varepsilon^2}.\tag{4.4.61}$$

Combining (4.4.59), (4.4.61) and (4.4.10) we immediately obtain (4.4.55). □

Proof of Theorem 4.4.1. The proof will be proceeded by the method of mathematical induction and the energy method. For $n=0$, from the initial data in the MTI-FP (4.3.17)-(4.3.20) method and noticing the assumption (4.4.1), we have

$$\|e^0\|_{H^2}+\varepsilon^2\|\dot{e}^0\|_{H^2}=\|\phi_1-I_M\phi_1\|_{H^2}+\|\phi_2-I_M\phi_2\|_{H^2}\lesssim h^{m_0+2}\lesssim h^{m_0}.$$

In addition, using the triangle inequality, we know that there exists $h_1>0$ independent of ε such that for $0<h\le h_1$ and $\tau>0$

$$\|u_I^0\|_{H^2}\le\|\phi_1\|_{H^2}+\|e^0\|_{H^2}\le C_0+1,\qquad \|\dot{u}_I^0\|_{H^2}\le\frac{\|\phi_2\|_{H^2}}{\varepsilon^2}+\|\dot{e}^0\|_{H^2}\le\frac{C_0+1}{\varepsilon^2}.$$

Thus (4.4.5)-(4.4.6) are valid for $n=0$. Now we assume that (4.4.5)-(4.4.6) are valid for $0\le n\le m-1\le T/\tau-1$. Substracting (4.4.12) from (4.4.19), we have

$$\widehat{(e^{n+1})}_l=\widehat{u}_l(t_{n+1})-\widehat{(u_I^{n+1})}_l=\cos(\omega_l\tau)\widehat{(e^n)}_l+\frac{\sin(\omega_l\tau)}{\omega_l}\widehat{(\dot{e}^n)}_l+\widehat{\xi}_l^n-\widetilde{\eta}_l^n,\tag{4.4.62a}$$

$$\widehat{(\dot{e}^{n+1})}_l=\widehat{u}_l'(t_{n+1})-\widehat{(\dot{u}_I^{n+1})}_l=-\omega_l\sin(\omega_l\tau)\widehat{(e^n)}_l+\cos(\omega_l\tau)\widehat{(\dot{e}^n)}_l+\widehat{\dot{\xi}}_l^n-\widetilde{\dot{\eta}}_l^n.\tag{4.4.62b}$$

Using the Cauchy's inequality, we obtain

$$\left|\widehat{(e^{n+1})}_l\right|^2 \le (1+\tau)\left|\cos(\omega_l\tau)\widehat{(e^n)}_l + \frac{\sin(\omega_l\tau)}{\omega_l}\widehat{(\dot{e}^n)}_l\right|^2 + \frac{1+\tau}{\tau}\left|\widehat{\xi}_l^n - \widetilde{\eta}_l^n\right|^2, \tag{4.4.63a}$$

$$\left|\widehat{(\dot{e}^{n+1})}_l\right|^2 \le (1+\tau)\left|\cos(\omega_l\tau)\widehat{(\dot{e}^n)}_l - \omega_l\sin(\omega_l\tau)\widehat{(e^n)}_l\right|^2 + \frac{1+\tau}{\tau}\left|\widehat{\dot{\xi}}_l^n - \widetilde{\dot{\eta}}_l^n\right|^2. \tag{4.4.63b}$$

Multiplying (4.4.63a) and (4.4.63b) by $(\mu_l^2+\frac{1}{\varepsilon^2})(1+\mu_l^2+\mu_l^4)$ and $\varepsilon^2(1+\mu_l^2+\mu_l^4)$, respectively, and then summing them up for $l=-M/2,\ldots,M/2-1$, we obtain

$$\mathcal{E}(e_M^{n+1},\dot{e}_M^{n+1}) \le (1+\tau)\mathcal{E}(e_M^n,\dot{e}_M^n) + \frac{1+\tau}{\tau}\mathcal{E}(\xi^n-\eta^n,\dot{\xi}^n-\dot{\eta}^n).$$

Using the Cauchy's inequality, we get

$$\mathcal{E}(e_M^{n+1},\dot{e}_M^{n+1}) - \mathcal{E}(e_M^n,\dot{e}_M^n) \lesssim \tau\mathcal{E}(e_M^n,\dot{e}_M^n) + \frac{1+\tau}{\tau}\left[\mathcal{E}(\xi^n,\dot{\xi}^n)+\mathcal{E}(\eta^n,\dot{\eta}^n)\right]. \tag{4.4.64}$$

Inserting (4.4.55) and the second inequality in (4.4.37) into (4.4.64), we get

$$\mathcal{E}\left(e_M^{n+1},\dot{e}_M^{n+1}\right) - \mathcal{E}\left(e_M^n,\dot{e}_M^n\right) \lesssim \tau\mathcal{E}\left(e_M^n,\dot{e}_M^n\right) + \frac{\tau h^{2m_0}}{\varepsilon^2} + \frac{\tau^5}{\varepsilon^6}.$$

Summing the above inequality for $0\le n\le m-1$ and then applying the discrete Gronwall's inequality, we have

$$\mathcal{E}\left(e_M^m,\dot{e}_M^m\right) \lesssim \frac{h^{2m_0}}{\varepsilon^2} + \frac{\tau^4}{\varepsilon^6}. \tag{4.4.65}$$

Similarly, by using the first inequality in (4.4.37), we obtain

$$\mathcal{E}\left(e_M^m,\dot{e}_M^m\right) \lesssim \frac{h^{2m_0}}{\varepsilon^2} + \frac{\tau^4}{\varepsilon^2} + \varepsilon^2. \tag{4.4.66}$$

Combining (4.4.10), (4.4.9), (4.4.65) and (4.4.66), we get that (4.4.5) is valid for $n=m$, which implies [34, 68]

$$\|e^m\|_{H^2} + \varepsilon^2\|\dot{e}^m\|_{H^2} \le h^{m_0} + \tau.$$

Using the triangle inequality, we obtain that these exist $h_2>0$ and $\tau_2>0$ independent of ε such that

$$\|u_I^m\|_{H^2} \le \|u(\cdot,t_m)\|_{H^2} + \|\dot{e}^m\|_{H^2} \le C_0+1,$$
$$\|\dot{u}_I^m\|_{H^2} \le \|\partial_t u(\cdot,t_m)\|_{H^2} + \|\dot{e}^m\|_{H^2} \le \frac{C_0+1}{\varepsilon^2}, \qquad 0<h\le h_2, \quad 0<\tau\le\tau_2.$$

Thus (4.4.6) is also valid for $n = m$. Then the proof is completed by choosing $\tau_0 = \min\{\tau_1, \tau_2\}$ and $h_0 = \min\{h_1, h_2\}$. □

Remark 4.4.1. *Here we emphasize that Theorem 4.4.1 holds in 2D and 3D and the above approach can be directly extended to the higher dimensions without any extra efforts. The only thing needs to be taken care of is the Sobolev inequality used in Lemma 4.4.5 in 2D and 3D,*

$$\begin{aligned} &\|u\|_{L^\infty(\Omega)} \le C\|u\|_{H^2(\Omega)}, \quad \text{in 2D and 3D,} \\ &\|u\|_{W^{1,p}(\Omega)} \le C\|u\|_{H^2(\Omega)}, \quad 1 < p < 6 \text{ in 2D and 3D,} \end{aligned} \tag{4.4.67}$$

where Ω is a bounded domain in 2D or 3D. By using assumption (4.4.6), Lemma 4.4.5 will still hold in 2D and 3D. (4.4.6) and error bounds can be proved by induction since our scheme is explicit.

Under a weaker assumption of the regularity

$$\text{(B)} \quad u \in C^1\left([0,T]; H_p^{m_0+3}(\Omega)\right), \quad \|u\|_{L^\infty([0,T];H^{m_0+3})} + \varepsilon^2 \|\partial_t u\|_{L^\infty([0,T];H^{m_0+3})} \lesssim 1,$$

with $m_0 \ge 2$, we can have the H^1-error estimates of the MTI-FP method by a very similar proof with all the H^2-norms in above changed into H^1-norms.

Theorem 4.4.2. *Under the assumption (B), there exist two constants $0 < h_0 \le 1$ and $0 < \tau_0 \le 1$ sufficiently small and independent of ε such that, for any $0 < \varepsilon \le 1$, when $0 < h \le h_0$ and $0 < \tau \le \tau_0$, we have*

$$\|e^n\|_{H^1} + \varepsilon^2 \|\dot{e}^n\|_{H^1} \lesssim h^{m_0} + \frac{\tau^2}{\varepsilon^2}, \ \|e^n\|_{H^1} + \varepsilon^2 \|\dot{e}^n\|_{H^1} \lesssim h^{m_0} + \tau^2 + \varepsilon^2, \tag{4.4.68}$$

$$\|u^n\|_{l^\infty} \le C_0 + 1, \quad \|\dot{u}^n\|_{l^\infty} \le \frac{C_0 + 1}{\varepsilon^2}, \qquad 0 \le n \le \frac{T}{\tau}. \tag{4.4.69}$$

Remark 4.4.2. *In 1D case, Theorem 4.4.2 holds without any CFL-type conditions. However for higher dimensional cases, i.e. $d = 2$ or $d = 3$, due to the use of inverse inequality to provide the l^∞ control of the numerical solution [13], one has to impose the technical condition*

$$\tau \lesssim \rho_d(h), \qquad \text{with} \quad \rho_d(h) = \begin{cases} 1/|\ln h|, & d = 2, \\ \sqrt{h}, & d = 3. \end{cases}$$

If the solution of the KGE is smooth enough, we can always turn to Theorem 4.4.1 and such CFL type conditions are unnecessary.

Remark 4.4.3. *If the periodic boundary condition for the KGE (4.3.3) is replaced by the homogeneous Dirichlet or Neumann boundary condition, then the MTI-FP method and its error estimates are still valid provided that the Fourier basis is replaced by sine or cosine basis.*

Remark 4.4.4. *Here we only consider the multiscale time integrator based on the decomposition by frequency, which is corresponding to the MTI-F (2.5.23) given in Section 2.5.2. For the other MTI-FA (2.5.16) proposed in Section 2.5.1, we remark that although the integrator can be applied to solve the KGE (4.1.1) as well, it suffers from stability problems based on our analysis and numerical experience. The stability problem is essentially caused by the approximations of the second order time derivative of function $z_\pm$ in the remainder equation of r. Meanwhile, the second error bound of (2.5.25) for the MTI-FA obtained by Theorem 2.5.1 is no longer valid when it is extended to the KGE, because now the Schrödinger type equations in (2.4.16) can not be solved exactly in the PDE case.*

Remark 4.4.5. *If the cubic nonlinearity in the KGE (4.1.1) is replaced by a general gauge invariant nonlinearity, the general MTI-FP method can be designed similarly to those in Chapter 2.*

4.5 Numerical results

In this section, we present numerical results of the MTI-FP method to confirm our error estimates. We take $d = 1$ and $f(u) = |u|^2 u$ in (4.1.1) and choose the initial data as

$$\phi_1(x) = (1+i)\mathrm{e}^{-x^2/2}, \qquad \phi_2(x) = \frac{3\mathrm{e}^{-x^2/2}}{2}, \qquad x \in \mathbb{R}. \tag{4.5.1}$$

The problem is solved on a bounded interval $\Omega = [-16, 16]$, i.e. $b = -a = 16$, which is large enough to guarantee that the periodic boundary condition does not

Table 4.1: Spatial error analysis: $\mathrm{e}_{\varepsilon}^{\tau,h}(T=1)$ with $\tau = 5\times 10^{-6}$ for different ε and h.

$\mathrm{e}_{\varepsilon}^{\tau,h}(T)$	$h_0=1$	$h_0/2$	$h_0/4$	$h_0/8$
$\varepsilon_0 = 0.5$	1.65E−1	3.60E−3	1.03E−6	7.34E−11
$\varepsilon_0/2^1$	2.65E−1	9.70E−3	9.07E−7	5.03E−11
$\varepsilon_0/2^2$	9.02E−1	1.34E−2	1.73E−7	4.60E−11
$\varepsilon_0/2^3$	1.13E+0	2.98E−2	2.25E−7	4.10E−11
$\varepsilon_0/2^4$	4.67E−1	3.14E−2	1.79E−7	4.78E−11
$\varepsilon_0/2^5$	7.41E−1	2.73E−2	2.50E−7	5.49E−11
$\varepsilon_0/2^7$	7.41E−1	2.62E−2	2.12E−7	4.96E−11
$\varepsilon_0/2^9$	6.33E−1	3.57E−2	1.92E−7	5.04E−11
$\varepsilon_0/2^{11}$	9.19E−1	2.44E−2	2.19E−7	6.18E−11
$\varepsilon_0/2^{13}$	1.18E+0	2.38E−2	2.59E−7	5.86E−11

introduce a significant aliasing error relative to the original problem. To quantify the error, we introduce two error functions:

$$\mathrm{e}_{\varepsilon}^{\tau,h}(T) := \left\| u(\cdot, T=M\tau) - u_I^M \right\|_{H^2}, \qquad \mathrm{e}_{\infty}^{\tau,h}(T) := \max_{\varepsilon} \left\{ \mathrm{e}_{\varepsilon}^{\tau,h}(T) \right\}.$$

Since the analytical solution to this problem is not available, so the 'exact' solution is obtained numerically by the MTI-FP method (4.3.17)-(4.3.20) with very fine mesh $h = 1/32$ and time step $\tau = 5\times 10^{-6}$. Tab. 4.1 shows the spatial error of MTI-FP method at $T=1$ under different ε and h with a very small time step $\tau = 5\times 10^{-6}$ such that the discretization error in time is negligible. Tab. 4.2 shows the temporal error of MTI-FP method at $T=1$ under different ε and τ with a small mesh size $h = 1/8$ such that the discretization error in space is negligible. The profiles of the solutions at $\varepsilon = 1/4$ and $\varepsilon = 1/8$ are given in Fig. 4.2.

From Tabs. 4.1-4.2 and extensive additional results not shown here for brevity, we can draw the following observations:

Table 4.2: Temporal error analysis: $\mathrm{e}_{\varepsilon}^{\tau,h}(T=1)$ a nd $\mathrm{e}_{\infty}^{\tau,h}(T=1)$ with $h=1/8$ for different ε and τ.

$\mathrm{e}_{\varepsilon}^{\tau,h}(T)$	$\tau_0 = 0.2$	$\tau_0/2^2$	$\tau_0/2^4$	$\tau_0/2^6$	$\tau_0/2^8$	$\tau_0/2^{10}$	$\tau_0/2^{12}$
$\varepsilon_0 = 0.5$	7.17E-1	5.72E-2	3.50E-3	2.14E-4	1.33E-5	8.14E-7	3.67E-8
rate	—	1.82	2.02	2.01	2.00	2.01	2.20
$\varepsilon_0/2^1$	5.40E-1	1.58E-1	1.12E-2	6.74E-4	4.15E-5	2.54E-6	1.18E-7
rate	—	0.89	1.91	2.02	2.01	2.01	2.21
$\varepsilon_0/2^2$	5.23E-1	1.47E-1	3.70E-2	2.70E-3	1.62E-4	9.87E-6	4.62E-7
rate	—	0.91	0.99	1.90	2.02	2.01	2.20
$\varepsilon_0/2^3$	6.30E-1	6.28E-2	4.13E-2	8.90E-3	6.51E-4	3.92E-5	1.82E-6
rate	—	1.66	0.30	1.11	1.89	2.02	2.21
$\varepsilon_0/2^4$	6.11E-1	3.00E-2	1.16E-2	1.05E-2	2.20E-3	1.60E-4	7.41E-6
rate	—	2.17	0.68	0.07	1.13	1.89	2.21
$\varepsilon_0/2^5$	6.17E-1	3.01E-2	2.70E-3	2.90E-3	2.80E-3	5.26E-4	2.98E-5
rate	—	2.17	1.75	-0.04	0.02	1.17	2.07
$\varepsilon_0/2^7$	6.16E-1	2.90E-2	1.80E-3	2.37E-4	1.37E-4	1.96E-4	1.91E-4
rate	—	2.20	2.01	1.46	0.40	-0.26	0.02
$\varepsilon_0/2^9$	6.13E-1	2.90E-2	1.69E-3	1.12E-4	1.09E-5	5.51E-6	1.69E-6
rate	—	2.20	2.03	1.96	1.68	0.49	0.85
$\varepsilon_0/2^{11}$	6.16E-1	2.90E-2	1.69E-3	1.05E-4	6.95E-6	9.97E-7	3.38E-7
rate	—	2.20	2.03	2.00	1.96	1.40	0.78
$\varepsilon_0/2^{13}$	6.20E-1	2.92E-2	1.69E-3	1.06E-4	6.61E-6	3.94E-7	2.38E-8
rate	—	2.20	2.04	2.00	2.00	2.03	2.02
$\mathrm{e}_{\infty}^{\tau,h}(T)$	7.17E-1	1.58E-1	4.13E-2	1.05E-2	2.80E-3	5.26E-4	1.91E-4
rate	—	1.09	0.97	0.99	1.00	1.15	0.74

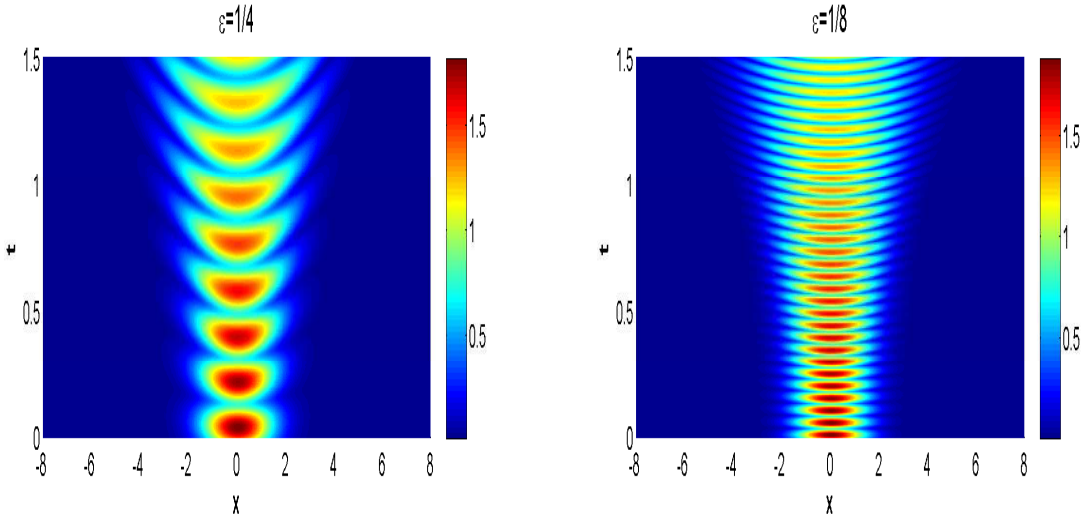

Figure 4.2: Profiles of the solutions of 1D KGE (4.5.1) under different ε.

(i) The MTI-FP method is spectrally accurate in space, which is uniformly for $0 < \varepsilon \leq 1$ (cf. Tab. 4.1).

(ii) The MTI-FP method converges uniformly and linearly in time for $\varepsilon \in (0, \tau]$ (cf. last row in Tab. 4.2). In addition, for each fixed $\varepsilon = \varepsilon_0 > 0$, when τ is small enough, it converges quadratically in time (cf. each row in the upper triangle of Tab. 4.2); and for each fixed ε small enough, when τ satisfies $0 < \varepsilon < \tau$, it also converges quadratically in time (cf. each row in the lower triangle of Tab. 4.2).

(iii) The MTI-FP method is uniformly accurate for all $\varepsilon \in (0, 1]$ under the mesh strategy (or ε-scalability) $\tau = O(1)$ and $h = O(1)$.

With the MTI-FP method, we can solve the KGE (4.1.1) in the nonrelativistic limit regime effectively in 2D and 3D cases. Fig. 4.3 and Fig. 4.3 show the contour plots of the solutions of the KGE in 2D case, i.e. $d = 2$ with $f(u) = |u|^2 u$ and

$$\begin{aligned} \phi_1(x, y) &= \exp\left(-(x+2)^2 - y^2\right) + \exp\left(-(x-2)^2 - y^2\right), \\ \phi_2(x, y) &= \exp\left(-x^2 - y^2\right), \end{aligned} \tag{4.5.2}$$

in (4.1.1) under different ε. Fig. 4.5 shows the isosurface plots of the solutions of

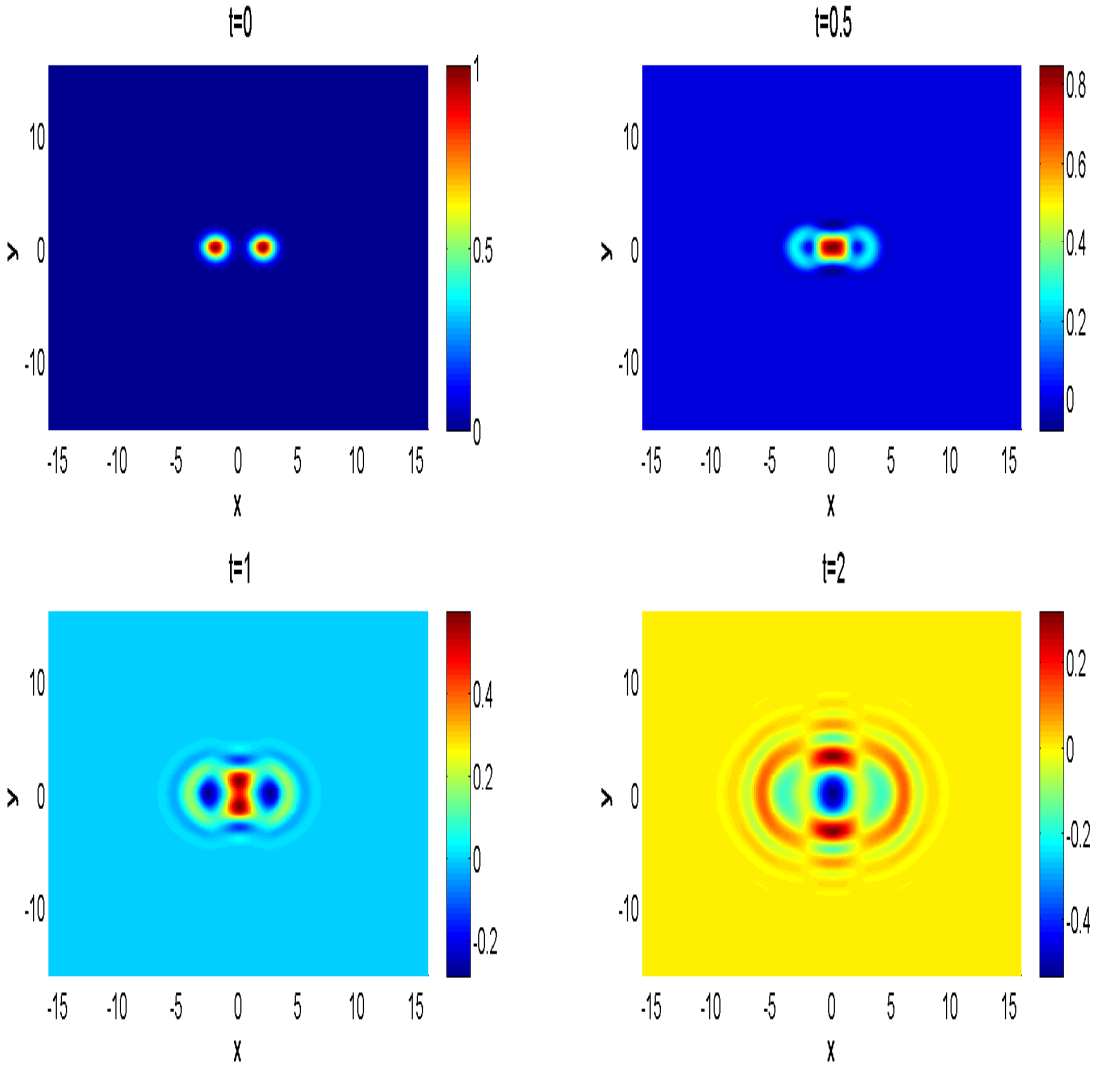

Figure 4.3: Contour plots of the solutions of 2D KGE with (4.5.2) at different time t under $\varepsilon = 5E-3$.

the KGE in 3D case, i.e. $d = 3$ with $f(u) = |u|^2 u$ and

$$\begin{aligned} \phi_1(x,y,z) &= 2\exp\left(-x^2 - 2y^2 - 3z^2\right), \\ \phi_2(x,y) &= \exp\left(-(x+0.5)^2 - y^2 - z^2\right), \end{aligned} \tag{4.5.3}$$

in (4.1.1).

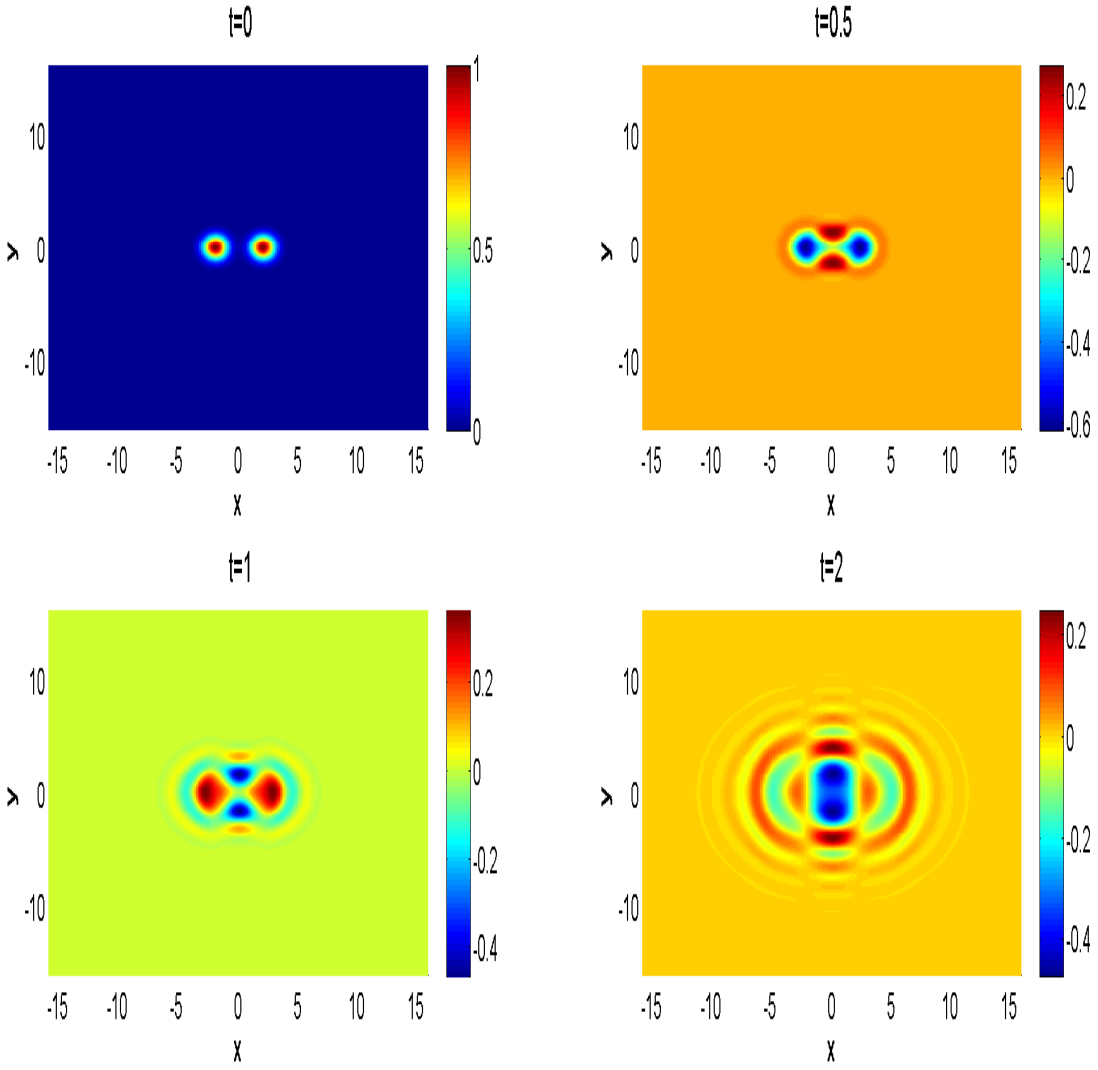

Figure 4.4: Contour plots of the solutions of 2D KGE with (4.5.2) at different time t under $\varepsilon = 2.5E-3$.

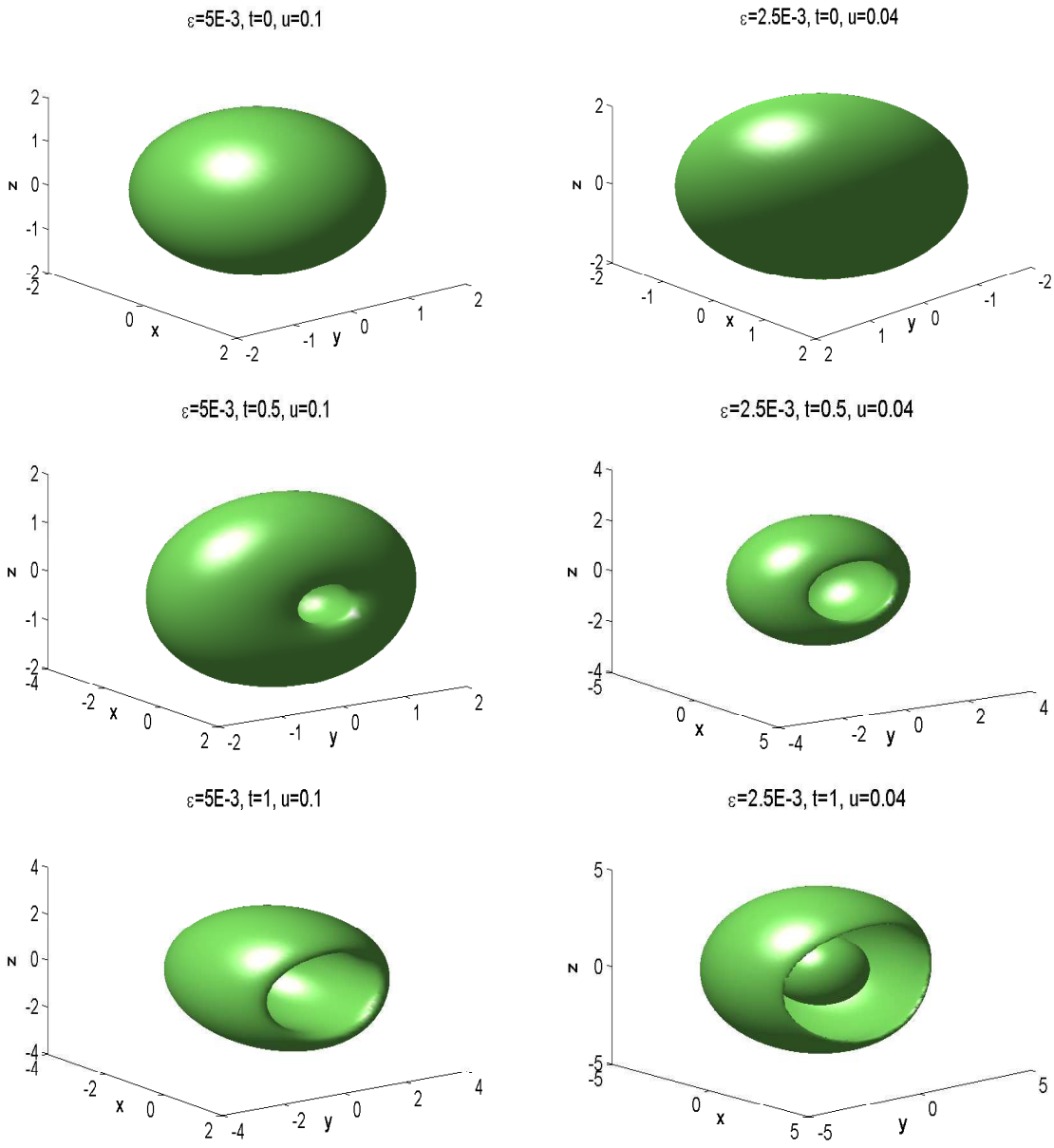

Figure 4.5: Isosurface plots of the solutions of 3D KGE with (4.5.3) at different time t under ε.

Chapter 5

Applications to the Klein-Gordon-Zakharov system

5.1 Introduction

In this chapter, we consider the following dimensionless Klein-Gordon-Zakharov (KGZ) system in d-dimensions ($d = 1, 2, 3$) as given in Section 1.3.3, which is a classical model describing the interaction between the Langmuir waves and ion acoustic waves in a plasma [20, 35],

$$\varepsilon^2 \partial_{tt}\psi(\mathbf{x},t) - \Delta\psi(\mathbf{x},t) + \frac{1}{\varepsilon^2}\psi(\mathbf{x},t) + \psi(\mathbf{x},t)\phi(\mathbf{x},t) = 0, \tag{5.1.1a}$$

$$\gamma^2 \partial_{tt}\phi(\mathbf{x},t) - \Delta\phi(\mathbf{x},t) - \Delta\left(\psi^2(\mathbf{x},t)\right) = 0, \qquad \mathbf{x} \in \mathbb{R}^d, \quad t > 0, \tag{5.1.1b}$$

with initial conditions:

$$\psi(\mathbf{x},0) = \psi^{(0)}(\mathbf{x}),\ \partial_t\psi(\mathbf{x},0) = \psi^{(1)}(\mathbf{x}),\ \phi(\mathbf{x},0) = \phi^{(0)}(\mathbf{x}),\ \partial_t\phi(\mathbf{x},0) = \phi^{(1)}(\mathbf{x}). \tag{5.1.1c}$$

Here, the real-valued functions $\psi = \psi(\mathbf{x},t)$ and $\phi = \phi(\mathbf{x},t)$ are the fast time scale component of electric field raised by electrons and the derivation of ion density from its equilibrium, respectively; $0 < \varepsilon \leq 1$ and $0 < \gamma \leq 1$ are two dimensionless parameters which are inversely proportional to the plasma frequency and speed of

sound, respectively. It is well-known that the KGZ system (5.3.1a)-(5.3.1c) is time symmetric or time reversible, and conserves the total *energy* [78, 79], i.e. for $t \geq 0$,

$$E(t) := \int_{\mathbb{R}^d} \left[\varepsilon^2 \left(\partial_t \psi\right)^2 + |\nabla \psi|^2 + \frac{1}{\varepsilon^2}\psi^2 + \frac{\gamma^2}{2}|\nabla \varphi|^2 + \frac{1}{2}\phi^2 + \phi\psi^2 \right] d\mathbf{x} \equiv E(0), \tag{5.1.2}$$

where φ is defined via $\Delta\varphi = \partial_t \phi$ with $\lim_{|\mathbf{x}|\to\infty} \varphi = 0$.

For fixed $\varepsilon = \varepsilon_0 > 0$ and $\gamma = \gamma_0 > 0$, i.e. $O(1)$-plasma frequency and speed of sound regime, the above KGZ system has been studied in both analytical and numerical aspects. Along the analytical front, the local well-posedness of the Cauchy problem (5.3.1a)-(5.3.1c) in the energy space $H^1 \times L^2$ was performed by Ozawa et al. [84] when $\varepsilon = O(1)$ and $\gamma = O(1)$ with $\varepsilon \neq \gamma$. In addition, as pointed out in [78, 78] that there is no null form structure as in [70] for the KGZ system, which suggests that the KGZ system (5.3.1a)-(5.3.1c) may be locally ill-posed in the energy space when $\varepsilon = \gamma$. Along the numerical front, Wang et al. [105] presented an energy conservative finite difference method and established its error estimate.

However, in the high-plasma-frequency limit regime, i.e. $\varepsilon \to 0$ and $\gamma = O(1)$, or in the simultaneous high-plasma-frequency and subsonic limit regime, i.e. $(\varepsilon, \gamma) \to 0$ under $\varepsilon \lesssim \gamma$, the analysis of the KGZ system are more complicated. The analysis difficulty is also mainly due to that the energy $E(t)$ in (5.1.2) is unbounded when $\varepsilon \to 0$ or $(\varepsilon, \gamma) \to 0$ under $\varepsilon \lesssim \gamma$. In these two limit regimes, Masmoudi et al. [78] showed that the energy $E(t)$ is at least $O(\varepsilon^{-2})$ when $\varepsilon \to 0$. They investigated the convergence in $H^s \times H^{s-1}$ $(s > 3/2)$ as $\varepsilon \to 0$ under $\varepsilon \lesssim \gamma$ and subsequently showed the convergence results in the energy space $H^1 \times L^2$ [79]. Based on their results [78, 79], in the subsonic limit, i.e. $\gamma \to 0$, the KGZ system converges to the KGE (1.3.7); and in the high-plasma-frequency limit, the KGZ system converges to the Zakharov system [17, 69]. In addition, the solutions ψ and ϕ of the KGZ system propagate waves with wavelength $O(\varepsilon^2)$ and $O(\varepsilon)$, respectively, in time when $0 < \varepsilon \ll 1$ under $\varepsilon \lesssim \gamma$. This highly oscillatory nature in time provides severe numerical burdens which is similar to the case of numerical resolution for the KGE

in the nonrelativistic limit regime, making the computation in the limit regime extremely challenging. So far there are few results on the numerics of the KGZ system in this regime.

Based on our investigation in previous chapters on the various numerical methods for solving the HODEs (1.3.1) or KGE (1.3.7) in the nonrelativistic limit regime where the solution has the similar oscillatory behavior as that of the KGZ system (5.1.1), in order to compute 'correct' solutions, the frequently used FDTD methods [1, 38, 74, 99] share the same ε-scalability: time step $\tau = O(\varepsilon^3)$ and mesh size $h = O(1)$. The Gautschi-type EWI spectral method for the KGE improves the ε-scalability to $\tau = O(\varepsilon^2)$, and the Deuflhard-type EWI or equivalently the time-splitting spectral method furthermore shows smaller temporal error bound. Finally, the multiscale time integrator (MTI) spectral method could achieve $\tau = O(1)$.

In this chapter, we are going to apply those numerical methods established before to solve the KGZ system in the highly oscillatory regims. In detail, the two kinds of EWIs for solving the KGZ in the simultaneous high-plasma-frequency and subsonic limit regime are proposed in Section 5.2, and the MTI method to KGZ in the high-plasma-frequency limit regime is established in Section 5.3, followed by numerical results given in Section 5.4.

5.2 Exponential wave integrators

For simplicity of notation, we shall only present the methods in 1D as usual. Generalization to higher dimensions are straightforward and results remain valid with tensor products. In practice, we truncate the whole-space problem (5.3.1a)-(5.3.1c) into an interval $\Omega = (a, b)$ with homogeneous Dirichlet boundary conditions.

In 1D, the problem collapses to

$$\varepsilon^2\partial_{tt}\psi(x,t) - \partial_{xx}\psi(x,t) + \frac{1}{\varepsilon^2}\psi(x,t) + \psi(x,t)\phi(x,t) = 0,\ x\in\Omega,\ t>0, \tag{5.2.1a}$$

$$\gamma^2\partial_{tt}\phi(x,t) - \partial_{xx}\phi(x,t) - \partial_{xx}\left(\psi^2(x,t)\right) = 0, \quad x\in\Omega, \quad t>0, \tag{5.2.1b}$$

$$\psi(a,t) = \psi(b,t) = 0, \quad \phi(a,t) = \phi(b,t) = 0, \quad t\geq 0, \tag{5.2.1c}$$

$$\psi(x,0) = \psi^{(0)}(x), \quad \partial_t\psi(x,0) = \psi^{(1)}(x), \quad x\in\overline{\Omega} = [a,b], \tag{5.2.1d}$$

$$\phi(x,0) = \phi^{(0)}(x), \quad \partial_t\phi(x,0) = \phi^{(1)}(x), \quad x\in\overline{\Omega}. \tag{5.2.1e}$$

We remark here that the boundary conditions considered here are inspired by the inherent physical nature of the system and they have been widely used in the literatures for dealing with analysis and computation of the KGZ system (see, e.g. [105] and references therein). It could be replaced by periodic boundary conditions which makes little difference in numerical aspects but would cost more effort in the error estimates.

Choose the mesh size $h := \Delta x = (b-a)/M$ with M a positive integer and denote grid points as $x_j := a + jh$ for $j = 0, 1, \ldots, M$. Define

$$X_M := \text{span}\left\{\sin(\mu_l(x-a)) \ :\ x\in\overline{\Omega},\ \mu_l = \frac{\pi l}{b-a},\ l = 1,\ldots,M-1\right\},$$

$$Y_M := \left\{\mathbf{v} = (v_0, v_1, \ldots, v_M)\in\mathbb{C}^{M+1} \mid v_0 = v_M = 0\right\},\ \|\mathbf{v}\|_{l^2} = h\sum_{j=1}^{M-1}|v_j|^2.$$

For a function $v(x)$ on $\overline{\Omega}$ and a vector $\mathbf{v}\in Y_M$, let $P_M : L^2(\Omega)\to X_M$ be the standard L^2-projection operator, and $I_M : C(\Omega)\to X_M$ or $Y_M\to X_M$ be the trigonometric interpolation operator [51, 95], i.e.

$$(P_M v)(x) = \sum_{l=1}^{M-1}\widehat{v}_l\sin(\mu_l(x-a)), \quad (I_M v)(x) = \sum_{l=1}^{M-1}\widetilde{v}_l\sin(\mu_l(x-a)), \tag{5.2.2}$$

where $\widehat{v}_l$ and $\widetilde{v}_l$ are the sine and discrete sine transform coefficients of the periodic function $v(x)$ and vector $\mathbf{v}$, respectively, defined as

$$\widehat{v}_l = \frac{2}{b-a}\int_a^b v(x)\sin(\mu_l(x-a))dx, \qquad \widetilde{v}_l = \frac{2}{M}\sum_{j=1}^{M-1}v_j\sin(\mu_l(x_j-a)). \tag{5.2.3}$$

Now, the sine spectral discretization [51, 95] for (5.2.1a)-(5.2.1b) is as follows:

Find $\psi_M(x,t)$ and $\phi_M(x,t) \in Y_M$, i.e.

$$\psi_M(x,t) = \sum_{l=1}^{M-1} \widehat{\psi}_l(t) \sin(\mu_l(x-a)), \quad \phi_M(x,t) = \sum_{l=1}^{M-1} \widehat{\phi}_l(t) \sin(\mu_l(x-a))), \tag{5.2.4}$$

such that

$$\varepsilon^2 \partial_{tt}\psi_M - \partial_{xx}\psi_M + \frac{1}{\varepsilon^2}\psi_M + \mathcal{P}_M\left(\psi_M \phi_M\right) = 0, \tag{5.2.5}$$

$$\gamma^2 \partial_{tt}\phi_M - \partial_{xx}\phi_M - \partial_{xx}\left(\mathcal{P}_M\left((\psi_M)^2\right)\right) = 0, \qquad x \in \overline{\Omega}, \quad t \geq 0. \tag{5.2.6}$$

Plugging (5.2.4) into (5.2.5)-(5.2.6), noticing the orthogonality of the sine bases, we have for $l = 1, \ldots, M-1$ and $w \in \mathbb{R}$, when t is near t_n $(n = 0, 1, \ldots)$,

$$\frac{d^2}{dw^2}\widehat{\psi}_l(t_n + w) + \beta_l^2 \widehat{\psi}_l(t_n + w) + \frac{1}{\varepsilon^2}\widehat{f}_l^n(w) = 0, \tag{5.2.7}$$

$$\frac{d^2}{dw^2}\widehat{\phi}_l(t_n + w) + \theta_l^2 \widehat{\phi}_l(t_n + w) + \theta_l^2 \widehat{g}_l^n(w) = 0, \tag{5.2.8}$$

where

$$\theta_l = \frac{\mu_l}{\gamma}, \ \beta_l = \frac{\sqrt{1+\varepsilon^2\mu_l^2}}{\varepsilon^2}, \ \widehat{f}_l^n(w) = (\widehat{\psi_M \phi_M})_l(t_n + w), \ \widehat{g}_l^n(w) = (\widehat{(\psi_M)^2})_l(t_n + w).$$

Using the variation-of-constants formula, for $n \geq 0$ and $w \in \mathbb{R}$, the general solutions of the above second order ODEs are

$$\widehat{\psi}_l(t_n + w) = \cos(\beta_l w)\, \widehat{\psi}_l(t_n) + \frac{\sin(\beta_l w)}{\beta_l}\widehat{\psi}_l'(t_n) - \int_0^w \widehat{f}_l^n(s) \frac{\sin(\beta_l(w-s))}{\varepsilon^2 \beta_l} ds, \tag{5.2.9}$$

$$\widehat{\phi}_l(t_n + w) = \cos(\theta_l w)\, \widehat{\phi}_l(t_n) + \frac{\sin(\theta_l w)}{\theta_l}\widehat{\phi}_l'(t_n) - \theta_l \int_0^w \widehat{g}_l^n(s) \sin(\theta_l(w-s))\, ds. \tag{5.2.10}$$

Differentiating (5.2.9) and (5.2.10) with respect to w, we obtain with $t = t_n + w$

$$\widehat{\psi}_l'(t) = -\beta_l \sin(\beta_l w)\, \widehat{\psi}_l(t_n) + \cos(\beta_l w)\, \widehat{\psi}_l'(t_n) - \int_0^w \widehat{f}_l^n(s) \frac{\cos(\beta_l(w-s))}{\varepsilon^2} ds, \tag{5.2.11}$$

$$\widehat{\phi}_l'(t) = -\theta_l \sin(\theta_l w)\, \widehat{\phi}_l(t_n) + \cos(\theta_l w)\, \widehat{\phi}_l'(t_n) - \theta_l^2 \int_0^w \widehat{g}_l^n(s) \cos(\theta_l(w-s))\, ds. \tag{5.2.12}$$

When $n = 0$, from the initial conditions (5.2.1d)-(5.2.1e), we have

$$\widehat{\psi}_l(0) = \widehat{(\psi^{(0)})}_l, \quad \widehat{\psi}'_l(0) = \widehat{(\psi^{(1)})}_l, \quad \widehat{\phi}_l(0) = \widehat{(\phi^{(0)})}_l, \quad \widehat{\phi}'_l(0) = \widehat{(\phi^{(1)})}_l. \quad (5.2.13)$$

Then based on the different quadratures applied to the above unknown integrations as introduced before, we can derive the following EWI with Gautschi's quadrature sine pseudospectral (EWI-GSP) method and the EWI with Deuflhard's quadrature sine pseudospectral (EWI-DSP) method.

5.2.1 EWI-GSP

Evaluating (5.2.9)-(5.2.10) and (5.2.11)-(5.2.12) with $w = \tau$ and $n = 0$, we get

$$\widehat{\psi}_l(t_1) = \cos(\beta_l\tau)\,\widehat{(\psi^{(0)})}_l + \frac{\sin(\beta_l\tau)}{\beta_l}\widehat{(\psi^{(1)})}_l - \int_0^\tau \widehat{f}_l^0(s)\frac{\sin(\beta_l(\tau-s))}{\varepsilon^2\beta_l}ds, \quad (5.2.14)$$

$$\widehat{\phi}_l(t_1) = \cos(\theta_l\tau)\,\widehat{(\phi^{(0)})}_l + \frac{\sin(\theta_l\tau)}{\theta_l}\widehat{(\phi^{(1)})}_l - \theta_l\int_0^\tau \widehat{g}_l^0\sin(\theta_l(\tau-s))\,ds, \quad (5.2.15)$$

$$\widehat{\psi}'_l(t_1) = -\beta_l\sin(\beta_l\tau)\,\widehat{(\psi^{(0)})}_l + \cos(\beta_l\tau)\,\widehat{(\psi^{(1)})}_l - \int_0^\tau \widehat{f}_l^0(s)\frac{\cos(\beta_l(\tau-s))}{\varepsilon^2}ds, \quad (5.2.16)$$

$$\widehat{\phi}'_l(t_1) = -\theta_l\sin(\theta_l\tau)\,\widehat{(\phi^{(0)})}_l + \cos(\theta_l\tau)\,\widehat{(\phi^{(1)})}_l - \theta_l^2\int_0^\tau \widehat{g}_l^0(s)\cos(\theta_l(\tau-s))\,ds. \quad (5.2.17)$$

For $n \geq 1$, choosing $w = \tau$ and $w = -\tau$, respectively, in (5.2.9)-(5.2.10), and then summing the corresponding equations together [45, 52, 53], we obtain

$$\widehat{\psi}_l(t_{n+1}) = 2\cos(\beta_l\tau)\,\widehat{\psi}_l(t_n) - \widehat{\psi}_l(t_{n-1}) - \int_0^\tau \widehat{(f^+)}_l^n(s)\frac{\sin(\beta_l(\tau-s))}{\varepsilon^2\beta_l}ds, \quad (5.2.18)$$

$$\widehat{\phi}_l(t_{n+1}) = 2\cos(\theta_l\tau)\,\widehat{\phi}_l(t_n) - \widehat{\phi}_l(t_{n-1}) - \theta_l\int_0^\tau \widehat{(g^+)}_l^n(s)\sin(\theta_l(\tau-s))\,ds, \quad (5.2.19)$$

where

$$\widehat{(f^+)}_l^n(s) := \widehat{f}_l^n(s) + \widehat{f}_l^n(-s), \qquad \widehat{(g^+)}_l^n(s) := \widehat{g}_l^n(s) + \widehat{g}_l^n(-s).$$

Carrying out the similar procedure to (5.2.11)-(5.2.12) by subtracting instead of summing [54, 62], we get

$$\widehat{\psi}_l'(t_{n+1}) = \widehat{\psi}_l'(t_{n-1}) - 2\beta_l \sin(\beta_l\tau)\,\widehat{\psi}_l(t_n) - \int_0^\tau \widehat{(f^+)}_l^n(s)\frac{\cos(\beta_l(\tau-s))}{\varepsilon^2}ds, \tag{5.2.20}$$

$$\widehat{\phi}_l'(t_{n+1}) = \widehat{\phi}_l'(t_{n-1}) - 2\theta_l \sin(\theta_l\tau)\,\widehat{\phi}_l(t_n) - \theta_l^2\int_0^\tau \widehat{(g^+)}_l^n(s)\cos(\theta_l(\tau-s))\,ds. \tag{5.2.21}$$

Then we adopt the following Gautschi's type quadrature with $A \in C([0,\tau])$ and $0 \neq \delta \in \mathbb{R}$ [45]

$$\int_0^\tau A(s)\sin(\delta(\tau-s))\,ds \approx A(0)\int_0^\tau \sin(\delta(\tau-s))\,ds = \frac{1-\cos(\delta\tau)}{\delta}A(0), \tag{5.2.22}$$

$$\int_0^\tau A(s)\cos(\delta(\tau-s))\,ds \approx A(0)\int_0^\tau \cos(\delta(\tau-s))\,ds = \frac{\sin(\delta\tau)}{\delta}A(0), \tag{5.2.23}$$

to approximate all the integrals in (5.2.14)-(5.2.21), and then replace all the integrals defining the sine transform coefficients by intercalations for the pseudospectral method.

Choosing $\psi_M^0(x)$, $(\psi_t)_M^0(x)$, $\phi_M^0(x)$ and $(\dot{\phi})_M^0(x)$ as the interpolations of $\psi^{(0)}(x)$, $\psi^{(1)}(x)$, $\phi^{(0)}(x)$ and $\phi^{(1)}(x)$ on the grids, respectively, and approximating the integrals by a quadrature rule on the grids [51, 95]. Let ψ_j^n, ϕ_j^n, $(\dot{\psi})_j^n$ and $(\dot{\phi})_j^n$ be the approximations of $\psi(x_j,t_n)$, $\phi(x_j,t_n)$, $\partial_t\psi(x_j,t_n)$, and $\partial_t\phi(x_j,t_n)$, respectively, for $j = 0,1,\ldots,M$ and $n \geq 0$, and denote ψ^n, ϕ^n, $(\dot{\psi})^n$ and $(\dot{\phi})^n$ be the vector with components ψ_j^n, ϕ_j^n $(\dot{\psi})_j^n$ and $(\dot{\phi})_j^n$, respectively. Choosing $\psi_j^0 = \psi^{(0)}(x_j)$, $\phi_j^0 = \phi^{(0)}(x_j)$, $(\dot{\psi})_j^0 = \psi^{(1)}(x_j)$ and $(\dot{\phi})_j^0 = \phi^{(1)}(x_j)$ for $j = 0,1,\ldots,M$, then a Gautschi-type exponential wave integrator sine pseudospectral (EWI-GSP) discretization for computing

ψ^{n+1}, ϕ^{n+1}, $\dot{\psi}^{n+1}$ and $\dot{\phi}^{n+1}$ for $n \geq 0$ reads

$$\psi_j^{n+1} = \sum_{l=1}^{M-1} \widetilde{(\psi^{n+1})}_l \sin(\mu_l(x_j - a)), \quad \phi_j^{n+1} = \sum_{l=1}^{M-1} \widetilde{(\phi^{n+1})}_l \sin(\mu_l(x_j - a)), \tag{5.2.24}$$

$$(\dot{\psi})_j^{n+1} = \sum_{l=1}^{M-1} \widetilde{\left(\dot{\psi}\right)}_l^{n+1} \sin(\mu_l(x_j - a)), \quad (\dot{\phi})_j^{n+1} = \sum_{l=1}^{M-1} \widetilde{\left(\dot{\phi}\right)}_l^{n+1} \sin(\mu_l(x_j - a)), \tag{5.2.25}$$

where for $n = 0$

$$\begin{aligned}
\widetilde{(\psi^1)}_l &= \cos(\beta_l\tau)\,\widetilde{(\psi^0)}_l + \frac{\sin(\beta_l\tau)}{\beta_l}\widetilde{\left(\dot{\psi}\right)}_l^0 + \frac{\cos(\beta_l\tau) - 1}{(\varepsilon\beta_l)^2}\widetilde{f}_l^0, \\
\widetilde{(\phi^1)}_l &= \cos(\theta_l\tau)\,\widetilde{(\phi^0)}_l + \frac{\sin(\theta_l\tau)}{\theta_l}\widetilde{\left(\dot{\phi}\right)}_l^0 + [\cos(\theta_l\tau) - 1]\,\widetilde{g}_l^0, \\
\widetilde{(\dot{\psi})}_l^1 &= -\beta_l \sin(\beta_l\tau)\,\widetilde{(\psi^{(0)})}_l + \cos(\beta_l\tau)\,\widetilde{(\psi^{(1)})}_l - \frac{\sin(\beta_l\tau)}{\varepsilon^2\beta_l}\widetilde{f}_l^0\,, \\
\widetilde{(\dot{\phi})}_l^1 &= -\theta_l \sin(\theta_l\tau)\,\widetilde{(\phi^{(0)})}_l + \cos(\theta_l\tau)\,\widetilde{(\phi^{(1)})}_l - \theta_l \sin(\theta_l\tau)\,\widetilde{g}_l^0\,;
\end{aligned}$$

and for $n \geq 1$

$$\begin{aligned}
\widetilde{(\psi^{n+1})}_l &= -\widetilde{(\psi^{n-1})}_l + 2\cos(\beta_l\tau)\,\widetilde{(\psi^n)}_l + \frac{2[\cos(\beta_l\tau) - 1]}{(\varepsilon\beta_l)^2}\widetilde{f}_l^n\,, \\
\widetilde{(\phi^{n+1})}_l &= -\widetilde{(\phi^{n-1})}_l + 2\cos(\theta_l\tau)\,\widetilde{(\phi^n)}_l + 2[\cos(\theta_l\tau) - 1]\,\widetilde{g}_l^n\,, \\
\widetilde{(\dot{\psi})}_l^{n+1} &= \widetilde{(\dot{\psi})}_l^{n-1} - 2\beta_l \sin(\beta_l\tau)\,\widetilde{(\psi^n)}_l - \frac{2\sin(\beta_l\tau)}{\varepsilon^2\beta_l}\widetilde{f}_l^n\,, \\
\widetilde{(\dot{\phi})}_l^{n+1} &= \widetilde{(\dot{\phi})}_l^{n-1} - 2\theta_l \sin(\theta_l\tau)\,\widetilde{(\phi^n)}_l - 2\theta_l \sin(\theta_l\tau)\,\widetilde{g}_l^n\,.
\end{aligned}$$

with $f^n = (\psi_0^n\phi_0^n, \ldots, \psi_M^n\phi_M^n)^T$, $g^n = \left((\psi_0^n)^2, \ldots, (\psi_M^n)^2\right)^T$.

5.2.2 EWI-DSP

For $n \geq 0$, by applying the standard trapezoidal rule or the Deuflhard-type quadrature [36] directly to those unknown integrations in (5.2.9)- (5.2.12), and then

setting $w = \tau$, we get

$$\widehat{\psi}_l(t_{n+1}) \approx \cos(\beta_l\tau)\,\widehat{\psi}_l(t_n) + \frac{\sin(\beta_l\tau)}{\beta_l}\widehat{\psi}_l'(t_n) - \frac{\tau\sin(\beta_l\tau)}{2\beta_l}\widehat{f}_l^n(0), \tag{5.2.26a}$$

$$\widehat{\phi}_l(t_{n+1}) \approx \cos(\theta_l\tau)\,\widehat{\phi}_l(t_n) + \frac{\sin(\theta_l\tau)}{\theta_l}\widehat{\phi}_l'(t_n) - \frac{\tau\theta_l\sin(\theta_l\tau)}{2}\widehat{g}_l^n(0), \tag{5.2.26b}$$

$$\widehat{\psi}_l'(t_{n+1}) \approx -\beta_l\sin(\beta_l\tau)\,\widehat{\psi}_l(t_n) + \cos(\beta_l\tau)\,\widehat{\psi}_l'(t_n) - \frac{\tau}{2}\left[\cos(\beta_l\tau)\,\widehat{f}_l^n(0) + \widehat{f}_l^n(\tau)\right], \tag{5.2.26c}$$

$$\widehat{\phi}_l'(t_{n+1}) \approx -\theta_l\sin(\theta_l\tau)\,\widehat{\phi}_l(t_n) + \cos(\theta_l\tau)\,\widehat{\phi}_l'(t_n) - \frac{\tau\theta_l^2}{2}\left[\cos(\theta_l\tau)\,\widehat{g}_l^n(0) + \widehat{g}_l^n(\tau)\right]. \tag{5.2.26d}$$

Then a detailed Deuflhard-type exponential wave integrator sine pseudospectral (EWI-DSP) method reads as follows. Denote ψ_j^n, $\dot{\psi}_j^n$, ϕ_j^n and $\dot{\phi}_j^n$ ($j = 0,\ldots,M,\ n = 0,1,\ldots$) be the approximations to $\psi(x_j,t_n)$, $\partial_t\psi(x_j,t_n)$, $\phi(x_j,t_n)$ and $\partial_t\phi(x_j,t_n)$, respectively. Choose $\psi_j^0 = \psi_j^{(0)}$, $\dot{\psi}_j^0 = \psi_j^{(1)}$, $\phi_j^0 = \phi_j^{(0)}$, $\dot{\phi}_j^0 = \phi_j^{(1)}$, then for $n = 0,1,\ldots,$

$$\psi_j^{n+1} = \sum_{l=1}^{M-1}\widetilde{\psi}_l^{n+1}\sin(\mu_l(x_j-a)), \quad \phi_j^{n+1} = \sum_{l=1}^{M-1}\widetilde{\phi}_l^{n+1}\sin(\mu_l(x_j-a)), \tag{5.2.27a}$$

$$\dot{\psi}_j^{n+1} = \sum_{l=1}^{M-1}\widetilde{\left(\dot{\psi}\right)}_l^{n+1}\sin(\mu_l(x_j-a)), \quad \dot{\phi}_j^{n+1} = \sum_{l=1}^{M-1}\widetilde{\left(\dot{\phi}\right)}_l^{n+1}\sin(\mu_l(x_j-a)), \tag{5.2.27b}$$

where

$$\widetilde{\psi}_l^{n+1} = \cos(\beta_l\tau)\,\widetilde{\psi}_l^n + \frac{\sin(\beta_l\tau)}{\beta_l}\widetilde{\left(\dot{\psi}\right)}_l^n - \frac{\tau\sin(\beta_l\tau)}{2\beta_l}\widetilde{f}_l^n, \tag{5.2.28a}$$

$$\widetilde{\phi}_l^{n+1} = \cos(\theta_l\tau)\,\widetilde{\phi}_l^n + \frac{\sin(\theta_l\tau)}{\theta_l}\widetilde{\left(\dot{\phi}\right)}_l^n - \frac{\tau\theta_l\sin(\theta_l\tau)}{2}\widetilde{g}_l^n, \tag{5.2.28b}$$

$$\widetilde{\left(\dot{\psi}\right)}_l^{n+1} = -\beta_l\sin(\beta_l\tau)\,\widetilde{\psi}_l^n + \cos(\beta_l\tau)\,\widetilde{\left(\dot{\psi}\right)}_l^n - \frac{\tau}{2}\left[\cos(\beta_l\tau)\,\widetilde{f}_l^n + \widetilde{f}_l^{n+1}\right], \tag{5.2.28c}$$

$$\widetilde{\left(\dot{\phi}\right)}_l^{n+1} = -\theta_l\sin(\theta_l\tau)\,\widetilde{\phi}_l^n + \cos(\theta_l\tau)\,\widetilde{\left(\dot{\phi}\right)}_l^n - \frac{\tau\theta_l^2}{2}\left[\cos(\theta_l\tau)\,\widetilde{g}_l^n + \widetilde{g}_l^{n+1}\right], \tag{5.2.28d}$$

with $f^n = (\psi_0^n\phi_0^n,\ldots,\psi_M^n\phi_M^n)^T$, $g^n = \left((\psi_0^n)^2,\ldots,(\psi_M^n)^2\right)^T$.

Similarly to that shown in Chapter 3 (refer to Theorem 3.4.1), the TSSP method is equivalent to an EWI with Deulhard's quadrature for solving the KGZ system.

The above EWI-GSP and EWI-DSP methods for the KGZ system are explicit, time symmetric and easy to extend to 2D and 3D. The memory cost is $O(M)$ and computational cost per time step is $O(M \ln M)$ thanks to fast sine transform.

5.2.3 Convergence analysis

Here we give the convergence results of the EWI-GSP and EWI-DSP methods in the regime: $\varepsilon = O(1)$ and $\gamma = O(1)$. Without loss of generality and for the simplicity of notation, we set $\varepsilon = \gamma = 1$ in this subsection. Let T^* be the maximum existence time for the solutions of the KGZ system [78,79,84] and denote $0 < T < T^*$. Assume the exact solutions (ψ, ϕ) of (5.2.1a)-(5.2.1e) satisfy

$$\begin{aligned} &\psi \in C\left([0,T]; W^{1,\infty} \cap H^{m_0} \cap H_0^2\right) \cap C^1\left([0,T]; W^{1,4}\right) \cap C^2\left([0,T]; H^1\right), \\ &\phi \in C\left([0,T]; L^\infty(\Omega) \cap H^{m_0} \cap H_0^1\right) \cap C^1\left([0,T]; L^4\right) \cap C^2\left([0,T]; L^2\right), \end{aligned} \tag{5.2.29}$$

for some integer $m_0 \geq 3$. Under the assumptions (5.2.29), we denote, for $\Omega_T := \Omega \times [0,T]$,

$$\begin{aligned} K_1 &:= \max\left\{\|\psi\|_{L^\infty([0,T];L^\infty\cap H^2)}, \|\partial_t\psi\|_{L^\infty([0,T];H^1)}\right\}, \\ K_2 &:= \max\left\{\|\phi\|_{L^\infty([0,T];L^\infty\cap H^1)}, \|\partial_x\varphi\|_{L^\infty([0,T];L^2)}\right\}. \end{aligned}$$

Denote the trigonometric interpolations of numerical solutions as

$$\psi_I^n(x) := I_M(\psi^n)(x), \quad \phi_I^n(x) := I_M(\phi^n)(x), \quad \dot{\psi}_I^n(x) := I_M(\dot{\psi}^n)(x), \quad x \in \Omega, \tag{5.2.30}$$

and an auxiliary function instead of $\dot{\phi}^n$ as

$$\rho_I^n(x) = \sum_{l=1}^{M-1} \widetilde{\rho}_l^n \sin(\mu_l(x-a)), \quad \text{with} \quad \widetilde{\rho}_l^n := \frac{1}{\mu_l}\widetilde{\left(\dot{\phi}\right)}_l^n. \tag{5.2.31}$$

Define the 'error' functions as

$$e_\psi^n(x) := \psi(x,t_n) - \psi_I^n(x), \quad e_\phi^n(x) := \phi(x,t_n) - \phi_I^n(x), \quad n = 0, 1\ldots, \tag{5.2.32a}$$

$$\dot{e}_\psi^n(x) := \partial_t\psi(x,t_n) - \dot{\psi}_I^n(x), \quad e_\rho^n(x) := \partial_x\varphi(x,t_n) - \rho_I^n(x), \quad x \in \Omega, \tag{5.2.32b}$$

then we have the following two convergence theorem of the EWI-GSP and EWI-DSP, respectively [11].

Theorem 5.2.1 (Convergence of EWI-GSP). *Let ψ^n and ϕ^n be the approximations obtained from the EWI-GSP (5.2.24)-(5.2.25). Under the assumption (5.2.29), there exists $h_0 > 0$ and $\tau_0 > 0$ sufficiently small and independent of h and τ, such that for any $0 < h \le h_0$ and $0 < \tau \le \tau_0$ satisfying $\tau \le \frac{\pi h}{3\sqrt{h^2+\pi^2}}$,, we have*

$$\left\|e_\psi^n\right\|_{H^1(\Omega)} + \left\|e_\phi^n\right\|_{L^2(\Omega)} \lesssim \tau^2 + h^{m_0}, \quad 0 \le n \le \frac{T}{\tau}, \tag{5.2.33}$$

$$\|\psi_I^n\|_{L^\infty(\Omega)} \le K_1 + 1, \quad \left\|\frac{d}{dx}\psi_I^n\right\|_{L^\infty(\Omega)} \le K_1 + 1, \quad \|\phi_I^n\|_{L^\infty(\Omega)} \le K_2 + 1. \tag{5.2.34}$$

Proof. The proof of Theorem 5.2.1 is quite similar to the proof of Theorem 3.2.2, so we omit here for brevity. □

Theorem 5.2.2 (Convergence of EWI-DSP). *Let ψ^n, ϕ^n, $\dot\psi^n$ and $\dot\phi^n$ be the numerical approximations obtained from the EWI-DSP method (5.2.27)-(5.2.28). Under the assumption (5.2.29), there exist two constants τ_0, $h_0 > 0$, independent of τ (or n) and h , such that for any $0 < \tau < \tau_0$, $0 < h < h_0$,*

$$\|\dot e_\psi^n\|_{L^2} + \|e_\psi^n\|_{H^1} + \|e_\rho^n\|_{L^2} + \|e_\phi^n\|_{L^2} \lesssim \tau^2 + h^{m_0}, \quad n = 0, 1, \ldots, \frac{T}{\tau}, \tag{5.2.35a}$$

$$\|\psi_I^n\|_{H^1} \le K_1 + 1, \qquad \|\phi_I^n\|_{L^2} \le K_2 + 1, \qquad \|\psi^n\|_{l^\infty} \le K_1 + 1, \tag{5.2.35b}$$

$$\|\dot\psi_I^n\|_{L^2} \le K_1 + 1, \qquad \|\rho_I^n\|_{L^2} \le K_2 + 1. \tag{5.2.35c}$$

To proceed to the proof of Theorem 5.2.2, we introduce the following notations. Let ψ, ϕ be the exact solution of the KGZ system (5.2.1) with $\varepsilon = \gamma = 1$. Denote the L^2-projected solution as

$$\begin{aligned} \psi_M(x,t) &:= P_M(\psi(x,t)) = \sum_{l=1}^{M-1} \widehat{\psi}_l(t)\sin(\mu_l(x-a)), \\ \phi_M(x,t) &:= P_M(\phi(x,t)) = \sum_{l=1}^{M-1} \widehat{\phi}_l(t)\sin(\mu_l(x-a)), \qquad x \in \Omega, \quad t \ge 0, \end{aligned} \tag{5.2.36}$$

and the projected error functions as

$$\begin{aligned} &e^n_{\psi,M}(x) := P_M(e^n_\psi(x)), \quad e^n_{\phi,M}(x) := P_M(e^n_\phi(x)), \\ &\dot{e}^n_{\psi,M}(x) := P_M(e^n_\psi(x)), \quad e^n_{\rho,M}(x) := P_M(e^n_\rho(x)), \qquad n = 0, 1, \ldots, \frac{T}{\tau}, \end{aligned} \tag{5.2.37}$$

where from (5.2.32), the corresponding coefficients in frequency space should satisfy

$$\begin{aligned} &\widehat{(e_\psi)}^n_l = \widehat{\psi}_l(t_n) - \widetilde{\psi}^n_l, \qquad \widehat{(e_\phi)}^n_l = \widehat{\phi}_l(t_n) - \widetilde{\phi}^n_l, \qquad l = 1, \ldots, M-1, \\ &\widehat{(\dot{e}_\psi)}^n_l = \widehat{\psi}'_l(t_n) - \widetilde{\left(\dot{\psi}\right)}^n_l, \qquad \widehat{(e_\rho)}^n_l = \frac{1}{\mu_l}\widehat{\phi}'_l(t_n) - \widetilde{\rho}^n_l, \qquad n = 0, 1, \ldots, \frac{T}{\tau}. \end{aligned} \tag{5.2.38}$$

Based on (5.2.26), define the local truncation errors for $n = 0, 1, \ldots, \frac{T}{\tau} - 1$ as

$$\begin{aligned} &\xi^n_\psi(x) := \sum_{l=1}^{M-1} \widehat{(\xi_\psi)}^n_l \sin(\mu_l(x_j - a)), \quad \xi^n_\phi(x) := \sum_{l=1}^{M-1} \widehat{(\xi_\phi)}^n_l \sin(\mu_l(x_j - a)), \\ &\dot{\xi}^n_\psi(x) := \sum_{l=1}^{M-1} \widehat{(\dot{\xi}_\psi)}^n_l \sin(\mu_l(x_j - a)), \quad \xi^n_\rho(x) := \sum_{l=1}^{M-1} \widehat{(\xi_\rho)}^n_l \sin(\mu_l(x_j - a)), \ x \in \Omega, \end{aligned}$$

where

$$\widehat{(\xi_\psi)}^n_l = \widehat{\psi}_l(t_{n+1}) - \cos(\beta_l\tau)\,\widehat{\psi}_l(t_n) - \frac{\sin(\beta_l\tau)}{\beta_l}\widehat{\psi}'_l(t_n) + \frac{\tau\sin(\beta_l\tau)}{2\beta_l}\widehat{f}^n_l(0), \tag{5.2.39a}$$

$$\widehat{(\xi_\phi)}^n_l = \widehat{\phi}_l(t_{n+1}) - \cos(\mu_l\tau)\,\widehat{\phi}_l(t_n) - \frac{\sin(\mu_l\tau)}{\mu_l}\widehat{\phi}'_l(t_n) + \frac{\tau\mu_l\sin(\mu_l\tau)}{2}\widehat{g}^n_l(0), \tag{5.2.39b}$$

$$\begin{aligned} \widehat{(\dot{\xi}_\psi)}^n_l =& \widehat{\psi}'_l(t_{n+1}) + \beta_l\sin(\beta_l\tau)\,\widehat{\psi}_l(t_n) - \cos(\beta_l\tau)\,\widehat{\psi}'_l(t_n) \\ &+ \frac{\tau}{2}\left[\cos(\beta_l\tau)\,\widehat{f}^n_l(0) + \widehat{f}^n_l(\tau)\right], \end{aligned} \tag{5.2.39c}$$

$$\begin{aligned} \widehat{(\xi_\rho)}^n_l =& \frac{1}{\mu_l}\widehat{\phi}'_l(t_{n+1}) + \sin(\mu_l\tau)\,\widehat{\phi}_l(t_n) - \frac{\cos(\mu_l\tau)}{\mu_l}\widehat{\phi}'_l(t_n) \\ &+ \frac{\tau\mu_l}{2}\left[\cos(\mu_l\tau)\,\widehat{g}^n_l(0) + \widehat{g}^n_l(\tau)\right], \end{aligned} \tag{5.2.39d}$$

with

$$f^n(x,s) := \psi\phi(x, t_n + s), \quad g^n(x,s) := |\psi(x, t_n + s)|^2. \tag{5.2.40}$$

Subtracting the local truncation errors (5.2.39) from the scheme (5.2.28) and noting (5.2.31), we are led to the error equations for $n = 0, 1, \ldots, \frac{T}{\tau}-1$ and $l = 1, \ldots, M-1$,

$$\widehat{(e_\psi)}_l^{n+1} = \cos(\beta_l\tau)\,\widehat{(e_\psi)}_l^{n} + \frac{\sin(\beta_l\tau)}{\beta_l}\widehat{(\dot{e}_\psi)}_l^{n} + \widehat{(\xi_\psi)}_l^{n} - \widehat{(\eta_\psi)}_l^{n}, \tag{5.2.41a}$$

$$\widehat{(e_\phi)}_l^{n+1} = \cos(\mu_l\tau)\,\widehat{(e_\phi)}_l^{n} + \sin(\mu_l\tau)\,\widehat{(e_\rho)}_l^{n} + \widehat{(\xi_\phi)}_l^{n} - \widehat{(\eta_\phi)}_l^{n}, \tag{5.2.41b}$$

$$\widehat{(\dot{e}_\psi)}_l^{n+1} = -\beta_l\sin(\beta_l\tau)\,\widehat{(e_\psi)}_l^{n} + \cos(\beta_l\tau)\,\widehat{(\dot{e}_\psi)}_l^{n} + \widehat{\left(\dot{\xi}_\psi\right)}_l^{n} - \widehat{(\dot{\eta}_\psi)}_l^{n}, \tag{5.2.41c}$$

$$\widehat{(e_\rho)}_l^{n+1} = -\sin(\mu_l\tau)\,\widehat{(e_\phi)}_l^{n} + \cos(\mu_l\tau)\,\widehat{(e_\rho)}_l^{n} + \widehat{(\xi_\rho)}_l^{n} - \widehat{(\eta_\rho)}_l^{n}, \tag{5.2.41d}$$

where

$$\widehat{(\eta_\psi)}_l^{n} = \frac{\tau\sin(\beta_l\tau)}{2\beta_l}\left(\widehat{f}_l^{n}(0) - \widetilde{f}_l^{n}\right), \quad \widehat{(\eta_\phi)}_l^{n} = \frac{\tau\mu_l\sin(\mu_l\tau)}{2}\left(\widehat{g}_l^{n}(0) - \widetilde{g}_l^{n}\right), \tag{5.2.42a}$$

$$\widehat{(\dot{\eta}_\psi)}_l^{n} = \frac{\tau}{2}\left[\cos(\beta_l\tau)\left(\widehat{f}_l^{n}(0) - \widetilde{f}_l^{n}\right) + \widehat{f}_l^{n}(\tau) - \widetilde{f}_l^{n+1}\right], \tag{5.2.42b}$$

$$\widehat{(\eta_\rho)}_l^{n} = \frac{\tau\mu_l}{2}\left[\cos(\mu_l\tau)\left(\widehat{g}_l^{n}(0) - \widetilde{g}_l^{n}\right) + \widehat{g}_l^{n}(\tau) - \widetilde{g}_l^{n+1}\right], \tag{5.2.42c}$$

with the nonlinear error functions defined as

$$\eta_\psi^n(x) := \sum_{l=1}^{M-1}\widehat{(\eta_\psi)}_l^{n}\sin(\mu_l(x_j-a)), \quad \eta_\phi^n(x) := \sum_{l=1}^{M-1}\widehat{(\eta_\phi)}_l^{n}\sin(\mu_l(x_j-a)),$$

$$\dot{\eta}_\psi^n(x) := \sum_{l=1}^{M-1}\widehat{(\dot{\eta}_\psi)}_l^{n}\sin(\mu_l(x_j-a)), \quad \eta_\rho^n(x) := \sum_{l=1}^{M-1}\widehat{(\eta_\rho)}_l^{n}\sin(\mu_l(x_j-a)), \quad x\in\Omega.$$

Define the error energy functional as

$$\mathcal{E}(P,Q,R,S) := \|P\|_{L^2}^2 + \|Q\|_{H^1}^2 + \|R\|_{L^2}^2 + \|S\|_{L^2}^2, \tag{5.2.43}$$

for some arbitrary functions $P(x)$, $Q(x)$, $R(x)$ and $S(x)$ on Ω.

In order to prove Theorem 5.2.2, we establish the following lemmas. Define the discrete H^1-norm as

$$\|v\|_{Y,1} := \sqrt{\|v\|_{l^2}^2 + \|\delta_x^+ v\|_{l^2}^2},$$

where

$$\|v\|_{l^2}^2 = h\sum_{j=1}^{M-1}|v_j|^2, \quad \|\delta_x^+ v\|_{l^2}^2 = h\sum_{j=0}^{M-1}|\delta_x^+ v_j|^2,$$

for some $v \in Y_M$. For the local truncation errors (5.2.39), we have estimates stated in the following lemma.

Lemma 5.2.1. *Based on assumptions (5.2.29), we have estimates for the local truncation errors as*

$$\mathcal{E}\left(\dot{\xi}_\psi^n, \xi_\psi^n, \xi_\rho^n, \xi_\phi^n\right) \lesssim \tau^6, \qquad n = 0, 1, \ldots, \frac{T}{\tau} - 1. \tag{5.2.44}$$

Proof. Applying the L^2-projection on both sides of (5.2.1), due to the orthogonality of basis functions and the variation-of-constant formula, the sine transform coefficients $\widehat{\psi}_l(t_n)$ and $\widehat{\phi}_l(t_n)$ should satisfy

$$\widehat{\psi}_l(t_{n+1}) = \cos(\beta_l\tau)\,\widehat{\psi}_l(t_n) + \frac{\sin(\beta_l\tau)}{\beta_l}\widehat{\psi}_l'(t_n) - \int_0^\tau \frac{\sin(\beta_l(\tau-s))}{\beta_l}\widehat{f}_l^n(s)ds, \tag{5.2.45a}$$

$$\widehat{\phi}_l(t_{n+1}) = \cos(\mu_l\tau)\,\widehat{\phi}_l(t_n) + \frac{\sin(\mu_l\tau)}{\mu_l}\widehat{\phi}_l'(t_n) - \mu_l\int_0^\tau \sin(\mu_l(\tau-s))\,\widehat{g}_l^n(s)ds, \tag{5.2.45b}$$

$$\widehat{\psi}_l'(t_{n+1}) = -\beta_l\sin(\beta_l\tau)\,\widehat{\psi}_l(t_n) + \cos(\beta_l\tau)\,\widehat{\psi}_l'(t_n) - \int_0^\tau \cos(\beta_l(\tau-s))\,\widehat{f}_l^n(s)ds, \tag{5.2.45c}$$

$$\frac{1}{\mu_l}\widehat{\phi}_l'(t_{n+1}) = \frac{\cos(\mu_l\tau)}{\mu_l}\widehat{\phi}_l'(t_n) - \sin(\mu_l\tau)\,\widehat{\phi}_l(t_n) - \mu_l\int_0^\tau \cos(\mu_l(\tau-s))\,\widehat{g}_l^n(s)ds. \tag{5.2.45d}$$

Subtracting (5.2.39) from (5.2.45), we get

$$\begin{aligned}
\widehat{(\xi_\psi)}_l^n &= \int_0^\tau \frac{\sin(\beta_l(\tau-s))}{\beta_l}\widehat{f}_l^n(s)ds - \frac{\tau\sin(\beta_l\tau)}{2\beta_l}\widehat{f}_l^n(0),\\
\widehat{(\xi_\phi)}_l^n &= \mu_l\int_0^\tau \sin(\mu_l(\tau-s))\,\widehat{g}_l^n(s)ds - \frac{\tau\mu_l\sin(\mu_l\tau)}{2}\widehat{g}_l^n(0),\\
\widehat{(\dot{\xi}_\psi)}_l^n &= \int_0^\tau \cos(\beta_l(\tau-s))\,\widehat{f}_l^n(s)ds - \frac{\tau}{2}\left[\cos(\beta_l\tau)\widehat{f}_l^n(0) + \widehat{f}_l^n(\tau)\right],\\
\widehat{(\xi_\rho)}_l^n &= \mu_l\int_0^\tau \cos(\mu_l(\tau-s))\,\widehat{g}_l^n(s)ds - \frac{\tau\mu_l}{2}\left[\cos(\mu_l\tau)\widehat{g}_l^n(0) + \widehat{g}_l^n(\tau)\right].
\end{aligned}$$

Thus, the local truncation errors here are in fact the error introduced by applying the trapezoidal rule. By the standard error formula [22] of the trapezoidal rule for a general function $v(s) \in C^2[0,\tau]$, i.e.

$$\int_0^\tau v(s)ds - \frac{\tau}{2}\left[v(0)+v(\tau)\right] = \frac{\tau^3}{12}v''(\kappa), \quad \text{for some} \quad \kappa \in [0,\tau], \tag{5.2.46}$$

we have

$$\begin{aligned}
\widehat{(\xi_\psi)}_l^n =& \frac{\tau^3}{12\beta_l}\Big[\sin(\beta_l\kappa_2)\left(\widehat{f}_l^n\right)''(\kappa_1) - 2\beta_l\cos(\beta_l\kappa_2)\left(\widehat{f}_l^n\right)'(\kappa_1) \\
& - \beta_l^2\sin(\beta_l\kappa_2)\widehat{f}_l^n(\kappa_1)\Big], \qquad (5.2.47a)\\
\widehat{(\xi_\phi)}_l^n =& \frac{\tau^3\mu_l}{12}\Big[\sin(\mu_l\kappa_2)\left(\widehat{g}_l^n\right)''(\kappa_1) - 2\mu_l\cos(\mu_l\kappa_2)\left(\widehat{g}_l^n\right)'(\kappa_1) \\
& - \mu_l^2\sin(\mu_l\kappa_2)\widehat{g}_l^n(\kappa_1)\Big], \qquad (5.2.47b)\\
\widehat{\left(\dot{\xi}_\psi\right)}_l^n =& \frac{\tau^3}{12}\Big[\cos(\beta_l\kappa_2)\left(\widehat{f}_l^n\right)''(\kappa_1) + 2\beta_l\sin(\beta_l\kappa_2)\left(\widehat{f}_l^n\right)'(\kappa_1) \\
& - \beta_l^2\cos(\beta_l\kappa_2)\widehat{f}_l^n(\kappa_1)\Big], \qquad (5.2.47c)\\
\widehat{(\xi_\rho)}_l^n =& \frac{\tau^3\mu_l}{12}\Big[\cos(\mu_l\kappa_2)\left(\widehat{g}_l^n\right)''(\kappa_1) + 2\mu_l\sin(\mu_l\kappa_2)\left(\widehat{g}_l^n\right)'(\kappa_1) \\
& - \mu_l^2\cos(\mu_l\kappa_2)\widehat{g}_l^n(\kappa_1)\Big], \qquad (5.2.47d)
\end{aligned}$$

for some $\kappa_2 = \tau - \kappa_1$ and $\kappa_1 \in [0,\tau]$.

Taking square on both sides of the inequalities in (5.2.47) and then using Cauchy's inequality, we get

$$\begin{aligned}
\left|\widehat{(\xi_\psi)}_l^n\right|^2 &\lesssim \frac{\tau^6}{\beta_l^2}\left[\left|\left(\widehat{f}_l^n\right)''(\kappa_1)\right|^2 + \beta_l^2\left|\left(\widehat{f}_l^n\right)'(\kappa_1)\right|^2 + \beta_l^4\left|\widehat{f}_l^n(\kappa_1)\right|^2\right], \qquad (5.2.48a)\\
\left|\widehat{(\xi_\phi)}_l^n\right|^2 &\lesssim \tau^6\mu_l^2\left[\left|\left(\widehat{g}_l^n\right)''(\kappa_1)\right|^2 + \mu_l^2\left|\left(\widehat{g}_l^n\right)'(\kappa_1)\right|^2 + \mu_l^4\left|\widehat{g}_l^n(\kappa_1)\right|^2\right], \qquad (5.2.48b)\\
\left|\widehat{\left(\dot{\xi}_\psi\right)}_l^n\right|^2 &\lesssim \tau^6\left[\left|\left(\widehat{f}_l^n\right)''(\kappa_1)\right|^2 + \beta_l^2\left|\left(\widehat{f}_l^n\right)'(\kappa_1)\right|^2 + \beta_l^4\left|\widehat{f}_l^n(\kappa_1)\right|^2\right], \qquad (5.2.48c)\\
\left|\widehat{(\xi_\rho)}_l^n\right|^2 &\lesssim \tau^6\mu_l^2\left[\left|\left(\widehat{g}_l^n\right)''(\kappa_1)\right|^2 + \mu_l^2\left|\left(\widehat{g}_l^n\right)'(\kappa_1)\right|^2 + \mu_l^4\left|\widehat{g}_l^n(\kappa_1)\right|^2\right]. \qquad (5.2.48d)
\end{aligned}$$

Multiplying (5.2.48a) on both sides by $\beta_l^2 = 1+\mu_l^2$ and then summing up for $l = 1,\ldots,M-1$, by Paserval's identity, we get

$$\left\|\xi_\psi^n\right\|_{H^1}^2 \lesssim \tau^6\left[\|\partial_{tt}f^n(\cdot,\kappa_1)\|_{L^2}^2 + \|\partial_t f^n(\cdot,\kappa_1)\|_{H^1}^2 + \|f^n(\cdot,\kappa_1)\|_{H^2}^2\right].$$

By assumption (5.2.29) and noting (5.2.40), we get

$$\left\|\xi_{\psi}^{n}\right\|_{H^1}^2 \lesssim \tau^6, \qquad n=0,\ldots,\frac{T}{\tau}-1. \tag{5.2.49}$$

Summing (5.2.48b) up directly for $l=1,\ldots,M-1$ and noting (5.2.29) and (5.2.40) again, we can get

$$\begin{aligned}\left\|\xi_{\phi}^{n}\right\|_{L^2}^2 &\lesssim \tau^6\left[\|\partial_{tt}g^n(\cdot,\kappa_1)\|_{H^1}^2+\|\partial_t g^n(\cdot,\kappa_1)\|_{H^2}^2+\|g^n(\cdot,\kappa_1)\|_{H^3}^2\right]\\ &\lesssim \tau^6, \quad n=0,\ldots,\frac{T}{\tau}-1.\end{aligned} \tag{5.2.50}$$

Similarly for (5.2.48c) and (5.2.48d), we can get

$$\left\|\dot{\xi}_{\psi}^{n}\right\|_{L^2}^2,\ \left\|\xi_{\rho}^{n}\right\|_{L^2}^2 \lesssim \tau^6, \qquad n=0,\ldots,\frac{T}{\tau}-1. \tag{5.2.51}$$

Combing (5.2.49)-(5.2.51) and noting (5.2.43), we get assertion (5.2.44). □

For the nonlinear error terms, we have estimates stated as the following lemma.

Lemma 5.2.2. *Based on assumption (5.2.29), and assume (5.2.35b) holds for some* $0\le n\le \frac{T}{\tau}-1$ *(which will be given by induction later), then we have*

$$\begin{aligned}\mathcal{E}\left(\dot{\eta}_{\psi}^{n},\eta_{\psi}^{n},\eta_{\rho}^{n},\eta_{\phi}^{n}\right)\lesssim&\tau^2\left[\mathcal{E}\left(\dot{e}_{\psi,M}^{n},e_{\psi,M}^{n},e_{\rho,M}^{n},e_{\phi,M}^{n}\right)+\mathcal{E}\left(\dot{e}_{\psi,M}^{n+1},e_{\psi,M}^{n+1},e_{\rho,M}^{n+1},e_{\phi,M}^{n+1}\right)\right]\\&+\tau^2h^{2m_0}.\end{aligned} \tag{5.2.52}$$

Proof. From (5.2.42), we have

$$\begin{aligned}&\left|\widehat{(\eta_{\psi})_l}^{n}\right|\lesssim\frac{\tau}{\beta_l}\left|\widehat{f}_l^{n}(0)-\widetilde{f}_l^{n}\right|,\quad \left|\widehat{(\eta_{\phi})_l}^{n}\right|\lesssim\tau\mu_l\left|\widehat{g}_l^{n}(0)-\widetilde{g}_l^{n}\right|,\\&\left|\widehat{(\dot{\eta}_{\psi})_l}^{n}\right|\lesssim\tau\left[\left|\widehat{f}_l^{n}(0)-\widetilde{f}_l^{n}\right|+\left|\widehat{f}_l^{n}(\tau)-\widetilde{f}_l^{n+1}\right|\right],\qquad n=0,\ldots,\frac{T}{\tau}-1,\\&\left|\widehat{(\eta_{\rho})_l}^{n}\right|\lesssim\tau\mu_l\left[\left|\widehat{g}_l^{n}(0)-\widetilde{g}_l^{n}\right|+\left|\widehat{g}_l^{n}(\tau)-\widetilde{g}_l^{n+1}\right|\right],\qquad l=1,\ldots,M-1.\end{aligned}$$

Similarly as before, we can get for $n=0,\ldots,\frac{T}{\tau}-1$,

$$\left\|\eta_{\psi}^{n}\right\|_{H^1}\lesssim\tau\left\|f^n(\cdot,0)-I_Mf^n\right\|_{L^2},\quad \left\|\eta_{\phi}^{n}\right\|_{L^2}\lesssim\tau\left\|g^n(\cdot,0)-g^n\right\|_{H^1}, \tag{5.2.53a}$$

$$\left\|\dot{\eta}_{\psi}^{n}\right\|_{L^2}\lesssim\tau\left[\left\|f^n(\cdot,0)-I_Mf^n\right\|_{L^2}+\left\|f^n(\cdot,\tau)-I_Mf^{n+1}\right\|_{L^2}\right], \tag{5.2.53b}$$

$$\left\|\eta_{\rho}^{n}\right|_{L^2}\lesssim\tau\left[\left\|g^n(\cdot,0)-I_Mg^n\right\|_{H^1}+\left\|g^n(\cdot,\tau)-I_Mg^{n+1}\right\|_{H^1}\right]. \tag{5.2.53c}$$

By Parserval's identity, we have

$$\begin{aligned}
&\|f^n(\cdot,0) - I_M f^n\|_{L^2} \lesssim \|I_M f^n(\cdot,0) - I_M f^n\|_{L^2} + \|f^n(\cdot,0) - I_M f^n(\cdot,0)\|_{L^2} \\
&\lesssim \|f^n(\cdot,0) - f^n\|_{l^2} + h^{m_0} \\
&\lesssim \|\psi(\cdot,t_n)\phi(\cdot,t_n) - \psi^n\phi^n\|_{l^2} + \left\||\psi|^2\psi(\cdot,t_n) - |\psi^n|^2\psi^n\right\|_{l^2} + h^{m_0}. \qquad (5.2.54)
\end{aligned}$$

Then by triangle inequality, under assumption (5.2.29) and (5.2.35b), we have

$$\begin{aligned}
\|\psi(\cdot,t_n)\phi(\cdot,t_n) - \psi^n\phi^n\|_{l^2} &\lesssim \left\|e_\psi^n \cdot \phi(\cdot,t_n)\right\|_{l^2} + \left\|\psi^n \cdot e_\phi^n\right\|_{l^2} \\
&\lesssim \left\|e_\psi^n\right\|_{l^2} + \left\|e_\phi^n\right\|_{l^2} \lesssim \left\|e_\psi^n\right\|_{L^2} + \left\|e_\phi^n\right\|_{L^2}.
\end{aligned}$$

Similarly,

$$\left\||\psi|^2\psi(\cdot,t_n) - |\psi^n|^2\psi^n\right\|_{l^2} \lesssim \left\|e_\psi^n\right\|_{L^2}.$$

Plugging the above two estimates back to (5.2.54), we get

$$\|f^n(\cdot,0) - I_M f^n\|_{L^2} \lesssim \left\|e_\psi^n\right\|_{L^2} + \left\|e_\phi^n\right\|_{L^2} + h^{m_0}. \qquad (5.2.55)$$

Also we have

$$\begin{aligned}
\|g^n(\cdot,0) - I_M g^n\|_{H^1} &\lesssim \|I_M g^n(\cdot,0) - I_M g^n\|_{H^1} + \|g^n(\cdot,0) - I_M f^n(\cdot,0)\|_{H^1} \\
&\lesssim \|g^n(\cdot,0) - g^n\|_{Y,1} + h^{m_0} \\
&\lesssim \left\||\psi(\cdot,t_n)|^2 - |\psi^n|^2\right\|_{Y,1} + h^{m_0} \\
&\lesssim \left\|e_\psi^n \cdot \psi(\cdot,t_n)\right\|_{Y,1} + \left\|\psi^n \cdot e_\psi^n\right\|_{Y,1} + h^{m_0}. \qquad (5.2.56)
\end{aligned}$$

Then with assumption (5.2.29),

$$\begin{aligned}
\left\|e_\psi^n \cdot \psi(\cdot,t_n)\right\|_{Y,1} &\lesssim \left\|e_\psi^n \cdot \psi(\cdot,t_n)\right\|_{l^2} + \left\|\left(\delta_x^+ e_\psi^n\right) \cdot \psi(\cdot,t_n)\right\|_{l^2} + \left\|e_\psi^n \cdot \left(\delta_x^+ \psi(\cdot,t_n)\right)\right\|_{l^2} \\
&\lesssim \left\|e_\psi^n\right\|_{l^2} + \left\|\delta_x^+ e_\psi^n\right\|_{l^2} + \left\|e_\psi^n\right\|_{l^2} \\
&\lesssim \left\|e_\psi^n\right\|_{Y,1} \lesssim \left\|e_\psi^n\right\|_{H^1}.
\end{aligned}$$

By assumption (5.2.29) and applying the discrete Sobelov's inequality [85],

$$\begin{aligned}
\left\|\psi^n \cdot e_\psi^n\right\|_{Y,1} &\lesssim \left\|\psi^n \cdot e_\psi^n\right\|_{l^2} + \left\|\left(\delta_x^+ e_\psi^n\right) \cdot \psi^n\right\|_{l^2} + \left\|e_\psi^n \cdot \left(\delta_x^+ \psi^n\right)\right\|_{l^2} \\
&\lesssim \left\|e_\psi^n\right\|_{l^2} + \left\|\delta_x^+ e_\psi^n\right\|_{l^2} + \left\|e_\psi^n\right\|_{l^\infty} \\
&\lesssim \left\|e_\psi^n\right\|_{Y,1} \lesssim \left\|e_\psi^n\right\|_{H^1}.
\end{aligned}$$

Plugging the above two estimates back to (5.2.56), we get

$$\|g^n(\cdot,0) - I_M g^n\|_{H^1} \lesssim \left\|e_\psi^n\right\|_{H^1} + h^{m_0}. \tag{5.2.57}$$

As for the estimates of $\|f^n(\cdot,\tau) - I_M f^{n+1}\|_{L^2}$ and $\|g^n(\cdot,\tau) - I_M g^{n+1}\|_{H^1}$ in (5.2.53), following the same manner as above, we only need to show that under the induction assumption (5.2.35b) for some n, the numerical solutions ψ_I^{n+1} and ϕ_I^{n+1} are also bounded. In fact from the scheme (5.2.28), we can find

$$\left\|\psi_I^{n+1}\right\|_{H^1} \le \|\psi_I^n\|_{H^1} + \left\|\dot{\psi}_I^n\right\|_{L^2} + \frac{\tau}{2}\|I_M f^n\|_{L^2} \le 2K_1 + 2 + \|I_M f^n\|_{L^2}\,, \tag{5.2.58a}$$

$$\left\|\phi_I^{n+1}\right\|_{L^2} \le \|\phi_I^n\|_{L^2} + \|\rho_I^n\|_{L^2} + \frac{\tau}{2}\|I_M g^n\|_{H^1} \le 2K_2 + 2 + \|I_M g^n\|_{H^1}\,. \tag{5.2.58b}$$

Noting by Parserval's identity and (5.2.35b),

$$\|I_M f^n\|_{L^2} \le \|\psi^n \phi^n\|_{l^2} \le (K_1+1)(K_2+1),$$
$$\|I_M g^n\|_{H^1} \le \left\||\psi^n|^2\right\|_{Y,1} \le 2(K_1+1)^2,$$

which together with (5.2.58) show the boundedness of ψ_I^{n+1} and ϕ_I^{n+1}. Thus, similarly as before, we can get

$$\left\|f^n(\cdot,\tau) - I_M f^{n+1}\right\|_{L^2} \lesssim \left\|e_\psi^{n+1}\right\|_{L^2} + \left\|e_\phi^{n+1}\right\|_{L^2} + h^{m_0}, \tag{5.2.59a}$$

$$\left\|g^n(\cdot,\tau) - I_M g^{n+1}\right\|_{H^1} \lesssim \left\|e_\psi^{n+1}\right\|_{H^1} + h^{m_0}. \tag{5.2.59b}$$

At last, plugging (5.2.55), (5.2.57) and (5.2.59) back to (5.2.53), and noticing by applying the projection and triangle inequality,

$$\left\|e_\psi^n\right\|_{H^1} \le \left\|e_{\psi,M}^n\right\|_{H^1} + \|\psi(\cdot,t_n) - \psi_M(\cdot,t_n)\|_{H^1} \lesssim \left\|e_{\psi,M}^n\right\|_{H^1} + h^{m_0},$$
$$\left\|e_\phi^n\right\|_{L^2} \le \left\|e_{\phi,M}^n\right\|_{L^2} + \|\phi(\cdot,t_n) - \phi_M(\cdot,t_n)\|_{L^2} \lesssim \left\|e_{\phi,M}^n\right\|_{L^2} + h^{m_0}, \quad n = 0,\ldots,\frac{T}{\tau}.$$

so we have

$$\left\|\eta_\psi^n\right\|_{H^1} \lesssim \tau\left[\left\|e_{\psi,M}^n\right\|_{H^1} + \left\|e_{\phi,M}^n\right\|_{L^2} + h^{m_0}\right], \quad \left\|\eta_\phi^n\right\|_{L^2} \lesssim \tau\left[\left\|e_{\psi,M}^n\right\|_{H^1} + h^{m_0}\right],$$
$$\left\|\dot{\eta}_\psi^n\right\|_{L^2} \lesssim \tau\left[\left\|e_{\psi,M}^n\right\|_{H^1} + \left\|e_{\phi,M}^n\right\|_{L^2} + \left\|e_{\psi,M}^{n+1}\right\|_{H^1} + \left\|e_{\phi,M}^{n+1}\right\|_{L^2} + h^{m_0}\right],$$
$$\left\|\eta_\rho^n\right|_{L^2} \lesssim \tau\left[\left\|e_{\psi,M}^n\right\|_{H^1} + \left\|e_{\psi,M}^{n+1}\right\|_{H^1} + h^{m_0}\right], \qquad n = 0,\ldots,\frac{T}{\tau} - 1.$$

Then by (5.2.43) and Cauchy's inequality, we get

$$\begin{aligned}
&\mathcal{E}\left(\dot{\eta}_{\psi}^{n}, \eta_{\psi}^{n}, \eta_{\rho}^{n}, \eta_{\phi}^{n}\right) \lesssim \tau^{2}\left[\left\|e_{\psi,M}^{n}\right\|_{H^{1}}^{2}+\left\|e_{\phi,M}^{n}\right\|_{L^{2}}^{2}+\left\|e_{\psi,M}^{n+1}\right\|_{H^{1}}^{2}+\left\|e_{\phi,M}^{n+1}\right\|_{L^{2}}^{2}\right]+\tau^{2} h^{2 m_{0}} \\
&\lesssim \tau^{2}\left[\mathcal{E}\left(\dot{e}_{\psi,M}^{n}, e_{\psi,M}^{n}, e_{\rho,M}^{n}, e_{\phi,M}^{n}\right)+\mathcal{E}\left(\dot{e}_{\psi,M}^{n+1}, e_{\psi,M}^{n+1}, e_{\rho,M}^{n+1}, e_{\phi,M}^{n+1}\right)\right]+\tau^{2} h^{2 m_{0}}.
\end{aligned}$$

and we complete the proof. □

With the error energy functional notation (5.2.43), it is ready to show the following fact.

Lemma 5.2.3. *For $n=0, \ldots, \frac{T}{\tau}-1$, we have*

$$\begin{aligned}
&\mathcal{E}\left(\dot{e}_{\psi,M}^{n+1}, e_{\psi,M}^{n+1}, e_{\rho,M}^{n+1}, e_{\phi,M}^{n+1}\right)-\mathcal{E}\left(\dot{e}_{\psi,M}^{n}, e_{\psi,M}^{n}, e_{\rho,M}^{n}, e_{\phi,M}^{n}\right) \\
&\lesssim \tau \mathcal{E}\left(\dot{e}_{\psi,M}^{n}, e_{\psi,M}^{n}, e_{\rho,M}^{n}, e_{\phi,M}^{n}\right)+\frac{1}{\tau}\left[\mathcal{E}\left(\dot{\xi}_{\psi}^{n}, \xi_{\psi}^{n}, \xi_{\rho}^{n}, \xi_{\phi}^{n}\right)+\mathcal{E}\left(\dot{\eta}_{\psi}^{n}, \eta_{\psi}^{n}, \eta_{\rho}^{n}, \eta_{\phi}^{n}\right)\right].
\end{aligned} \tag{5.2.61}$$

Proof. Taking square on both sides of (5.2.41) and applying Cauchy's inequality, we get

$$\begin{aligned}
\left|\widehat{\left(e_{\psi}\right)}_{l}^{n+1}\right|^{2} \leq & (1+\tau)\left|\cos\left(\beta_{l} \tau\right) \widehat{\left(e_{\psi}\right)}_{l}^{n}+\frac{\sin\left(\beta_{l} \tau\right)}{\beta_{l}} \widehat{\left(\dot{e}_{\psi}\right)}_{l}^{n}\right|^{2} \\
& +\left(1+\frac{1}{\tau}\right)\left|\widehat{\left(\xi_{\psi}\right)}_{l}^{n}-\widehat{\left(\eta_{\psi}\right)}_{l}^{n}\right|^{2}, \qquad (5.2.62a) \\
\left|\widehat{\left(e_{\phi}\right)}_{l}^{n+1}\right|^{2} \leq & (1+\tau)\left|\cos\left(\mu_{l} \tau\right) \widehat{\left(e_{\phi}\right)}_{l}^{n}+\sin\left(\mu_{l} \tau\right) \widehat{\left(e_{\rho}\right)}_{l}^{n}\right|^{2} \\
& +\left(1+\frac{1}{\tau}\right)\left|\widehat{\left(\xi_{\phi}\right)}_{l}^{n}-\widehat{\left(\eta_{\phi}\right)}_{l}^{n}\right|^{2}, \qquad (5.2.62b) \\
\left|\widehat{\left(\dot{e}_{\psi}\right)}_{l}^{n+1}\right|^{2} \leq & (1+\tau)\left|-\beta_{l} \sin\left(\beta_{l} \tau\right) \widehat{\left(e_{\psi}\right)}_{l}^{n}+\cos\left(\beta_{l} \tau\right) \widehat{\left(\dot{e}_{\psi}\right)}_{l}^{n}\right|^{2} \\
& +\left(1+\frac{1}{\tau}\right)\left|\widehat{\left(\dot{\xi}_{\psi}\right)}_{l}^{n}-\widehat{\left(\dot{\eta}_{\psi}\right)}_{l}^{n}\right|^{2}, \qquad (5.2.62c) \\
\left|\widehat{\left(e_{\rho}\right)}_{l}^{n+1}\right|^{2} \leq & (1+\tau)\left|-\sin\left(\mu_{l} \tau\right) \widehat{\left(e_{\phi}\right)}_{l}^{n}+\cos\left(\mu_{l} \tau\right) \widehat{\left(e_{\rho}\right)}_{l}^{n}\right|^{2} \\
& +\left(1+\frac{1}{\tau}\right)\left|\widehat{\left(\xi_{\rho}\right)}_{l}^{n}-\widehat{\left(\eta_{\rho}\right)}_{l}^{n}\right|^{2}, \qquad (5.2.62d)
\end{aligned}$$

Multiplying (5.2.62a) by β_{l}^{2} and then adding to (5.2.62c), we get

$$\begin{aligned}
&\left(1+\mu_{l}^{2}\right)\left|\widehat{\left(e_{\psi}\right)}_{l}^{n+1}\right|^{2}+\left|\widehat{\left(\dot{e}_{\psi}\right)}_{l}^{n+1}\right|^{2} \leq(1+\tau)\left[\left(1+\mu_{l}^{2}\right)\left|\widehat{\left(e_{\psi}\right)}_{l}^{n}\right|^{2}+\left|\widehat{\left(\dot{e}_{\psi}\right)}_{l}^{n}\right|^{2}\right] \\
&+\left(1+\frac{1}{\tau}\right)\left[\left(1+\mu_{l}^{2}\right)\left|\widehat{\left(\xi_{\psi}\right)}_{l}^{n}-\widehat{\left(\eta_{\psi}\right)}_{l}^{n}\right|^{2}+\left|\widehat{\left(\dot{\xi}_{\psi}\right)}_{l}^{n}-\widehat{\left(\dot{\eta}_{\psi}\right)}_{l}^{n}\right|^{2}\right].
\end{aligned} \tag{5.2.63}$$

Adding (5.2.62b) to (5.2.62d), we get

$$\left|\widehat{(e_\phi)_l}^{n+1}\right|^2+\left|\widehat{(e_\rho)_l}^{n+1}\right|^2 \leq (1+\tau)\left[\left|\widehat{(e_\phi)_l}^{n}\right|^2+\left|\widehat{(e_\rho)_l}^{n}\right|^2\right] + \left(1+\frac{1}{\tau}\right)\left[\left|\widehat{(\xi_\phi)_l}^{n}-\widehat{(\eta_\phi)_l}^{n}\right|^2+\left|\widehat{(\xi_\rho)_l}^{n}-\widehat{(\eta_\rho)_l}^{n}\right|^2\right]. \tag{5.2.64}$$

Adding (5.2.63) to (5.2.64), and then summing up for $l=1,\ldots,M-1$, noting (5.2.43), we get

$$\begin{aligned}\mathcal{E}\left(\dot{e}^{n+1}_{\psi,M},e^{n+1}_{\psi,M},e^{n+1}_{\rho,M},e^{n+1}_{\phi,M}\right) \leq & (1+\tau)\mathcal{E}\left(\dot{e}^{n}_{\psi,M},e^{n}_{\psi,M},e^{n}_{\rho,M},e^{n}_{\phi,M}\right)\\ &+\left(1+\frac{1}{\tau}\right)\mathcal{E}\left(\dot{\xi}^n_\psi-\dot{\eta}^n_\psi,\xi^n_\psi-\eta^n_\psi,\xi^n_\rho-\eta^n_\rho,\xi^n_\phi-\eta^n_\phi\right),\end{aligned}$$

which with triangle inequality prove assertion (5.2.61). □

Now, combining the Lemma 5.2.1-5.2.3, we give the proof of Theorem 5.2.2 by energy method with the help of mathematical induction argument [10], or the equivalent cut-off technique [7] for the boundedness of numerical solutions.

Proof of Theorem 5.2.2. For $n=0$, from the scheme and assumption (5.2.29), we have

$$\begin{aligned}&\|\dot{e}^0_\psi\|_{L^2}+\|e^0_\psi\|_{H^1}+\|e^0_\phi\|_{L^2}\\ &\lesssim \|\psi^{(1)}-I_M\psi^{(1)}\|_{L^2}+\|\psi^{(0)}-I_M\psi^{(0)}\|_{H^1}+\|\phi^{(0)}-I_M\phi^{(0)}\|_{L^2}\lesssim h^{m_0},\end{aligned}$$

Moreover, noting (5.2.31) and (5.2.38), we get

$$\|e^0_\rho\|_{L^2}\lesssim \|\phi^{(1)}-I_M\phi^{(1)}\|_{L^2}\lesssim h^{m_0}.$$

Then by triangle inequality,

$$\begin{aligned}&\|\psi^n_I\|_{H^1}\leq \|\psi(\cdot,t_n)\|_{H^1}+\|e^n_\psi\|_{H^1}\leq K_1+1,\\ &\|\phi^n_I\|_{L^2}\leq \|\phi(\cdot,t_n)\|_{L^2}+\|e^n_\phi\|_{L^2}\leq K_2+1,\\ &\|\dot{\psi}^n_I\|_{L^2}\leq \|\partial_t\psi(\cdot,t_n)\|_{L^2}+\|\dot{e}^n_\psi\|_{L^2}\leq K_1+1,\\ &\|\rho^n_I\|_{L^2}\leq \|\partial_x\varphi(\cdot,t_n)\|_{L^2}+\|e^n_\rho\|_{L^2}\leq K_2+1,\end{aligned}$$

for $0 < h \le h_1$, where h_1 is a constant independent of τ and h. Obviously, $\|\psi^0\|_{l^\infty} \le K_1 + 1$. Thus (5.2.35) is true for $n = 0$.

Assume (5.2.35) is valid for $n \le N \le T/\Delta t - 1$. Now we need to show the results still hold for $n = M + 1$. First of all, by triangle inequality and projection error estimate with assumption (5.2.29), we have

$$\begin{aligned} &\|\dot{e}_\psi^{M+1}\|_{L^2} + \|e_\psi^{M+1}\|_{H^1} + \|e_\rho^{M+1}\|_{L^2} + \|e_\phi^{M+1}\|_{L^2} \\ &\lesssim \|\dot{e}_{\psi,M}^{M+1}\|_{L^2} + \|e_{\psi,M}^{M+1}\|_{H^1} + \|e_{\rho,M}^{M+1}\|_{L^2} + \|e_{\phi,M}^{M+1}\|_{L^2} + h^{m_0}. \end{aligned} \tag{5.2.65}$$

Since (5.2.35b) is assumed to be true under induction for all $n \le N$, so we can plug the estimates (5.2.44) from Lemma 5.2.1 and (5.2.52) from Lemma 5.2.2 into (5.2.61) and get for $n = 0, \dots, N$,

$$\begin{aligned} &\mathcal{E}\left(\dot{e}_{\psi,M}^{n+1}, e_{\psi,M}^{n+1}, e_{\rho,M}^{n+1}, e_{\phi,M}^{n+1}\right) - \mathcal{E}\left(\dot{e}_{\psi,M}^{n}, e_{\psi,M}^{n}, e_{\rho,M}^{n}, e_{\phi,M}^{n}\right) \\ &\lesssim \tau\left[\mathcal{E}\left(\dot{e}_{\psi,M}^{n+1}, e_{\psi,M}^{n+1}, e_{\rho,M}^{n+1}, e_{\phi,M}^{n+1}\right) + \mathcal{E}\left(\dot{e}_{\psi,M}^{n}, e_{\psi,M}^{n}, e_{\rho,M}^{n}, e_{\phi,M}^{n}\right)\right] + \tau^5 + \tau \cdot h^{2m_0}. \end{aligned} \tag{5.2.66}$$

Summing (5.2.66) up for $n = 0, 1, \dots, N$, and then by the discrete Gronwall's inequality, we get

$$\mathcal{E}\left(\dot{e}_{\psi,M}^{n+1}, e_{\psi,M}^{n+1}, e_{\rho,M}^{n+1}, e_{\phi,M}^{n+1}\right) \lesssim \tau^4 + h^{2m}.$$

Thus, we have

$$\|\dot{e}_{\psi,M}^{N+1}\|_{L^2} + \|e_{\psi,M}^{N+1}\|_{H^1} + \|e_{\rho,M}^{N+1}\|_{L^2} + \|e_{\phi,M}^{N+1}\|_{L^2} \lesssim \tau^2 + h^{m_0},$$

which together with (5.2.65) show that (5.2.35b) is valid for $n = N + 1$. Then by triangle inequality,

$$\begin{aligned} &\|\psi_I^{N+1}\|_{H^1} \le \|\psi(\cdot, t_{N+1})\|_{H^1} + \|e_\psi^{N+1}\|_{H^1} \le K_1 + 1, \\ &\|\phi_I^{N+1}\|_{L^2} \le \|\phi(\cdot, t_{N+1})\|_{L^2} + \|e_\phi^{N+1}\|_{L^2} \le K_2 + 1, \\ &\|\dot{\psi}_I^{N+1}\|_{L^2} \le \|\partial_t\psi(\cdot, t_{N+1})\|_{L^2} + \|\dot{e}_\psi^{N+1}\|_{H^1} \le K_1 + 1, \\ &\|\rho_I^{N+1}\|_{L^2} \le \|\partial_x\varphi(\cdot, t_{N+1})\|_{L^2} + \|e_\rho^{N+1}\|_{L^2} \le K_2 + 1, \end{aligned} \qquad 0 < \tau \le \tau_1, \;\; 0 < h \le h_2,$$

for some constants τ_1, $h_2 > 0$ independent of τ and h. Noting the Sobolev's inequality

$$\|e_\psi^{N+1}\|_{L^\infty} \lesssim \|e_\psi^{N+1}\|_{H^1},$$

we also have

$$\|\psi^{N+1}\|_{l^\infty} \le \|\psi_I^{N+1}\|_{L^\infty} \le \|\psi(\cdot, t_{N+1})\|_{L^\infty} + \|e_u^{N+1}\|_{L^\infty} \le K_1 + 1, \quad ,$$

for $0 < \tau \le \tau_2$, $0 < h \le h_3$, where τ_2, $h_3 > 0$ are two constants independent of τ and h. Therefore, the proof is completed by choosing $\tau_0 = \min\{\tau_1, \tau_2\}$ and $h_0 = \min\{h_1, h_2, h_3\}$. □

Remark 5.2.1. *Here we only managed to get the error estimates of the numerical methods in regime $\varepsilon = \gamma = O(1)$. As we have mentioned, different from the KGE, ψ and ϕ in the KGZ stay in different energy spaces. When the small parameters step in, it is hard to find a suitable pair of energy spaces to establish the rigorous error estimates in the limit regimes via energy method. We will continue to study this problem in our future.*

5.3 Multiscale method

In this section, we shall derive a MTI with sine pesudospectral method to solve the KGZ system in the high-plasma-frequency limit regime. Without loss of generality, we take $\gamma = 1$ in (5.1.1), i.e.

$$\varepsilon^2 \partial_{tt}\psi(\mathbf{x}, t) - \Delta\psi(\mathbf{x}, t) + \frac{1}{\varepsilon^2}\psi(\mathbf{x}, t) + \psi(\mathbf{x}, t)\phi(\mathbf{x}, t) = 0, \tag{5.3.1a}$$

$$\partial_{tt}\phi(\mathbf{x}, t) - \Delta\phi(\mathbf{x}, t) - \Delta\left(\psi^2(\mathbf{x}, t)\right) = 0, \qquad \mathbf{x} \in \mathbb{R}^d, \quad t > 0, \tag{5.3.1b}$$

$$\psi(\mathbf{x}, 0) = \psi_0(\mathbf{x}),\ \partial_t\psi(\mathbf{x}, 0) = \frac{1}{\varepsilon^2}\psi_1(\mathbf{x}),\ \phi(\mathbf{x}, 0) = \phi_0(\mathbf{x}),\ \partial_t\phi(\mathbf{x}, 0) = \phi_1(\mathbf{x}), \tag{5.3.1c}$$

where $0 < \varepsilon \le 1$, with the uniform convergence in purpose. To illustrate the oscillations in this case, Fig. 5.1 shows the solutions $\psi(0, t)$, $\phi(0, t)$, $\psi(x, 1)$ and $\phi(x, 1)$ of the KGZ system at different ε, with $d = 1$, $\psi_0(x) = e^{-x^2/2}$, $\psi_1(x) = 3\psi_0(x)/2$, $\phi_0(x) = sech(x^2/2)$, $\phi_1(x) = e^{-x^2/2}$ in (5.3.1a)-(5.3.1c). Similarly as before, we will first derive the decomposition system and then propose the MTI based on it.

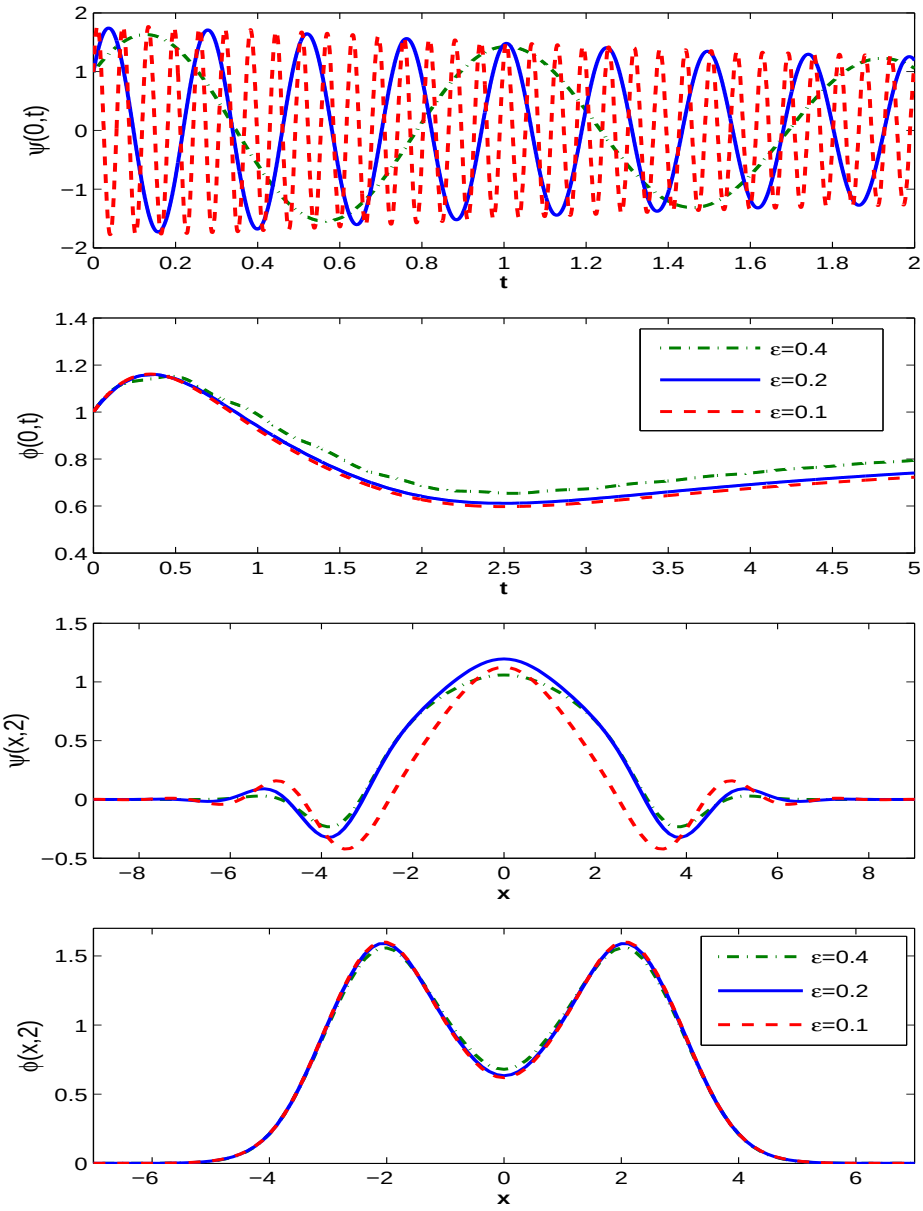

Figure 5.1: Profile of the solutions of KGZ with $d = 1$ for different ε.

5.3.1 Multiscale decomposition

Let $\tau = \Delta t > 0$ be the step size, and denote time steps by $t_n = n\tau$ for $n = 0, 1, \ldots$. In this section, we apply the multiscale decomposition by frequency which

is established for the KGE in Section 4.2 to the solution of the KGZ system (5.3.1a)-(5.3.1b) on the time interval $[t_n, t_{n+1}]$ with given initial data at $t = t_n$ as

$$\psi(\mathbf{x}, t_n) = \psi_0^n(\mathbf{x}) = O(1), \qquad \partial_t \psi(\mathbf{x}, t_n) = \frac{1}{\varepsilon^2}\psi_1^n(\mathbf{x}) = O\left(\frac{1}{\varepsilon^2}\right), \tag{5.3.2a}$$

$$\phi(\mathbf{x}, t_n) = \phi_0^n(\mathbf{x}) = O(1), \qquad \partial_t \phi(\mathbf{x}, t_n) = \phi_1^n(\mathbf{x}) = O(1). \tag{5.3.2b}$$

Apply the ansatz to the variable $\psi(\mathbf{x}, t) := \psi(\mathbf{x}, t_n + s)$ of (5.3.1a) on the time interval $[t_n, t_{n+1}]$ with (5.3.2)

$$\psi(\mathbf{x}, t_n + s) = \mathrm{e}^{\frac{is}{\varepsilon^2}} z^n(\mathbf{x}, s) + \mathrm{e}^{-\frac{is}{\varepsilon^2}} \overline{z^n}(\mathbf{x}, s) + r^n(\mathbf{x}, s), \quad \mathbf{x} \in \mathbb{R}^d, \ \ 0 \le s \le \tau. \tag{5.3.3}$$

We remark here since ψ is real-valued, so (5.3.3) implies that r^n is a real-valued function. Differentiating (5.3.3) with respect to s, we have

$$\begin{aligned} \partial_s \psi(\mathbf{x}, t_n + s) =& \mathrm{e}^{\frac{is}{\varepsilon^2}} \left[\partial_s z^n(\mathbf{x}, s) + \frac{i}{\varepsilon^2} z^n(\mathbf{x}, s)\right] + \partial_s r^n(\mathbf{x}, s) \\ &+ \mathrm{e}^{-\frac{is}{\varepsilon^2}} \left[\partial_s \overline{z^n}(\mathbf{x}, s) - \frac{i}{\varepsilon^2} \overline{z^n}(\mathbf{x}, s)\right], \quad \mathbf{x} \in \mathbb{R}^d, \ 0 \le s \le \tau. \end{aligned} \tag{5.3.4}$$

Plugging (5.3.3) into (5.3.1a), we get for $\mathbf{x} \in \mathbb{R}^d$, $0 \le s \le \tau$ and $\phi(\mathbf{x}, t_n + s) =: \phi^n(\mathbf{x}, s)$

$$\begin{aligned} &\mathrm{e}^{\frac{is}{\varepsilon^2}} \left[\varepsilon^2 \partial_{ss} z^n(\mathbf{x}, s) + 2i\partial_s z^n(\mathbf{x}, s) - \Delta z^n(\mathbf{x}, s) + z^n \phi^n(\mathbf{x}, s)\right] \\ &+ \mathrm{e}^{-\frac{is}{\varepsilon^2}} \left[\varepsilon^2 \partial_{ss} \overline{z^n}(\mathbf{x}, s) - 2i\partial_s \overline{z^n}(\mathbf{x}, s) - \Delta \overline{z^n}(\mathbf{x}, s) + \overline{z^n} \phi^n(\mathbf{x}, s)\right] \\ &+ \varepsilon^2 \partial_{ss} r^n(\mathbf{x}, s) + \Delta r^n(\mathbf{x}, s) + \frac{r^n(\mathbf{x}, s)}{\varepsilon^2} + r^n \phi^n(\mathbf{x}, s) = 0. \end{aligned}$$

Multiplying the above equation by $\mathrm{e}^{-\frac{is}{\varepsilon}}$ or $\mathrm{e}^{\frac{is}{\varepsilon^2}}$, respectively, we can decompose it into a coupled system for a ε^2-frequency wave with the unknown $z^n(\mathbf{x}, s) := z^n$ and the rest frequency waves with the unknown $r^n(\mathbf{x}, s) := r^n$ as

$$\begin{cases} \varepsilon^2 \partial_{ss} z^n + 2i\partial_s z^n - \Delta z^n + z^n \phi^n = 0, \\ \varepsilon^2 \partial_{ss} r^n - \Delta r^n + \dfrac{1}{\varepsilon^2} r^n + r^n \phi^n = 0, \end{cases} \quad \mathbf{x} \in \mathbb{R}^d, \quad 0 \le s \le \tau. \tag{5.3.5}$$

By plugging (5.3.3) directly into (5.3.1b), we get

$$\begin{cases} \partial_{ss} \phi^n - \Delta \phi^n - \mathrm{e}^{\frac{2is}{\varepsilon^2}} \Delta\left((z^n)^2\right) - \mathrm{e}^{-\frac{2is}{\varepsilon^2}} \Delta\left((\overline{z^n})^2\right) - 2\mathrm{e}^{\frac{is}{\varepsilon^2}} \Delta(z^n r^n) \\ \quad - 2\mathrm{e}^{-\frac{is}{\varepsilon^2}} \Delta(\overline{z^n} r^n) - \Delta\left(2|z^n|^2 + (r^n)^2\right) = 0, \quad \mathbf{x} \in \mathbb{R}^d, \ \ 0 < s \le \tau, \\ \phi^n(\mathbf{x}, 0) = \phi_0^n(\mathbf{x}), \quad \partial_s \phi^n(\mathbf{x}, 0) = \phi_1^n(\mathbf{x}), \quad \mathbf{x} \in \mathbb{R}^d. \end{cases} \tag{5.3.6}$$

For initial conditions for the system (5.3.5) coupled with (5.3.6), similarly as (4.2.5), we have

$$\begin{cases} z^n(\mathbf{x},0)+\overline{z^n}(\mathbf{x},0)+r^n(\mathbf{x},0)=\psi_0^n(\mathbf{x}), \quad \mathbf{x}\in\mathbb{R}^d, \\ \dfrac{i}{\varepsilon^2}\left[z^n(\mathbf{x},0)-\overline{z^n}(\mathbf{x},0)\right]+\partial_s z^n(\mathbf{x},0)+\partial_s\overline{z^n}(\mathbf{x},0)+\partial_s r^n(\mathbf{x},0)=\dfrac{\psi_1^n(\mathbf{x})}{\varepsilon^2}. \end{cases} \tag{5.3.7}$$

Then we decompose the above initial data similarly as (4.2.6) to get

$$\begin{cases} z^n(\mathbf{x},0)=\dfrac{1}{2}\left[\psi_0^n(\mathbf{x})-i\psi_1^n(\mathbf{x})\right], \\ \partial_s z^n(\mathbf{x},0)=\dfrac{i}{2}\left[-\Delta z^n(\mathbf{x},0)+z^n(\mathbf{x},0)\phi^n(\mathbf{x},0)\right], \quad \mathbf{x}\in\mathbb{R}^d, \\ r^n(\mathbf{x},0)=0, \qquad \partial_s r^n(\mathbf{x},0)=-\partial_s z^n(\mathbf{x},0)-\partial_s\overline{z^n}(\mathbf{x},0). \end{cases} \tag{5.3.8}$$

The initial data for (5.3.6) comes naturally from (5.3.2b).

After solving the decomposed system (5.3.5)-(5.3.6) with the initial data (5.3.8), we get

$$\phi^n(\mathbf{x},\tau)=:\phi_0^{n+1}(\mathbf{x}), \qquad \partial_s\phi^n(\mathbf{x},\tau)=:\phi_1^{n+1}(\mathbf{x}),$$

and $z^n(\mathbf{x},\tau)$, $\partial_s z^n(\mathbf{x},\tau)$, $r^n(\mathbf{x},\tau)$, $\partial_s r^n(\mathbf{x},\tau)$. Then we can reconstruct the variable to (5.3.1a) at $t=t_{n+1}$ by setting $s=\tau$ in (5.3.3) and (5.3.4), i.e.,

$$\begin{cases} \psi(\mathbf{x},t_{n+1})=\mathrm{e}^{i\tau/\varepsilon^2}z^n(\mathbf{x},\tau)+\mathrm{e}^{-i\tau/\varepsilon^2}\overline{z^n}(\mathbf{x},\tau)+r^n(\mathbf{x},\tau)=:\psi_0^{n+1}(\mathbf{x}), \\ \partial_t\psi(\mathbf{x},t_{n+1})=\dfrac{1}{\varepsilon^2}\psi_1^{n+1}(\mathbf{x}), \qquad \mathbf{x}\in\mathbb{R}^d, \end{cases} \tag{5.3.9}$$

with

$$\psi_1^{n+1}(\mathbf{x}):=\mathrm{e}^{\frac{i\tau}{\varepsilon^2}}\left[\varepsilon^2\partial_s z^n(\mathbf{x},\tau)+iz^n(\mathbf{x},\tau)\right]+\mathrm{e}^{-\frac{i\tau}{\varepsilon^2}}\left[\varepsilon^2\partial_s\overline{z^n}(\mathbf{x},\tau)-i\overline{z^n}(\mathbf{x},\tau)\right]+\varepsilon^2\partial_s r^n(\mathbf{x},\tau).$$

5.3.2 MTI

In one space dimension for simplicity, with the whole-space problem (5.3.1a)-(5.3.1c) truncated into an finite interval $\Omega=(a,b)$ with homogenous Dirichlet

boundary conditions, the decomposed system reads:

$$\begin{cases} \varepsilon^2\partial_{ss}z^n + 2i\partial_s z^n - \partial_{xx}z^n + z^n\phi^n = 0, \\ \varepsilon^2\partial_{ss}r^n - \partial_{xx}r^n + \dfrac{1}{\varepsilon^2}r^n + r^n\phi^n = 0, \\ \partial_{ss}\phi^n - \partial_{xx}\phi^n - \mathrm{e}^{\frac{2is}{\varepsilon^2}}\partial_{xx}\left((z^n)^2\right) - \mathrm{e}^{-\frac{2is}{\varepsilon^2}}\partial_{xx}\left((\overline{z^n})^2\right) - 2\mathrm{e}^{\frac{is}{\varepsilon^2}}\partial_{xx}(z^n r^n) \\ -2\mathrm{e}^{-\frac{is}{\varepsilon^2}}\partial_{xx}(\overline{z^n}r^n) - \partial_{xx}\left(2|z^n|^2 + (r^n)^2\right) = 0, \quad a < x < b,\ 0 < s \le \tau. \end{cases} \tag{5.3.10}$$

The initial and boundary conditions for the above system are

$$\begin{cases} z^n(a,s) = z^n(b,s) = 0, \quad r^n(a,s) = r^n(b,s) = 0, \\ \phi^n(a,s) = \phi^n(b,s) = 0, \quad 0 \le s \le \tau; \\ z^n(x,0) = \dfrac{1}{2}\left[\psi_0^n(x) - i\psi_1^n(x)\right], \\ \partial_s z^n(x,0) = \dfrac{i}{2}\left[-\partial_{xx}z^n(x,0) + z^n(x,0)\phi^n(x,0)\right], \\ r^n(x,0) = 0, \qquad \partial_s r^n(x,0) = -\partial_s z^n(x,0) - \partial_s\,\overline{z^n}(x,0), \\ \phi^n(x,0) = \phi_0^n(x), \qquad \partial_s\phi^n(x,0) = \phi_1^n(x), \qquad a \le x \le b. \end{cases} \tag{5.3.11}$$

Following the same notation introduced in the previous section, we begin with a sine spectral discretization for (5.3.10): find $z_M^n := z_M^n(x,s)$, $r_M^n := r_M^n(x,s)$, $\phi_M^n := \phi_M^n(x,s) \in X_M$ for $0 \le s \le \tau$, i.e.

$$\begin{aligned} z_M^n(x,s) &= \sum_{l=1}^{M-1}\widehat{(z_M^n)}_l(s)\sin(\mu_l(x-a)),\ r_M^n(x,s) = \sum_{l=1}^{M-1}\widehat{(r_M^n)}_l(s)\sin(\mu_l(x-a)), \\ \phi_M^n(x,s) &= \sum_{l=1}^{M-1}\widehat{(\phi_M^n)}_l(s)\sin(\mu_l(x-a)), \end{aligned} \tag{5.3.12}$$

such that for $0 < s < \tau$,

$$\begin{cases} \varepsilon^2\partial_{ss}z_M^n + 2i\partial_s z_M^n - \partial_{xx}z_M^n + P_M\left(z_M^n\phi_M^n\right) = 0, \quad a < x < b, \\ \varepsilon^2\partial_{ss}r_M^n - \partial_{xx}r_M^n + \dfrac{1}{\varepsilon^2}r_M^n + P_M(r_M^n\phi_M^n) = 0, \\ \partial_{ss}\phi_M^n - \partial_{xx}\phi_M^n - \partial_{xx}(P_M f_M^n)(x,s) = 0, \end{cases} \tag{5.3.13}$$

where

$$\begin{aligned} f_M^n(x,s) :=& \mathrm{e}^{\frac{2is}{\varepsilon^2}}(z_M^n)^2 + \mathrm{e}^{-\frac{2is}{\varepsilon^2}}(\overline{z_M^n})^2 + 2\mathrm{e}^{\frac{is}{\varepsilon^2}}(z_M^n r_M^n) + 2\mathrm{e}^{-\frac{is}{\varepsilon^2}}(\overline{z_M^n}r_M^n) \\ &+ 2|z_M^n|^2 + (r_M^n)^2. \end{aligned} \tag{5.3.14}$$

Substituting (5.3.12) into (5.3.13) and noticing the orthogonality of bases, we get

$$\begin{cases} \varepsilon^2\widehat{(z_M^n)}_l''(s)+2i\widehat{(z_M^n)}_l'(s)+\mu_l^2\widehat{(z_M^n)}_l(s)+\widehat{(z_M^n\phi_M^n)}_l(s)=0, \\ \varepsilon^2\widehat{(r_M^n)}_l''(s)+\left(\mu_l^2+\dfrac{1}{\varepsilon^2}\right)\widehat{(r_M^n)}_l(s)+\widehat{(r_M^n\phi_M^n)}_l(s)=0, \\ \widehat{(\phi_M^n)}_l''(s)+\mu_l^2\widehat{(\phi_M^n)}_l(s)+\mu_l^2\widehat{(f_M^n)}_l(s)=0, \quad 0<s\le\tau,\ 1\le l\le M-1, \end{cases} \tag{5.3.15}$$

In order to apply the EWIs for integrating (5.3.15) in time, for each fixed $1\le l\le M-1$, we rewrite (5.3.15) by using the variation-of-constant formulas

$$\begin{cases} \widehat{(z_M^n)}_l(s)=a_l(s)\widehat{(z_M^n)}_l(0)+\varepsilon^2 b_l(s)\widehat{(z_M^n)}_l'(0)-\displaystyle\int_0^s b_l(s-\theta)\widehat{(z_M^n\phi_M^n)}_l(\theta)\,d\theta, \\ \widehat{(r_M^n)}_l(s)=\dfrac{\sin(\omega_l s)}{\omega_l}\widehat{(r_M^n)}_l'(0)-\displaystyle\int_0^s\frac{\sin\left(\omega_l(s-\theta)\right)}{\varepsilon^2\omega_l}\widehat{(r_M^n\phi_M^n)}_l(\theta)\,d\theta, \\ \widehat{(\phi_M^n)}_l(s)=\cos(\mu_l s)\widehat{(\phi_M^n)}_l(0)+\dfrac{\sin(\mu_l s)}{\mu_l}\widehat{(\phi_M^n)}_l'(0) \\ \qquad\qquad -\mu_l\displaystyle\int_0^s\sin\left(\mu_l(s-\theta)\right)\widehat{(f_M^n)}_l(\theta)\,d\theta, \qquad 0\le s\le\tau, \end{cases} \tag{5.3.16}$$

where

$$\begin{cases} a_l(s):=\dfrac{\lambda_l^+\mathrm{e}^{is\lambda_l^-}-\lambda_l^-\mathrm{e}^{is\lambda_l^+}}{\lambda_l^+-\lambda_l^-}, \qquad b_l(s):=i\dfrac{\mathrm{e}^{is\lambda_l^+}-\mathrm{e}^{is\lambda_l^-}}{\varepsilon^2(\lambda_l^--\lambda_l^+)}, \quad 0\le s\le\tau, \\ \lambda_l^\pm=-\dfrac{1}{\varepsilon^2}\left(1\pm\sqrt{1+\mu_l^2\varepsilon^2}\right), \qquad \omega_l=\dfrac{\sqrt{1+\mu_l^2\varepsilon^2}}{\varepsilon^2}. \end{cases} \tag{5.3.17}$$

Differentiating (5.3.16) with respect to s, we obtain

$$\begin{cases} \widehat{(z_M^n)}_l'(s)=a_l'(s)\widehat{(z_M^n)}_l(0)+\varepsilon^2 b_l'(s)\widehat{(z_M^n)}_l'(0)-\displaystyle\int_0^s b_l'(s-\theta)\widehat{(z_M^n\phi_M^n)}_l(\theta)\,d\theta, \\ \widehat{(r_M^n)}_l'(s)=\cos(\omega_l s)\widehat{(r_M^n)}_l'(0)-\displaystyle\int_0^s\frac{\cos\left(\omega_l(s-\theta)\right)}{\varepsilon^2}\widehat{(r_M^n\phi_M^n)}_l(\theta)\,d\theta, \\ \widehat{(\phi_M^n)}_l'(s)=-\mu_l\sin(\mu_l s)\widehat{(\phi_M^n)}_l(0)+\cos(\mu_l s)\widehat{(\phi_M^n)}_l'(0) \\ \qquad\qquad -\mu_l^2\displaystyle\int_0^s\cos\left(\mu_l(s-\theta)\right)\widehat{(f_M^n)}_l(\theta)\,d\theta, \qquad 0\le s\le\tau, \end{cases} \tag{5.3.18}$$

where

$$a_l'(s)=i\lambda_l^+\lambda_l^-\frac{\mathrm{e}^{is\lambda_l^-}-\mathrm{e}^{is\lambda_l^+}}{\lambda_l^+-\lambda_l^-}, \qquad b_l'(s)=\frac{\lambda_l^+\mathrm{e}^{is\lambda_l^+}-\lambda_l^-\mathrm{e}^{is\lambda_l^-}}{\varepsilon^2(\lambda_l^+-\lambda_l^-)}, \qquad 0\le s\le\tau.$$

Taking $s = \tau$ in (5.3.16) and (5.3.18), and using (5.3.14) we get

$$\begin{cases} \widehat{(z_M^n)}_l(\tau) = a_l(\tau)\widehat{(z_M^n)}_l(0) + \varepsilon^2 b_l(\tau)\widehat{(z_M^n)}'_l(0) - \displaystyle\int_0^\tau b_l(\tau-\theta)\widehat{(z_M^n\phi_M^n)}_l(\theta)\,d\theta, \\ \widehat{(z_M^n)}'_l(\tau) = a_l'(\tau)\widehat{(z_M^n)}_l(0) + \varepsilon^2 b_l'(\tau)\widehat{(z_M^n)}'_l(0) - \displaystyle\int_0^\tau b_l'(\tau-\theta)\widehat{(z_M^n\phi_M^n)}_l(\theta)\,d\theta, \\ \widehat{(r_M^n)}_l(\tau) = \dfrac{\sin(\omega_l\tau)}{\omega_l}\widehat{(r_M^n)}'_l(0) - \displaystyle\int_0^\tau \frac{\sin\left(\omega_l(\tau-\theta)\right)}{\varepsilon^2\omega_l}\widehat{(r_M^n\phi_M^n)}_l(\theta)\,d\theta, \\ \widehat{(r_M^n)}'_l(\tau) = \cos(\omega_l\tau)\widehat{(r_M^n)}'_l(0) - \displaystyle\int_0^\tau \frac{\cos\left(\omega_l(\tau-\theta)\right)}{\varepsilon^2}\widehat{(r_M^n\phi_M^n)}_l(\theta)\,d\theta, \\ \widehat{(\phi_M^n)}_l(\tau) = \cos(\mu_l\tau)\widehat{(\phi_M^n)}_l(0) + \dfrac{\sin(\mu_l\tau)}{\mu_l}\widehat{(\phi_M^n)}'_l(0) - (F_M^n)_l, \\ \widehat{(\phi_M^n)}'_l(\tau) = -\mu_l\sin(\mu_l\tau)\widehat{(\phi_M^n)}_l(0) + \cos(\mu_l\tau)\widehat{(\phi_M^n)}'_l(0) - (\dot{F}_M^n)_l, \end{cases} \tag{5.3.19}$$

where

$$\begin{aligned} (F_M^n)_l =& \mu_l\int_0^\tau \sin\left(\mu_l(\tau-\theta)\right)\left[\mathrm{e}^{\frac{2i\theta}{\varepsilon^2}}\widehat{((z_M^n)^2)}_l(\theta) + \mathrm{e}^{-\frac{2i\theta}{\varepsilon^2}}\widehat{((\overline{z_M^n})^2)}_l(\theta)\right]d\theta \\ &+ \mu_l\int_0^\tau \sin\left(\mu_l(\tau-\theta)\right)\left[2\widehat{(|z_M^n|^2)}_l(\theta) + \widehat{((r_M^n)^2)}_l(\theta)\right]d\theta \\ &+ \mu_l\int_0^\tau \sin\left(\mu_l(\tau-\theta)\right)\left[2\mathrm{e}^{\frac{i\theta}{\varepsilon^2}}\widehat{(z_M^n r_M^n)}_l(\theta) + 2\mathrm{e}^{-\frac{i\theta}{\varepsilon^2}}\widehat{(\overline{z_M^n} r_M^n)}_l(\theta)\right]d\theta, \\ (\dot{F}_M^n)_l =& \mu_l^2\int_0^\tau \cos\left(\mu_l(\tau-\theta)\right)\left[\mathrm{e}^{\frac{2i\theta}{\varepsilon^2}}\widehat{((z_M^n)^2)}_l(\theta) + \mathrm{e}^{-\frac{2i\theta}{\varepsilon^2}}\widehat{((\overline{z_M^n})^2)}_l(\theta)\right]d\theta \\ &+ \mu_l^2\int_0^\tau \cos\left(\mu_l(\tau-\theta)\right)\left[2\widehat{(|z_M^n|^2)}_l(\theta) + \widehat{((r_M^n)^2)}_l(\theta)\right]d\theta \\ &+ \mu_l^2\int_0^\tau \cos\left(\mu_l(\tau-\theta)\right)\left[2\mathrm{e}^{\frac{i\theta}{\varepsilon^2}}\widehat{(z_M^n r_M^n)}_l(\theta) + 2\mathrm{e}^{-\frac{i\theta}{\varepsilon^2}}\widehat{(\overline{z_M^n} r_M^n)}_l(\theta)\right]d\theta. \end{aligned}$$

Approximating the integrals in (5.3.19) either by the Gautschi's quadrature or by the standard trapezoidal rule, we get

$$\begin{cases} \widehat{(z_M^n)}_l(\tau) \approx a_l(\tau)\widehat{(z_M^n)}_l(0) + \varepsilon^2 b_l(\tau)\widehat{(z_M^n)}'_l(0) - c_l\widehat{(z_M^n\phi_M^n)}_l(0) - d_l\widehat{(z_M^n\phi_M^n)}'_l(0), \\ \widehat{(z_M^n)}'_l(\tau) \approx a_l'(\tau)\widehat{(z_M^n)}_l(0) + \varepsilon^2 b_l'(\tau)\widehat{(z_M^n)}'_l(0) - \dot{c}_l\widehat{(z_M^n\phi_M^n)}_l(0) - \dot{d}_l\widehat{(z_M^n\phi_M^n)}'_l(0), \\ \widehat{(r_M^n)}_l(\tau) \approx \dfrac{\sin(\omega_l\tau)}{\omega_l}\widehat{(r_M^n)}'_l(0), \\ \widehat{(r_M^n)}'_l(\tau) \approx \cos(\omega_l\tau)\widehat{(r_M^n)}'_l(0) - \dfrac{\tau}{2\varepsilon^2}\widehat{(r_M^n\phi_M^n)}_l(\tau), \end{cases} \tag{5.3.20}$$

and

$$\begin{cases} (F_M^n)_l \approx p_l(\widehat{(z_M^n)^2})_l(0) + q_l(\widehat{(z_M^n)^2})_l'(0) + \overline{p_l}(\widehat{(\overline{z_M^n})^2})_l(0) + \overline{q_l}(\widehat{(\overline{z_M^n})^2})_l'(0) \\ \qquad\quad + \tau\mu_l \sin(\mu_l\tau)(\widehat{|z_M^n|^2})_l(0), \\ (\dot{F}_M^n)_l \approx \dot{p}_l(\widehat{(z_M^n)^2})_l(0) + \dot{q}_l(\widehat{(z_M^n)^2})_l'(0) + \overline{\dot{p}_l}(\widehat{(\overline{z_M^n})^2})_l(0) + \overline{\dot{q}_l}(\widehat{(\overline{z_M^n})^2})_l'(0) \\ \qquad\quad + \tau\mu_l^2\Big[\cos(\mu_l\tau)(\widehat{|z_M^n|^2})_l(0) + (\widehat{|z_M^n|^2})_l(\tau) + \frac{1}{2}(\widehat{(r_M^n)^2})_l(\tau) \\ \qquad\quad + \mathrm{e}^{\frac{i\tau}{\varepsilon^2}}(\widehat{z_M^n r_M^n})_l(\tau) + \mathrm{e}^{-\frac{i\tau}{\varepsilon^2}}(\widehat{\overline{z_M^n} r_M^n})_l(\tau)\Big], \end{cases}$$

where

$$\begin{cases} c_l = \displaystyle\int_0^\tau b_l(\tau-\theta)\,d\theta, \quad p_l = \mu_l \int_0^\tau \sin\left(\mu_l(\tau-\theta)\right)\mathrm{e}^{\frac{2i\theta}{\varepsilon^2}}\,d\theta, \\ d_l = \displaystyle\int_0^\tau b_l(\tau-\theta)\theta\,d\theta, \quad q_l = \mu_l \int_0^\tau \sin\left(\mu_l(\tau-\theta)\right)\mathrm{e}^{\frac{2i\theta}{\varepsilon^2}}\theta\,d\theta, \\ \dot{c}_l = \displaystyle\int_0^\tau b_l'(\tau-\theta)\,d\theta, \quad \dot{p}_l = \mu_l^2 \int_0^\tau \cos\left(\mu_l(\tau-\theta)\right)\mathrm{e}^{\frac{2i\theta}{\varepsilon^2}}\,d\theta, \\ \dot{d}_l = \displaystyle\int_0^\tau b_l'(\tau-\theta)\theta\,d\theta, \quad \dot{q}_l = \mu_l^2 \int_0^\tau \cos\left(\mu_l(\tau-\theta)\right)\mathrm{e}^{\frac{2i\theta}{\varepsilon^2}}\theta\,d\theta. \end{cases} \tag{5.3.21}$$

Inserting (5.3.20) into (5.3.12) with $s = \tau$, and noticing (5.3.9), we immediately obtain a multiscale time integrator sine spectral method based on (5.3.10) for the problem (5.3.1). Furthermore, let Ψ_j^n, $\dot{\Psi}_j^n$, Φ_j^n and $\dot{\Phi}_j^n$ be approximations of $\psi(x_j,t_n)$, $\partial_t\psi(x_j,t_n)$, $\phi(x_j,t_n)$ and $\partial_t\phi(x_j,t_n)$, respectively; and Z_j^{n+1}, $\dot{Z}_j^{n+1}$, R_j^{n+1} and $\dot{R}_j^{n+1}$ be approximations of $z^n(x_j,\tau)$, $\partial_s z^n(x_j,\tau)$, $r^n(x_j,\tau)$ and $\partial_s r^n(x_j,\tau)$, respectively, for $j = 1,\ldots,M-1$. Choosing $\Psi_j^0 = \psi_0(x_j)$, $\dot{\Psi}_j^0 = \psi_1(x_j)/\varepsilon^2$, $\Phi_j^0 = \phi_0(x_j)$ and $\dot{\Phi}_j^0 = \phi_1(x_j)$ for $0 \le j \le M$ and noticing (5.3.9), (5.3.12) with $s = \tau$, (5.3.20),

(5.3.11) and (2.4.1), then a multiscale time integrator sine pseudospectral (MTI-SP) discretization for the KGZ (5.3.1) in 1D reads: for $n \geq 0$,

$$\begin{cases} \Psi_j^{n+1} = \mathrm{e}^{i\tau/\varepsilon^2} Z_j^{n+1} + \mathrm{e}^{-i\tau/\varepsilon^2} \overline{Z_j^{n+1}} + R_j^{n+1}, \quad j = 1, \ldots, M-1, \\ \dot{\Psi}_j^{n+1} = \mathrm{e}^{i\tau/\varepsilon^2} \left(\dot{Z}_j^{n+1} + \frac{i}{\varepsilon^2} Z_j^{n+1} \right) + \mathrm{e}^{-i\tau/\varepsilon^2} \left(\overline{\dot{Z}_j^{n+1}} - \frac{i}{\varepsilon^2} \overline{Z_j^{n+1}} \right) + \dot{R}_j^{n+1}, \\ \Phi_j^{n+1} = \sum_{l=1}^{M-1} \widetilde{(\Phi^{n+1})}_l \sin(\mu_l (x_j - a)), \ \dot{\Phi}_j^{n+1} = \sum_{l=1}^{M-1} \widetilde{(\dot{\Phi}^{n+1})}_l \sin(\mu_l (x_j - a)), \\ Z_j^{n+1} = \sum_{l=1}^{M-1} \widetilde{(Z^{n+1})}_l \sin(\mu_l (x_j - a)), \ R_j^{n+1} = \sum_{l=1}^{M-1} \widetilde{(R^{n+1})}_l \sin(\mu_l (x_j - a)), \\ \dot{Z}_j^{n+1} = \sum_{l=1}^{M-1} \widetilde{(\dot{Z}^{n+1})}_l \sin(\mu_l (x_j - a)), \ \dot{R}_j^{n+1} = \sum_{l=1}^{M-1} \widetilde{(\dot{R}^{n+1})}_l \sin(\mu_l (x_j - a)), \end{cases} \tag{5.3.22}$$

where for $1 \leq l \leq M-1$,

$$\begin{aligned} \widetilde{(Z^{n+1})}_l =& a_l(\tau) \widetilde{(Z^0)}_l + \varepsilon^2 b_l(\tau) \widetilde{(\dot{Z}^0)}_l - c_l \widetilde{(Z^0 \Phi^n)}_l - d_l \widetilde{(\dot{Z}^0 \Phi^n)}_l \\ & - d_l \widetilde{(Z^0 \dot{\Phi}^n)}_l \end{aligned} \tag{5.3.23a}$$

$$\begin{aligned} \widetilde{(\dot{Z}^{n+1})}_l =& a_l'(\tau) \widetilde{(Z^0)}_l + \varepsilon^2 b_l'(\tau) \widetilde{(\dot{Z}^0)}_l - \dot{c}_l \widetilde{(Z^0 \Phi^n)}_l - \dot{d}_l \widetilde{(\dot{Z}^0 \Phi^n)}_l \\ & - \dot{d}_l \widetilde{(Z^0 \dot{\Phi}^n)}_l, \end{aligned} \tag{5.3.23b}$$

$$\widetilde{(R^{n+1})}_l = \frac{\sin(\omega_l \tau)}{\omega_l} \widetilde{(\dot{R}^0)}_l, \quad \widetilde{(\dot{R}^{n+1})}_l = \cos(\omega_l \tau) \widetilde{(\dot{R}^0)}_l - \frac{\tau}{2\varepsilon^2} \widetilde{(R^{n+1})}_l, \tag{5.3.23c}$$

$$\widetilde{(\Phi^{n+1})}_l = \cos(\mu_l \tau) \widetilde{(\Phi^n)}_l + \frac{\sin(\mu_l \tau)}{\mu_l} \widetilde{(\dot{\Phi}^n)}_l - \mathcal{F}_l^n, \tag{5.3.23d}$$

$$\widetilde{(\dot{\Phi}^{n+1})}_l = -\mu \sin(\mu_l \tau) \widetilde{(\Phi^n)}_l + \cos(\mu_l \tau) \widetilde{(\dot{\Phi}^n)}_l - \dot{\mathcal{F}}_l^n, \tag{5.3.23e}$$

with

$$\begin{cases} \widetilde{(Z^0)}_l = \dfrac{1}{2}\left[\widetilde{(\Psi^n)}_l - i\varepsilon^2\widetilde{\left(\dot{\Psi}^n\right)}_l\right], \quad \widetilde{\left(\dot{R}^0\right)}_l = -\widetilde{\left(\dot{Z}^0\right)}_l - \widetilde{\left(\overline{\dot{Z}^0}\right)}_l, \\ \widetilde{\left(\dot{Z}^0\right)}_l = \dfrac{i}{2}\left[\dfrac{2}{\tau}\sin\left(\dfrac{1}{2}\mu_l^2\tau\right)\widetilde{(Z^0)}_l + \widetilde{(Z^0\Phi^n)}_l\right], \\ \mathcal{F}_l^n = p_l\widetilde{((Z^0)^2)}_l + 2q_l\widetilde{(Z^0\dot{Z}^0)}_l + \overline{p_l}\widetilde{((\overline{Z^0})^2)}_l + 2\overline{q_l}\widetilde{\left(\overline{Z^0\dot{Z}^0}\right)}_l \\ \qquad +\tau\mu_l\sin(\mu_l\tau)\widetilde{(|Z^0|^2)}_l, \\ \dot{\mathcal{F}}_l^n = \dot{p}_l\widetilde{((Z^0)^2)}_l + 2\dot{q}_l\widetilde{\left(Z^0\dot{Z}^0\right)}_l + \overline{\dot{p}_l}\widetilde{\left((\overline{Z^0})^2\right)}_l + 2\overline{\dot{q}_l}\widetilde{\left(\overline{Z^0\dot{Z}^0}\right)}_l \\ \qquad +\tau\mu_l^2\Big[\widetilde{(|Z^{n+1}|^2)}_l + \dfrac{1}{2}\widetilde{((R^{n+1})^2)}_l + \mathrm{e}^{\frac{i\tau}{\varepsilon^2}}\widetilde{(Z^{n+1}R^{n+1})}_l \\ \qquad +\mathrm{e}^{-\frac{i\tau}{\varepsilon^2}}\widetilde{\left(\overline{Z^{n+1}}R^{n+1}\right)}_l + \cos(\mu_l\tau)\widetilde{(|Z^0|^2)}_l\Big]. \end{cases} \tag{5.3.24}$$

This MTI-SP method for the KGZ equation (5.3.1) (or (5.3.1a)-(5.3.1b)) is clearly explicit, accurate, easy to implement and very efficient due to the fast discrete sine transform, and its memory cost is $O(M)$ and the computational cost per time step is $O(M\log M)$.

5.4 Numerical results

Since the methods are extensions from those established for the KGE (1.3.7), so the numerical results for the KGZ system (5.1.1) are very much similar to those of KGE. The results of EWI-GSP and EWI-DSP for KGZ in the simultaneous high-plasma-frequency and subsonic limit regime are similar to Tabs 3.5&3.6. For brevity, we only present the numerical results of MTI-SP for solving the KGZ system (5.1.1) in high-plasma-frequency limit regime. We choose the initial data in (5.3.1) as

$$\psi_0(x) = \mathrm{e}^{-\frac{x^2}{2}}, \quad \psi_1(x) = \frac{3\psi_0(x)}{2\varepsilon^2}, \quad \phi_0(x) = sech(x^2), \quad \phi_1(x) = 0. \tag{5.4.1}$$

The problem is solved on a bounded interval $\Omega = [-16, 16]$, i.e. $b = -a = 16$, which is large enough to guarantee that the zero boundary condition does not introduce a significant truncation error relative to the original problem. To quantify the error,

we introduce the error functions:

$$e_{\psi}^{\varepsilon}(T) := \left\|\psi(\cdot,T) - \psi_I^M\right\|_{H^2}, \quad e_{\psi}^{\infty}(T) := \max_{0<\varepsilon\leq 1}\left\{e_{\psi}^{\varepsilon}(T)\right\},$$
$$e_{\phi}^{\varepsilon}(T) := \left\|\phi(\cdot,T) - \phi_I^M\right\|_{H^1}, \quad e_{\phi}^{\infty}(T) := \max_{0<\varepsilon\leq 1}\left\{e_{\phi}^{\varepsilon}(T)\right\},$$

with $M = \frac{T}{\tau}$. Since the analytical solution to this problem is not available, so the 'exact' solution here is obtained numerically by the MTI-SP method (5.3.22)-(5.3.24) with very fine mesh $h = 1/32$ and time step $\tau = 5 \times 10^{-6}$. Tab. 5.1 and Tab. 5.2 show the spatial error of MTI-SP method at $T = 1$ under different ε and h with a very small time step $\tau = 5 \times 10^{-6}$ such that the discretization error in time is negligible. Tab. 5.3 and Tab. 5.4 show the temporal error of MTI-SP method at $T = 1$ under different ε and τ with a small mesh size $h = 1/8$ such that the discretization error in space is negligible. Fig 5.2 shows the profiles of the solutions of the KGZ (5.3.1) with (5.4.1) during the dynamics under different ε. Fig 5.3 shows the solutions of the KGZ (5.2.1) with the initial data (5.4.1) in the simultaneous high-plasma-frequency and subsonic limit regime under different ε with $\gamma = 2\varepsilon$.

From Tabs. 5.1-5.4 and extensive additional results not shown here for brevity, we can draw the following observations:

(i) The MTI-SP method is spectrally accurate in space, which is uniformly for $0 < \varepsilon \leq 1$ (cf. Tabs. 5.1&5.2).

(ii) The MTI-SP method converges uniformly and linearly in time for $\varepsilon \in (0, \tau]$ (cf. last row in Tabs. 5.3&5.4). In addition, for each fixed $\varepsilon = \varepsilon_0 > 0$, when τ is small enough, it converges quadratically in time (cf. each row in the upper triangle of Tabs. 5.3&5.4); and for each fixed ε small enough, when τ satisfies $0 < \varepsilon < \tau$, it also converges quadratically in time (cf. each row in the lower triangle of Tabs. 5.3&5.4).

(iii) The MTI-SP method is uniformly accurate for all $\varepsilon \in (0, 1]$ under the mesh strategy (or ε-scalability) $\tau = O(1)$ and $h = O(1)$.

With the MTI-FP method, similarly as before, we can solve the KGZ system (5.3.1) in the high-frequency limit regime effectively in high dimensional cases. Fig.

Table 5.1: Spatial error analysis: $e_\phi^\varepsilon(T)$ at $T = 1$ with $\tau = 5 \times 10^{-6}$ for different ε and h.

$e_\phi^\varepsilon(T)$	$h_0 = 1$	$h_0/2$	$h_0/4$	$h_0/8$
$\varepsilon_0 = 0.5$	3.84E-02	7.85E-04	1.53E-07	8.36E-12
$\varepsilon_0/2^1$	3.79E-02	2.00E-03	1.49E-07	7.51E-12
$\varepsilon_0/2^2$	3.72E-02	2.10E-03	8.49E-08	7.53E-12
$\varepsilon_0/2^3$	3.69E-02	2.10E-03	8.14E-08	7.39E-12
$\varepsilon_0/2^4$	3.68E-02	2.10E-03	8.05E-08	7.44E-12
$\varepsilon_0/2^5$	3.67E-02	2.10E-03	8.02E-08	7.43E-12
$\varepsilon_0/2^7$	3.68E-02	2.10E-03	8.01E-08	7.40E-12
$\varepsilon_0/2^9$	3.68E-02	2.10E-03	8.01E-08	7.46E-12
$\varepsilon_0/2^{11}$	3.68E-02	2.10E-03	8.01E-08	7.54E-12
$\varepsilon_0/2^{13}$	3.68E-02	2.10E-03	8.01E-08	7.42E-12

5.4 and Fig. 5.5 show the contour plots of the solutions of the KGE in 2D case, i.e. $d = 2$, with initial data

$$\begin{aligned} \psi_0(x,y) &= \exp\left(-(x+2)^2 - y^2\right) + \exp\left(-(x-2)^2 - y^2\right), \\ \phi_0(x,y) &= sech(x^2 + (y+2)^2) + sech(x^2 + (y-2)^2), \\ \psi_1(x,y) &= \exp\left(-x^2 - y^2\right), \quad \phi_1(x,y) = sech(x^2 + y^2), \end{aligned} \tag{5.4.2}$$

in (5.3.1) under different ε and t.

Table 5.2: Spatial error analysis: $e_{\psi}^{\varepsilon}(T)$ at $T = 1$ with $\tau = 5 \times 10^{-6}$ for different ε and h.

$e_{\psi}^{\varepsilon}(T)$	$h_0 = 1$	$h_0/2$	$h_0/4$	$h_0/8$
$\varepsilon_0 = 0.5$	1.07E-01	2.40E-03	9.23E-08	5.77E-11
$\varepsilon_0/2^1$	1.29E-01	2.10E-03	2.13E-07	3.68E-11
$\varepsilon_0/2^2$	2.25E-01	1.90E-03	2.20E-07	3.36E-11
$\varepsilon_0/2^3$	2.17E-01	2.10E-03	4.27E-07	3.94E-11
$\varepsilon_0/2^4$	1.03E-01	7.70E-04	1.62E-07	4.21E-11
$\varepsilon_0/2^5$	7.52E-02	1.00E-03	4.06E-07	4.62E-11
$\varepsilon_0/2^7$	9.20E-02	1.20E-03	3.58E-07	4.99E-11
$\varepsilon_0/2^9$	1.87E-01	1.80E-03	1.72E-07	3.90E-11
$\varepsilon_0/2^{11}$	1.14E-01	1.40E-03	3.70E-07	3.91E-11
$\varepsilon_0/2^{13}$	2.33E-01	2.50E-03	3.72E-07	4.71E-11

Table 5.3: Temporal error analysis: $e_\phi^\varepsilon(T)$ and $e_\phi^\infty(T)$ at $T = 1$ with $h = 1/8$ for different ε and τ.

$e_\phi^\varepsilon(T)$	$\tau_0 = 0.2$	$\tau_0/2^2$	$\tau_0/2^4$	$\tau_0/2^6$	$\tau_0/2^8$	$\tau_0/2^{10}$	$\tau_0/2^{12}$
$\varepsilon_0 = 0.5$	1.41E-01	1.16E-02	6.85E-04	4.19E-05	2.60E-06	1.60E-07	7.37E-09
rate	—	1.80	2.04	2.02	2.00	2.01	2.21
$\varepsilon_0/2^1$	4.08E-02	2.92E-02	2.10E-03	1.22E-04	7.51E-06	4.60E-07	2.14E-08
rate	—	0.24	1.90	2.05	2.01	2.01	2.21
$\varepsilon_0/2^2$	3.81E-02	1.55E-02	6.80E-03	4.63E-04	2.75E-05	1.66E-06	7.77E-08
rate	—	0.65	0.59	1.94	2.04	2.02	2.21
$\varepsilon_0/2^3$	5.25E-02	4.40E-03	6.70E-03	1.70E-03	1.12E-04	6.58E-06	3.03E-07
rate	—	1.79	-0.30	0.99	1.96	2.05	2.21
$\varepsilon_0/2^4$	5.29E-02	2.60E-03	1.80E-03	1.90E-03	4.12E-04	2.75E-05	1.23E-06
rate	—	2.17	0.26	-0.04	1.10	1.95	2.24
$\varepsilon_0/2^5$	5.31E-02	3.00E-03	1.22E-04	4.92E-04	4.86E-04	1.01E-04	5.19E-06
rate	—	2.07	2.31	-1.01	0.01	1.13	2.14
$\varepsilon_0/2^7$	5.38E-02	3.40E-03	1.95E-04	2.53E-05	2.59E-05	4.05E-05	3.95E-05
rate	—	1.99	2.06	1.47	-0.02	-0.32	0.02
$\varepsilon_0/2^9$	5.39E-02	3.40E-03	2.10E-04	1.21E-05	1.09E-06	9.34E-07	3.38E-07
rate	—	1.99	2.01	2.06	1.73	0.11	0.73
$\varepsilon_0/2^{11}$	5.39E-02	3.40E-03	2.11E-04	1.31E-05	7.14E-07	8.43E-08	3.33E-08
rate	—	1.99	2.00	2.00	2.10	1.54	0.67
$\varepsilon_0/2^{13}$	5.39E-02	3.40E-03	2.11E-04	1.31E-05	8.24E-07	5.75E-08	2.42E-09
rate	—	1.99	2.01	2.00	2.00	1.92	2.28
$e_\phi^\infty(T)$	1.41E-01	2.92E-02	6.80E-03	1.90E-03	4.86E-04	1.01E-04	3.95E-05
rate	—	1.13	1.05	0.92	0.98	1.13	0.68

Table 5.4: Temporal error analysis: $e_\psi^\varepsilon(T)$ and $e_\psi^\infty(T)$ at $T = 1$ with $h = 1/8$ for different ε and τ.

$e_\psi^\varepsilon(T)$	$\tau_0 = 0.2$	$\tau_0/2^2$	$\tau_0/2^4$	$\tau_0/2^6$	$\tau_0/2^8$	$\tau_0/2^{10}$	$\tau_0/2^{12}$
$\varepsilon_0 = 0.5$	4.52E-02	4.10E-03	2.62E-04	1.63E-05	1.02E-06	6.26E-08	2.86E-09
rate	—	1.73	1.99	2.00	2.00	2.01	2.22
$\varepsilon_0/2^1$	6.66E-02	1.28E-02	1.10E-03	6.74E-05	4.20E-06	2.58E-07	1.20E-08
rate	—	1.19	1.77	2.01	2.00	2.01	2.21
$\varepsilon_0/2^2$	6.35E-02	1.66E-02	4.00E-03	3.18E-04	1.99E-05	1.22E-06	5.71E-08
rate	—	0.97	1.03	1.83	2.00	2.01	2.20
$\varepsilon_0/2^3$	5.88E-02	7.80E-03	5.00E-03	9.82E-04	7.73E-05	4.77E-06	2.23E-07
rate	—	1.46	0.32	1.17	1.83	2.01	2.20
$\varepsilon_0/2^4$	6.66E-02	4.30E-03	1.30E-03	1.20E-03	2.11E-04	1.64E-05	7.80E-07
rate	—	1.98	0.86	0.06	1.25	1.84	2.19
$\varepsilon_0/2^5$	6.34E-02	4.10E-03	3.61E-04	2.95E-04	2.95E-04	4.85E-05	2.92E-06
rate	—	1.98	1.75	0.15	0.00	1.30	2.02
$\varepsilon_0/2^7$	6.21E-02	3.90E-03	2.51E-04	3.19E-05	1.48E-05	1.98E-05	1.98E-05
rate	—	1.99	1.98	1.49	0.55	-0.21	0.00
$\varepsilon_0/2^9$	6.80E-02	4.10E-03	2.56E-04	1.65E-05	1.32E-06	7.10E-07	2.15E-07
rate	—	2.02	2.00	1.98	1.82	0.45	0.86
$\varepsilon_0/2^11$	6.11E-02	3.80E-03	2.39E-04	1.50E-05	9.95E-07	1.30E-07	4.70E-08
rate	—	2.00	1.99	2.00	1.96	1.47	0.73
$\varepsilon_0/2^13$	6.11E-02	3.80E-03	2.38E-04	1.49E-05	9.27E-07	5.70E-08	7.76E-09
rate	—	2.00	2.00	2.00	2.00	2.01	1.45
$e_\psi^\infty(T)$	6.66E-02	1.66E-02	5.00E-03	1.20E-03	2.95E-04	4.85E-05	1.98E-05
rate	—	1.00	0.87	1.02	1.01	1.30	0.65

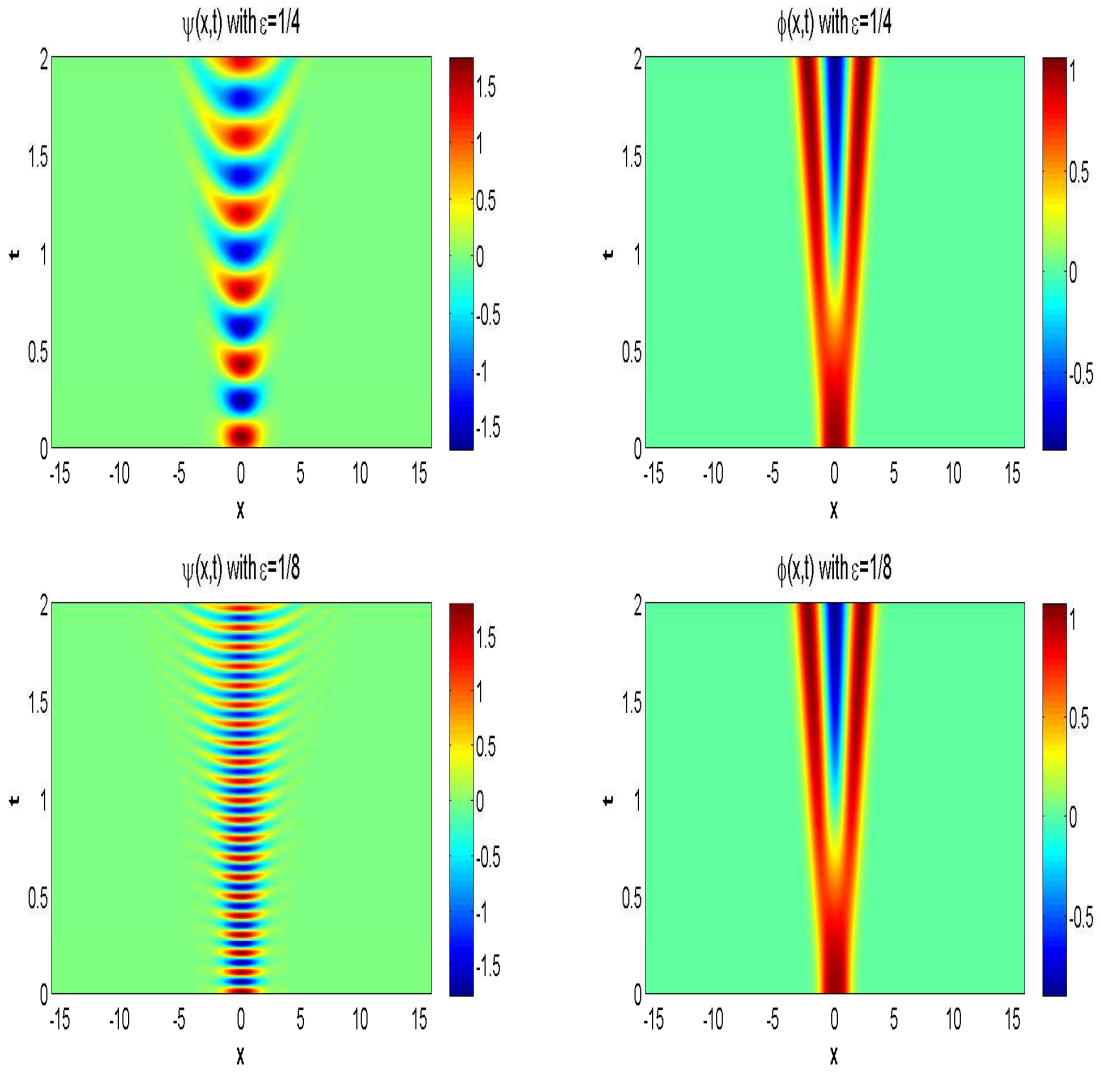

Figure 5.2: Solutions of the KGZ (5.3.1) with (5.4.1) in the high-plasma-frequency limit regime under different ε.

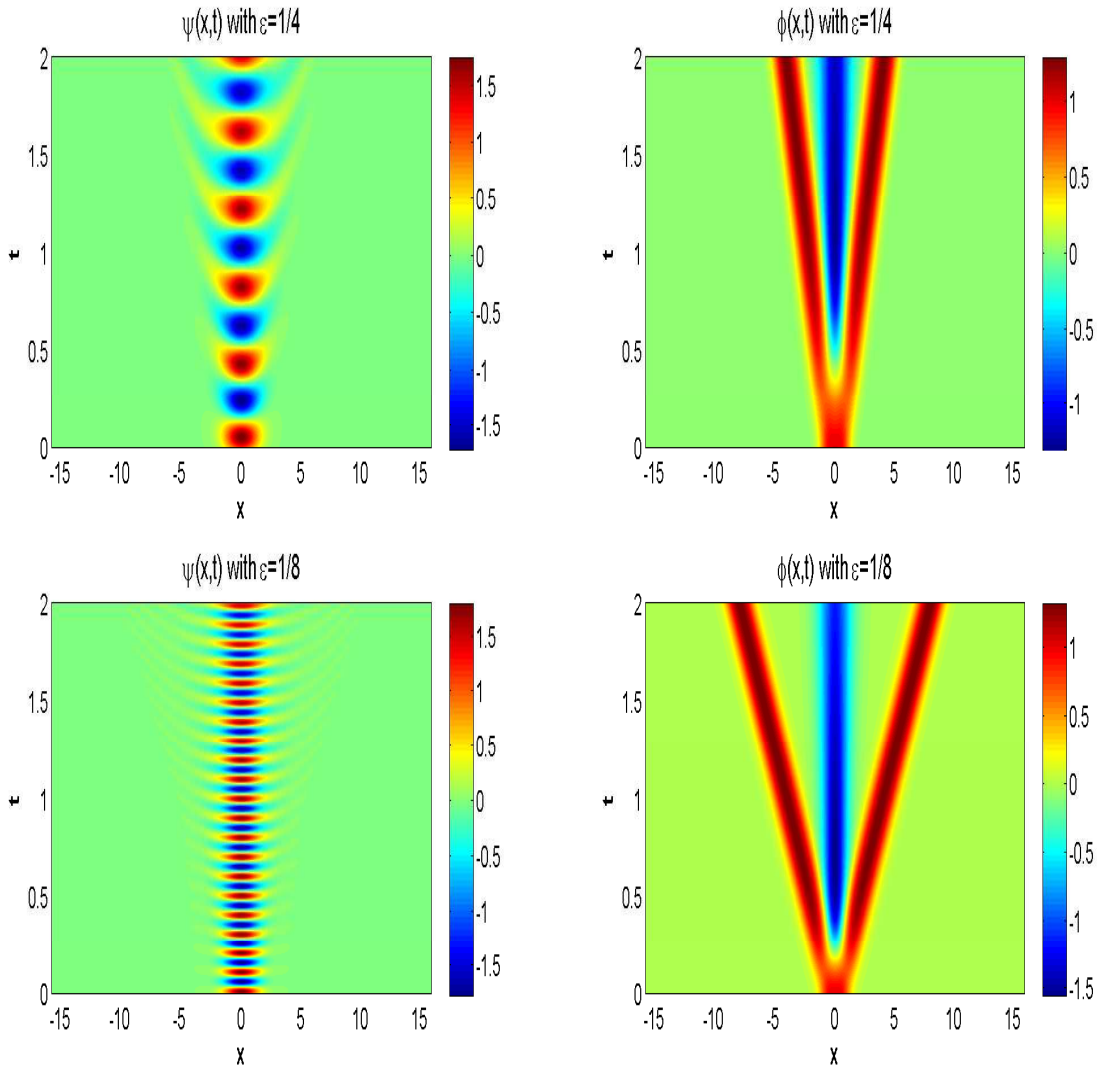

Figure 5.3: Solutions of the KGZ (5.2.1) with (5.4.1) in the simultaneously high-plasma-frequency and subsonic limit regime under different ε with $\gamma = 2\varepsilon$.

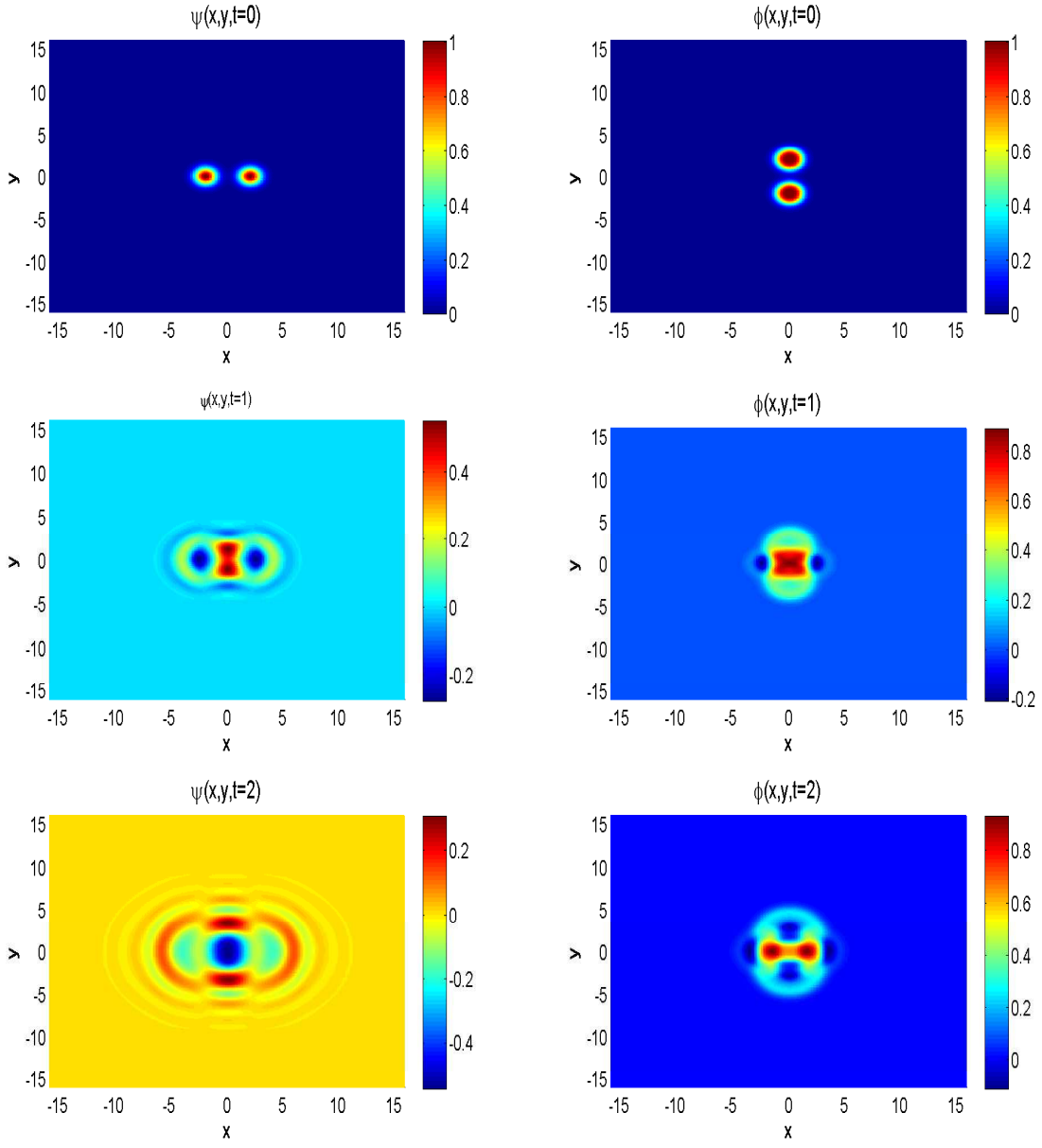

Figure 5.4: Solutions of the 2D KGZ (5.3.1) with (5.4.2) at different t under $\varepsilon = 5E-3$.

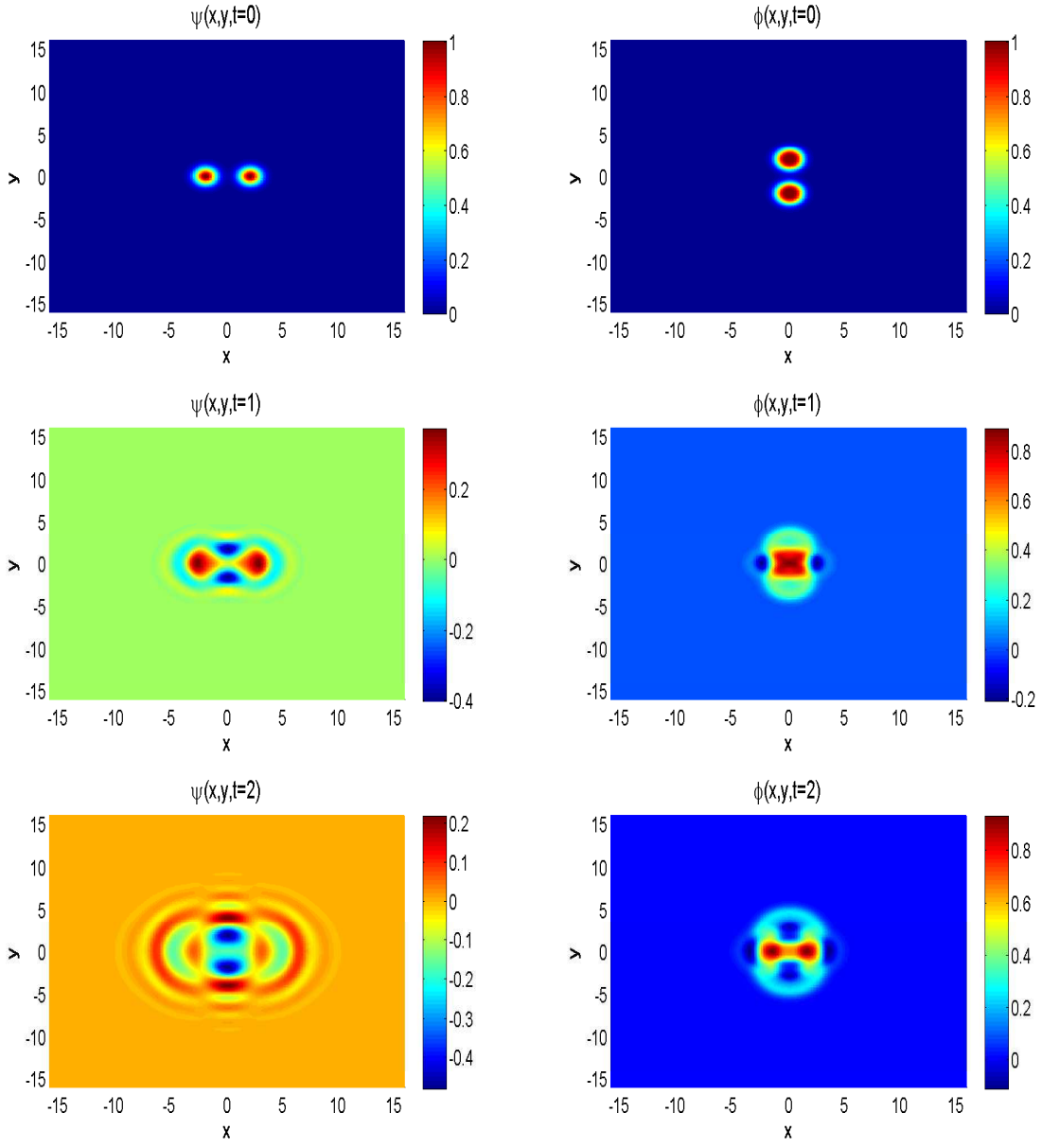

Figure 5.5: Solutions of the 2D KGZ (5.3.1) with (5.4.2) at different t under $\varepsilon = 2.5E-3$.

Chapter 6

Conclusion remarks and future work

This thesis is devoted to study efficient and accurate numerical methods for solving highly oscillatory differential equations with focus on proposing and analyzing multiscale methods. The subjects studied here include the high oscillatory second order differential equations (HODEs) (1.3.1), Klein-Gordon equation (KGE) (1.3.7) in nonrelativistic limit regime and Klein-Gordon-Zakharov (KGZ) system (1.3.11)-(1.3.12) in high-plasma-frequency and subsonic limit regime. The concluding remarks on each topic and possible future studies are drawn as follows.

1. On the high oscillatory second order differential equations

In Chapter 2, different numerical methods were either designed or reviewed as well as compared with each other for solving the HODEs with a dimensionless parameter $0 < \varepsilon \leq 1$ which is inversely proportional to the speed of light, especially in the nonrelativistic limit regime $0 < \varepsilon \ll 1$. In this regime, the solution propagates waves at wavelength $O(\varepsilon^2)$ and amplitude at $O(1)$, which brings significantly numerical burdens in practical computation. Based on two types of multiscale decomposition by either frequency or frequency and amplitude, two multiscale time integrators (MTIs), e.g. MTI-FA and MTI-F, were designed for solving the problem when the nonlinearity is taken as either a pure power nonlinearity or a general gauge invariant nonlinearity. Two independent error bounds at $O(\tau^2/\varepsilon^2)$ and $O(\varepsilon^2)$ for $\varepsilon \in (0, 1]$ of the two MTIs were rigorously established when the nonlinearity is

taken as a pure power nonlinearity, which immediately imply that the two MTIs converge uniformly with linear convergence rate at $O(\tau)$ for $\varepsilon \in (0, 1]$ and optimally with quadratic convergence rate at $O(\tau^2)$ in the regimes when either $\varepsilon = O(1)$ or $0 < \varepsilon \leq \tau$. For comparison, classical methods, such as exponential wave integrators (EWIs) and finite difference (FD) methods, were also presented for solving the problem. Error bounds for them were given with explicitly dependence on the parameter ε. Those rigorous error estimates lead to the conclusion that, in the regime $0 < \varepsilon \ll 1$, the ε-scalability for the two MTIs is $\tau = O(1)$ which is independent of ε, where it is at $\tau = O(\varepsilon^2)$ and $\tau = O(\varepsilon^3)$ for EWIs and FD methods, respectively. Therefore, the proposed MTIs offer compelling advantages over those classical methods in the regime $0 < \varepsilon \ll 1$. Numerical results confirmed our analytical error bounds. We remark here that both MTI-FA and MTI-F and their error estimates can be extended to (2.1.3) when $g(\rho)$ in (2.1.4) is a polynomial in ρ.

For future studies, we will give mathematical analysis to the MTIs for solving the HODEs with general nonlinearities. We will try to furthermore improve the performance of the MTIs and apply them to solve massive problems arising from molecular dynamics.

2. On the Klein-Gordon equation

Chapter 3 studied the classical numerical methods including finite difference time domain (FDTD) methods, exponential wave integrators (EWIs) and the time-splitting method with spectral spatial discretization for solving the KGE with a dimensionless parameter $\varepsilon \in (0, 1]$ that is inversely proportional the speed of the light. The existing popular FDTD methods and an EWI with Gautschi's quadrature Fourier pseudospectral (EWI-GFP) method given in [10] were reviewed with special attentions paid to the error bounds in the highly oscillatory regime, i.e. the nonrelativistic limit regime $0 < \varepsilon \ll 1$. As a known result, the EWI-GFP method has much better performance than the FD methods due to the released temporal resolution capacity in the nonrelativistic limit regime. Then a time-splitting Fourier pseudospectral (TSFP) discretization, which was derived for a simple equivalent

first-order-in-time form of the KG equation, was applied and analyzed for the KGE. It was shown that the TSFP is essentially equivalent to an EWI with the Deulfhard's type quadrature pseudospectral method, and thanks to the fact, rigorous and optimal error estimates of the TSFP method were achieved for the regime $\varepsilon = O(1)$. Extensive numerical studies carried out in the nonrelativistic limit regime $0 < \varepsilon \ll 1$ demonstrated that the TSFP has uniform spectral accuracy in spatial discretization, and has the temporal discretization error bound within the convergence regime as $O(\varepsilon^{-2}\tau^2)$, whereas that of the EWI-GFP method is $O(\varepsilon^{-4}\tau^2)$, where τ denotes the time step. Comparisons between the methods show that TSFP offers compelling better temporal approximations over the EWI-GFP method, and consequently TSFP has the optimal performance among all the classical numerical methods for directly solving the KGE in the nonrelativistic limit regime. Rigorous arguments for optimal error bounds of the TSFP when $0 < \varepsilon \ll 1$ are of great interests and it is proposed to be done in a future work.

In Chapter 4, a multiscale time integrator Fourier pseudospectral (MTI-FP) method was proposed and analyzed for solving the KGE with the dimensionless parameter $0 < \varepsilon \leq 1$. The key ideas for designing the MTI-FP method are based on (i) carrying out a multiscale decomposition by frequency at each time step with proper choice of transmission conditions between time steps, and (ii) adapting the Fourier spectral for spatial discretization and the EWI for integrating second-order highly oscillating ODEs. Rigorous error bounds for the MTI-FP method were established, which imply that the MTI-FP method converges uniformly and optimally in space with spectral convergence rate, and uniformly in time with linear convergence rate for $\varepsilon \in (0, 1]$ and optimally with quadratic convergence rate in the regimes when either $\varepsilon = O(1)$ or $0 < \varepsilon \leq \tau$. Numerical results confirmed these error bounds and suggested that they are sharp. The MTI method has wide future potential applications to solve other nonlinear equations arising from quantum and plasma physics in some limit physical regimes, where similar oscillations happen. For example, the Klein-Gordon-Schrödinger equations in the nonrelativistic limit regime [18], and the

Zakharov-Rubenchik system in the adiabatic limit regime [82, 83]....

3. On the Klein-Gordon-Zakharov system

We successfully applied and extended the EWI and MTI methods from previous chapters to solve the KGZ system in highly oscillatory regimes in Chapter 5. In this chapter, a Gautschi-type EWI sine pseudospectral method and a Deflhard-type sine pseudospectral method were proposed for the KGZ in the simultaneous high-plasma-frequency and subsonic limit regime. Error estimates of the two EWIs were established in non-limit regime. A MTI sine spectral was proposed to the KGZ in high-plasma-frequency limit regime with uniform convergence. All the proposed methods have similar numerical performance as that in the KGE case.

The future studies on multiscale methods for the KGZ are fruitful. Firstly, the coupling of two nonlinear equations and the small parameters make the error estimates of the numerical methods very hard to be established rigorously in the limit regimes. So far, it has not been done yet even for finite difference methods. Thus, establishing the rigorous error bounds of the EWIs and MTI is a challenging mathematical work. Secondly, here the MTI method is only proposed to the KGZ in the single high-plasma-frequency limit regime. The technique used here is mainly based on our study of KGE in the nonrelativistic limit regime. However, in the subsonic limit regime of the KGZ, it is completely a different story. Thus another challenging work is to propose MTIs for solving the KGZ in the subsonic limit regime and even in the simultaneously high-plasma-frequency and subsonic limit regime.

Bibliography

[1] M. Ablowitz, M. Kruskal, and J. Ladik, *Solitary wave collisions*, SIAM J. Appl. Math., 36 (1979), pp. 428–437.

[2] G. Adomian, *Nonlinear klein-gordon equation*, Appl. Math. Lett., 9 (1996), pp. 9–10.

[3] G. Ariel, B. Engquist, and R. Tsai, *A multiscale method for highly oscillatory ordinary differential equations with resonance*, Math. Comput., 78 (2009), pp. 929–956.

[4] Z. Artstein, J. Linshiz, and E. Titi, *Young measure approach to computing slowly advancing fast oscillations*, SIAM Multiscale Model. Simul., 6 (2007), pp. 1085–1097.

[5] W. Bao and Y. Cai, *Uniform error estimates of finite difference methods for the nonlinear Schrödinger equation with wave operator*, SIAM J. Numer. Anal., 50 (2012), pp. 492–521.

[6] ——, *Mathematical theory and numerical methods for Bose-Einstein condensation*, Kinet. Relat. Mod., 6 (2013), pp. 1–135.

[7] ——, *Optimal error estimates of finite difference methods for the Gross-Pitaevskii equation with angular momentum rotation*, Math. Comp., 82 (2013), pp. 99–128.

[8] ——, *Uniform and optimal error estimates of an exponential wave integrator sine pseudospectral method for the nonlinear Schrödinger equation with wave operator*, SIAM J. Numer. Anal., 52 (2014), pp. 1103–1127.

[9] W. Bao, Y. Cai, and X. Zhao, *Uniformly correct multiscale time integrator pseudospectral method for klein-gordon equation in the non-relativistic limit regime*, SIAM J. Numer. Anal., 52 (2014), pp. 2488–2511.

[10] W. Bao and X. Dong, *Analysis and comparison of numerical methods for the Klein-Gordon equation in the nonrelativistic limit regime*, Numer. Math., 120 (2012), pp. 189–229.

[11] W. Bao, X. Dong, and X. Zhao, *An exponential wave integrator pseudospectral method for the Klein-Gordon-Zakharov system*, SIAM J. Sci. Comput., 35 (2013), pp. A2903–A2927.

[12] ——, *Uniformly correct multiscale time integrators for highly oscillatory second order differential equations*, J. Math. Study, 47 (2014), pp. 111–150.

[13] W. Bao, D. Jaksch, and P. Markowich, *Numerical solution of the Gross-Pitaevskii equation for Bose-Einstein condensation*, J. Comput. Phys., 187 (2003), pp. 318–342.

[14] W. Bao, S. Jin, and P. Markowich, *Numerical study of time-splitting spectral discretizations of nonlinear Schrödinger equations in the semiclassical regimes*, SIAM J. Sci. Comput., 25 (2002), pp. 27–64.

[15] ——, *Time-splitting spectral approximations for the Schrödinger equation in the semiclassical regime*, J. Compt. Phys., 175 (2002), pp. 487–524.

[16] W. Bao and J. Shen, *A fourth-order time-splitting Laguerre-Hermite pseudo-spectral method for Bose-Einstein condensates*, SIAM J. Sci. Comput., 26 (2005), pp. 2010–2028.

[17] W. Bao and F. Sun, *Efficient and stable numerical methods for the generalized and vector Zakharov system*, SIAM J. Sci. Comput., 26 (2005), pp. 1057–1088.

[18] W. Bao and L. Yang, *Efficient and accurate numerical methods for the Klein-Gordon-Schrödinger equations*, J. Comput. Phys., 225 (2007), pp. 1863–1893.

[19] D. Baĭnov and E. Minchev, *Nonexistence of global solutions of the initial-boundary value problem for the nonlinear Klein-Gordon equation*, J. Math. Phys., 36 (1995), pp. 756–762.

[20] P. Bellan, *Fundamentals of Plasmas Physics*, Cambridge University Press, Cambridge, 2006.

[21] P. Brenner and W. V. Wahl, *Global classical solutions of non-linear wave equations*, Math. Z., 176 (1981), pp. 87–121.

[22] L. Burden and J. Douglas, *Numerical Analysis*, Thomson/Brooks/Cole, 2005.

[23] M. Calvo, P. Chartier, A. Murua, and J. Sanz-Serna, *A stroboscopic numerical method for highly oscillatory problems*. Preprint available at http://www.irisa.fr/ipso/fichiers/strob3.pdf.

[24] W. Cao and B. Guo, *Fourier collocation method for solving nonlinear Klein-Gordon equation*, J. Comput. Phys., 108 (1993), pp. 296–305.

[25] F. Castella, P. Chartier, F. Méhats, and A. Murua, *Stroboscopic averaging for the nonlinear Schrödinger equation*. Preprint available at http://www.irisa.fr/ipso/fichiers/sav-6.pdf.

[26] P. Chartier, N. Crouseilles, M. Lemou, and F. Méhats, *Uniformly accurate numerical schemes for highly oscillatory Klein-Gordon and nonlinear Schrödinger equations*. Preprint available at arXiv:math.NA1308.0507.

[27] D. Cohen, *Analysis and numerical treatment of highly oscillatory differential equations*, PhD thesis, Université de Genève, 2004.

[28] ——, *Conservation properties of numerical integrators for highly oscillatory Hamiltonian systems*, IMA J. Numer. Anal., 26 (2005), pp. 34–59.

[29] D. Cohen, E. Hairer, and C. Lubich, *Modulated Fourier expansions of highly oscillatory differential equations*, Found. Comput. Math., 3 (2003), pp. 327–345.

[30] D. Cohen, E. Hairer, and C. Lubich, *Conservation of energy, momentum and actions of numerical discretization of non-linear wave equations*, Numer. Math., 110 (2008), pp. 113–143.

[31] M. Condona, A. D. no, and A. Iserles, *On second order differential equations with highly oscillatory forcing terms*, Proc. R. Soc. A, 466 (2010), pp. 1809–1828.

[32] A. Davydov, *Quantum Mechanics, 2nd Edition*, Pergamon, Oxford, 1976.

[33] E. Deeba and S. Khuri, *A decomposition method for solving the nonlinear Klein-Gordon equation*, J. Comput. Phys., 124 (1996), pp. 442–448.

[34] P. Degond, J. Liu, and M. Vignal, *Analysis of an asymptotic preserving scheme for the Euler-Poisson system in the quasineutral limit*, SIAM J. Numer. Anal., 46 (2008), pp. 1298–1322.

[35] R. Dendy, *Plasma Dynamics*, Oxford University Press, Oxford, 1990.

[36] P. Deuflhard, *A study of extrapolation methods based on multistep schemes without parasitic solutions*, ZAMP., 30 (1979), pp. 177–189.

[37] X. Dong and X. Zhao, *On time-splitting pseudospectral discretization for nonlinear klein-gordon equation in nonrelativistic limit regime*, Commun. Comput. Phys., 16 (2014), pp. 440–466.

[38] D. Duncan, *Symplectic finite difference approximations of the nonlinear Klein-Gordon equation*, SIAM J. Numer. Anal., 34 (1997), pp. 1742–1760.

[39] W. E, *Principles of Multiscale Modeling*, Cambridge University Press, 2011.

[40] W. E and B. Engquist, *The heterogeneous multiscale methods*, Comm. Math. Sci., 1 (2003), pp. 87–132.

[41] W. E., B. Engquist, X. Li, W. Ren, and E. Vanden-Eijnden, *The heterogeneous multiscale method: a review*, Commun. Comput. Phys., 2 (2007), pp. 367–450.

[42] B. Engquist and Y. Tsai, *Heterogeneous multiscale methods for stiff ordinary differential equations*, Math. Comp., 74 (2005), pp. 1707–1742.

[43] E. Faou and K. Schratz, *Asympotic preserving schemes for the Klein-Gordon equation in the non-relativistic limit regime*, Numer. Math., 126 (2014), pp. 441–469.

[44] B. Garcia-Archilla, J. Sanz-Serna, and R. Skeel, *Long-time-step methods for oscillatory differential equations*, SIAM J. Sci. Comput., 20 (1998), pp. 930–963.

[45] W. Gautschi, *Numerical integration of ordinary differential equations based on trigonometric polynomials*, Numer. Math., 3 (1961), pp. 381–397.

[46] D. Germund and B. A. ke, *Numerical Methods in Scientific Computing: Vol. 1*, SIAM, 2008.

[47] J. Ginibre and G. Velo, *The global Cauchy problem for the nonlinear Klein-Gordon equation*, Math. Z., 189 (1985), pp. 487–505.

[48] ——, *The global cauchy problem for the nonlinear Klein-Gordon equationii*, Ann. Inst. H. Poincaré Anal. Non Linéaire, 6 (1989), pp. 15–35.

[49] R. Glassey, *On the asymptotic behavior of nonlinear wave equations*, Trans. Am. Math. Soc., 182 (1973), pp. 187–200.

[50] R. Glassey and M. Tsutsumi, *On uniqueness of weak solutions to semi-linear wave equations*, Commun. Partial Differ. Eqn., 7 (1982), pp. 153–195.

[51] D. Gottlieb and S. Orszag, *Numerical Analysis of Spectral Methods: Theory and Applications*, Society for Industrial and Applied Mathematics, Philadelphia, 1993.

[52] V. Grimm, *A note on the Gautschi-type method for oscillatory second-order differential equations*, Numer. Math., 102 (2005), pp. 61–66.

[53] ——, *On error bounds for the Gautschi-type exponential integrator applied to oscillatory second-order differential equations*, Numer. Math., 100 (2005), pp. 71–89.

[54] V. Grimm and M. Hochbruck, *Error analysis of exponential integrators for oscillatory second-order differential equations*, J. Phys. A: Math. Gen., 39 (2006), pp. 5495–5507.

[55] E. Hairer and C. Lubich, *Long-time energy conservation of numerical methods for oscillatory differential equations*, SIAM J. Numer. Anal., 38 (2000), pp. 414–441.

[56] ——, *On the energy disctribution in Fermi-Pasta-Ulam lattices*, Arch. Ration. Mech. Anal., 205 (2012), pp. 993–1029.

[57] E. Hairer, C. Lubich, and G. Wanner, *Geometric Numerical Integration: Structure-Preserving Algorithms for Ordinary Differential Equations*, Springer, Berlin, 2006.

[58] E. Hairer, S. Nørsett, and G. Wanner, *Solving Ordinary Differential Equations: Stiff And Differential-Algebraic Problems*, Springer, 1993.

[59] ——, *Solving ordinary differential equations: Nonstiff problems*, SIAM Journal on Matrix Analysis and Applications, 31 (2009), pp. 1432–1457.

[60] R. Hardin and F. Tappert, *Applications of the split-step Fourier method to the numerical solution of nonlinear and variable coefficient wave equations*, SIAM Rev., 15 (1973), p. 423.

[61] J. Hesthaven, S. Gottlieb, and D. Gottlieb, *Spectral Methods for Time-Dependent Problems*, Cambridge University Press, Cambridge, New York, 2007.

[62] M. Hochbruck and C. Lubich, *A Gautschi-type method for oscillatory second-order differential equations*, Numer. Math., 83 (1999), pp. 402–426.

[63] S. Ibrahim, M. Majdoub, and N. Masmoudi, *Global solutions for a semilinear, two-dimensional Klein-Gordon equation with exponential-type nonlinearity*, Comm. Pure Appl. Math., 59 (2006), pp. 1639–1658.

[64] A. Iserles, *On the numerical quadrature of highly-oscillating integrals i: Fourier transforms.*, IMA J. Numer. Anal., 24 (2004), pp. 365–391.

[65] ——, *On the numerical quadrature of highly-oscillating integrals ii: Fourier transforms.*, IMA J. Numer. Anal., 25 (2005), p. 2544.

[66] A. Iserles and S. Nørsett, *Efficient quadrature of highly oscillatory integrals using derivatives*, Proc. R. Soc. A, 461 (2005), p. 13831399.

[67] S. Jiménez and L. Vázquez, *Analysis of four numerical schemes for a nonlinear Klein-Gordon equation*, Appl. Math. Comput., 35 (1990), pp. 61–94.

[68] S. Jin, *Efficient asymptotic-preserving (ap) schemes for some multiscale kinetic equations*, SIAM J. Sci. Comp., 21 (1999), pp. 441–454.

[69] S. Jin, P. Markowich, and Z. Xiong, *Numerical simulation of a generalized Zakharov system*, J. Comput. Phys., 201 (2004), pp. 376–395.

[70] S. Klainerman and M. Machedon, *Space-time estimates for null forms and the local existence theorem*, Commun. Pure Appl. Math., 46 (1993), pp. 1221–1268.

[71] R. Kosecki, *The unit condition and global existence for a class of nonlinear Klein-Gordon equations*, J. Diff. Eqn., 100 (1992), pp. 257–268.

[72] N. Krylov and N. Bogoliubov, *Introduction to non-linear mechanics*, Princeton: Princeton Univ. Press., 1947.

[73] B. Leimkuhler and S. Reich, *Simulating Hamiltonian Dynamics*, 2004.

[74] S. Li and L. Vu-Quoc, *Finite difference calculus invariant structure of a class of algorithms for the nonlinear Klein-Gordon equation*, SIAM J. Numer. Anal., 32 (1995), pp. 1839–1875.

[75] S. Machihara, *The nonrelativistic limit of the nonlinear Klein-Gordon equation*, Funkcial. Ekvac., 44 (2001), pp. 243–252.

[76] S. Machihara, K. Nakanishi, and T. Ozawa, *Nonrelativistic limit in the energy space for nonlinear Klein-Gordon equations*, Math. Ann., 322 (2002), pp. 603–621.

[77] N. Masmoudi and K. Nakanishi, *From nonlinear Klein-Gordon equation to a system of coupled nonlinear Schrödinger equations*, Math. Ann., 324 (2002), pp. 359–389.

[78] ——, *From the Klein-Gordon-Zakharov system to the nonlinear schrödinger equation*, J. Hyperbolic Differ. Equ., 2 (2005), pp. 975–1008.

[79] ——, *Energy convergence for singular limits of Zakharov type systems*, Invent. Math., 172 (2008), pp. 535–583.

[80] C. Morawetz and W. Strauss, *Decay and scattering of solutions of a nonlinear relativistic wave equation*, Comm. Pure Appl. Math., 25 (1972), pp. 1–31.

[81] B. Najman, *The nonrelativistic limit of the nonlinear Klein-Gordon equation*, Nonlinear Anal., 15 (1990), pp. 217–228.

[82] F. Oliveira, *Stability of the solitons for the one-dimensional Zakharov-Rubenchik equation*, Physica D, 175 (2003), pp. 220–240.

[83] ——, *Adiabatic limit of the Zakharov-Rubenchik equation*, Rep. Math. Phys., 61 (2008).

[84] T. Ozawa, K. Tsutaya, and Y. Tsutsumi, *Well-posedness in energy space for the Cauchy problem of the Klein-Gordon-Zakharov equations with different propagation speeds in three space dimensions*, Math. Ann., 313 (1999), pp. 127–140.

[85] B. Pachpatte, *Inequalities for Finite Difference Equations. Monographs and Textbooks in Pure and Applied Mathematics*, Marcel Dekker Inc., New York, 2002.

[86] G. Pavliotis and A. Stuart, *Multiscale methods: averaging and homogenization*, Springer, 2007.

[87] H. Pecher, *Nonlinear small data scattering for the wave and Klein-Gordon equation*, Math. Z., 185 (1984), pp. 261–270.

[88] L. Petzold, L. Jay, and J. Yen, *Numerical solution of highly oscillatory ordinary differential equations.*

[89] J. Sakurai, *Advanced Quantum Mechanics*, Addison Wesley, New York, 1967.

[90] J. Sanders, F. Verhulst, and J. Murdock, *Averaging Methods in Nonlinear Dynamical Systems*, Springer, New York, 2007.

[91] J. Sanz-Serna, *Mollified impulse methods for highly oscillatory differential equations*, SIAM J. Numer. Anal., 46 (1998), pp. 1040–1059.

[92] J. Sanz-Serna and M. Calvo, *Numerical Hamiltonian Problems*, Chapman and Hall, London, 1994.

[93] I. Segal, *The global Cauchy problem for a relativistic scalar field with power interaction*, Bull. Soc. Math. Fr., 91 (1963), pp. 129–135.

[94] J. Shatah, *Normal forms and quadratic nonlinear Klein-Gordon equations*, Commun. Pure Appl. Math., 35 (1985), pp. 685–696.

[95] J. Shen and T. Tang, *Spectral and High-Order Methods with Applications*, Science Press, Beijing, 2006.

[96] J. Simon and E. Taflin, *The Cauchy problem for nonlinear Klein-Gordon equations*, Commun. Math. Phys., 152 (1993), pp. 433–478.

[97] G. Strang, *On the construction and comparison of difference schemes*, SIAM J. Numer. Anal., 5 (1968), pp. 506–517.

[98] W. Strauss, *Decay and asymptotics for* $\Box u = f(u)$, J. Funct. Anal., 2 (1968), pp. 409–457.

[99] W. Strauss and L. Vázquez, *Numerical solution of a nonlinear Klein-Gordon equation*, J. Comput. Phys., 28 (1978), pp. 271–278.

[100] C. Sulem and P. Sulem, *The Nonlinear Schrödinger Equation: Self-Focusing and Wave Collapse*.

[101] M. Tao, H. Owhadi, and J. Marsden, *Nonintrusive and structure preserving multiscale integration of stiff odes, sdes and hamiltonian systems with*

hidden slow dynamics via flow averaging, SIAM Multiscale Model Simul., 8 (2010), pp. 1269–1324.

[102] T. Tao, *Local and Global Analysis of Nonlinear Dispersive and Wave Equations*, CBMS Regional Series in Mathematics, 2006.

[103] Y. Tourigny, *Product approximation for nonlinear Klein-Gordon equations*, IMA J. Numer. Anal., 9 (1990), pp. 449–462.

[104] M. Tsutsumi, *Nonrelativistic approximation of nonlinear Klein-Gordon equations in two space dimensions*, Nonlinear Anal., 8 (1984), pp. 637–643.

[105] T. Wang, J. Chen, and L. Zhang, *Conservative difference methods for the Klein-Gordon-Zakharov equations*, J. Comput. App. Math., 205 (2007), pp. 430–452.

[106] J. Weideman and B. Herbst, *Split-step methods for the solution of the nonlinear Schrödinger equation*, SIAM J. Numer. Anal., 23 (1986), pp. 485–507.

[107] H. Yoshida, *Construction of higher order symplectic integrators*, Phys. Lett. A, 150 (1990), pp. 262–268.

[108] V. Zakharov, *Collapse of langmuir waves*, Sov. Phys. JETP, 35 (1972), pp. 908–914.

List of Publications

[1] *An exponential wave integrator pseudospectral method for the Klein-Gordon-Zakharov system* (with Weizhu Bao and Xuanchun Dong), SIAM J. Sci. Comput., 35, pp. A2903–A2927 (2013).

[2] *Numerical methods and simulations for the dynamics of one-dimensional Zakharov-Rubenchik equations,* (with Ziyi Li), J. Sci. Comput., 59, pp. 412–438 (2014).

[3] *Uniformly correct multiscale time integrators for highly oscillatory second order differential equations* (with Weizhu Bao and Xuanchun Dong), J. Math. Study, 47, pp. 111–150 (2014).

[4] *On time-splitting pseudospectral discretization for nonlinear Klein-Gordon equation in nonrelativistic limit regime* (with Xuanchun Dong), Commun. Comput. Phys., 16, pp. 440–466 (2014).

[5] *Scalar-field theory of dark matter* (with Kerson Huang and Chi Xiong), Int. J. Mod Phys A, 29, 1450074 (2014).

[6] *Optimal error estimates of finite difference methods for the coupled Gross-Pitaevskii equations in high dimensions,* (with Tingchun Wang), Sci. China Math., 57, pp. 2189–2214 (2014).

[7] *Uniformly correct multiscale time integrator pseudospectral method for Klein-Gordon equation in the non-relativistic limit regime,* (with Weizhu Bao and Yongyong Cai), SIAM J. Numer. Anal., 52, pp. 2488–2511 (2014).

[8] *On multichannel solutions of nonlinear Schrödinger equations: algorithm, analysis and numerical explorations* (with Avy Soffer), submitted to J. Phys. A (2014).

Multiscale methods and analysis for highly oscillatory differential equations **Zhao Xiaofei** **2014**